THE DEVELOPMENT OF CO_2-SWITCHABLE TECHNOLOGIES FOR SEPARATION OF ORGANIC COMPOUNDS

by

Sean M. Mercer

A thesis submitted to the Department of Chemistry

In conformity with the requirements for

the degree of Doctor of Philosophy

Queen's University

Kingston, Ontario, Canada

December, 2012

Abstract

The increasing environmental impact of society has created the need for the modification of current and the implementation of new industrial processes which are less environmentally harmful. However, these new or modified processes must be less material-, time-, and cost-intensive such that they are more economically beneficial than the processes they are to supplant. The described research was inspired by these two ideas and is comprised of two projects, both focused on the creation of recyclable, CO_2-switchable methods of separating organic compounds.

The development and optimization of switchable water, a CO_2-switchable ionic strength aqueous solvent is described. The solvent system, an amine/aqueous mixture, had the ability to switch from low to high ionic strength via the application and removal of CO_2. This solvent system was able to achieve salting-out of water-miscible organics in comparable amounts to several inorganic salts typically used for salting-out.

The switchable water system was explored for use in several industrial applications. A homogeneous catalysis recycling system was developed for the hydroformylation of styrene. A catalyst was able to be recovered and recycled five times with minimal loss of activity. The use of switchable water to expedite the settling of clay suspensions was also explored. Switchable water, when used as process water did not settle bulk clay solids as quickly as a CO_2-only treatment, but did however increase the settling rate of small clay fines resulting in lower turbidities of the supernatant. The solvent could be recovered from settled clay suspensions and recycled up to three times.

Finally, efforts towards the realization of CO_2-switchable chiral resolving agents are presented. It is hypothesized that chiral nitrogenous bases could be used as switchable

resolving agents by forming diastereomeric salt pairs with racemic alcohols via the application of CO_2. After separation of the diastereomers, removal of CO_2 would afford the resolved alcohol enantiomers and the chiral base. Efforts towards the synthesis of a library of chiral nitrogenous bases and the screening of their reactivity with CO_2-treated alcohols are described. Several bases were generated, but the necessary reactivity between the bases and the racemic alcohols in the presence of CO_2 was not observed.

Acknowledgements

During the past four years at Queen's I've been extremely fortunate to make many new friends and to truly grow as a scientist and as a person. I would first like to thank Professor Jessop for his guidance and mentorship. Your knowledge, enthusiasm, and eagerness to teach (or to let me figure it out for myself) has instilled me with an even greater passion for research, science, and the environment. I would be remiss to not extend gratitude to the many academic and industrial collaborators that I had the opportunity to work with. I am also very thankful for the generous support of many government and industrial agencies that supported my work as well as the Department of Chemistry at Queen's, particularly the faculty and support staff that served as mentors, readers, and supervisory committee members.

My colleagues in the Jessop group have been an absolute pleasure to work, play, and commiserate with. I'd specifically like to thank Trisha Ang, Alaina Boyd, Vanessa Little, and Darrell Dean whom I had the great privilege to have as friends for the entirety of my time in Kingston. I would also like to specifically thank the people that greatly influenced me during my time at Queen's. Drs. Tobias Robert, Dominik Wechsler, Keith Huynh, and Jitendra Harjani, you have all provided with so much help for the future by showing me how excellent scientists conduct themselves.

I'd like to thank my friends and family whom have been constantly supportive of me despite my 8+ year (and growing) reluctance to get a real job. I would especially like to thank my Mom and Dad whom instilled me with a love of science and learning at a very young age. I love you both!

Finally, I would like to thank my beautiful and inspiring wife, Victoria. You have been my biggest supporter and I will never be able to thank you enough for the sacrifices that you've made so that I could pursue my dreams. I am the luckiest man in the world to have you in my life and I hope that our lives together will continue to be full of fun, love, laughter, and highly-cited journal publications.

I hope that in the future that I will be able pay forward the mentorship, friendship, and love that I have been fortunate enough to receive during these past several years.

Slainte Mhath!

Statement of Originality

I hereby certify that all of the work described within this thesis is the original work of the author. Any published (or unpublished) ideas and/or techniques from the work of others are fully acknowledged in accordance with the standard referencing practices. Any and all contributions from collaborators are clearly noted below.

In Chapter 3, Mr. Daniel Dixon and Mr. Chien-Shun Chen participated in the data collection of organic compound salting out. Dr. Jitendra Harjani and Ms. Zahra Ghoshouni developed a preliminary procedure for the synthesis of compound **3.11**, which was later modified. Dr. Tobias Robert synthesized and studied compounds **3.1** and **3.10**. Prof. Natalie Cann assisted with computational calculations. Prof. Gilles Peslherbe and Mr. Soran Jahangiri of Concordia University participated in the formulation of hypotheses and development of the final conclusions as to what factors dictate the salting out behaviour of diammonium salts in aqueous solution.

In Chapter 4, Dr. Tobias Robert and Mr. Daniel Dixon participated in method development and screening of pre-catalysts. Dr. Alemayehu Asfaw and Prof. Diane Beauchemin performed the ICP-MS measurements.

In Chapter 5, Dr. Tobias Robert and Mr. Chien-Shun Chen participated in data collection of clay settling. Ms. Ying Lau contributed to the initial method development and zeta potential measurements. The results of her initial study are presented in their entirety in her M.Sc. thesis (Queen's University, Sept. 2010). Mr. Ian Rupar assisted with light microscopy.

In addition, all X-ray structures described were solved by Dr. Ruiyao Wang and all high-res mass spectra were collected by Dr. Jiaxi Wang and Mr. James Lei at Queen's University.

Portions of the dissertation have been published previously:

Chapter 2: i) S. M. Mercer, P.G. Jessop, *ChemSusChem* **2010**, *3*, 467-470. Reproduced with permission of John Wiley & Sons, 2012.

Chapter 3: i) S.M. Mercer, T. Robert, D.V. Dixon, C-S. Chen, Z Ghoshouni, J.R. Harjani, S. Jahangiri, G.H. Peslherbe, P.G. Jessop, *Green Chemistry* **2012**, *14*, 832-839. Reproduced with permission of the Royal Society of Chemistry, 2012.

Chapter 4: i) S.M. Mercer, T. Robert, D.V. Dixon, P.G. Jessop, *Catalysis Science & Technology* **2012**, *2*, 1315-1318. Reproduced with permission of the Royal Society of Chemistry, 2012.

Chapter 5: i) C-S Chen, Y-Y. Lau, S.M. Mercer, T. Robert, J.H. Horton, P.G. Jessop, *ChemSusChem* **2012**, DOI: 10.1002/cssc.201200465. Reproduced with permission of John Wiley & Sons, 2012.

Sean M. Mercer

December, 2012

Table of Contents

List of Figures

List of Tables

List of Abbreviations

B:L	Branched product/linear product
BHT	Butylated hydroxytoluene
BINAM	1,1'-Binaphthyl-2,2'-diamine
BINAP	2,2'-Bis(diphenylphosphino)-1,1'-binaphthyl
CCC	Critical coagulation concentration
CHELPG	Charges from electrostatic potentials using a grid based method
DIAD	Diisopropylazodicarboxylate
DIH	1,3-diiodo-5,5-dimethylhydantoin
DPPA	Diphenylphosphoryl azide
DMEA	*N*,*N*-dimethylethanolamine
DMSO	Dimethylsulfoxide
DBU	1,8-Diazobicyclo[5.4.0]undec-7-ene
DMF	Dimethylformamide
DMSO	Dimethyl sulfoxide
e.u.	Electronic unit
HRMS	High resolution mass spectrometry
i.d.	Inner diameter
L:B	Linear product/branched product
ICP-MS	Inductively coupled plasma mass spectrometry
IR	Infrared spectroscopy
MDEA	*N*-Methyldiethanolamine
MEA	Monoethanolamine
MeCN	Acteonitrile
NMR	Nuclear magnetic resonance spectroscopy
NTU	Nephelometric turbidity unit
OATS	Organic-aqueous tunable solvent
ppm	Parts per million
PDI	Polydispersity index
pH	Negative logarithm of the concentration of hydronium ions
pK_a	Negative logarithm of the acid dissociation constant
pK_{aH}	Negative logarithm of the conjugate acid dissociation constant
RPM	Revolutions per minute
RRR	Resolution-recycle-racemization synthetic strategy
$[Rh(COD)Cl]_2$	Chloro(1,5-cyclooctadiene)rhodium (I) dimer
SAS	CO_2-Switchable anionic surfactant
SCS	CO_2-Switchable cationic surfactant
SHS	CO_2-Switchable hydrophilicity solvent
SPS	CO_2-Switchable polarity solvent
TAML	Tetra-amido macrocycle ligand
THF	Tetrahydrofuran
TMDAB	*N,N,N',N'*-Tetramethyl-1,4-diaminobutane

TPP	Triphenylphosphine
TPPTS	Triphenylphosphine-3,3',3"-trisulfonic acid trisodium salt hydrate

List of Symbols

α	The first carbon from an attached functional group
a	Activity
$a_{\pm}$	Mean ionic activity
β	The second carbon from an attached functional group
B	Base
C	Conversion
c	Concentration
δ	NMR chemical shift
e	Charge of a proton (1.60 x 10^{-19} C)
ε_0	Permittivity of free space (8.85 x 10^{-12} C N^{-1} m^{-2})
ε_r	Dielectric constant
ee	Enantiomeric excess
γ	Activity coefficient
$\gamma_{\pm}$	Mean ionic activity coefficient
I	Ionic strength
J	NMR coupling constant
κ	Inverse of Debye screening length
K_a	Acid dissociation constant
K_A	Association constant
K_{salt}	Setschenow constant
k	Boltzmann constant (1.38 x 10^{-23} J K^{-1})
k_H	Henry's Law constant
k_R	Rate constant for a reaction involving an R enantiomer
k_S	Rate constant for a reaction involving an S enantiomer
μ	Chemical potential
$\mu_{\pm}$	Mean chemical potential
M	Molarity
M^+	Molecular ion
m	Molality
m^0	1 Mol solute per kilogram solvent
$m_{\pm}$	Mean ionic molality
N_A	Avogadro constant (6.02 x 10^{23} mol^{-1})
n	Number of basic sites on a polyamine
ω	The final carbon from an attached functional group
Φ	Electrostatic potential
P	Partial pressure
P^*	Partial pressure of a pure substance
π	Pi bond
R	Ideal Gas Constant (8.314 J K^{-1} mol^{-1})
R	Enantiomer with Cahn-Ingold-Prelog priority decreasing in a clockwise direction
r	Radius

S	Enantiomer with Cahn-Ingold-Prelog priority decreasing in a counterclockwise direction
S	Aqueous solubility of a substrate in the presence of a salt
S_0	Aqueous solubility of a substrate
SF	Selectivity factor
T	Temperature
x	Mole fraction
Z	Charge number

List of Numbered Compounds

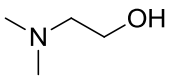

2.1

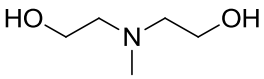

2.2

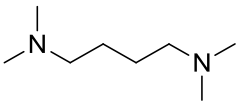

2.3

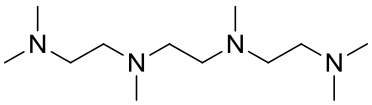

2.4

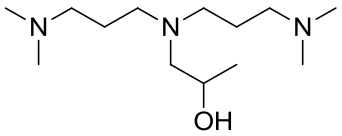

2.5

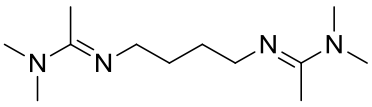

3.1

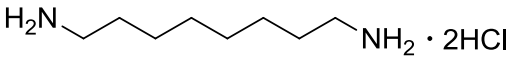

3.2

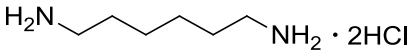

3.3

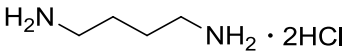

3.4

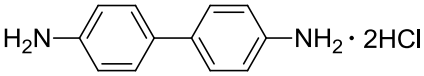

3.5

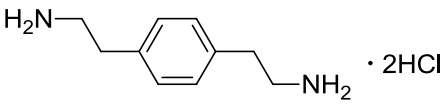

3.6

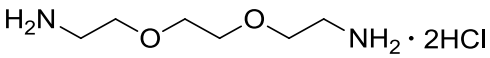

3.7

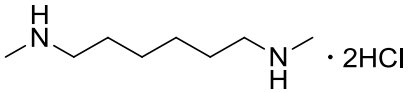

3.8

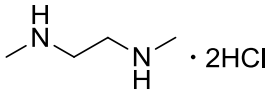

3.9

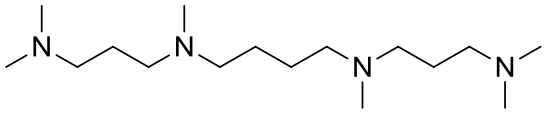

3.10

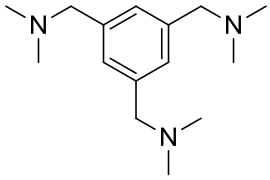

3.11

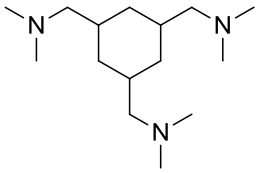

3.12

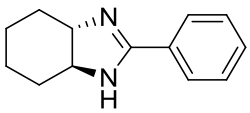

6.1

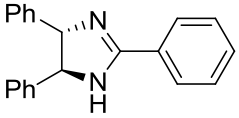

6.2

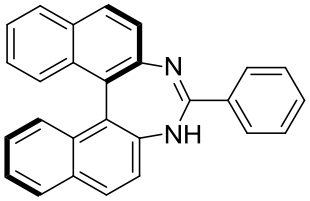

6.3

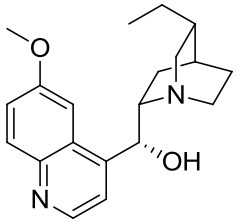

6.4

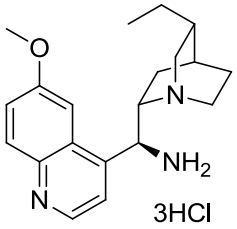

6.5

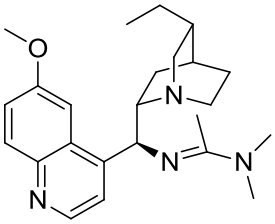

6.6

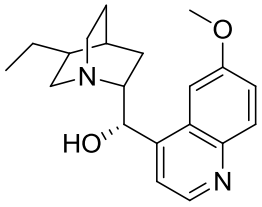

6.7

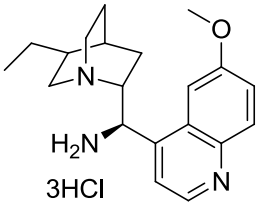

6.8

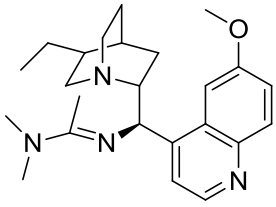

6.9

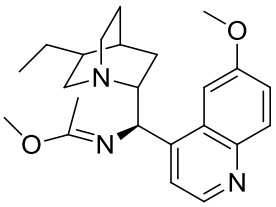

6.10

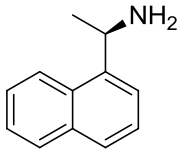

6.11

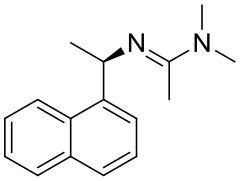

6.12

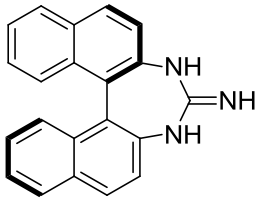

6.13

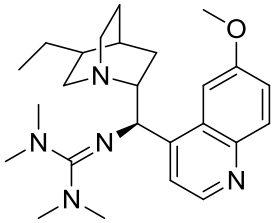

6.14

Chapter 1

Introduction

1.1 Green Chemistry

1.1.1 Ideals & Principles

Green chemistry is broadly defined as the "design, development, and implementation of chemical products and processes to reduce or eliminate the use and generation of substances hazardous to human health and the environment".[1] This branch of chemistry connects all four of the traditional realms of chemistry, organic, inorganic, analytical, and physical/theoretical, in the pursuit of more efficient and less environmentally harmful chemistry. The field is reliant on contributions from both fundamental and applied chemistry where the former provides the foundation on which new ideas are developed and the latter provides the means to develop those ideas into real-world practice. The field also encompasses expertise from many other fields of science truly making it a multi-disciplinary field of study. Knowledge in subjects such as environmental and chemical engineering and toxicology allow green chemistry practitioners to appropriately identify hazardous substances and subsequently design chemical processes that circumvent their use.

A set of twelve principles were developed in the 1990s by Warner and Anastas which provided a preliminary guide to practitioners of green chemistry (Table 1.1).[2] The primary focus was the efficient synthesis and use of more benign materials while

redesigning chemical processes such that waste was not formed in the process. This was in contrast to traditional real-world pollution prevention where waste was not minimized, but merely mitigated at the end of the process.

Table 1.1. The twelve principles of green chemistry.[2]

1. **Prevention**: *It is better to prevent waste than to treat or clean up waste after it has been created.*
2. **Atom Economy**: *Synthetic methods should be designed to maximize the incorporation of all materials used in the process into the final product.*
3. **Less Hazardous Chemical Syntheses**: *Wherever practicable, synthetic methods should be designed to use and generate substances that possess little or no toxicity to human health and the environment.*
4. **Designing Safer Chemicals**: *Chemical products should be designed to affect their desired function while minimizing their toxicity.*
5. **Safer Solvents and Auxiliaries**: *The use of auxiliary substances (eg. solvents, separation agents, etc.) should be made unnecessary whenever possible and innocuous when used.*
6. **Design for Energy Efficiency**: *Energy requirements of chemical processes should be recognized for their environmental and economical impacts and should be minimized. If possible, synthetic methods should be conducted at ambient temperature and pressure.*
7. **Use of Renewable Feedstocks**: *A raw material or feedstock should be renewable rather than depleting whenever technically and economically practicable.*
8. **Reduce Derivatives**: *Unnecessary derivatization (use of blocking groups, protection/deprotection, temporary modification of physical/chemical processes) should be minimized or avoided if possible, because such steps require additional reagents and can generate waste.*
9. **Catalysis**: *Catalytic reagents (as selective as possible) are superior to stoichiometric reagents.*
10. **Design for Degradation**: *Chemical products should be designed so that at the end of their function they break down into innocuous degradation products and do not persist in the environment.*
11. **Real-time Analysis for Pollution Prevention**: *Analytical methodologies need to be further developed to allow for the real-time, in-process monitoring and control prior to the formation of hazardous substances.*
12. **Inherently Safer Chemistry for Accident Prevention**: *Substances and the form of a substance used in a chemical process should be chosen to minimize the potential for chemical accidents, including releases, explosions, and fires.*

This broad philosophy was later extended into a set of twelve principles for green engineering by Anastas and Zimmerman (Table 1.2).[3]

Table 1.2. The twelve principles of green engineering.[3]

1. **Inherent Rather Than Circumstantial**: *Designers need to strive to ensure that all material and energy inputs and outputs are as inherently nonhazardous as possible.*
2. **Prevention Instead of Treatment**: *It is better to prevent waste than to treat or clean up waste after it is formed.*
3. **Design for Separation**: *Separation and purification operations should be designed to minimize energy consumption and materials use.*
4. **Maximize Efficiency**: *Products, processes and systems should be designed to maximize mass, energy, space and time efficiency.*
5. **Output-Pulled Versus Input-Pushed**: *Products, processes and systems should be "output pulled" rather than "input pushed" through the use of energy and materials.*
6. **Conserve Complexity**: *Embedded entropy and complexity must be viewed as an investment when making design choices on recycle, reuse, or beneficial disposition.*
7. **Durability Rather Than Immortality**: *Targeted durability, not immortality, should be a design goal.*
8. **Meet Need, Minimize Excess**: *Design for unnecessary capacity or capability (eg. "one size fits all") solutions should be considered a design flaw.*
9. **Minimize Material Diversity**: *Material diversity in multi-component products should be minimized to promote disassembly and value retention.*
10. **Integrate Local Material and Energy Flows**: *Design of products, processes and systems must include integration and interconnectivity with available energy and material flows.*
11. **Design for Commercial "Afterlife"**: *Products, processes and systems should be designed for performance in a commercial "afterlife".*
12. **Renewable Rather Than Depleting**: *Material and energy inputs should be renewable rather than depleting.*

Although these guiding principles offer an excellent foundation for pursuits in green chemistry and engineering, they are not steadfast rules and often a set of principles must supersede another. Thus the discussion of which process, compound, or even company is "green" has become a large topic of scientific debate.

1.1.2 Metrics

The process of labeling a compound or material "green" generally stems from a quantitative measure of "greenness". However, one must always ensure that such a label is never used as an absolute term. The term "green" as an absolute is ultimately

unattainable as every material or process will incorporate some degree of hazard or risk. However “green”, as a relative term, can be used to compare one material or process to another (i.e. this is “greener” than that) as hazard and risk are continually minimized as new technologies are developed. A material that is currently considered “green” compared to existing materials may eventually have this label supplanted in the future by a better material or process which is less harmful.

To perform comparisons of “greenness”, a number of metrics have been developed. These metric systems range from uni- to multi-variate, from brief “reaction only” to comprehensive “cradle-to-gate” or “cradle-to-grave”, and from calculations requiring seconds to studies that require many weeks of research.[4] Ultimately, the more comprehensive a metric system is, the better it is for assigning the 'greenness' of a process.

The most popular metrics used to assign “greenness” of a chemical reaction are atom economy and E-factor. Every chemical reaction can be assigned an atom economy and/or E-factor and comparisons of “greenness” between reactions can be made from this data. Atom economy, as developed by Trost,[5] reflects the percentage of atoms from reagents that emerge from a chemical reaction incorporated into the desired product (Eqn. 1.1).

$$\%\ Atom\ Economy = \frac{Molecular\ Weight\ of\ Desired\ Product}{Molecular\ Weight\ of\ All\ Reactants}\ x\ 100 \qquad \textbf{(1.1)}$$

Some reactions, such as the azide-alkyne Huisgen cycloaddition,[6] are 100% atom economical as all atoms in the reagents are incorporated into the desired final product.

The environmental factor or "E-Factor", developed by Sheldon,[7] is the ratio of the mass of the total waste generated by a reaction per unit mass of product produced (Eqn. 1.2).

$$E\ Factor = \frac{Mass\ of\ Waste\ Generated}{Mass\ of\ Product\ Produced} \qquad \textbf{(1.2)}$$

This metric is an improvement upon atom economy as it better reflects a total chemical process rather than a chemical reaction alone. A reaction that is 100% atom economical may, for example, produce a large amount of solvent waste, where a reaction with a lower atom economy may not. The E-factor will reflect this difference in waste generation where the atom economy will not.

These uni-variate metrics have been embraced for their simplicity, but they provide insufficient information on the potential hazards, risks, and waste produced by a reaction and often do not consider an entire chemical process.[8] For example, a set of reactions may be found to have a series of differing E-Factor values. With no specific identification of the waste produced, a true determination of which route is "greenest" is not possible. One reaction may generate hundreds of kilograms of benign waste, per kilogram of product, while another may generate a few kilograms of hazardous waste. The route that generates the hazardous waste is then ultimately the less green process

despite its lower E-factor. A real-world comparative demonstration of the differing results provided by a series of metrics was recently performed by Beckman and co-workers.[9] The more information that can be solicited from a chemical reaction will ultimately lead to the most appropriate assessment of its "greenness". It must also be remembered that not only reactions can be assessed for "greenness". Materials and separations can also be labeled as "green" or not, but atom economy and E-factor do not provide a means of assessment for these materials and processes.

Currently, the most comprehensive system for determining "greenness" of materials, reactions, and separations, comes from cradle-to-grave life cycle assessment.[10] In these studies a set of multi-variate metrics corresponding to a wide variety of environmental and hazard implications are determined for raw material acquisition, material synthesis, material distribution, and subsequent material degradation. This system allows for a comprehensive analysis of the inherent waste, hazard, and risk produced by not only a material, but all processes involved in its lifetime. This system affords a balanced platform for a comparison of "greenness".

1.1.3 Practice in Industry

Many industries have begun to embrace green chemistry and engineering and now use their philosophies in material and process development. This is of paramount importance to the green chemistry and engineering movement. Although the philosophies

were developed in academic and government laboratories, the practice of green chemistry and engineering must be taken up in industry to enact the greatest amount of change globally. Industry has taken up green chemistry and engineering practice not only to protect the environment but also to assist in public relations and increase profits. The basis of green chemistry and engineering in reaction and engineering efficiency often helps to make processes more streamlined and economical, minimizing production costs.[11]

Examples where industry has made strides in environmental protection and improvements in efficiency are numerous. Those that have arguably received the most attention are those that have been awarded the Presidential Green Chemistry Challenge Award by the United States Environmental Protection Agency.[11] Industrial examples in pharmaceutical production (minimization of waste generation in Ibuprofen synthesis), polymer manufacturing (use of CO_2 as a blowing agent in polystyrene) and paper production (TAML oxidant catalysts for delignification) easily demonstrate the multi-disciplinary nature of green chemistry and engineering.[11] These few examples also highlight the potential wide-spread positive ramifications of further incorporation of green chemistry and engineering into industrial practices.

1.2 Carbon Dioxide

1.2.1 Background, Structure & Bonding

Carbon dioxide, CO_2, is a colourless gas first recognized as a distinct compound in the 16th century as a by-product of combustion.[12] CO_2 is a centrosymmetric molecule and therefore has no dipole moment. By molecular orbital theory (Fig. 1.1), the compound has equal distribution of its 16 valence electrons in two σ bonding, two π bonding orbitals and four non-bonding orbitals, however the compound is considered weakly electrophilic. This stems from the greater electronegativity of the oxygen atoms withdrawing electron density in the bonding orbitals from the central carbon[13] (3.61 vs. 2.54 on the Pauling Scale)[14].

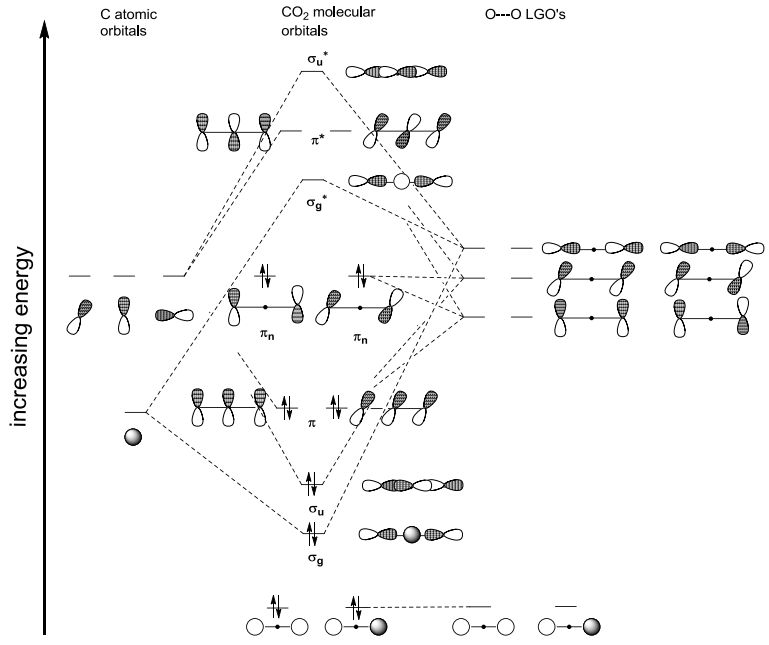

Fig. 1.1. Molecular orbital diagram of CO_2.

Beyond combustion, CO_2 is also a by-product of many industrial processes including hydrogen production, fermentation, and calcinations.[12] CO_2 is a vital compound in the environment. The gas circulates around in the Earth's carbon cycle serving as a reagent in photosynthesis and as a waste product of cellular respiration.[15] CO_2 is a topic of great relevance for the atmospheric and environmental sciences as it is considered a greenhouse gas and is thought to be contributing to increasing global temperatures. The atmospheric concentration of CO_2 has risen from roughly 270 ppm, pre-industrial revolution, to approximately 370 ppm during the past decade.[15] Mitigation of CO_2 released from industrial processes, particularly fossil fuel combustion, has become a large field of study. The majority of research is currently devoted to methods of capture, sequestration, and/or fixation of CO_2 into value-added products.

CO_2 is also an important additive in process chemistry. When used at elevated pressures, compressed CO_2 has become a popular medium for chemical reactions and extractions due to its low cost, as well being benign and operable at low temperatures. When pressurized over the critical point (72.9 atm, 31.1 °C), supercritical CO_2 has been successfully used a reaction medium and extracting solvent.[16] Elevated pressures of CO_2, below the critical pressure, have also been used to generate new reaction environments. Chemical reactions and extractions have been successfully performed with CO_2-expanded liquids.[17] The elevation in CO_2 pressure generally increases the physical solubility of CO_2 in a solvent thereby manipulating the solvent properties. The mixture of the dissolved gas (which is dictated by the pressure) and the organic solvent provides a

continuum of liquid media of varying properties, ranging from those of the neat solvent to that of supercritical CO_2. Upon release of the pressure, the solvent reverts to its ambient CO_2 solubility and original (neat) physical properties, thus providing a solvent system with many accessible sets of physical properties. Liquid CO_2 can also be used as a reaction medium. Its properties resemble that of typical hydrocarbon solvents save a greater capacity for hydrogen-bonding.[18]

1.2.2 Reactivity

Generally, CO_2 is not very reactive at ambient temperature unless in the presence of a catalyst or strong nucleophile. Typical synthetic procedures which use CO_2 are carboxylation reactions to install a C1 source which can later be reduced or transformed to less oxidized functionalities. Phenols can undergo base-promoted carboxylations to give salicylic acid derivatives via the Kolbe-Schmitt reaction (Eqn. 1.3).[19]

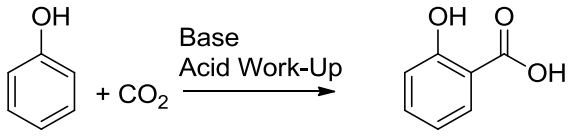

(**1.3**)

CO_2 is known to insert into metal-carbon bonds to afford higher carbon-number carboxylic acids and is also known to react with carbanions on aromatic structures via directed lithiation chemistry.[20] CO_2 can also form β-keto acids from ketones in the

presence of a strong base[20], such as 1,8-diazobicyclo[5.4.0]undec-7-ene, DBU (Eqn. 1.4).[21]

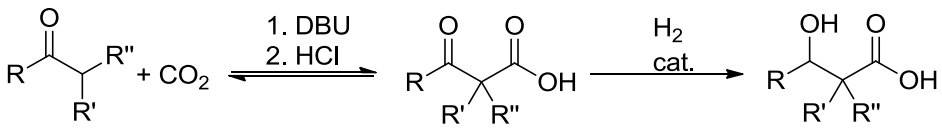

(**1.4**)

Arguably, the most important commercial reaction involving CO_2 is the production of urea, where CO_2 reacts with two equivalents of ammonia to generate ammonium carbamate.[12] Subsequent dehydration of the intermediate ammonium carbamate affords urea (Eqn. 1.5).

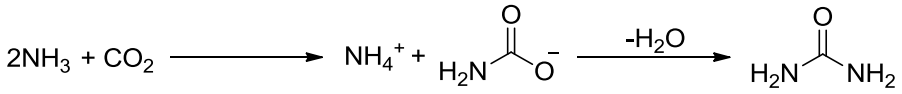

(**1.5**)

In a similar vein structurally, CO_2 can be used to generate carbonates.[22] Linear carbonates have particular industrial relevance as they have been used in place of phosgene in bulk polymer synthesis providing a less hazardous replacement for this dangerous chemical.[23] Cyclic carbonate polymers can also be synthesized from CO_2 potentially affording value-added products while fixing a greenhouse gas simultaneously (Eqn. 1.6).[24]

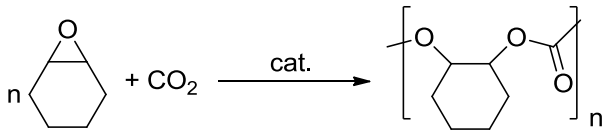

(**1.6**)

CO_2 also has the ability to form carbamic acids with primary and secondary amines which then often leads to carbamate salt formation with a second equivalent of an amine (Eqn. 1.7).[25] Such reactivity has been readily exploited in scrubbing technology as a means to trap and remove CO_2 from fossil fuel combustion sources such as coal-fired power plants.[26]

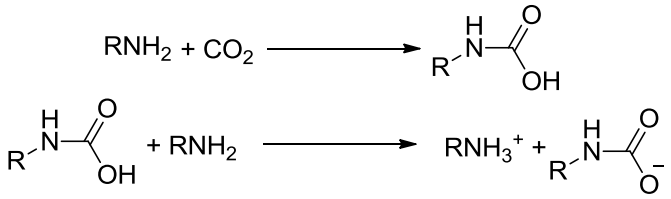

(**1.7**)

Esters of carbamic acids can be generated from the parent carbamic acid via a series of metal catalyzed reactions and addition of an organic substrate such as an alkyl halide (Eqn. 1.8).[27] These reactions provide a means of obtaining many phosgene related compounds without the use of phosgene itself.[20]

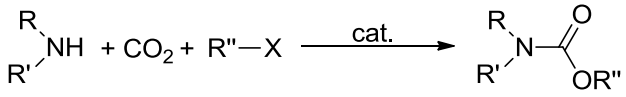

(**1.8**)

The dissolution of CO_2 in water affords a series of acid/base equilibria. The dissolution of CO_2 into water is dictated by Henry's Law (Eqn. 1.9) where the concentration of dissolved CO_2, c, is proportional to the CO_2 partial pressure, P, and inversely proportional to the Henry's Law constant, k_H, which for CO_2 in water at 298 K is 29.41 L·atm mol^{-1}.

$$c = \frac{P}{k_H} \tag{1.9}$$

The reaction of dissolved CO_2 with water then generates carbonic acid, H_2CO_3, a weak acid with an apparent pK_a of 6.4.[28] The apparent pK_a reflects the combination of the CO_2 hydration equilibria and the first dissociation of H_2CO_3 (Eqn. 1.10).

$$\begin{aligned} CO_{2(g)} &\rightleftharpoons CO_{2(aq)} \\ CO_{2(aq)} + H_2O_{(l)} &\rightleftharpoons H_2CO_{3(aq)} \\ H_2CO_{3(aq)} &\rightleftharpoons HCO_3^-{}_{(aq)} + H^+_{(aq)} \\ HCO_3^-{}_{(aq)} &\rightleftharpoons CO_3^{2-}{}_{(aq)} + H^+_{(aq)} \end{aligned} \tag{1.10}$$

As carbonic acid is a polyprotic acid, its two actual pK_{00} values have been measured as 3.8[29] and 10.3[28] respectively. The extent of dissociation and therefore the population of each species, H_2CO_3, HCO_3^-, and CO_3^{2-}, is pH dependent (Fig. 1.2). Acting as a common

acid, the dissociation of this compound acts to acidify water, which is a growing concern in large bodies of water due to the increasing atmospheric CO_2 concentration.[29] The acid can be neutralized by common alkaline compounds such as amines, serving to generate bicarbonate and carbonate salts.

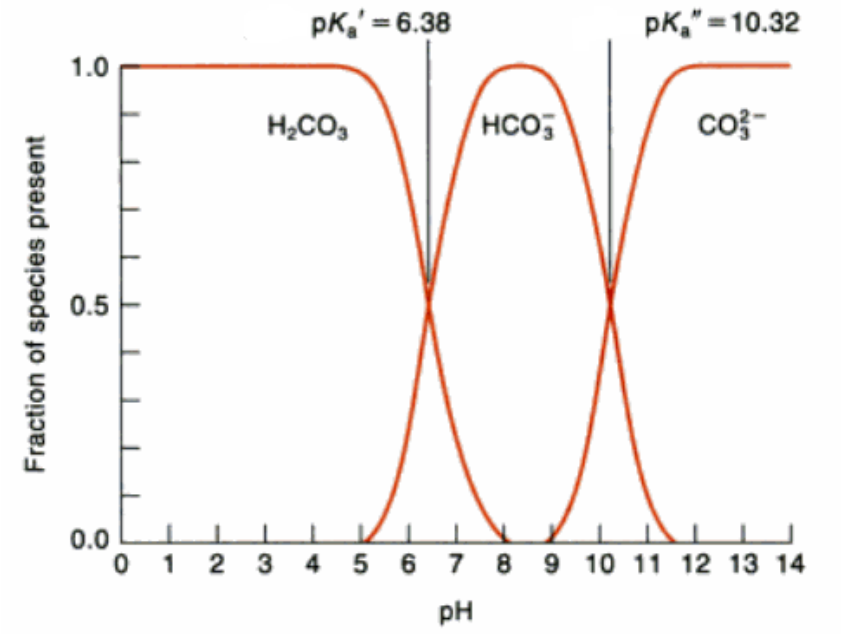

Fig. 1.2. A distribution plot of carbonic acid (hydrated CO_2 & H_2CO_3) and the subsequent dissociated species based on pH.[28]

1.3 CO_2-Switchable Technologies

1.3.1 Switchable Materials

A "switchable" material is one that possesses two sets of physical or chemical properties that are accessible via the application or removal of a stimulus, often referred to as the trigger. There are many stimuli-responsive materials, often labeled "smart" materials, which are switchable in one direction, such as drug-delivery vehicles.[31,32] Ideally however, a switchable material is readily interchangeable between two states so that the material may be readily recycled in the process in which it is being used.

Previous materials which have been explicitly labeled as switchable include surfactants and surfaces.[32,33] The stimuli used to trigger the change between physical and/or chemical property sets have included redox reactions,[34-41] acid/base chemistry,[42-44] and light.[45,46] A CO_2-switchable material is one where CO_2 acts as the trigger. The removal of CO_2 from the system is typically achieved by heating the system and flushing with an inert gas such as N_2, Ar or air. To achieve switchability, the application or removal of CO_2 often exploits the inherent acid/base reactivity of a substrate to enact the change between two sets of chemical and/or physical properties.[47]

1.3.2 CO_2-Switchable Solvents

CO_2-switchable solvents were primarily developed as reaction media that allowed for a chemical reaction to occur in one form of the solvent and, upon application of CO_2,

provide a solvent which allowed for selective extraction or precipitation of a product.[47] Such a switchable solvent would eliminate the need for more than one solvent in a chemical process, reducing solvent waste.

The switchable polarity solvents, SPS, were the first CO_2-switchable materials created in the Jessop group, and developed in collaboration with the research group of Eckert and Liotta. The solvent system exists in two forms: the first, with CO_2 absent, being a low polarity liquid and the second, where CO_2 is present, a higher polarity liquid (Fig. 1.3).[48] The initial system consisted of an equimolar mixture of an amidine, DBU, and small chain alcohol acting as the low polarity solvent. The introduction of CO_2, to afford the high polar solvent, formed alkyl-carbonic acid with the alcohol. The acid was subsequently neutralized by DBU, generating an amidinium alkyl-carbonate ionic liquid (Eqn. 1.11).

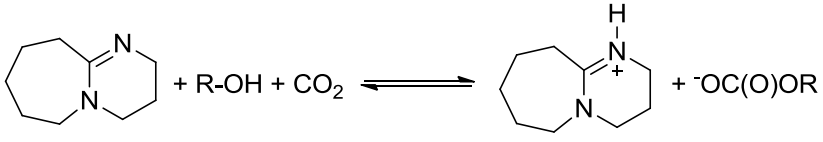

(1.11)

Since its initial development, multiple variations of the solvent system have been developed by Jessop, Eckert, Liotta and contemporaries.[47] Additional amidine-containing solvents[49,50] in addition to systems employing other nitrogenous bases such as guanidines[49,51] and amines,[52-56] alone or in conjunction with amidines, have been used to generate ionic liquids in the presence of CO_2.

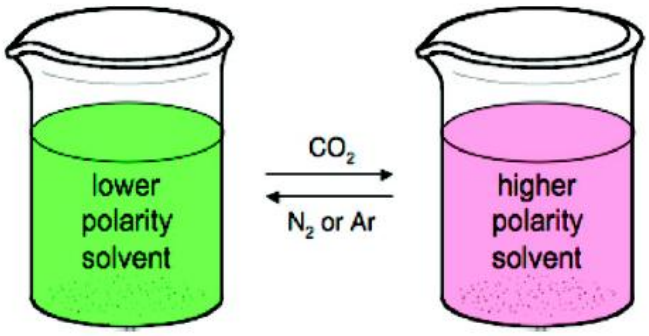

Fig. 1.3. A conceptual scheme of a switchable polarity solvent (SPS).[48]

The second generation of switchable solvents were the switchable hydrophilicity solvents, SHS (Fig. 1.4).[57] A nitrogenous base with minimal miscibility with water is capable of acting as a solvent for hydrophobic solutes and creates a biphasic system when mixed with water. The introduction of CO_2 into the system leads to the protonation of the nitrogenous base solvent, converting it into a bicarbonate salt. The newly formed ionic species are much more hydrophilic and become miscible with water. The removal of CO_2 then returns the nitrogenous base solvent back to its original hydrophobic form (Eqn. 1.12). This strategy allows for the hydrophobic form of the SHS to extract hydrophobic organic substrates and later leave them isolated, without the need for distillation or filtration, as the solvent is drawn into carbonated water. The removal of CO_2 allows for recycling of the solvent.

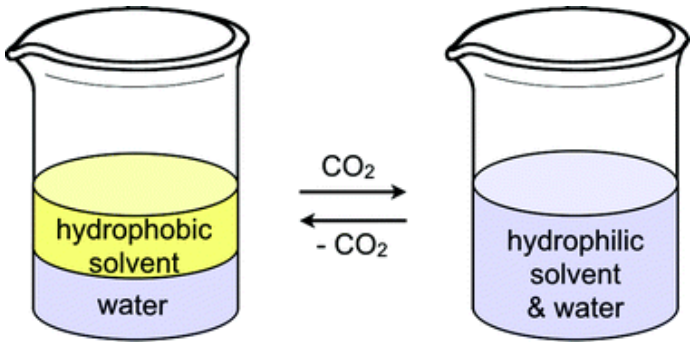

Fig. 1.4. A conceptual scheme of a switchable hydrophilicity solvent (SHS).[57]

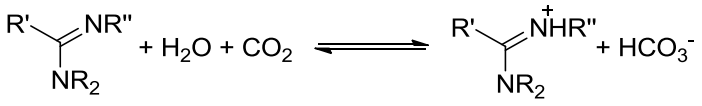

(**1.12**)

The use of SHS as a recyclable extraction solvent has already been demonstrated for numerous industrially relevant substrates including: extracting oils from soybean flakes,[57] algae,[58] oil sands,[59] and recycling polystyrene foams.[60] CO_2 need not only act as a trigger to induce miscibility, but can in fact cause immiscibility. Ohno and co-workers have previously developed an ionic liquid which is miscible with water but not with carbonated water,[61] providing a complementary technology to those developed by Jessop and co-workers.

1.3.3 CO_2-Switchable Surfactants

A compound which can be made to reversibly change between a surfactant or demulsifier is very relevant for industrial chemists. The first switchable cationic surfactant, SCS, comprised an acetamidine appended to a long hydrocarbon tail. Upon protonation by carbonic acid, an amidinium bicarbonate species is generated as the cationic surfactant (Fig. 1.5).[62] This surfactant system demonstrated the ability to stabilize crude oil/water emulsions in the presence of CO_2 and act as a demulsifier in the absence of CO_2. Additional studies into the design of the head[63-65] and tail[66,67] groups showed the emulsion stabilization/demulsifying performance could be tailored depending on the structure of the SCS used.

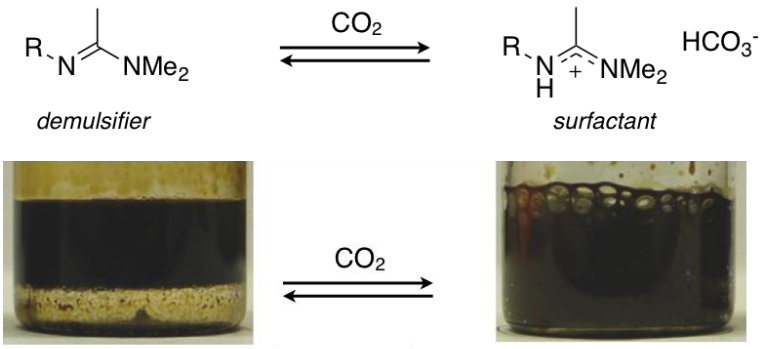

Fig. 1.5. The reaction scheme of switchable cationic surfactants and their resulting effect upon an oil/water biphasic system before and after a CO_2-treatment .[62]

The use of CO_2 to affect the surface activity had been previously hypothesized. In the 1980s the first use of CO_2 as a means to decrease the surface activity of a compound was demonstrated by Moore and Lefevre during the coagulation of latex from an emulsion polymerization.[68] CO_2 was introduced in water to reprotonate the anionic surfactant sodium oleate. Jessop and co-workers would later demonstrate the recyclability of similar anionic surfactant, SAS, systems comprised of long-tail carboxylates and phenolates (Fig. 1.6).[69]

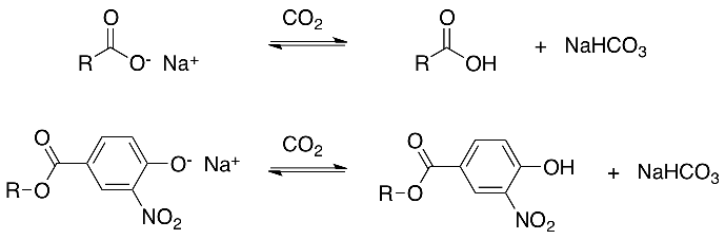

Fig. 1.6. Reaction schemes of several switchable anionic surfactants, SAS, studied by Jessop and co-workers.[69]

1.3.4 CO_2-Switchable Polymers

Recently, the incorporation of pendant nitrogenous base functional groups on polymer chains has been used to generate polymers which have switchable hydrophilicity,[70] conductance,[71] and critical solution temperatures[72] upon reaction with carbonic acid. Reversible organogels, developed by Weiss and co-workers, have

employed CO_2 as a reversible gelling agent.[73,74] CO_2 has also been used as a means to achieve reversible polymerization and crosslinking of monomer or oliogomer units. Rudkevich and co-workers developed a series of amine-containing monomers which upon treatment with CO_2 would polymerize via carbamate linkages.[75,76] The polymeric structures were far less soluble than their monomer components so the carbamate polymer could be easily removed from solution. Monomer units which incorporated appropriate supramolecular hosts, such as crown ethers, were developed as a means of scavenging undesired metal ions from solution.[77,78] The groups of Weiss and Nagai have demonstrated reversible and controllable cross-linking of amine-functionalized polymer chains as a means to obtaining adhesive[79] and porous[80] materials respectively.

1.3.5 CO_2-Switchable Particles

The use of CO_2 as a means of enacting reversible chemical and physical changes upon particles is becoming a popular and varied area of research. The reversible coagulation and dispersion of suspensions, particularly latexes, has become a fast growing field of polymer chemistry. The Jessop and Cunningham groups, and later the Zhu group, demonstrated the ability of switchable surfactants to stabilize styrene and methacrylate latexes generated by emulsion polymerization which then could be coagulated by removal of CO_2 (Fig. 1.7).[81-85] The latexes could also be redispersed upon re-introduction of CO_2.[86] Latexes generated by surfactant-free polymerization have also

been shown to demonstrate CO_2-switchability if a CO_2-switchable initiator is used.[87] The incorporation of a CO_2-switchable monomer into co-polymer has also demonstrated reversible coagulation and dispersion in the presence or absence of CO_2.[88]

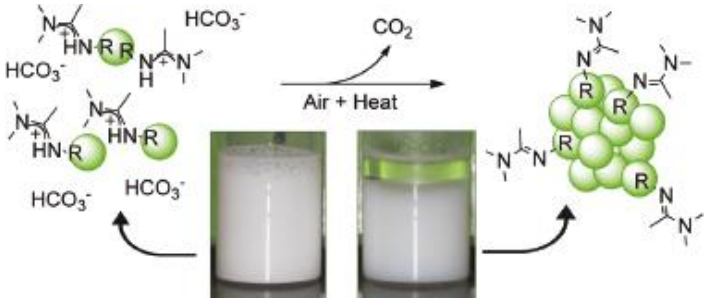

Fig. 1.7. Schematic and example of a dispersed latex stabilized by aminidinium bicarbonate switchable surfactants, followed by coagulation of latex after removal of CO_2.[81]

Reversible dispersions manipulated by CO_2 are not only limited to latexes. Zhang and co-workers have previously grafted amine-functional groups onto single-walled carbon nanotubes allowing CO_2 to act as a controlled dispersant of the nanotubes.[89] Oligo-amine based polyelectrolyte molecular cages[90] and nanocapsules[91] which "breathe" in the presence or absence of CO_2 have also been developed as a means of achieving controlled release of organic substrates.

1.3.6 CO_2-Switchable Catalysts & Solutes

In a similar vein to the CO_2-switchable polymers, the incorporation of nitrogenous base functionalities onto a molecular framework can allow for switchable chemical and physical properties upon reaction with CO_2 and allow for easier separation of substrates. Tagged-fluorescent dyes[92] and metal complexes with appropriate ligand frameworks[93-97] have been shown to partition from organic to aqueous phases and back again with the application and removal of CO_2. Hydrocarbons with appended nitrogenous bases have also shown variable fluorescence in the presence of CO_2 and have been proposed as CO_2 detectors.[98-100] The introduction of CO_2 into a switchable solvent system, such as carabamate ionic liquids, containing a solvent-responsive material has also afforded CO_2 sensors which are based on changes in fluorescence[101.102] as well as conductance.[103]

CO_2 can also be used to control the photochromism of dyes. Darwish and co-workers have shown that spiropyran dyes which undergo photo-isomerizations to merocyanines can have this process interrupted when DBU is present, as a new stable complex is formed. The introduction of CO_2 into such a DBU solution can disrupt this complex and allow for normal photo-isomerization to occur.[104] Incorporation of a pendant-amidine onto a spiropyran has afford another CO_2-sensing technology utilizing this reactivity.[105] CO_2 has also been shown to dictate activity of an organocatalyst. Introduction of CO_2 into a solution containing a benzamidine organocatalyst can shut down the catalyst's activity towards promoting the aldol reaction. The removal of CO_2 from the system restores the activity of the organocatalyst.[106]

1.3.7 Future Technologies

Despite the recent large advances of switchable-CO_2 chemistry, many unexplored areas of research remain with many potential green technologies still to be developed. The generation of electrolytes is a common theme in switchable-CO_2 chemistry, particularly in solvents, yet prior to the research to be described in subsequent chapters, no CO_2-switchable manipulations of ionic strength and/or salinity have been demonstrated in an aqueous solvent. Similarly, no demonstration of a chiral resolving agent for the isolation of chiral compounds using switchable-CO_2 chemistry has been achieved. Both recyclable chiral resolving agents and aqueous solvents with reversible ionic strength could afford industrially useful green technologies for the separation of organic compounds.

1.4 Electrolyte Solutions

1.4.1 Ideal, Non-ideal Solutions and Activity

An ideal solution, comprised of components A and B, is defined as one that follows Raoult's Law (Eqn. 1.13) at all mole fractions of either component.[106] Where the partial pressure of a substance, P_i, is proportional to the vapour pressure of the pure substance, P_i^*, multiplied by its mole fraction in solution, x_i.This results from equivalent A-A, B-B, and A-B interactions ultimately leading to the vapor pressure of a substance

being linearly proportional to its mole fraction in the overall solution. At equilibrium the chemical potential, μ_i, or the change in Gibbs free energy per mole of substance, of either component can be expressed as Equation 1.14 where the chemical potential of the component is a function of its mole fraction.

$$P_i = P_i^* x_i \tag{1.13}$$

$$\mu_i = \mu_i^* + RTln\frac{P_i}{P_i^*} \tag{1.14}$$

Often solutions do not follow Raoult's Law and thus are non-ideal. To account for this, the dimensionless term, activity (Eqn. 1.15) provides a modified expression for chemical potential (Eqn. 1.16) that reflects the non-ideality of the solution by scaling the mole fraction with the empirically determined activity coefficient, γ. If A is considered the solvent and B the solute, an ideal dilute solution can then be defined where the solvent follows Raoult's Law and the solute follows Henry's Law (Eqn. 1.9).

$$\mu_i = \mu_i^* + RTlna_i \tag{1.15}$$

$$a_i = \gamma_i x_i \tag{1.16}$$

Electrolytes are compounds that dissociate into free ions and impart electrical conductivity into the medium in which they are dissociated. Solutions of electrolytes do not follow the ideal dilute solution model due to electrostatic forces, which dominate the

solute-solute interactions and are not present in non-electrolyte solutions. As electrolyte species undergo dissociation, the ions' chemical potentials (μ_+ and μ_-) are not measurable. A mean chemical potential, $\mu_\pm$, can be measured (Eqn. 1.17). The mean chemical potential can be related to the standard state mean chemical potential via the mean ionic activity, $a_\pm$, (Eqn. 1.18) which itself is based on the mean ionic activity coefficient, $\gamma_\pm$ and the mean ionic molality, $m_\pm$ (Eqn. 1.19). The activity coefficient, which reflects deviation from ideality, can be measured through variance of colligative properties and in many cases can be modeled.

$$\mu_\pm = \mu_\pm^* + RTlna_\pm \quad \textbf{(1.17)}$$

$$a_\pm = \left(\frac{m_\pm}{m^\circ}\right)\gamma_\pm \quad \textbf{(1.18)}$$

$$\begin{gathered} m_\pm^\upsilon = m_+^{\upsilon_+} m_-^{\upsilon_-} \\ m_\pm = (\upsilon_+^{\upsilon_+}\upsilon_-^{\upsilon_-})^{\frac{1}{\upsilon}}\, m \\ \gamma_\pm^\upsilon = \gamma_+^{\upsilon_+}\gamma_-^{\upsilon_-} \\ \gamma_\pm = (\gamma_+^{\upsilon_+}\gamma_-^{\upsilon_-})^{\frac{1}{\upsilon}} \end{gathered} \quad \textbf{(1.19)}$$

1.4.2 Formulation of the Ionic Strength Term

For non-electrolyte solutions, the deviations from ideality are quite specific to the nature of the components and are thus difficult to model. This however is not the case for electrolytes as electrostatic forces dominate the solute-solute interactions and these interactions are far more general across the spectrum of solutes. Electrostatic, or coulombic, interactions are fundamentally based on ion charge and separation. A means to model the mean ionic activity coefficient of a solute, and thereby a way to model the departure of electrolyte solutions from ideality, was developed Debye and Hückel.[108] The model is based on coulombic interactions where a comparison of the electric potential of an isolated ion in solution versus the electric potential of a solvated ion dictates ion screening and deviation from ideality.

The electric potential of an isolated ion in a dielectric medium is described in Equation 1.20. Upon solvation, the electric potential is defined as Equation 1.21. The ratio of the two (Eqn. 1.22) utilizes a new term, κ, which represents the inverse of the Debye-Hückel screening length, a representation of the amount that an ion is screened away from other ions. It is assumed that an ion is surrounded by a spherical cloud of oppositely charged neighbours but ultimately the net charge of this spherical cloud is considered the same as the central ion. However when κ is large, the net charge of the cloud begins to decrease towards zero, resulting in $\gamma_{\pm} < 1$ and a departure from ideality. At large values of κ, the screening length ($1/\kappa$) is small and the central atom is thus well screened from the rest of the solution.

$$\Phi_{isolated\ ion}(r) = \frac{\pm Ze}{4\pi\varepsilon_0\varepsilon_r r} \quad \textbf{(1.20)}$$

$$\Phi_{solvated\ ion}(r) = \frac{\pm Ze}{4\pi\varepsilon_0\varepsilon_r r} e^{-\kappa r} \quad \textbf{(1.21)}$$

$$\frac{\Phi_{solvated\ ion}(r)}{\Phi_{isolated\ ion}(r)} = e^{-\kappa r} \quad \textbf{(1.22)}$$

The screening length term contains concentration dependant terms which were combined by Debye and Hückel into one term known as ionic strength, *I,* (Eqn. 1.23). The ionic strength term is defined as one half of the summation of the concentration term (each ion's molality, m), multiplied by the square of each ion's charge number, Z.[109] This definition of ionic strength afforded a way to calculate κ (Eqn. 1.24) and ultimately the mean ionic activity coefficient (Eqn. 1.25). Equation 1.25, the Debye-Hückel Limiting Law, provided means to model the thermodynamics of electrolyte solutions albeit at very low ionic strength. Modifications of Debye-Hückel theory by Davies[110] and Bromley[111] which included semi-empirical terms, have allowed for predictions of mean ionic activity coefficients at ionic strengths well above those that can be approximated with the original model by Debye and Hückel. Other models such as specific ion interaction theory[112] and Pitzer[113] equations have provided even more rigorous modeling systems.

$$I = \frac{1}{2}\sum_i (m_{i+} Z_{i+}^2 + m_{i-} Z_{i-}^2) \quad \textbf{(1.23)}$$

$$\kappa = \left(\sqrt{\left(\frac{2e^2 N_A}{\varepsilon_0 kT}\right)}\right)\sqrt{\frac{I}{\varepsilon_r}} \quad \textbf{(1.24)}$$

$$\ln \gamma_{\pm} = -|Z_+ Z_-| \frac{e^2 \kappa}{8\pi \varepsilon_0 \varepsilon_r kT} \quad \textbf{(1.25)}$$

1.4.3 Effects of Ionic Strength

The effect of increasing ionic strength fundamentally leads to a re-ordering of solvent structure as the dissociated ions are solvated to varying extents.[114] In aqueous solutions, the addition of salt and subsequent increase of the ionic strength is generally performed to decrease the solubility of other solutes, the "salting out" effect, and to destabilize a persistent colloid mixture. These behaviors are not universal however as for example a "salting in" effect can be induced where solubility of other solutes, such as some proteins, can increase with addition of charged species.[115] Additionally, other factors may play larger roles in dictating the solubility of solutes even with salts present. A common example of these effects is the pH-dependent solubility of many biological molecules in buffered solutions.

The salting out effect is hypothesized to be the result of the increased order of local water-structure in the presence of ions. A single water molecule can participate in up to four hydrogen bonds, providing a structured solvent matrix.[116] Solutes, particularly those which are considered nonpolar and/or hydrophobic, are not readily solvated as such a solvated state is not as energetically favourable as the original water matrix.[112] These

solutes then tend to aggregate to minimize disruption to the water matrix resulting in an observed "hydrophobic effect".[115] Upon solvation of charged species, which increases the ionic strength, the solvating water molecules can often adopt an even more organized structure. Although these ordering effects are generally in the local structure it is thought that long-range bulk effects cause the solvation of nonpolar substrates to become even less favourable.[114] At higher salt concentrations, the aggregation of a nonpolar substrate continues until it ultimately precipitates or creams out of the aqueous solution. Salts which induce an increase in the ordered water structure and cause salting out of a substrate are known as kosmotropes while salts that decrease water structure and induce a salting in effect on a substrate are known as chaotropes.[117]

Purely from the definition of ionic strength, the salting out efficiency of a salt is dictated by the valency of its dissociated ions. As ionic strength is proportional to the square of the charge number of an ion (Eqn. 1.23), a divalent ion provides a greater ionic strength than an equimolal concentration of a monovalent ion. A resulting salting out effect should be more prevalent for the divalent species; however this is not always the case. Many factors can contribute to the varied salting out ability of ions of different valency as well as those with the same valency. Such factors can include: substrate solubility, ion size, and ion-substrate interactions.[118] A number of empirically determined series have been determined for the salting out efficiency and have found particular relevance in biochemistry for mechanistic study and protein purification.[115] The first and most well-recognized series is the Hofmeister series which ranked the efficiency of egg

white protein precipitation by various ions.[119] Studies towards elucidating the source of these effects have been of great interest for many years and recently have called the salting out by hydrophobic effect hypothesis into question, instead referring to local interfacial effects giving rise to the ordered series.[120] The propensity of various substrates to be salted out by a common salt has also been empirically determined. The Setschenow equation (Eqn. 1.26)[121] relates a non-electrolyte substrate's solubility, S, to the concentration of a specific salt, c_{salt}, via an empirical constant, K_{salt}. The Setschenow constant has been previously correlated to molar volume of a solute[122] and more recently and correctly to the octanol-water partition coefficient of a solute.[123] Although there is still much future discussion and study to completely elucidate the nature of ionic strength and the resulting salting out effects, salt addition has been thoroughly demonstrated as a means to precipitate solids or cream out liquids from aqueous solutions.

$$\log \frac{S}{S_0} = -K_{salt} c_{salt} \qquad \textbf{(1.26)}$$

Dispersions are also known to be affected by variations in ionic strength. Emulsions stabilized by surfactants can be destabilized via the addition of salts. An interplay of micellization and salting out occurs upon salt addition to organic-water emulsions.[114] At low salt concentrations, the critical micelle concentration of surfactants are often lowered by the addition of salt, thus assisting in the persistence of an emulsion. However at higher salt concentrations, the surfactant can be salted out from the aqueous

into the organic layer thereby causing the micelles to break up and destabilize the emulsion.

Coagulation of particles can be induced in suspensions via increases in ionic strength. Colloidal suspensions are stabilized electrostatically by the repulsive forces of their like-charged neighbours. Particles hold a net charge due to their own composition or by ionic materials residing along the surface of the particle, such as surfactants. Suspended particles are surrounded by structured water molecules which create a diffuse electrical double layer around the particle disallowing coagulation due to repulsion.[124] Increases in ionic strength collapse this double layer and allow the particles to come together into loose flocs.

The use of salts to induce changes in ionic strength is ubiquitous in industrial processes. Industrial practices that frequently use manipulations of ionic strength for processing and that are relevant to the research that will be discussed in this dissertation include: dehydration of organics,[125] salting out for liquid-liquid extraction[126] or solid precipitation,[127] flocculation of particulates in wastewater treatment[128] and strip mining,[129] destabilization of organic/aqueous emulsions,[130] and coagulation of polymer latexes.[131]

1.5 Separation of Chiral Compounds

1.5.1 Methods of Obtaining Enantio-enriched Compounds

The generation of highly enantiopure compounds is of great relevance to the fine chemical and pharmaceutical industries.[132] In 2005 the sale of single-enantiomer drugs accounted for over 35% of total pharmaceutical sales with market share expected to increase.[133] The means to obtain enantio-enriched compounds can be broadly segmented into two categories, enantioselective synthesis and chiral resolution. As the need for enantio-enriched and even enantiopure compounds increases, a growing number of synthetic methodologies and resolution techniques are emerging.

Enantioselective synthesis by asymmetric catalysis offers an elegant and efficient means of generating a wide variety of chiral materials using a variety of synthetic methodologies.[134] Although these synthetic strategies are becoming a popular means of generating single enantiomer species in industry,[135] a great deal of ligand, catalyst, and substrate engineering may be required to generate the desired final product. Biocatalysis provides a supplementary means to achieve enantio-enriched products upon proper selection or engineering of an enzyme.[135]

Apart from chiral catalysis, enantioselective synthesis can be achieved from the derivatization of man-made or naturally occurring chiral materials from the chiral pool. Of course the chiral pool is only relevant if an available framework is appropriate for the desired target.[132] Compounds such as sugars and amino acids can be easily obtained as enantiopure materials and later functionalized while maintaining enantiopurity.

Alternatively, chiral auxiliaries, which often are obtained from the chiral pool, can be grafted onto molecules in a similar fashion to protecting groups. The transfer of chirality from the auxiliary to the entire molecule allows enantioselective reactions to take place upon the substrate. Upon completion of the transformation, the auxiliary is then removed to yield the final product.[136]

Resolution techniques where enantiomers are separated from one another by physical or chemical means provide an alternative to stereoselective synthesis. Unfortunately, due to the nature of racemic mixtures, yields of a desired enantiomer can never exceed 50% in a single classical resolution. However, systems where fast racemization between enantiomers occurs or where multiple racemization-resolution steps are undertaken can afford yields greater than 50%.

Gas and liquid chromatographic methods which exploit the temporary formation of diastereomers between the enantiomers and an enantiopure mobile or solid phase often allow for the separate elution of enantiomers from racemic mixture.[137] Generally though, chromatography is not an efficient resolution technique on an industrial scale.

Enrichment of starting materials for later stereoselective synthesis or for the removal of an undesired enantiomer from a final product can also often be achieved by kinetic resolution. This resolution technique exploits the different rate of reaction between each enantiomer of a racemate and an enantiopure chiral compound. As the reaction pathways to the formed diastereomers are not equivalent, varied rates of formation often exist. In such systems, a selectivity factor, SF, is defined as the ratio of

the rates of the reaction of two enantiomers with the enantiopure compound. The selectivity factor can also be related to conversion, C, and enantiomeric excess, ee of the resolution reaction (Eqn. 1.27).[138]

$$SF = \frac{k_R}{k_S} = \frac{\ln [(1 - C)(1 - ee)]}{\ln [(1 - C)(1 + ee)]} \quad \textbf{(1.27)}$$

It is generally accepted that for a reasonable separation and therefore yield of a desired enantiomer, the selectivity factor must be greater than twenty. When such variance in kinetic diastereomer formation does not exist and chromatography is not possible, other resolution techniques, such as crystallization, must be employed.

1.5.2 Chiral Resolution by Crystallization

The generation of enantio-enriched compounds has been performed by classical resolution, or crystallization, for over a century and is by far the oldest resolution technique.[139] Due to the often required "trial and error" practice in crystallizations, the practice is considered by industry as a less elegant method to obtain chiral materials than stereoselective synthesis. Nonetheless, it is still the most widely used set of techniques for obtaining chiral molecules in the pharmaceutical industry due to high reproducibility when a working system is eventually developed and streamlined.[139]

Resolution via crystallization occurs via two methods, direct and diastereomeric. A racemic compound may crystallize as it exists in solution as a racemic mixture of **R** and **S** isomers or as a racemic conglomerate where **R** and **S** enantiomers each crystallize in their own solid phase made up of one enantiomer. In the latter case, which represents approximately 10% of racemic compounds, the enantiomers may be physically separated by a direct crystallization step. Such a practice was performed by Pasteur in the original resolution of sodium ammonium tartrate.[140] When a racemic compound crystallizes as a racemic mixture, diastereomeric separation must be employed. To achieve a separation, each enantiomer is reacted with an enantiopure chiral resolving agent, often taken from the chiral pool, to form a set of diastereomers. These diastereomers, often a set of salt pairs, differ in physical properties such as solubility. Exploiting the differing physical properties of each diastereomer, one diastereomer is preferentially precipitated away from the other. The later removal of the chiral resolving agent then affords a single enantiomer. Unfortunately, this method typically generates large amounts of waste so industrial recycling programs of unwanted enantiomers and chiral resolving agents, such as the Resolution-Recycle-Racemization (RRR) synthetic strategy developed for Duloxetine at Eli Lilly, are employed.[141]

1.6 Research Objectives

The focus of this dissertation is twofold. The first being development and application of switchable water, a CO_2-switchable ionic strength aqueous solvent, and the second being efforts towards the development of switchable chiral resolving agents, a set of chiral CO_2-switchable compounds for the resolution of alcohol racemates by diastereomeric crystallization. Chapter 2 concerns the initial development of the switchable water solvent system. Chapter 3 is focused upon the development of additional generations of switchable water additives. Chapters 4 and 5 describe several industrial applications of switchable water which include homogeneous catalyst recycling as well as reversible destabilizations of suspensions. Chapter 6 outlines efforts made towards the development of CO_2-switchable chiral resolving agents.

1.7 References

1) "*Green Chemistry at a Glance*" American Chemical Society Green Chemistry Institute, 2012. http://www.acs.org/gci (accessed 09/2012).

2) P.T. Anastas, J.C. Warner, *Green Chemistry: Theory and Practice*. Oxford University Press: New York, **1998**.

3) P.T. Anastas, J.B. Zimmerman, *Environ. Sci. Technol*. **2003**, *37*, 94A-101A.

4) *Green Chemistry Metrics: Measuring and Monitoring Sustainable Processes*. A. Lapkin, D.J.C. Constable, Eds. John Wiley & Sons: New York, **2008**.

5) B.M. Trost, *Science* **1991**, *254*, 1471-1477.

6) *1,3-Dipolar Cycloaddition Chemistry*. A. Padwa, Ed. John Wiley & Sons: New York, **1984.**

7) R.A. Sheldon, *CHEMTECH* **1994**, *24*, 38-47.

8) S.M. Mercer, J. Andraos, P.G. Jessop, *J. Chem. Educ*. **2012**, *89*, 215-220.

9) M.D. Tabone, J.J. Cregg, EJ. Beckman, A.E. Landis, *Environ. Sci. Technol*. **2010**, *44*, 8264-8269.

10) *Handbook on Life Cycle Assessment*, J.B. Guinée, Ed. Kluwer Academic Publishers: Dordrecht, **2002**.

11) M.C. Cann, M.E. Connelly, *Real-World Cases in Green Chemistry* American Chemical Society: Washington D.C., **2000**.

12) R. Pierantozzi, *Carbon Dioxide*, In Kirk-Othmer Encyclopedia of Chemical Technology, John Wiley & Sons: New York, **2003**.

13) G.L. Miessler, D.A. Tarr, *Inorganic Chemistry* 3rd ed. Pearson Scientific: Upper Saddle River, **2004**.

14) J.B. Mann, T.L. Meek, L.C. Allen, *J. Am. Chem. Soc*. **2000**, *122*, 2780-2783.

15) P.H. Raven, G.B. Johnson, J.B. Losos, S R.Inger, *Biology* 7th ed. McGraw Hill: Boston, **2005**.

16) *Chemical Synthesis Using Supercritical Fluids*, P. G. Jessop, W. Leitner, Eds., VCH-Wiley: Weinheim, **1999**.

17) P.G. Jessop, B. Subramaniam, *Chem. Rev.* **2007**, *107*, 2666-2694.

18) J.A. Hyatt, *J. Org. Chem*. **1984**, *49*, 5097-5101.

19) A.S. Lindsey, H. Jeskey, *Chem. Rev*. **1957**, *57*, 583-620.

20) L.N. Mander, J.R. Andreatta, D.J. Darensbourg, *Carbon Dioxide* In Encyclopedia of Reagents for Organic Synthesis John Wiley & Sons: New York, **2008**.

21) B.J. Flowers, R. Gautreau-Service, P.G. Jessop, *Adv. Synth. Catal*. **2008**, *350*, 2947-2958.

22) W. McGhee, D. Riley, *J. Org. Chem*. **1995**, *60*, 6205-6207.

23) M.M. Green, H.A. Wittcoff, *Organic Chemistry Principles and Industrial Practice*, Wiley-VCH: Weinheim, **2003**.

24) D.J. Darensbourg, *Chem. Rev*. **2007**, *107*, 2388-2410.

25) L. Phan, J.R. Andreatta, L.K. Horvey, C.R. Edie, A-L. Luco, A. Mirchandani, D.J. Darensbourg, P.G. Jessop, *J. Org. Chem*. **2008**, *73*, 127-132.

26) G.T. Rochelle, *Science* **2009**, *325*, 1652-1654.

27) I. Omae, *Catal. Today* **2006**, *115*, 33-52.

28) R. Chang, *Physical Chemistry for the Biosciences*, University Science Books: Herndon, **2005**.

29) T. Loerting, J. Bernard, *ChemPhysChem* **2010**, *11*, 2305-2309.

30) S. Grund, M. Bauer, D. Fischer, *Adv. Eng. Mater.* **2011**, *13*, B61-B87.

31) C.T. Vogelson, *Mod. Drug Discovery* **2001**, *4*, 49-52.

32) A.M. Ross, H. Nandivada, J. Lahann, in *Handbook of Stimuli-Responsive Materials*, M.W. Urban, Ed., Wiley-VCH: Weinheim, **2011**.

33) X. Liu, N.L. Abbott, *J. Colloid Interface Sci*. **2009**, *339*, 1-18.

34) T. Saji, K. Hoshino, S. Aoyagui, *J. Am. Chem. Soc*. **1985**, *107*, 6865-6868.

35) P. Anton, P. Koeberle, A. Laschewsky, *Prog. Colloid Polym. Sci*. **1992**, *89*, 56-59.

36) N. Aydogan, N.L. Abbott, *Langmuir* **2001**, *17*, 5703-5706.

37) S.S. Datwani, V.N. Truskett, C.A. Rosslee, N.L. Abbott, K.J. Stebe, *Langmuir* **2003**, *19*, 8292-8301.

38) K. Tsuchiya, Y. Orihara, Y. Kondo, N. Yoshino, T. Ohkubo, H. Sakai, M. Abe, *J. Am. Chem. Soc*. **2004**, *126*, 12282-12283.

39) M.M. Schmittel, M. Lal, K. Graf, G. Jeschke, I. Suske, J. Salbeck, *Chem. Commun*. **2005**, 5650-5652.

40) Z. Cheng, B. Ren, M. Gao, X. Liu, Z. Tong, *Macromolecules* **2007**, *40*, 7638-7643.

41) S. Ghosh, K. Irvin, S. Thayumanavan, *Langmuir* **2007**, *23*,7916-7919.

42) C.B. Minkenberg, L. Florusse, R. Eelkema, G.J.M. Koper, J.H. v. Esch, *J. Am. Chem. Soc*. **2009**, *131*, 11274-11275.

43) A.S. Malcolm, A.F. Dexter, A.P.J. Middelberg, *Soft Matter* **2006**, *2*, 1057- 1066.

44) H. Sakai, M. Abe, In *Mixed Surfactant Systems* 2nd Ed., M. Abe, J. F. Scamehorn, Eds., Marcel Dekker: New York, **2005**.

45) P. Mirarefi, C.T. Lee Jr., *Biochim. Biophys. Acta, Proteins Proteomics* **2010**, *1804*, 106-114.

46) H. Sakai, A. Matsumura, S. Yokoyama, T. Saji, M. Abe, *J. Phys. Chem. B* **1999**, *103*, 10737-10740.

47) P.G. Jessop, S.M. Mercer, D.J. Heldebrant, *Energy Environ. Sci*. **2012**, *5*, 7240-7253.

48) P.G. Jessop, D.J. Heldebrant, L. Xiaowang, C.A. Eckert, C.L. Liotta, *Nature* **2005**, *436*, 1102.

49) L. Phan, X. Li, D.J. Heldebrant, R. Wang, D. Chiu, E. John, H. Huttenhower, P. Pollet, C.A. Eckert, C.L. Liotta, P.G. Jessop, *Ind. Eng. Chem. Res*. **2008**, *47*, 539-545.

50) I. Anugwom, Päivi Mäki-Arvela, P. Virtanen, P. Damlin, R. Sjöholm, J-P. Mikkola, *RSC Adv*. **2011**, *1*, 452-457.

51) C. Wang, H. Luo, D.-E. Jiang, H. Li, S. Dai, *Angew. Chem., Int. Ed*. **2010**, *49*, 5978-5981.

52) T. Yamada, P.J. Lukac, M. George, R.G. Weiss, *Chem. Mater*. **2007**, *19*, 967-969.

53) T. Yamada, P.J. Lukac, T. Yu, R.G. Weiss, *Chem. Mater*. **2007**, *19*, 4761-4768.

54) T. Yu, T. Yamada, G.C. Gaviola, R.G. Weiss, *Chem. Mater.* **2008**, *20*, 5337-5344.

55) L. Phan, J.R. Andreatta, L.K. Horvey, C.F. Edie, A.-L. Luco, A. Mirchandi, D.J. Darensbourg, P. G. Jessop, *J. Org. Chem.* **2008**, *73*, 127-132.

56) D.J. Heldebrant, P.K. Koech, T. Ang, C. Liang, J.E. Rainbolt, C.R. Yonker, P.G. Jessop, *Green Chem.* **2010**, *12*, 713-721.

57) P.G. Jessop, L. Phan, A. Carrier, S. Robinson, C.J. Dürr, J.R. Harjani, *Green Chem*. **2010**, *12*, 809-814.

58) A.R. Boyd, P. Champagne, P.J. McGinn, K.M. MacDougall, J.E. Melanson, P.G. Jessop, *Bioresour. Technol*. **2012**, *111*, 628-632.

59) A. Holland, D. Wechsler, A. Patel, B.M. Molloy, A.R. Boyd, P.G. Jessop, Can. *J. Chem*. **2012**, *90*, 805-810.

60) P.G. Jessop, L. Kozycz, Z.G. Rahami, D. Schoenmakers, A.R. Boyd, D. Wechsler, A.M. Holland, *Green Chem*. **2011**, *13*, 619-623.

61) Y. Kohno, H. Arai, H. Ohno, *Chem. Commun*. **2011**, *47*, 4772-4774.

62) Y. Liu, P.G. Jessop, M. Cunningham, C.A. Eckert, C.L. Liotta, *Science* **2006**, *313*, 958-960.

63) L. Wang, W. Qiao, C. Cao, Z. Li, *Colloids Surf., A* **2008**, *320*, 271-274.

64) Y. Qin, H. Yang, J. Ji, S. Yao, Y. Kong, Y. Wang, *Tenside Surf. Det*. **2009**, *46*, 294-296.

65) L.M. Scott, T. Robert, J.R. Jarjani, P.G. Jessop, *RSC Adv*. **2012**, *2*, 4925-4931.

66) C. Liang, J.R. Harjani, T. Robert, E. Rogel, D.Kuehne, C. Ovalles, V. Sampath, P.G. Jessop, *Energy Fuels* **2012**, *26*, 488-494.

67) J.R. Harjani, C. Liang, P.G. Jessop, *J. Org. Chem*. **2011**, *76*, 1683-1691.

68) E.R. Moore, N.A. Lefevre, U.S. Patent, 4,623,678, **1986**.

69) E. Ceschia, J.R. Harjani, C. Liang, Z. Ghoshouni, T. Andrea, R.S Brown, P.G. Jessop, *Environ. Sci. Technol.* **2012**, *Submitted*.

70) Z. Guo, Y. Feng, Y. Wang, J. Wang, Y. Wu, Y. Zhang, *Chem. Commun*. **2011**, *47*, 9348-9350.

71) K. Zhou, J. Li, Y. Lu, G. Zhang, Z. Xie, C. Wu, *Macromolecules* **2009**, *42*, 7146-7154.

72) D. Han, X. Tong, O. Boissière Y. Zhao, *ACS Macro Lett*. **2012**, *1*, 57-61.

73) M. George, R.G. Weiss, *J. Am. Chem. Soc*. **2001**, *123*, 10393-10394.

74) M. George, R.G. Weiss, *Langmuir* **2003**, *19*, 1017-1025.

75) H. Xu, E.M. Hampe, D.M. Rudkevich, *Chem. Commun.* **2003**, 2828-2829.

76) H. Xu, D.M. Rudkevich, *Chem. Eur. J.* **2004**, *10*, 5432-5442.

77) V. Stastny, D.M. Rudkevich, *J. Am. Chem. Soc*. **2007**, *129*, 1018-1019.

78) H. Zhang, D.M. Rudkevich, *Chem. Commun*. **2007**, 4893-4894.

79) T. Yu, K. Wakuda, D.L. Blair, R.G. Weiss, *J. Phys. Chem. C* **2009**, *113*, 11546-11553.

80) A. Suzuki, Y. Maki, H. Takeno, D. Nagai, *Chem. Commun*. **2011**, *47*, 8856-8858.

81) C.I. Fowler, C. Muchemu, R.E. Miller, L. Phan, C. O'Neill, M.F. Cunningham, P.G. Jessop, *Macromolecules* **2011**, *44*, 2501-2509.

82) C.I. Fowler, P.G. Jessop, M.F. Cunningham, *Macromolecules* **2012**, *45*, 2955-2962.

83) Q. Zhang, G. Yu, W-J. Wang, B-G. Li, S. Zhu, *Macromol. Rapid Commun*. **2012**, *33*, 916-921.

84) Q. Zhang, G. Yu, W-J. Wang, H. Yuan, B-G. Li, S. Zhu, *Langmuir* **2012**, *28*, 5940-5946.

85) Q. Zhang, W.-J. Wang, Y. Lu, B.-G. Li and S. Zhu, *Macromolecules* **2011**, *44*, 6539-6545.

86) M. Mihara, P. Jessop, M. Cunningham, *Macromolecules* **2011**, *44*, 3688-3693.

87) X. Su, P.G. Jessop, M.F. Cunningham, *Macromolecules* **2012**, *45*, 666-670.

88) J. Pinaud, E. Kowal, M. Cunningham, P. Jessop, *ACS Macro Lett*. **2012**, *1*, 1103-1107.

89) Y. Ding, S. Chen, H. Xu, Z. Wang, X. Zhang, T. H. Ngo, M. Smet, *Langmuir* **2010**, *26*, 16667-16671.

90) L. Hartmann, M. Bedard, H.G. Börner, H. Möhwald, G.B. Sukhorukov, M. Antonietti, *Soft Matter* **2008**, *4*, 534-539.

91) Q. Yan, R. Zhou, C. Fu, H. Zhang, Y. Yin, J. Yuan, *Angew. Chem. Int. Ed*. **2011**, *50*, 4923-4927.

92) L. Phan, P. G. Jessop, *Green Chem*. **2009**, *11*, 307-308.

93) A. Andreetta, G. Barberis, G. Gregorio, *Chim. Ind*. **1978**, *60*, 887-891.

94) A. Buhling, P.C.J. Kamer, P.W.N.M. van Leeuwen, J.W. Elgersma, K. Goubitz, J. Fraanje, *Organometallics* **1997**, *16*, 3027-3037.

95) A. Buhling, P.C.J. Kamer, P.W.N.M. van Leeuwen, J.W. Elgersma, *J. Mol. Catal. A: Chem*. **1997**, *116*, 297-308.

96) S.L. Desset, D.J. Cole-Hamilton, *Angew. Chem. Int. Ed*. **2009**, *48*, 1472-1474.

97) M. Mokhadinyana, S.L. Desset, D.B.G. Williams, D.J. Cole-Hamilton, *Angew. Chem. Int. Ed*. **2012**, *51*, 1648-1652.

98) P. Herman, Z. Murtaza, J.R. Lakowicz, *Anal. Biochem*. **1999**, *272*, 87-93.

99) E.M. Hampe, D.M. Rudkevich, *Chem. Commun*. **2002**, 1450-1451.

100) E.M. Hampe, D.M. Rudkevich, *Tetrahedron* **2003**, *59*, 9619-9625.

101) Y. Liu, Y. Tang, N.N. Barashkov, I.S. Irgibaeva, J.W.Y. Lam, R. Hu, D. Birimzhanova, Y. Yu, B.Z. Tang, *J. Am. Chem. Soc*. **2010**, *132*, 13951-13953.

102) S. Pandey, S.N. Baker, D. Pandey, G.A. Baker, *Chem. Commun*. **2012**, *48*, 7043-7045.

103) L. Chen, D. Huang, S. Ren, Y. Chi, G. Chen, *Anal. Chem*. **2011**, *83*, 6852-6867.

104) T.A. Darwish, R.A. Evans, M. James, N. Malic, G. Triani, T. L. Hanley, *J. Am. Chem. Soc.* **2010**, *132*, 10748-10755.

105) R.A. Evans, M. James, T. L. Hanley, T.A. Dariwsh, *Chem. Eur. J*. **2011**, *17*, 11399-11404.

106) F. Ilgen, B. König, *Z. Naturforsch., Teil B* **2009**, *64*, 1053-1056.

107) T. Engel, P. Reid, *Thermodynamics, Statistical Thermodynamics, and Kinetics*, Pearson Scientific: San Francisco, **2006**.

108) P. Debye, E. Hückel, *Physik. Z.* **1923**, *24*, 185-206.

109) I.N. Levine, *Physical Chemistry* 5th Ed. McGraw Hill: Boston, **2002**.

110) C.W. Davies, *Ion Association*, Butterworths: Washington DC, **1962**.

111) L.A. Bromley, *AIChE J*. **1979**, *19*, 313-320.

112) E.A. Guggenheim, J.C. Turgeon, *Trans. Faraday Soc*. **1955**, *51*, 747-761.

113) K.S. Pitzer, J.J. Kim, *J. Am. Chem. Soc*. **1974**, *96*, 5701-5707.

114) J.A. Beunen, E. Ruckenstein, *Adv. Colloid Interface Sci*. **1982**, *16*, 201-231.

115) T. Creighton, *Proteins: Structure and Molecular Properties*, 2nd Ed., W.H. Freeman: New York, **1984**,

116) A. Ben-Naim, *Molecular Theory of Water and Aqueous Solutions*, World Scientific: Singapore, **2009**.

117) Y. Zhang, P.S. Cremer, *Curr. Opin. Chem. Biol*. **2006**, *10*, 658-663.

118) J. Lyklema, *Chem. Phys. Lett*. **2009**, *467*, 217-222.

119) F. Hofmeister, *Arch. Exp. Pathol. Pharmacol*. **1888**, *24*, 247-260.

120) C.L.D. Gibb, B.C. Gibb, *J. Am. Chem . Soc*. **2011**, *133*, 7344-7347.

121) J.Z. Setschenow *Z. Physik. Chem*. **1889**, *4*, 117-125.

122) W-H. Xie, W-Y Shiu, D. Mackay, *Marine. Environ. Res*. **1997**, *44*, 429-444.

123) N. Ni, S.H. Yalkowsky, *Int. J. Pharm*. **2003**, *254*, 167-172.

124) D. Myers, *Surfaces, Interfaces, and Colloids: Principles and Applications*, 2nd Ed. John Wiley and Sons: Toronto, **1999**.

125) H.P. Meissner, C.A. Stokes, *Ind. Eng. Chem*. **1944**, *36*, 816-820.

126) M. Tabata, M. Kumamoto, J. Nishimoto, *Anal. Sci*. **1994**, *10*, 383-388.

127) S.D. Barnicki, C.A. Hoyme, J.J. Siirola, *Separation Process Synthesis* in Kirk-Othmer Encyclopedia of Chemical Technology, John Wiley & Sons: New York, **2006**.

128) J.M. Montgomery, *Water Treatment Principles and Design*, John Wiley & Sons: New York, **1985**.

129) R.J. Mikula, R. Zrobok, O. Omotoso, *J. Can. Pet. Technol*. **2004**, *43*, 48-52.

130) T.M. Schmitt, *Analysis of Surfactants* 2nd ed. Marcel Dekker, Inc.: New York, **2001**.

131) R.M. Fitch, *Polymer Colloids*, Academic Press: San Diego, **1997**.

132) J. Crosby, *Introduction* In Chirality in Industry: The Commercial Manufacture and Applications of Optically Active Compounds, A.N. Collins, G.N. Sheldrake, J. Crosby, Eds., John Wiley & Sons, New York, **1992**.

133) S. Erb, Pharmaceutical Technology, 10/03/2006 http://www.pharmtech.com/pharmtech/Active+ingredients/Single-Enantiomer-Drugs-Poised-for-Further-Market-/ArticleStandard/Article/detail/385859 (accessed 10/2012).

134) V. Caprio, J.M.J. Williams, *Catalysis in Asymmetric Synthesis*, John Wiley & Sons: New York, **2009**.

135) *Asymmetric Catalysis on Industrial Scale: Challenges, Approaches, and Solutions*, H.U. Blaser, H-J. Federsel, Eds., John Wiley and Sons: New York, **2011**.

136) Y. Gnas, F. Glorius, *Synthesis* **2006**, *12*, 1899-1930.

137) V.A. Davankov, *Pure Appl. Chem*. **1997**, *69*, 1469-1474.

138) H.B. Kagan, J.C. Fiaud, In *Topics in Steroechemistry* Vol. 18, E.L. Eliel, S.H. Wilen, Eds., John Wiley & Sons: New York, **1988**.

139) A. Bruggink, *Rational Design in Resolutions,* In Chirality in Industry II: Developments in the Manufacture and Applications of Optically Active Compounds, A.N. Collins, G.N. Sheldrake, J. Crosby, Eds., John Wiley & Sons: New York, **1997**.

140) W.M.L. Wood, *Crystal Science Techniques in the Manufacture of Chiral Compounds,* In Chirality in Industry II: Developments in the Manufacture and Applications of Optically Active Compounds, A.N. Collins, G.N. Sheldrake, J. Crosby, Eds., John Wiley & Sons: New York, **1997**.

141) Y. Fujima, M. Ikunaka, T. Inoue, J. Matsumoto, *Org. Process Res. Dev*. **2006**, *10*, 905-913.

Chapter 2

The Development of Switchable Water

2.1 Introduction

Water is undoubtedly the most commonly used solvent in industry. Unfortunately, the processes used to separate solutes from water, such as distillation, membrane filtration, and pervaporation, are often expensive in terms of energy, materials, and time. A particularly resource-demanding method of separating organic solutes from water is "salting out" which involves adding an electrolyte, such as NaCl, to increase the ionic strength of an aqueous solution until previously dissolved organic solutes are no longer soluble in the increasingly polar aqueous environment. Although the method is quite effective, the addition of salt to water is not readily reversible, so that the water cannot be recycled or discarded without treatment. Often then one or more of the separation methods listed above must be used to treat the salty water, further contributing to the environmental impact of many aqueous-based industrial processes.

It was hypothesized that an additive could be designed to dissolve in water and allow reversible switchable changes in ionic strength (Fig. 2.1). Such an additive could allow for drastic reductions in energy and materials required to separate organic solutes from water and encourage solvent recycling. Optimally, a switch from low to high ionic strength could be performed reversibly with the introduction or removal of a trigger, CO_2 without the need for traditional inorganic salts, such as NaCl. Such an additive could greatly increase the versatility and attractiveness of water as an industrial solvent.

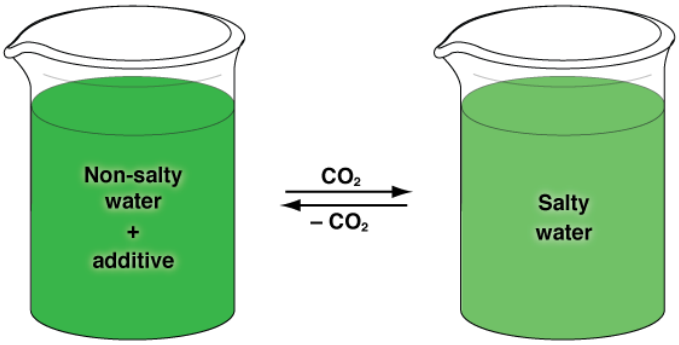

Fig. 2.1. Conceptual scheme of switchable ionic strength water. The reversible change of the additive into a salt would raise and lower the ionic strength of the water via the introduction or removal of CO_2.

The original concept of this solvent system involved the reversible reaction of a nitrogenous base additive dissolved in water with CO_2. Previous work in the Jessop group, along with collaborators, has previously demonstrated many applications for the reaction of nitrogenous bases with CO_2 to generate ionic species in solution. Such work has previously led to the development of switchable solvents, surfactants, and solutes.[1]

It was proposed that an aqueous solution of an organic, uncharged nitrogenous base additive would have low ionic strength if pure (ultimately non-zero due to the weak base dissociation in water). Upon the introduction of CO_2, carbonic acid would form and protonate the dissolved nitrogenous base additive, resulting in the formation of charged species (hydrogen carbonate (bicarbonate) salts). The removal of CO_2, by heating and

sparging with N_2, Ar or air, would reverse the reaction and return the aqueous system to a low ionic strength. Thus, the combination of a nitrogenous base solute in water and the use of CO_2 as a trigger would, theoretically, make an aqueous solution of switchable ionic strength. This reversible change in ionic strength could then be used to expel or "salt out" organic liquids or solids from an aqueous solution (Fig. 2.2).

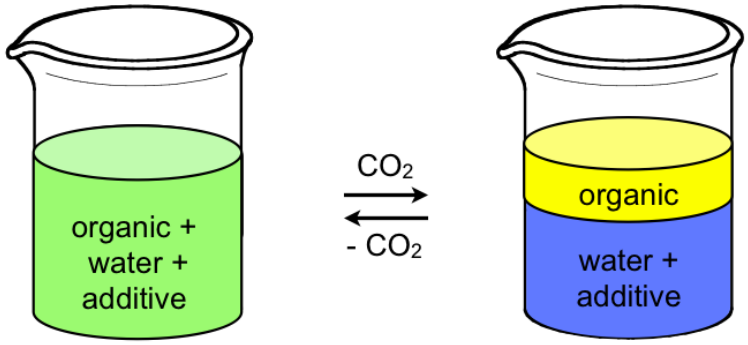

Fig. 2.2. Conceptual scheme of switchable water being used to reversibly salt out a water-miscible organic compound(s).

As the chemistry of CO_2 and nitrogenous bases, particularly amines, in water is well studied in the CO_2 capture literature,[2] this large body of research provided the inspiration to incorporate this reactivity in a switchable aqueous solvent. CO_2-capture by aqueous amine solutions has been envisioned since the early 1930s for industrial flue gas treatment, but only within the past 20-30 years has become an area of popular research and industrial use.[2] Recent advances in CO_2-capture agents and solvent technology have

allowed for greater CO_2 solubility in amine/aqueous solvents, greater absorption capacity, and easier CO_2 stripping (for later processing or sequestration). These and other advances have allowed the cost per ton of CO_2 captured to decrease over 30 % between 2001 and 2006 making the process much more economically viable.[2]

Typical amines used in CO_2-capture such as monoethanolamine, MEA, suggested that alkanolamines would be a suitable set of candidates for an aqueous switchable solvent due to their small size, high water solubility, and appropriate reactivity and basicity. Primary and secondary amines are preferentially used as CO_2-capture agents over tertiary amines due to their greater CO_2 absorption performance.[3] Tertiary amines however are generally much easier substrates to remove CO_2 from during recycling.[3] As efficient reversibility of the switchable solvent was a central goal of this research, it seemed that tertiary amine analogues of amines that have been found to be very effective for CO_2 capture would provide a good starting point for the present study.

These results have previously appeared in *ChemSusChem* **2010**, *3*, 467-470. The structure of the original manuscript has been modified and additional information has been added in several places to better reflect the progression of the study.

2.2 Results and Discussion

2.2.1 Confirmation of Additive Reversibility

A series of tertiary amines when dissolved in water and reacted with CO_2 generated aqueous solutions of significantly greater ionic strength than pure water through the formation of ammonium hydrogen carbonates (bicarbonates). This increased ionic strength was easily reduced by removing CO_2 through moderate heating and sparging with N_2 or air, thereby affording a switchable aqueous solvent (Eqn. 2.1).

$$NR_3 + H_2O + CO_2 \rightleftharpoons [NR_3H]^+ + [HCO_3]^- \quad \textbf{(2.1)}$$

Fortunately, the reversibility of this reaction for certain amines has been well established in the literature on CO_2 capture.[4] As stated previously, tertiary amines were ultimately chosen for this study because of their ease of switchability compared to amidines and to secondary and primary amines. Amines have more moderate pK_{aH} (the pK_a of the conjugate acid) values compared to many amidines (which appear in many Jessop-group switchable technologies), so that the reaction with CO_2 is more easily reversed. Compared to primary and secondary amines, tertiary amines lack hydrogen bond-donating ability and, most importantly, they are incapable of forming carbamates upon reaction with CO_2. Work by Mani and co-workers has shown that the removal of carbamate ions in water to give neutral amines by heating and sparging is quite difficult.[4]

Such carbamate formation would therefore decrease the efficiency of reverting a high ionic strength solvent back to a low ionic strength solvent.

The initial screening involved the tertiary amino alcohols *N*,*N*-dimethylethanolamine **2.1**, (DMEA, pK_{aH}=9.35)[5] and *N*-methyldiethanolamine **2.2** (MDEA, pK_{aH}=8.52),[6] the structures of which are shown in Figure 2.3. ^{1}H and ^{13}C NMR spectroscopy showed that these two amino alcohols in water formed the corresponding trialkylammonium bicarbonate salts when CO_2 was slowly bubbled through the aqueous solution for 20 min using a single narrow gauge steel needle.

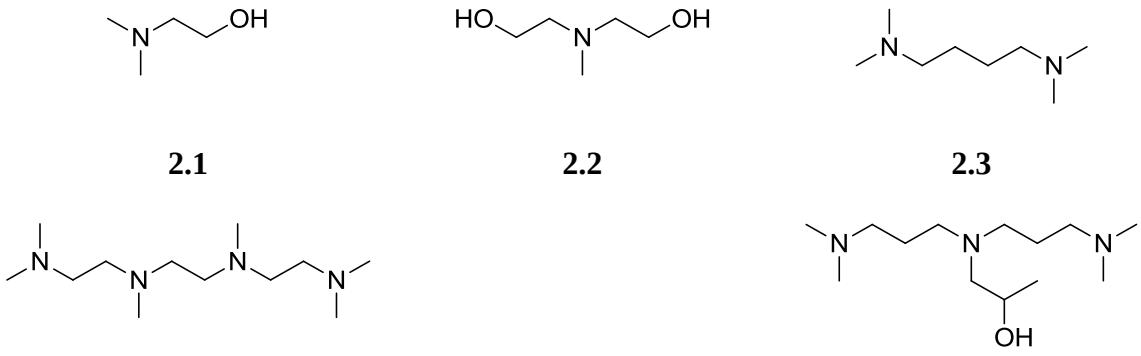

2.1 **2.2** **2.3**

2.4 **2.5**

Fig. 2.3. Molecular structures of the amines tested as switchable water additives.

A $^{13}C\{^{1}H\}$ NMR chemical shift around 160 ppm is comparable to shifts found by Mani and co-workers[7] and suggests that only bicarbonate anion formation was occurring rather than a mixture of bicarbonate and carbonate anions. The corresponding pH values (pH

~6) of the protonated amine solutions also suggested that only bicarbonate anions were present rather than a mixture of bicarbonates and carbonates (see Fig. 1.2). The trialkylammonium bicarbonates reverted back to the original uncharged species when the system was sparged with N_2 or air and gently heated for several hours. For these preliminary experiments, no attempt was made to optimize the rate of switching.

To determine the extent of trialkylammonium bicarbonate formation in the aqueous system, several ^{1}H NMR spectroscopy experiments were conducted. The NMR spectra of the 1:1 salts of these amines with strong acids were determined in order to obtain the chemical shifts of the trialkylammonium cations. Comparing the difference in ^{1}H chemical shifts (δ) between several atoms on the amines when fully protonated or deprotonated, the extent of protonation caused by carbonic acid was calculated using Eqn. 2.2. Tables of % protonation of amines by CO_2 over time and an example calculation and can be found in Appendix I.

$$\%\ Protonation = \left(1 - \frac{\left(\delta_{b,100\%} - \delta_{a,100\%}\right) - \left(\delta_{b,x\%} - \delta_{a,x\%}\right)}{\left(\delta_{b,100\%} - \delta_{a,100\%}\right) - \left(\delta_{b,0\%} - \delta_{a,0\%}\right)}\right) x\ 100 \qquad \textbf{(2.2)}$$

Comparison of the ^{1}H NMR chemical shifts showed that the two amino alcohols, **2.1** and **2.2**, in CO_2-saturated water were completely protonated, within experimental error. Because two ions were generated (trialkylammonium cation and bicarbonate anion), this corresponded to a jump in ionic strength in the aqueous system from approximately zero to a value equal to the molality of the amino alcohol. The removal of CO_2 then triggered

a decrease in the ionic strength as the neutral species are regenerated. By ^{1}H NMR spectroscopy, the conversion of **2.2** back to the neutral form was found to be roughly 96% complete.

Conductivity studies were performed to demonstrate the dramatic change in charge between the low ionic strength solution and the high ionic strength solution. Solutions of the amino alcohols and water (1:1 v/v) showed a large increase in conductivity, starting at ~0.07 mS cm^{-1} and increasing up to 22 mS cm^{-1} for **2.1** and 19 mS cm^{-1} for **2.2,** upon the introduction of CO_2 (Fig. 2.4). In contrast, bubbling CO_2 through only water (starting at 0.06 mS cm^{-1}) raised the conductivity only to 0.6 mS cm^{-1}.

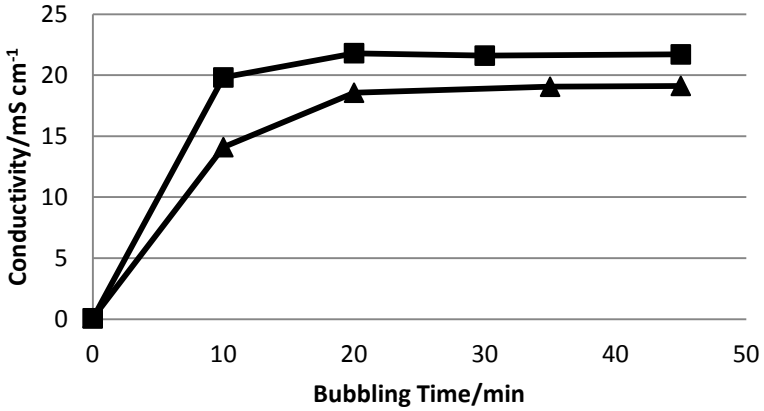

Fig. 2.4. A plot showing the conductivity of ■ (1:1 (v/v) **2.1**/H_2O) and ▲ (1:1 (v/v) **2.2**/H_2O) when reacted with a CO_2 flow of 3-5 mL min^{-1} through a fritted-glass apparatus at 25 °C.

Sparging and heating of the solutions showed the expected decrease in conductivity as the CO_2 was removed, decreasing the conductivity to ~2 mS cm^{-1} for both **2.1** and **2.2** (Fig. 2.5). This represented an approximate 90 % decrease from the maximum conductivity for both systems. The drop in conductivity depended greatly on the amine choice, time and efficiency of bubbling. Although conductivity is not directly related to ionic strength, these studies provide confirmation of charge generation and reduction that reflect increasing and decreasing ionic strength (however for simplicity if one assumed that conductivity and ionic strength were linearly related, than a similar decrease to 90 % of the maximum ionic strength had occurred). Often to expedite these reactions, N_2 was bubbled through the aqueous solutions of the amino alcohols by means of a fritted-glass apparatus (see section 2.4.3) as opposed to a single narrow gauge steel needle. The increased dispersion of N_2 in the solution drastically reduced reaction times by reducing the mass transfer issues which hinder many gas/liquid reactions.

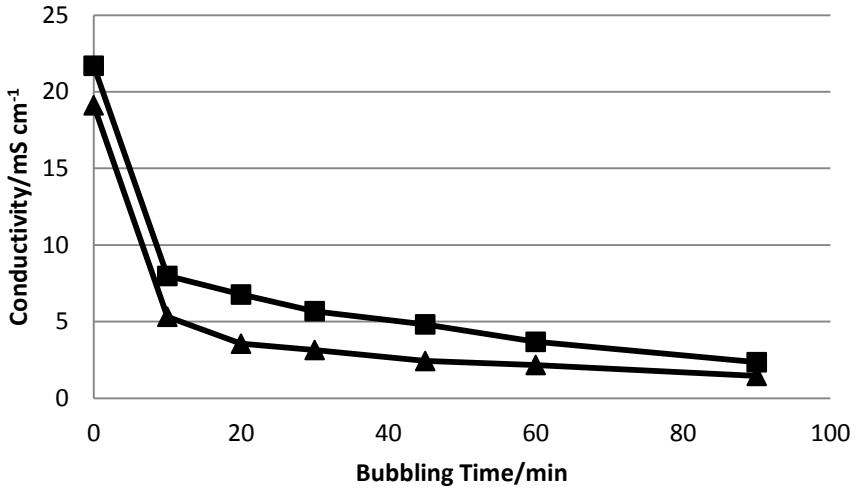

Fig. 2.5. A plot showing the conductivity of ■ (1:1 (v/v) **2.1**/H_2O) and ▲ (1:1 (v/v) **2.2**/H_2O) having already been protonated with CO_2 but then subsequently sparged with a N_2 flow of 3-5 mL min^{-1} through a fritted-glass apparatus at 80 °C.

2.2.2 Polybasic Amines

For the creation of a solution of high ionic strength, it is important that the ions have charges greater than one, where possible, because ionic strength is proportional to the square of the charge number of the ionic species. Whereas the anion in the present system is always bicarbonate, the cation is the only species that can be designed to have a greater charge number. Therefore amine additives with two or more basic sites were studied. If the additive was protonated by carbonic acid at n sites (Eqn. 2.3) and the

molality of the additive is m, then the ionic strength I switched from zero to $\frac{1}{2}m(n^2+n)$ (Eqn. 2.4).

$$B + nH_2O + nCO_2 \rightleftharpoons [BH_n]^{n+} + n[HCO_3]^- \quad \textbf{(2.3)}$$

$$I = \frac{1}{2}m(+n)^2 + \frac{1}{2}mn(-1)^2 = \frac{1}{2}m(n^2+n) \quad \textbf{(2.4)}$$

For example, the ionic strength of a solution of a diprotonated additive would be three times than that obtained with a monoprotonated additive. *N,N,N',N'*-tetramethyl-1,4-diaminobutane **2.3** has the capability for both basic sites to be reversibly protonated by carbonic acid (pK_{aH}=10.30, 8.77)[8] and showed great promise in increasing the efficiency of the switchable ionic strength system. 1,1,4,7,10,10-Hexamethyltriethylenetetramine **2.4** has two amine sites that can be protonated by carbonic acid (pK_{aH} = 9.23, 8.47, 5.36, 1.68).[9] ^{1}H NMR spectroscopy studies (see Appendix I) did show that approximately two out of the four basic sites of **2.4** can be protonated by reaction with CO_2 in D_2O. A triamine, 1-[bis[3-(dimethylamino)]propyl]amino]-2-propanol **2.5**, showed a similar amount of protonation compared to **2.4** with slightly more than two nitrogens being protonated by carbonic acid (Appendix I). These two polyamines possessed amine groups in differing chemical environments and Eqn. 2.2 could not provide a proper representation of the % protonation. In these two cases, the ^{1}H NMR chemical shifts were found for the amines when fractionally protonated by stong acids. The % protonation by

CO_2 was then estimated by comparing the chemical shifts of the fully protonated amines, the fractionally protonated amines, and the amines with CO_2 treatment.

2.2.3 Salting Out Studies

An envisaged practical application of this technology would be the reversible separation of water-miscible organic liquids from water. To this end, the ability of the additives to reversibly separate THF from water was evaluated (Fig. 2.6). An organic soluble dye, Oil Red O (Fig. 2.7), was used to assist in highlighting the separation of THF.

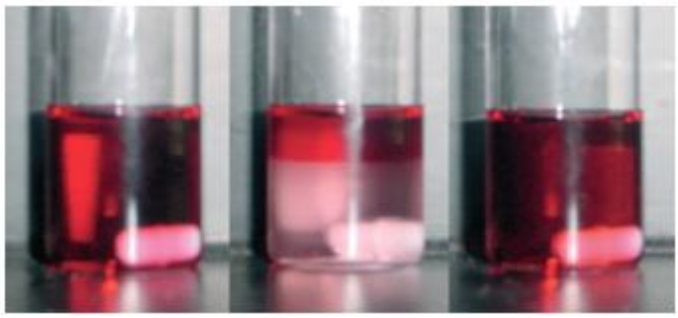

Fig. 2.6. From left to right: a 10:10:1 (w/w) mixture of H_2O/THF/**2.3** and Oil Red O dye shown before CO_2 bubbling, after 30 min of CO_2 bubbling through a single narrow gauge steel needle generating two phases at 25 °C, and finally, the solution after sparging with N_2 for 20 min at 50 °C.

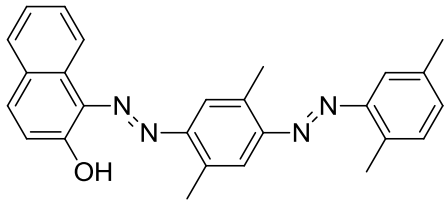

Fig. 2.7. Molecular strtucture of Oil Red O dye.

These studies involved bubbling CO_2 into the liquid through a single narrow gauge steel needle for 30 min. A visible phase separation occurred, resulting in an organic and an aqueous phase. With **2.3** at a 9 wt% loading of base (i.e., 5:5:1 THF/H_2O/amine), 87% of the THF was forced out of the aqueous phase while 99.6% of the additive was retained in the aqueous phase as determined by ^{1}H NMR spectroscopy (Table 2.1, procedure described in section 2.4.2). This is an extremely important characteristic as for the solvent to be recycled and remain functional the amine additive must be retained in the aqueous phase. Even at a 3 wt% loading of **2.3** (15:15:1 THF/H_2O/amine), 74% of the THF was forced out. However, in all of the experiments, the salting out effect could be reversed; the THF phase recombined with the aqueous phase to regenerate a one phase system when the mixture was heated and sparged with N_2 or air to remove CO_2. In many cases, greater additive loadings induced greater salting-out of THF, but lower additive retention. This was likely due to the salting-out of THF occurring prior to the complete protonation of the amine additive in solution leading to partitioning of some of the unprotonated amine into the organic layer. Additionally, polyamines generally had better retention in

the aqueous phase. This was likely because of the greater number of hydrophilic ammonium groups per molecule.

Table 2.1. A comparison of amine additive concentration and the separation of THF from 1:1 (w/w) solutions of THF and H_2O when reacted with CO_2. The subsequent % retention of the amine additive in the aqueous phase after reaction with CO_2 is also presented.

Base	THF/H_2O/Base (w/w/w)	% THF Separated[(a)]	% Additive Retained[(a)]
2.1	1:1:1	76 ± 1.7 %	73.5 ± 2.0 %
2.1	3:3:1	85 ± 2.2 %	93.9 ± 2.1 %
2.1	5:5:1	74 ± 5.6 %	91.7 ± 2.6 %
2.1	10:10:1	75 ± 0.3 %	98.3 ± 0.4 %
2.2	1:1:1	74 ± 3.0 %	90.7 ± 1.7 %
2.2	3:3:1	74 ± 3.8 %	95.7 ± 1.5 %
2.2	5:5:1	72 ± 0.3 %	95.2 ± 1.5 %
2.2	10:10:1	66 ± 3.0 %	96.6 ± 0.6 %
2.3	3:3:1	87 ± 1.3 %	87.1 ± 2.1 %
2.3	5:5:1	87 ± 0.6 %	99.6 ± 0.1 %
2.3	10:10:1	80 ± 0.5 %	99.5 ± 0.1 %
2.3	15:15:1	74 ± 0.9 %	98.4 ± 0.4 %
2.4	3:3:1	80 ± 4.0 %	95.6 ± 1.5 %
2.4	5:5:1	80 ± 3.0 %	98.4 ± 1.2 %
2.4	10:10:1	70 ± 1.3 %	97.7 ± 1.2 %
2.4	15:15:1	65 ± 4.9 %	96.6 ± 1.4 %
2.5	3:3:1	78 ± 6.1 %	87.1 ± 7.3 %
2.5	5:5:1	81 ± 1.0 %	98.4 ± 0.4 %
2.5	10:10:1	69 ± 1.4 %	96.0 ± 0.8 %
2.5	15:15:1	62 ± 1.1 %	94.4 ± 1.1 %

[(a)] Determined by ^{1}H NMR spectroscopy. Experiments were run in triplicate and standard deviations are reported as error.

To further demonstrate the increased efficiency and greater jump in ionic strength of the diprotonated additives versus the monoprotonated additives, a similar THF salting out study was carried out using the same molality for each additive (Table 2.2). Again, compound **2.3** was superior. This result for compound **2.3** was confirmed to be statistically different from all other additives by Student's t-test (P value = 1 x 10^{-4} comparing **2.3** to **2.4** and 6 x 10^{-4} comparing **2.3** to **2.5**).

Table 2.2. Comparison of the ability of 0.80 molal aqueous solutions of amine additives to separate THF from 1:1 (w/w) solutions of THF and H_2O when reacted with CO_2. The subsequent % retention of the amine additive in the aqueous phase after reaction with CO_2 is also presented.

Base	% THF Separated[(a)]	% Additive Retained[(a)]
2.1	70 ± 0.6 %	98.0 ± 0.2 %
2.2	61 ± 0.6 %	99.0 ± 1.3 %
2.3	82 ± 0.6 %	99.7 ± 0.2 %
2.4	78 ± 0.9 %	99.3 ± 0.4 %
2.5	79 ± 1.2 %	98.8 ± 0.4 %

[(a)] Determined by ^{1}H NMR spectroscopy. Experiments were run in triplicate and standard deviations are reported as error.

2.3 Conclusions

Switchable water, the first CO_2-switchable ionic strength aqueous solvent, was demonstrated. Aqueous solutions of **2.3** in water are capable of dissolving a large amount

of an organic compound such as THF, but exposing the solution to CO_2 triggered a change in the aqueous solution ionic strength so that the organic compound is forced out of solution. The change was reversible, although the reverse reaction was not 100% complete. This solvent system is hypothesized to offer a new, greener, and reversible method for the separation of organic compounds from water. Because CO_2 capture was not the goal of this work, it was not surprising, but notable nonetheless, that the best amine, **2.3**, for this work was different from the recommended amines (**2.1**[10] and **2.2**[11]) for CO_2 capture. The development of even more efficient additives was then pursued as will be described in chapter 3.

2.4 Experimental

2.4.1 General Reaction Conditions

All amine bases were used as received from Sigma-Aldrich and TCI. THF was used as received from Fisher Scientific and distilled water was used. Reactions were carried out in 6 dram glass vials sealed with rubber septa. To introduce CO_2, N_2 or air streams, a single narrow gauge steel needle was inserted and gas was bubbled through at a flow rate of 3-5 mL min^{-1} while being stirred on a magnetic plate. A second needle was inserted into the vial, but not into the liquid, to act as a gas outlet. Flow rates were measured using a J&W Scientific ADM 2000 Intelligent Flowmeter.

2.4.2 NMR Spectroscopic Methods

NMR spectroscopy was performed using a 400 MHz Bruker NMR spectrometer. Additives were dissolved in D_2O and the NMR tubes were sealed with rubber septa. To introduce CO_2, N_2 or air, two narrow gauge steel needles were inserted and gas was gently bubbled through one of them and into the solution at approximately 4-5 bubbles per second. The second needle served as a vent for the gas phase.

To establish the chemical shifts of the protonated amine bases, molar equivalents of several strong acids (HCl and HNO_3) were added to solutions of the amines in D_2O. A minimum of two spectra were acquired in for each amine and acid combination, providing four or more spectra representing 100 % protonation. An average value of each chemical shift or each protonated base was calculated. If the bases, when reacted with CO_2, displayed chemical shifts within the range of the amine/strong acid chemical shifts, they were considered to be 100 % protonated within experimental error. For several bases, spectra of the bases when reacted with fractional equivalents of a strong acid (i.e. 1/3 protonation of a triamine) were also obtained.

To measure the amount of THF being forced out of an aqueous layer and the amount of amine retained in the aqueous phase, 1:1 (w/w) solutions of THF and water (~ 3 g) were prepared in graduated cylinders. The appropriate mass of amine additive was added and the cylinders were capped with rubber septa. After 30 min of CO_2 bubbling through the liquid phase from a single narrow gauge steel needle, a visible phase separation could be observed. The volumes of each phase were recorded from visual

measurement. The error of the graduated cylinders (Chemglass model CG-1223) is noted as ± 0.1 mL, however measured volumes corresponding to weighed out amounts of water and an organic (n-decane) showed greater reproducibility than the quoted error. Aliquots of both layers were dissolved in d_3-MeCN in NMR tubes and a known amount of ethyl acetate was added to each NMR tube as an internal standard. ^{1}H NMR spectra were acquired and the ethyl acetate standard was integrated. Assuming that the density of the expelled organic layer was equal to that of THF and that no water or additive was lost to the expelled organic layer from the aqueous layer, a concentration of THF or additive was calculated. This value was then scaled up to reflect the total volume of the aqueous or organic phase giving a percentage of the compound being forced out or retained and the experiment was then repeated in triplicate.

2.4.3 Conductivity Measurements

Conductivity measurements were performed using a Jenway 470 conductivity meter (cell constant 1.02 cm^{-1}). 1:1 (v/v) solutions of the various additives and distilled water were prepared in 6 dram glass vials and transferred to a fritted glass apparatus which acted as the reaction vessel. CO_2, N_2, or air was bubbled through the solution at a flow rate of 3-5 mL min^{-1} as measured by a J&W Scientific ADM 2000 Intelligent Flowmeter. For each conductivity measurement, the solutions were transferred back to the vials, cooled to 298 K and measured in triplicate. The fritted glass apparatus consisted

of a long narrow glass tube leading to a fine glass frit roughly 4 cm in diameter. The other end of the frit was connected a cylindrical glass tube which held the solution during bubbling. A diagram showing both methods for gas bubbling is depicted in Fig. 2.8.

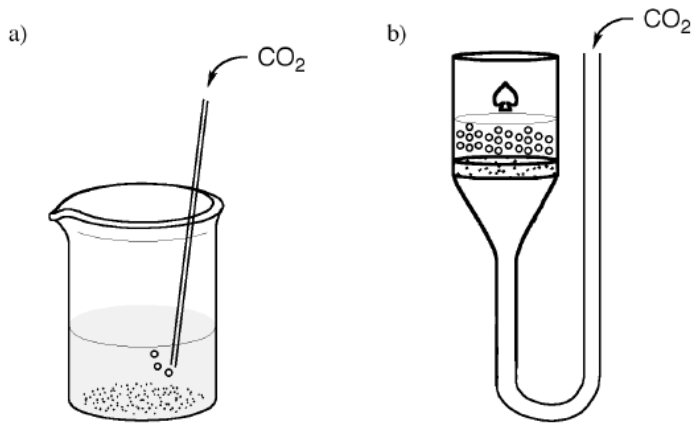

Fig. 2.8. Methods for bubbling gases through liquids on a lab bench scale, illustrating the difference between a) a single point source of bubbles using a single gauge narrow steel needle, and b) multiple sources of bubbles by passing the gas through a glass frit.

2.5 References

1) P.G. Jessop, S.M. Mercer, D.J. Heldebrant, *Energy Environ. Sci*. **2012**, *5*, 7240-7253.

2) G.T. Rochelle, *Science* **2009**, *325*, 1652-1654.

3) L. Dubois, D. Thomas, *Chem. Eng. Techol*. **2009**, *32*, 710-718.

4) F. Barzagli, F. Mani, M. Peruzzini, *Energy Environ. Sci*. **2009**, *2*, 322-330.

5) V. Somayaji, K.I. Skorey, R.S. Brown, R.G. Ball, *J. Org. Chem*. **1986**, *51*, 4866-4872.

6) D.E. Leyden, J.M. McCall, *Anal. Chim. Acta* **1970**, *49*, 77-81.

7) F. Mani, M. Perruzzini, P. Stoppioni, *Green Chem*. **2006**, *8*, 995-1000.

8) D.E. Leyden, J.M. McCall Jr., *J. Phys. Chem*. **1971**, *75*, 2400-2402.

9) G. Golub, H. Cohen, P. Paoletti, A. Bencini, D. Meyerstein, *J. Chem. Soc., Dalton Trans*. **1996**, *10*, 2055-2060.

10) G. Puxty, R. Rowland, A. Allport, Q. Yang, M. Bown, R. Burns, M. Maeder, M. Attalla, *Environ. Sci. Technol*. **2009**, *43*, 6427-6433.

11) K-Y. Tomizaki, S. Shimizu, M. Onoda, Y. Fujioka, *Chem. Lett*. **2008**, *37*, 516-517.

Chapter 3

Design, Synthesis and Solution Behaviour of Switchable Water Additives

3.1 Introduction

Addition of salt to water has many practical applications, from the breaking of emulsions, foams and suspensions to the removal of organic contaminants from water by salting out. However, the addition of salt to water is generally avoided industrially because it is energetically costly to remove the salt from the water afterwards and the water can be neither recycled nor discarded while salty. In Chapter 2, switchable water, an aqueous solution of switchable salinity was described. The solvent consisted of an amine or polyamine dissolved in water. In the absence of CO_2, the ionic strength of the solution was very low (it would be zero but for the small dissociation of the amine in water as well as water itself). In the presence of CO_2, however, the additive was converted to the bicarbonate salt, resulting in a dramatic and reversible rise in the ionic strength. While the chemistry is quite similar to that used in CO_2 capture, the utility of the solution is quite different; not surprisingly, then, in the preliminary screening of amine additives it was found that those which were most effective for switchable water are different from those that were most effective for CO_2 capture.

As evident from equation 2.4, the ionic strength, I, of the solution is strongly dependent on the number of protonatable sites on the amine additive, but only if equation 1.23 applies. Because ionic strength is not easily measured directly, the salting out of

THF from a switchable water solution has been used as both an indirect measure of the ionic strength of the solution as well as a direct measure of the effectiveness of the switchable water additive for the salting out application. Salting out was certainly not the only application envisioned for switchable water additives, but it has the benefit of being easily and rapidly tested.

In general, the desired performance characteristics of a switchable water additive used for salting out are rapid switching, high level of THF expulsion from the aqueous phase, and high retention of the additive in the aqueous phase. Optimally, these additives should be commercially available or be easily synthesized from readily available and inexpensive starting materials. In Chapter 2 it was demonstrated that several diamines have a greater ability to salt out THF from water than an equimolal concentration of monoamines in the presence of CO_2. Here, the results of efforts towards further delineating the structural design parameters that control the effectiveness of switchable water additives, along with the syntheses of new additives, are presented.

The work described in this chapter has previously appeared in *Green Chemistry* **2012**, 14, 832-839. The structure of the manuscript has been modified in some places to better reflect the progression of the study.

3.2 Results and Discussion

3.2.1 Comparison of Salting Out Efficiencies

Before attempting to find more new amine additives, the amount of THF salted out by common inorganic salts (NaCl and $(NH_4)_2SO_4$) at the standard test molality of 0.8 molal (Table 3.1, entries 6 and 8) was determined. Additionally, a ceiling amount of THF that could be removed from water by such inorganic salts at higher concentrations (Table 3.1, entries 7 and 9) was determined. The slightly larger amount of THF that was removed via these salts compared to the amine additives at equimolal loading (Table 3.1, compare entries 1–6 and 8) showed that improvement of switchable water additives was necessary to match the performance of typical non-switchable salts used in salting-out processes.

Table 3.1. A comparison of the ability of several tertiary amine, amidine, and inorganic salt additives to separate THF from 1:1 w/w solutions of H_2O and THF when reacted with CO_2. The subsequent % retention of the additive in the aqueous phase after reaction with CO_2 is also presented.

Entry	Base or Salt	Loading	% THF Separated[a]	% Amine Retained[a]
1	**2.1**	0.80 molal	70 ± 0.6 %[b]	98.0 ± 0.2 %[b]
2	DBU	0.80 molal	59 ± 0.7 %	96.5 ± 1.7 %
3	**3.1**[c]	0.80 molal	75 ± 2.3 %	98.1 ± 2.2 %
4	**2.3**	0.80 molal	82 ± 0.6 %[b]	99.2 ± 0.4 %[b]
5	**2.4**[d]	0.80 molal	78 ± 0.9 %[b]	99.3 ± 0.4 %[b]
6	NaCl	0.80 molal	88 ± 1.6 %	n/a
7	NaCl	varied[e]	98 ± 0.5 %	n/a
8	$(NH_4)_2SO_4$	0.80 molal	92 ± 1.2 %	n/a
9	$(NH_4)_2SO_4$	varied[e]	99 ± 0.6 %	n/a

[a] Determined by ^{1}H NMR spectroscopy. Experiments were performed in triplicate and standard deviations are reported as error. [b] From Chapter 2. [c] This additive (synthesized in ~90 % purity) was able to salt out organics upon reaction with CO_2, but CO_2 could not be released under working conditions to allow for recycling. [d] This additive, a tetramine, could only be protonated at two sites by carbonic acid, as determined by ^{1}H NMR spectroscopy. [e] Salt was added until a consistent volume of THF separated from the aqueous solution was observed.

Amidine bases, such as DBU and compound **3.1** (Fig. 3.1), were briefly explored as switchable water additives but ultimately are not preferred because the reversion from the amidinium bicarbonate species was too difficult at moderate temperatures. In addition, amidines are more expensive and suffer from hydrolytic instability at alkaline conditions.[1]

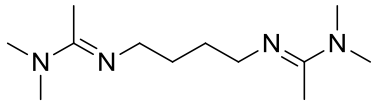

3.1

Fig. 3.1. Molecular structure of compound **3.1**, a diamidine tested as a switchable water additive.

To approach the salting-out capabilities of the inorganic salts studied, diamines and larger polyamines, which when protonated generate bolaform electrolytes in solution, should be more effective than monoamines, according to equation 2.4. A bolaform electrolyte is a polyvalent electrolyte species where the sites of charge are separated from each other by a series of atoms.[2] Evidence supporting this hypothesis was already obtained using the diamine **2.3** (TMDAB), which was more effective than monoamines at salting out THF from 1 : 1 w/w solutions of THF and H_2O (Table 2.2). However, these salts were still not as capable of salting out organics as the inorganic salts shown in Table 3.1, so further improvement and development of larger polyamines was necessary.

3.2.2 Basicity Considerations

For effective switching, the amine sites on an additive must be neither too basic nor insufficiently basic (similar to the findings for ionic liquids used for CO_2 capture).[3] From the initial screening of amine additives it was determined that a pK_{aH} (the pK_a value

of the protonated species) range of 8 to 10.5 was appropriate. If the amine was insufficiently basic, then CO_2 at 1 atm would be insufficient to protonate the amine with high conversion. If the amine was too basic, then the reversion would require severe conditions, take too long, or be impractical to achieve.

For polyamines, it is desirable to have as many amine sites as possible fall within this pK_{aH} window to maximize effectiveness of ionic strength generation but still allow for easy switchability. Symmetry arguments predict that symmetric diprotic acids, a diprotonated diamine for example, with chemically equivalent functional groups should possess two dissociation constant values with a ratio of four ($K_1/K_2 = 4$, $pK_{aH(1)} - pK_{aH(2)} \sim 0.6$) if the ionization events are completely independent of one another.[4-6] A deviation resulting in a ratio greater than four would represent some sort of dependence of the second ionization event upon the first ionization event. One possible intra-molecular based explanation of this deviation[7-9] is that when the two functional groups are too close, a single ionization event at one group affects the electron density and therefore acidity or basicity of the second functional group. Therefore, it must then be ensured that protonation events at one amine functional group on a polyamine chain do not greatly decrease the capacity of subsequent amine groups to be protonated (i.e. $pK_{aH(1)} - pK_{aH(2)}$ should be close to 0.6).

For linear ditertiary diamines $Me_2N(CH_2)_xNMe_2$, the trends in the first and second pK_{aH} values show that four carbons are necessary to insulate the one basic site electronically from the other and thus to ensure that both pK_{aH} values fall within the

range that is appropriate for facile switching (Fig. 3.2). TMDAB, compound **2.3**, was the smallest ditertiary diamine that had both pK_{aH} values within the specified working range, although the pK_a values for corresponding propanediamine were close to the desired range. It was then concluded that polyamines should have a minimum of four carbons between each amine group to maintain appropriate basicity of each amine after the protonation of a neighbouring group.

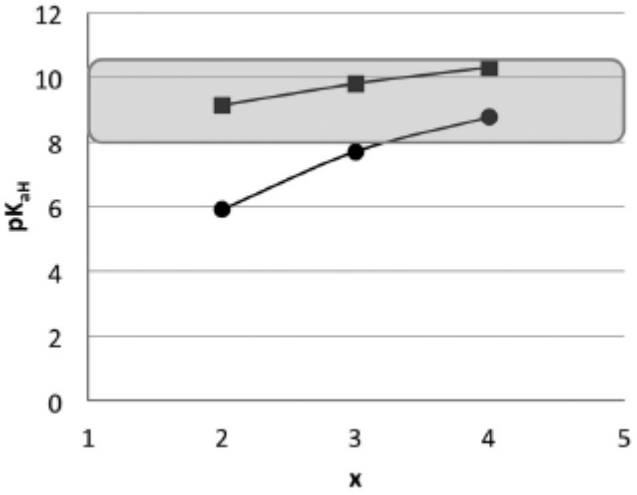

Fig. 3.2. A plot of the pK_{aH} values of $Me_2N(CH_2)_xNMe_2$ (● = $pK_{aH(1)}$, ■ = $pK_{aH(2)}$) relative to the number of carbons (**x**) found between the two amine groups.[10-12] The shaded region highlights the desired range of pK_{aH} values for a switchable water additive.

How large an increase in the ionic strength could one expect when applying CO_2 to a solution of 0.1 molal of **2.3**? The approximate ionic strength can be calculated by

assuming solution ideality and by using molarity rather than molality. A 0.1 M solution of **2.3** has a pH of 11.6 and the relevant ions would be [**2.3**·$2H^+$] (0.006 mM), [**2.3**·H^+] (4 mM), [OH^-] (4 mM) and a negligible concentration of H^+, giving a total ionic strength of ~4 mM. Adding CO_2 at 1 bar to that solution lowers the pH to 6.8, giving a solution containing [**2.3**·$2H^+$] (99 mM), [**2.3**·H^+] (1 mM), [HCO_3^-] (199 mM) and negligible concentrations of CO_3^{2-}, H^+ and OH^-, giving a total ionic strength of ~300 mM. Therefore, in this idealized case, the ionic strength has jumped two orders of magnitude upon addition of CO_2.

3.2.3 Long-Linker Bolaform Electrolytes

Once the minimum number of carbons between amine nitrogen atoms had been found to be four, it was wondered whether there was either an optimum number or an upper limit beyond which salting-out ability would be lost. It was hypothesized that if the carbon spacer were excessively long, then the dication would begin to function more like a pair of singly charged cations and the Z term in equation 1.23 would thus fall to 1 instead of 2.

To observe this threshold value of spacer length, a series of salting out experiments using 1:1 w/w solutions of THF and H_2O was performed. Using a series of nonswitchable α,ω-diaminoalkane dihydrochloride salts $[H_3N(CH_2)_xNH_3]Cl_2$ with a varying number of carbons between the ammonium groups, the amount of THF expelled

from each aqueous solution upon dissolution of the salts in the aqueous solution was observed (Fig. 3.3).

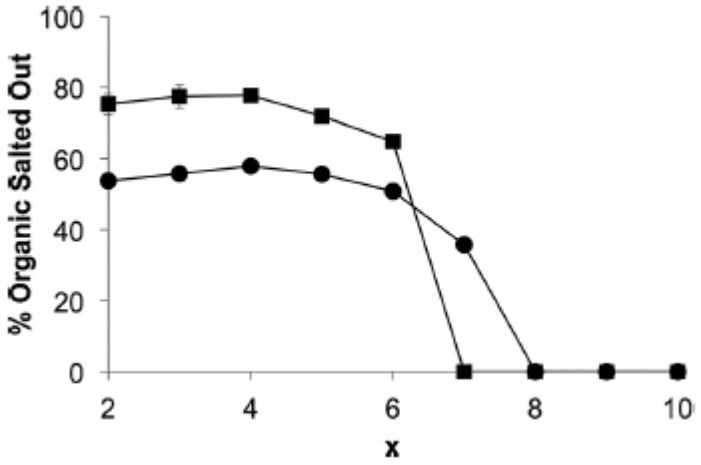

Fig. 3.3. A plot showing the amount of a organic compound salted out from 1:1 w/w mixtures of ●:THF/H_2O or ■:MeCN/H_2O with a 0.50 molal loading of α,ω-diaminoalkane dihydrochloride salts, $[H_3N(CH_2)_xNH_3]Cl_2$, where **x** is the number of carbons between the ammonium groups.

As shown, the amount of THF salted out is essentially independent of x up to a value of 6, but the amount of THF salted out quickly decreased with the 1,7-diaminoheptane dihydrochloride salt and ultimately to zero salting out when the eight-, nine-, and 10-carbon spaced salts were used. A similar trend was observed with 1:1 w/w solutions of acetonitrile (MeCN) and water (Fig. 3.3). With either solvent, there appeared to be a very

weak maximum at x = 4. On a practical level, it was clear that a four-carbon spacer was best, but the reason for the poor performance at x > 6 was not immediately clear. The reasons for the cause of the diminished salting out effect of diamine dihydrochloride salts with longer spacers were then pursued.

3.2.4 Accounting for the Diminishing Salting Out Effect

In the attempt to rationalize these observations, four possible hypotheses were explored.

Hypothesis #1. The first hypothesis was that intra-molecular (through-bond) communication between the two ammonium groups diminished or was lost when the carbon spacer was larger than six carbons, so that the two charge centres were functioning essentially as two monocations as far as equation 1.23 was concerned. To determine the spacer length at which electronic communication was lost, the dependence of basicity on spacer length was explored. A survey of the pK_{aH} values of primary α,ω-diaminoalkane dihydrochlorides from the literature[13-15] (Fig. 3.4) showed that the ratio of the first and second K_{aH} dissociation constants leveled off at a value of roughly 4 (or $pK_{aH(1)} - pK_{aH(2)} \sim 0.6$) as the number of carbons between the two functional groups exceeded six. This suggested that simple diamines with carbon spacers of greater than

six, when protonated, have two ammonium groups that are electronically independent of each other.

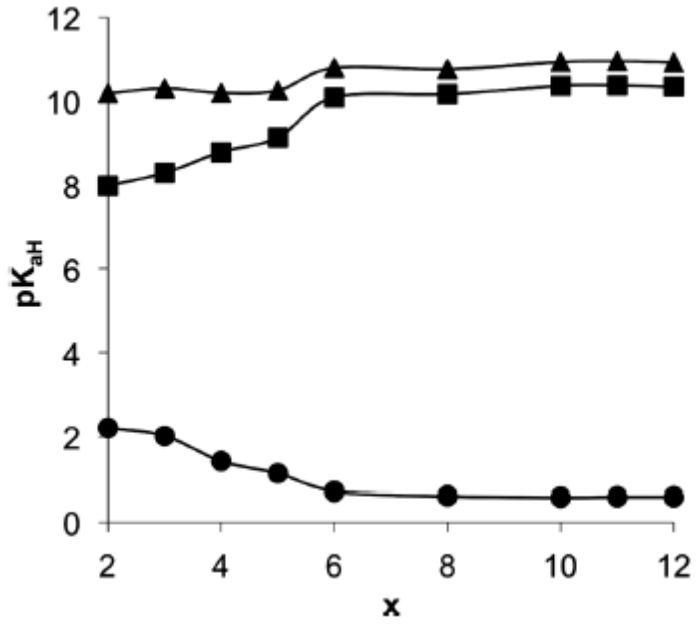

Fig. 3.4. A plot showing the comparison of pK_{aH} values of linear α,ω-diaminoalkane hydrochlorides versus the number of carbons, **x**, separating the two amine groups.[13-15] ■ $pK_{aH(1)}$, ▲$pK_{aH(2)}$, ● $pK_{aH(1)} - pK_{aH(2)}$.

To determine whether a lack of electronic communication was the deciding factor in disallowing salting out by diammonium salts with long carbon spacers, another set of THF salting out experiments was performed, this time using benzidine dihydrochloride, **3.5**, a biphenyl analogue (Table 3.2). This species had pK_{aH} values of 3.85 and 4.95[16]

resulting in $K_{aH(1)}/K_{aH(2)}$ ratio much greater than 4, showing that electronic communication still existed between the N atoms. One may then have expected this salt to have acted similarly to the simple diamines of six carbons or fewer. However, this salt did not cause salting out of THF at 0.30 molal loading. The same experiment was performed using the slightly less rigid diamine 1,4-benzenediethanamine dihydrochloride, **3.6**, at 0.30 molal loading, however, a similar result to the benzidine salt was obtained. A very long chain diamine with ether linkages (compound **3.7** in Table 3.2) could salt out THF however. It was concluded that the presence or absence of electronic communication throughout the backbone linking the ammonium groups is not the deciding factor that determines the salting-out abilities of these diammonium species.

Table 3.2. A comparison of the ability of various diamine dihydrochloride salts to salt out THF from a 1:1 w/w solution of H_2O and THF.

Compound	Structure	Loading	% THF Separated
3.2	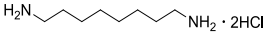	0.50 molal	0 %
3.3	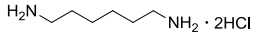	0.50 molal	51 %
3.3	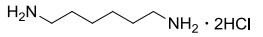	0.30 molal	46 %
3.4	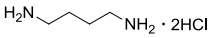	0.50 molal	58 %
3.5[a]	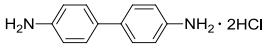	0.30 molal	0 %
3.6[a]	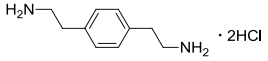	0.30 molal	0 %
3.7	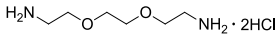	0.50 molal	53 %
3.8	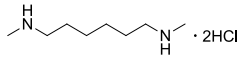	0.50 molal	68 %
3.9	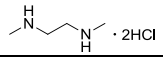	0.50 molal	73 %

[a] 0.30 molal was used rather than the typical 0.50 molal loading due to low solubility of this salt in water.

In an effort to support the aforementioned conclusion, each salt was modeled using density functional theory in an attempt to assign atomic charges. These charges were calculated using the B3LYP/6-311G(d,p) level with theory[17] along with CHELPG (Charges from Electrostatic Potentials using a Grid based method).[18] It was hypothesized that any atom in the backbone between the two charged ammonium groups which possessed little to no charge represented a break in through-bond electronic communication (i.e. a loss of inductive effect). It was hypothesized that if any of the atom charges (which generally ranged from |~1 to $1x10^{-2}$| electronic units, e.u.) decreased below |$1x10^{-3}$| e.u., the charge could be denoted as zero signifying a break in communication. Unfortunately, no supporting evidence to the previous conclusion could be drawn from the modeling studies as the CHELPG charges of the atoms along each dication's backbone never decreased below the set threshold in a distinguishable pattern (see Appendix II).

Hypothesis #2. In the second hypothesis, it was proposed that intra-molecular communication (through-space) was diminishing or was lost past a separation of six carbons, again providing an ion which contained two monocations rather than a single dication. As a model, photoelectron spectroscopy literature on lone-pair interactions of diamines was consulted to see if a potential through space communication effect could be leading to the enhanced salting out ability of the diamine salts with ≤6 carbon spacers. However, such a through space effect was not likely leading to the effect as it has been

previously suggested that radical cation species with terminal nitrogens would have little chance of interacting intra-molecularly through space when the number of carbons between the amine groups are greater than four. This has been attributed to the great number of possible orientations of the nitrogen groups in space which are unfavorable towards lone-pair interaction.[19-21] As the diminishing salting out effect was not noticeably prevalent until the seven-carbon spaced species, rather than the four-carbon spaced species, it was concluded this was not the cause of the observations.

Hypothesis #3. An increase in ion-pairing of the alkylammonium and chloride ions occurring at greater spacer lengths, reducing the effective ionic strength generated by the α,ω-diaminoalkane dihydrochloride salts, was then hypothesized. Past literature has noted that bolaform electrolytes are prone to extensive ion-pairing in aqueous solution.[2] If this phenomenon is dependent on the carbon spacer length between the diammonium ions, this could account for the lack of salting-out ability of the longer salts due to a diminished effective concentration of charged species and resulting ionic strength in solution. However, a recent study of ion-pair association constants of similar diamine dihydrohalide species has shown that the association constant values, K_A, of the diamine dihydrohalide ion pairs decrease as the number of carbon spacers between ammonium groups is increased.[22]

Hypothesis #4. Attention was then focused upon the increasing organic content of the salts. It was proposed that the increase of organic content in the longer bolaform electrolytes was helping to solubilize the organic substrates in aqueous solution, thus preventing a salting-out effect despite the high ionic strength. Previous modeling studies by Wang and co-workers have shown that a dicarboxylate dianion, when adequately solvated, will fold in, bringing its two charged termini closer than expected. Remarkably, the aqueous solvation stabilization overcomes electrostatic repulsions of the two charged ends leaving the organic backbone sticking out in the aqueous solution.[23] A similar result was very recently found for 1,7-diammoniumheptane models by Williams and co-workers.[24] It was then thought that a folding of the diammonium species may be occurring, which could give increasingly large pockets of organic content as the carbon spacers of the diammonium salts were increased. An increasing size of local organic environments in aqueous solution might have stabilized the THF or MeCN in aqueous solution via a hydrophobic effect, despite the higher ionic strength environment in the bulk solution.

To support this hypothesis, salting out experiments were performed using 1,8-diamino-3,6-dioxaoctane dihydrochloride, **3.7**, a 1,8-diaminooctane dihydrochloride analogue with two oxygen atoms in the backbone ($pK_{aH(1)}$ = 8.74, $pK_{aH(2)}$ = 9.68).[25] This salt provided considerable salting out of THF from aqueous solution despite having a linker length of eight atoms between the ammonium groups. The presence of a more hydrophilic backbone and an observed salting out effect suggested that the carbon content

of the bolaform electrolyte must be taken into account when assessing salting out capability. Additional diammonium dihydrochloride salts shown in Table **3.2** (compounds **3.8** and **3.9**) demonstrated that it was hydrophobic organic content far from the centres of charge (in these cases in the chain between the ammonium groups) which diminished the salting out effect; additional methyl groups on the *N* atoms seem to make little difference. Compound **3.8**, despite having eight carbon atoms, was closer in performance to compound **3.3** than compound **3.2**.

It was also observed that shorter-chain salts at low ionic strength could still expel organics from aqueous solution, while longer-chain salts at a supposed greater ionic strength were still unable to salt out these organics, further suggesting that the organic content of the salt may play a role in its salting out ability. For example (Table 3.3), a 0.50 molal solution of the 1,8-diaminooctane dihydrochloride salt, **3.2**, provided no salting out of THF despite an ionic strength of 1.5 molal (if the salt acted as a $Z = 2$ dication) or an ionic strength of 1.0 molal if it is assumed that the two ammonium sites were independent of one another (resulting in two singly charged cations). However, a 0.30 molal solution of 1,6-diaminohexane dihydrochloride, **3.3**, provided a lower ionic strength of 0.90 molal (if the ammonium sites were considered to be giving a doubly charged cation) and still salted out roughly 46 % of THF in conditions similar to those presented in Fig. **3.3**. While these calculations cannot be considered accurate because they assumed ideality, this result cannot be purely explained by the lack of electronic

communication between the ammonium groups, but could be explained by the greater organic content of salt **3.2**.

Table 3.3. A comparison of various loadings of α,ω-diaminoalkane dihydrochlorides and the ionic strength of those solutions given two scenarios of solution behavior. Also included is the observed ability of each species to salt out THF from 1:1 (w/w) solutions of H_2O and THF.

Salt	Loading	Ionic Strength Assuming Single Dication	Ionic Strength Assuming Two Monocations	% THF Separated
3.2	0.50 molal	1.5 molal	1.0 molal	0 %
3.3	0.30 molal	0.9 molal	0.6 molal	46 %

The notion of the organic character of a salt lowering its salting-out ability was not limited to the bolaform electrolytes studied. A similar set of salting out studies using monoamine hydrochloride salts, $[H(CH_2)_xNH_3]Cl$, (Fig. 3.5) again showed a decrease in the salting out efficiency of the alkylammonium salts as the carbon chain was lengthened.

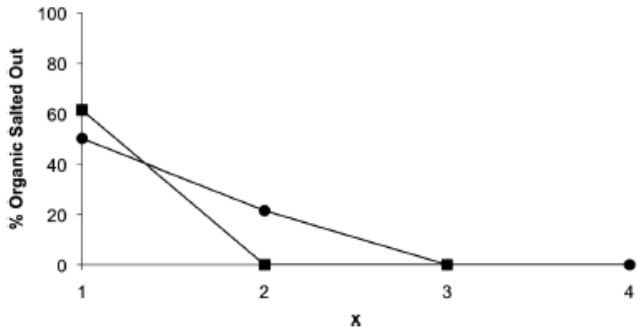

Fig. 3.5. A plot showing ●: the amount of THF salted out and ■: the amount of MeCN salted out from a 1:1 w/w solution of THF or MeCN and H_2O with a 1.00 molal loading of alkylammonium chloride salts, $[H(CH_2)_xNH_3]Cl$, where **x** was the number of carbons on the alkyl chain.

While the ability of the organic chain in α,ω-diaminoalkane salts to solubilize organic molecules such as THF was believed to be the reason for the poor salting-out ability, a further hypothesis might have been that the salts, when folded in half, could have acted as surfactants. A plot of conductivity as a function of salt concentration in water was found not to have a sharp break, which would have been indicative of a critical micelle concentration[26] (see Fig 3.6). Therefore the solubilizing effect of the long-chain salts is merely by inter-molecular association and not likely by micelle formation.

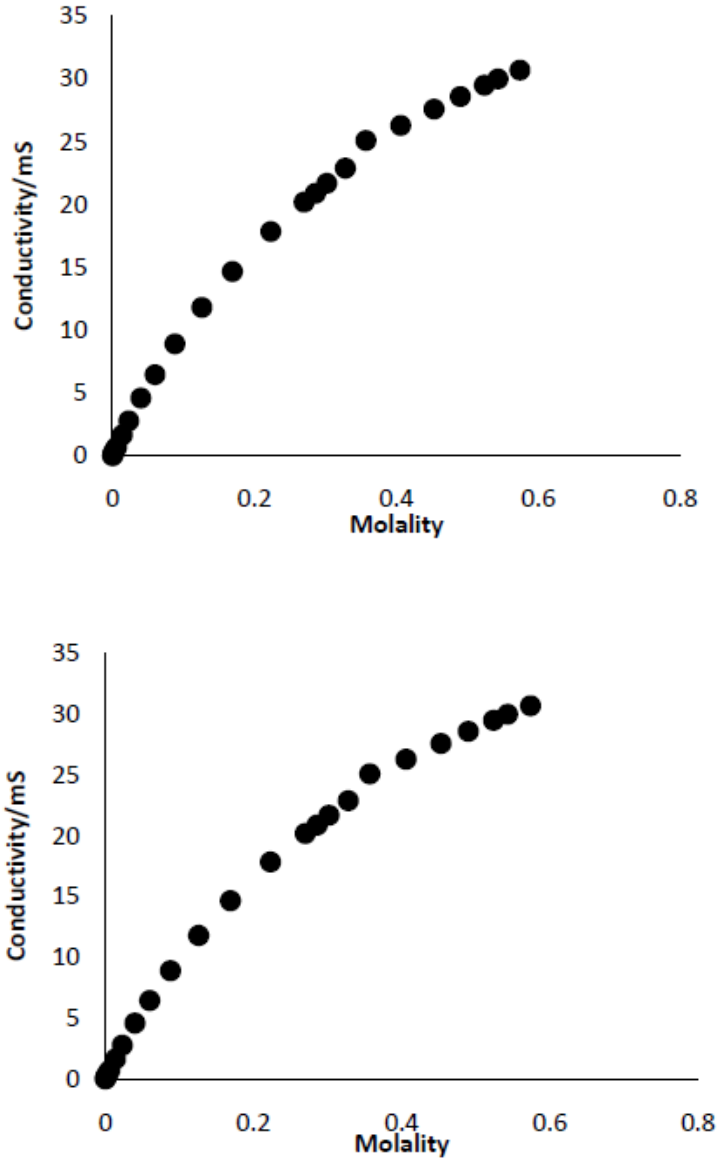

Fig. 3.6. A plot of the conductivity of aqueous solutions of 1,6-diaminohexane dihydrochloride, **3.3**, (above) and 1,8-diaminooctane dihydrochloride, **3.2**, (below) as a function of the salt concentration.

Ultimately, it would seem that even when studying very similar salts, a slight difference in carbon content results in a changed ability of the salt to induce organic substrates to salt out of aqueous solution. This finding is not only important to the design of switchable water additives but is likely to find use in other chemical separation technologies.

3.2.5 New Switchable Water Additives

With a reasonable set of principles for the design of polyamine additives, linear and cyclic polyamines from readily available precursors were prepared. A modified *N*-methylated spermine analogue, **3.10**, was envisioned (Fig. 3.7). Initially there were concerns about the presence of only three carbon positions between N1 and N2 and between N3 and N4, but all four pK_{aH} values of unmodified spermine ($pK_{aH(0.1\ N\ KCl)}$ = 7.95, 8.82, 10.05,10.86)[27] fell close to or within the acceptable working range of 8–10.5 and thus synthesis and testing for function as a switchable water additive was performed.

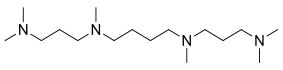

3.10

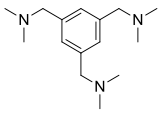

3.11

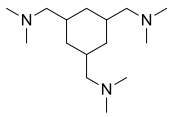

3.12

Fig. 3.7. Molecular structures of newly developed switchable water additives.

Compound **3.10** was synthesized using a modified method developed by Bieber and co-workers[28] in a 45 % yield. Compound **3.10** showed the ability to salt out approximately 85 % of THF from a 1:1 w/w system, the highest observed (Table 3.4) to this point, even though ^{1}H NMR spectroscopy showed that incomplete protonation of all the amine sites on compound **3.10** had occurred, as shown in Table 3.4. This again suggested that a minimum of four carbon positions between the amine groups are necessary to allow for full protonation by carbonic acid. Increasing the amount of compound **3.10** in solution did not yield a greater THF salting out (Table 3.4). This was likely due to the now greater organic content in solution helping to solubilize the THF.

Table 3.4. A comparison of the ability, at 0.80 molal loading, of switchable water polyamine additives to separate THF from 1:1 w/w solutions of H_2O and THF when reacted with CO_2. The resulting % retention of the additive in the aqueous phase and the average number of amine groups protonated during the treatment are also shown.

Compound	% THF Separated[a]	% Amine Retained[a]	Average *N* Atoms Protonated[c]
3.10	85 ± 1.2 %	99.8 ± 0.1 %	3.7
3.10[b]	84 ± 3.5 %	94.9 ± 2.2 %	3.7
3.11	76 ± 0.9 %	94.7 ± 0.3 %	2.8
3.12	86 ± 1.3 %	99.3 ± 0.4 %	3.0

[a] Determined by ^{1}H NMR spectroscopy. Experiments were run in triplicate and standard deviations are reported as error. [b] 1.2 molal loading of additive was used. [c] Determined by the comparison of ^{1}H NMR spectra of the additive when treated with strong acids, carbonic acid, and no treatment.

In an attempt to force the utilization of all amine functional groups available on a carbon scaffold, compound **3.11**, a triamine analogue of *N*,*N*-dimethylbenzylamine (pK_{aH} = 9.03),[29] where all the amine groups were separated by 5 carbons, was prepared. This molecular design was thought to minimize the impact of neighbouring ionization events while maintaining an enhanced ionic strength effect and avoiding the presence of excess organic content in the scaffolding. Compound **3.11** was synthesized in ~96 % purity using a modification of the method of Hirsch and co-workers.[30] Compound **3.11** showed the capacity to salt out roughly 76% THF from a 1:1 w/w solution of THF and H_2O. ^1H NMR spectroscopy again showed, however, that incomplete protonation of compound **3.11** had occurred when it was reacted with carbonic acid, which likely contributed to the lower than expected salting-out ability.

The synthesis of a saturated analogue of compound **3.11** was then pursued to eliminate the conjugation in the carbon backbone. A cis/trans mixture of compound **3.12** was synthesized in ~95 % purity using a modified preparation from Shirai and coworkers[31] followed by a $LiAlH_4$ reduction from the triamide to triamine. Compound **3.12** showed an improved ability to salt out THF from 1:1 w/w solutions of H_2O and THF, comparable to compound **3.10**, as shown in Table 3.4. A definitive conclusion as to what resulted in the similar salting out effect between the tetramine **3.10** and the triamine **3.12** was not obtained, but it was hypothesized that the less conformationally rigid compound **3.10** may have shielded some charge by folding onto itself when solvated, comparable to the conclusions in the modeling of Yang and Williams,[23,24] while

compound **3.12** could not undergo conformational shifts to such an extent. Nonetheless, both compounds **3.10** and **3.12** showed a greater salting out ability than any amine additive previously tested and were comparable in effectiveness to a equimolal loading of NaCl (88% THF removed). Additionally, compounds **3.10** and **3.12** at 0.8 molal were as good at salting out THF as a 2.3 molal solution of compound **2.3** but with 65 mol% less additive used. Higher loadings of compound **3.12** in THF/water systems were not possible due to insufficient solubility.

The time to remove CO_2 from the additives (to return the solution to the original ionic strength) varied between the additives (Fig. 3.8). The conversion of the bicarbonate salts to neutral amines was not complete even after several hours, but the conversion of all the additives was sufficient after N_2 sparging at 50 °C for 30–60 min to restore the miscibility of the THF/water mixture.

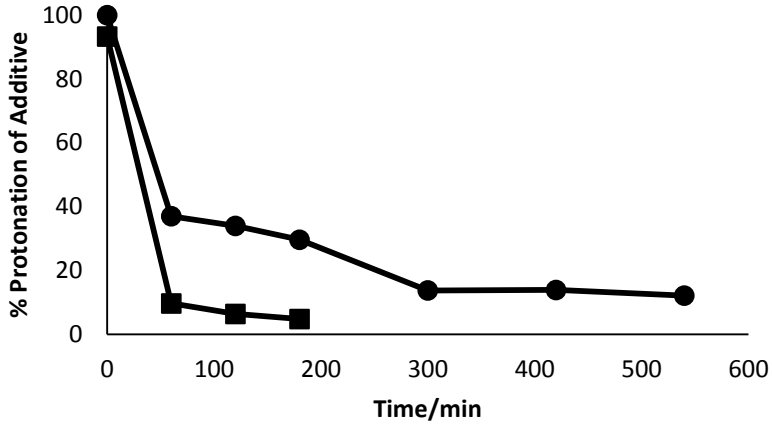

Fig. 3.8. A plot showing the % deprotonation of protonated (■) compound **3.11** and (●) compound **3.12** in D_2O as CO_2 is removed from the system as monitored by ^1H NMR spectroscopy. CO_2 was removed by sparging the solution with an inert gas at 75 °C.

3.2.6 Primary and Secondary Amines as Switchable Water Additives

In Chapter 2, it was stipulated that only tertiary amine additives would work well as switchable additives because they react with CO_2 in water to exclusively form bicarbonate salts rather than carbamate salts. Carbamate salt formation is not preferred because it is more difficult to reverse[32] and because it creates fewer ions in solution per mole of amine additive (compare equations 2.1 and 3.1). In the case of non-tertiary polyamines, there is also the risk that zwitterionic carbamate species can form[33] which would further decrease the ionic strength.

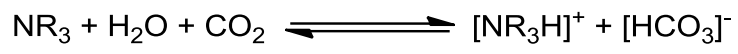

$$NR_3 + H_2O + CO_2 \rightleftharpoons [NR_3H]^+ + [HCO_3]^- \quad \textbf{(2.1)}$$

$$2\ NHR_2 + CO_2 \rightleftharpoons [NH_2R_2]^+ + [NR_2C(O)O]^- \quad \textbf{(3.1)}$$

However, the CO_2-capture literature has shown that carbamate formation from secondary amines can be prevented by sterically bulky groups near or attached to the nitrogen.[34-38] This potentially allowed for the development of a secondary amine switchable water additive. This would be attractive because secondary amines generally have faster kinetics for CO_2 uptake than tertiary amines[39] and still could afford the desired reverse reaction at moderate conditions.

Two sterically-hindered secondary amines, *N*-*tert*-butylethanolamine (*t*BuNHCH$_2$CH$_2$OH) and *N*-*tert*-butyl-methylamine (*t*BuNHMe), were found to reversibly salt out THF from 1:1 w/w THF/H_2O solutions via the introduction and removal of CO_2 and thus could function as switchable water additives (Table 3.5). Although these secondary amines were not as effective in salting out THF as the tertiary amine additives previously studied, they offered a proof that further exploration of secondary amines as switchable water additives was not necessarily a fruitless endeavor. Additionally, the secondary amine additives had excellent retention in the aqueous phase, which decreased losses of amine to the separated organic phase.

Table 3.5. A comparison of the ability of several sterically-hindered secondary amines to separate THF from 1:1 w/w solutions of H_2O and THF when reacted with CO_2. The resulting % retention of the additive in the aqueous phase after CO_2 treatment is also presented.

Base	Loading	% THF Separated	% Amine Retained[a]
*t*BuNHCH$_2$CH$_2$OH	1.60 molal	69 ± 0.4 %	99.8 ± 0.1 %
*t*BuNHMe	1.60 molal	68 ± 0.8 %	99.8 ± 0.1 %

[a] Determined by ^{1}H NMR spectroscopy. . Experiments were run in triplicate and standard deviations are reported as error.

Non-sterically hindered primary and secondary amines such as monoethanolamine, MEA, are readily switched to ionic species (bicarbonate salts and carbamate salts) but are less easily converted back to the neutral species. However, non-bulky secondary and primary amines are more hydrophilic than tertiary amines and bulky secondary amines. This additional hydrophilicity could be advantageous in switchable water systems because a) the amines could be soluble at higher loadings and b) because the ability of the salts of these amines to solvate THF may be lessened, compared to tertiary amines, by the greater hydrophilicity. Therefore the use of primary amines as switchable water additives for the salting out of THF was briefly evaluated. MEA, a monoamine, did salt out THF but not to a great extent. Among the primary diamines ($H_2N(CH_2)_xNH_2$), the chain length affects their ability to salt out THF when exposed to

CO_2 (Fig. 3.9) was explored. As was found with the diamine dihydrochloride salts (Fig. 3.3), the four carbon-spaced diamine (1,4-diaminobutane) showed a very weak maximum, but once again, all the salts with carbon spacers from 2 to 6 performed quite similarly. While these tests were performed at 0.8 molal loading, it was found that increasing the amount of 1,4-diaminobutane in the THF/water mixture to 1.2 molal increased the amount of THF expelled from the aqueous phase (Table 3.6) but increasing the loading of diamine even further did not help. This suggested that there is a balance between additive concentration to generate sufficient ionic strength and the resulting organic content being built up in the aqueous solution working against the ionic strength effects. In a similar salting out test, spermine (the non-methylated analogue of compound **3.10**) also demonstrated an impressive removal of THF at 0.80 and 1.2 molal loading (Table 3.6). This was likely due to all the nitrogens in the backbone participating in salt formation (whether as bicarbonates or carbamates). Spermine, in the presence of CO_2, was more effective than NaCl at equal molality (Table 3.1). A future design principle should be to synthesize additives with greater hydrophilicity so that they may counteract the effect of increasing organic content in aqueous solution.

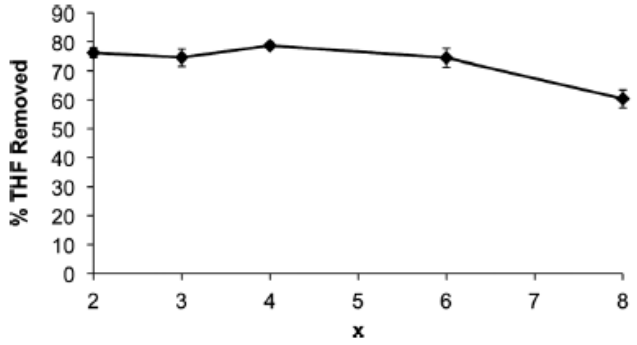

Fig. 3.9. A plot showing the percentage of THF salted out from 1:1 w/w solutions of THF/H_2O using 0.80 molal loadings of primary diamines ($H_2N(CH_2)_xNH_2$) with varying carbon spacer (**x**) when reacted with CO_2 for 30 min.

Table 3.6. A comparison of the ability of several primary and secondary amines to separate THF from 1:1 w/w solutions of H_2O and THF at various loadings when reacted with CO_2 for 30 min.

Base	Loading	% THF Separated[a]
MEA	0.80 molal	65 ± 0.8 %
1,4-diaminobutane	0.80 molal	79 ± 0.8 %
1,4-diaminobutane	1.20 molal	89 ± 0.4 %
1,4-diaminobutane	1.60 molal	86 ± 1.2 %
Spermine	0.80 molal	91 ± 3.3 %
Spermine	1.20 molal	92 ± 1.9 %

[a] Determined by ^{1}H NMR spectroscopy. Experiments were run in triplicate and standard deviations are reported as error.

While these primary and secondary amines, especially spermine, were impressive in their ability to salt out THF (spermine was the best at this point, at 92% expulsion), they were not easily switched back to the neutral form. Although MEA, upon treatment with CO_2, does salt out organics, the reverse reaction, removing CO_2, did not occur under the mild conditions of heating to 50 °C while bubbling an inert gas (N_2 or air) through the solution. Primary amines can be switched back to neutral at higher temperatures, as has already been demonstrated in the literature,[40] but often temperatures over 100 °C are required and thus were judged to be impractical for this application.

3.3 Conclusions

The ability to salt out organic compounds from water and then easily recycle the water without desalination should be an asset to industry both from environmental and cost perspectives. Use of switchable water, a switchable ionic strength aqueous solvent, offers a means of salting out water-miscible organic compounds from aqueous solutions through the use of CO_2. These solvent systems can also easily be recycled by removal of CO_2. To make these systems more attractive, alkylammonium bicarbonate salts derived from polyamines were required. These bicarbonate salts can provide solutions of greater ionic strength at lower loadings in water.

Before the synthesis of a new generation of additives could take place, a set of principles for future additive design was developed. These principles evolved from a

study of the dependence of diamine pK_{aH} on the chain length between the functional groups. Evidence was provided which suggested that the organic content in the backbone of a bolaform electrolyte plays a large role in its salting out capabilities, potentially due to enhanced interactions of the carbon backbone with organic substrates in aqueous solution.

It was found that polyamines should have a minimum of four carbon atoms between the amine groups (to allow for appropriate basicity) but otherwise a minimum of hydrophobic organic content (to allow for maximum salting out capacity). Several new small molecules were synthesized and tested and showed improved salting out capabilities compared to the original set of switchable water additives described in Chapter 2. Primary and secondary polyamines were more effective at salting out than tertiary polyamines, but the reversion of the primary and secondary polyamines to the neutral form required significantly more energy. Larger polymeric tertiary amine additives were later synthesized in the Jessop group. These polymers provided a complementary set of switchable water additives to the small molecule polyamines described here.[41]

3.4 Experimental

3.4.1 General Reaction Conditions

All chemicals were obtained from either Sigma Aldrich or TCI and were used as received without further purification. Solvents were obtained from Fisher Scientific and Commercial Alcohols and were used as received without purification. NMR spectroscopy was performed using Bruker 300 and 400 MHz spectrometers. IR spectra were acquired using a Nicolet 360 FTIR.

3.4.2 Synthesis of Diamine Dihydrochloride Salts

α,ω-Diaminoalkane dihydrochloride salts were synthesized from the reaction of HCl and an appropriate diamine. Diamine (5 mmol) was dissolved in 30 – 50 mL diethyl ether and, if necessary, 5 mL methanol to speed up dissolution. A slightly greater than two molar equivalent (to the diamine concentration) excess of 1.0 M HCl in diethyl ether was added to the solution dropwise with constant and vigorous stirring. A white precipitate immediately formed. The precipitate was collected by filtration, washed with diethyl ether and dried under vacuum. Salts without literature precedent were characterized by ^{1}H NMR spectroscopy in DMSO-d_6 with reference to TMS at 0 ppm. ^{1}H NMR spectra were found to represent symmetrical molecules, indicating the likely presence of a dication. All other salts used were commercially available and used as received.

1,7-diaminoheptane dihydrochloride: ^{1}H NMR (DMSO-d_6, 300 MHz): δ [ppm] = 8.10 (bs, 4H, NH_3), 2.73 (m, 4H), 1.56 (m, 4H), 1.32 – 1.28 (m, 6H).

1,8-diaminooctane dihydrochloride: ^{1}H NMR (DMSO-d_6, 300 MHz): δ [ppm] = 7.30 (bs, 6H, NH_3), 2.70 (t, J = 7.3 Hz, 4H), 1.52 (m, 4H), 1.27 (m, 8H). These chemical shifts match literature: (DMSO-d_6) δ [ppm] = 8.04 (bs, 6H, NH_3), 2.73 (m, 4H), 1.55 (m, 4H), 1.27 (bs, 8H).[42]

1,9-diaminononane dihydrochloride: ^{1}H NMR (DMSO-d_6, 300 MHz): δ [ppm] = 8.04 (bs, 6H, NH_3), 2.73 (m, 4H), 1.55 (m, 4H), 1.27 (m, 10H).

1,10-diaminodecane dihydrochloride: ^{1}H NMR (DMSO-d_6, 300 MHz): δ [ppm] = 8.08 (bs, 6H, NH_3), 2.71 (m, 4H), 1.55 (m, 4H), 1.26 (m, 12H). These chemical shifts match literature: (DMSO-d_6) δ [ppm] = 7.99 (bs, 6H, NH_3), 2.74 (t, 4H), 1.51 (m, 4H), 1.26 (bs, 12H).[42]

1,8-diamino-3,6-dioxaoctane dihydrochloride: ^{1}H NMR (DMSO-d_6, 300 MHz): δ [ppm] = 7.55 (bs, 6H, NH_3), 3.62-3.59 (overlapping signals, 8H), 2.92 (t, J = 5.3, 4H). These chemical shifts match literature: (DMSO-d_6) δ [ppm] = 8.11 (bs, 6H, NH_3), 3.64 (t, 4H), 3.59 (s, 4H), 2.95 (m, 4H).[42]

***N,N*'-dimethylethylenediamine dihydrochloride**: ^{1}H NMR (DMSO-d_6, 300 MHz): δ [ppm] = 9.51 (bs, 4H, NH_3), 3.25 (s, 4H), 2.57 (s, 6H).

***N,N*'-dimethyl-1,6-hexanediamine dihydrochloride**: ^{1}H NMR (D_2O, 400 MHz): δ [ppm] = 3.01 (t, J = 7.6 Hz, 4H), 2.69 (s, 6H), 1.69 (m, 4H), 1.42 (m, 4H). These

chemical shifts match literature: (20 mM phosphate buffer in D_2O) δ [ppm] = 2.90, 2.58, 1.55, 1.39 (no integrations reported).[43]

3.4.3 Salting Out of Water-Miscible Organics by α,ω-Diaminoalkane Dihydrochloride and Alkylamine Hydrochloride Salts

THF or acetonitrile (2.0 g) and distilled water (2.0 g) were mixed together in a graduated cylinder. An appropriate amount of α,ω-diaminoalkane dihydrochloride salt was added to the solution to give a 0.50 molal loading relative to water (1.00 molal for alkylamine hydrochloride salts). The cylinder was capped and inverted 30–50 times to allow for complete dissolution of the salts. Some mixtures required heating to 50 °C to speed up dissolution of the salts, but were cooled to room temperature after dissolution. If a phase separation occurred, then the volumes of the two layers were recorded.

Using the assumption that the top organic layer is comprised primarily of the organic that was salted out and the bottom aqueous contains all other components, the volume of the organic layer was multiplied by the density of the pure organic compound studied to give the mass of organic compound salted out. Comparing this amount to the original mass put into the mixture gave the percentage of organic compound salted out.

3.4.4 Synthesis of Compound 3.1, [(1E,1'E)-*N'*,*N''*-(Butane-1,4-diyl)bis(*N*,*N*-dimethylethanimidamide)]

This procedure was adapted from two previously published synthetic procedures.[44,45] A 100 mL flask was equipped with a condenser and a 1 cm stirring bar and was then placed over a stirplate. 1,4-Diaminobutane (1.14 mL, 11.3 mmol, 1 eq.) and dimethylacetamide dimethylacetal (3.64 mL, 24.9 mmol, 2.2 eq.) were placed into the flask. The reaction mixture was then stirred at 600 RPM and heated to 60 °C. After 2 h the reaction mixture was allowed to cool to room temperature and the resulting methanol was removed under reduced pressure to afford a yellow oil. Purification of the crude product was attempted by performing a bulb-to-bulb distillation using a short-path vacuum condenser. The liquid was transferred over at a maximum temperature of 218 °C (5 mbar) and 2.32 g of a yellow oil was obtained. An impurity (~10:1 product/impurity by ^{1}H NMR spectroscopy) was retained in the oil and by comparing to similar ^{1}H NMR chemical shifts[45] was hypothesized be the di-imidate ester, the mono-amidine/mono-imidate ester, or a mixture of the two. A ^{1}H NMR spectrum is included in Appexdix III.

^{1}H NMR ($CDCl_3$, 400 MHz): δ [ppm] = 3.09-3.19 (m, 4H), 2.79 (s, 12H), 1.80 (s, 6H), 1.45-1.53 (m, 4H). ^{13}C NMR ($CDCl_3$, 100.7 MHz): δ [ppm] = 158.7, 50.0, 37.9, 30.2, 12.3. MS (EI): m/z (%) = 227.22 (3), 226.21 (21), 198.16 (7), 182.17 (7), 141.14 (14), 140.13 (21), 128.11 (10), 127.10 (30), 114.11 (23), 113.11 (28), 112.09 (52), 99.09 (27), 70.07 (45), 56.05 (100). HRMS (EI): calc. for $[M]^+$: 226.2157, found: 226.2161.

3.4.5 Synthesis of Compound 3.6, [1,4-benzendiethanamine dihydrochloride]

The procedure was adapted from a previous literature preparation.[46] 1,4-Phenylene diacetonitrile (0.878 g, 5.62 mmol) was dissolved in 60 mL THF under nitrogen atmosphere. A 1.0 M BH_3·THF solution (40 mL) was added dropwise under nitrogen. The solution was refluxed for 24 h; some white precipitate formed during the reaction.

The solution was cooled to 0 °C and 40 mL of a 1:1 mixture of H_2O:THF was added very slowly dropwise. More white precipitate formed in the mixture. The mixture was warmed to room temperature and the solvents were removed *in vacuo*. The solids were then suspended in 90 mL absolute ethanol and 0.6 mL concentrated H_2SO_4. The mixture was refluxed for 30 min. The ethanol was removed *in vacuo* leaving a concentrated acidic solution. A solution of 1 M $NaOH_{(aq)}$ (15 mL) was added until the solution became basic to litmus paper. Some solid did not completely dissolve. The organic compounds were extracted from the aqueous solution by 3 x 150 mL chloroform extractions. The combined extracts were dried over $MgSO_4$ and the solvents were removed *in vacuo* to yield a yellow liquid which was used without further purification. ^{1}H NMR ($CDCl_3$, 400 MHz): δ [ppm] = 7.11 (s, 4H), 2.95 (t, 4H), 2.72 (d, 4H), 1.25, (bs, 4H, NH_2). These chemical shift match the literature: 7.11 (s, 4H), 2.92 (t, 4H), 2.69 (d, 4H), 1.08, (bs, 4H, NH_2).[46]

The yellow liquid was mixed with 100 mL chloroform and 12.0 mL of 2.0 M HCl in diethyl ether, forming a white precipitate. The solvent was removed *in vacuo* to yield

white solids. The solids were recrystallized from hot methanol to give 0.462 g of a white powder (35 % yield, m.p. >250 °C).

^{1}H NMR (D_2O, 400 MHz): δ [ppm] = 7.32 (s, 4H), 3.23 (t, J = 7.3 Hz, 4H), 2.98 (t, J = 7.3 Hz, 4H). Reference: 7.35 (s, 4H), 3.29 (t, J = 7.6 Hz, 4H), 3.00 (t, J = 7.6 Hz).[47] ^{13}C NMR (D_2O, 100.7 MHz): δ [ppm] = 135.6, 129.4, 40.5, 32.3.

3.4.6 Synthesis of Compound 3.10, [*N*1,*N*1'-(Butane-1,4-diyl)bis(*N*1,*N*3,*N*3-trimethylpropane-1,3-diamine) (hexa-methylated spermine)]

The procedure was adapted from a previous literature method.[28] Spermine (2.02 g, 10 mmol, 1.0 eq.) was placed in a 250 mL round-bottom flask and dissolved in 40 mL water. Afterwards, 9.72 mL (120 mmol, 12.0 eq.) formaldehyde solution (37% in H_2O) and 13.7 mL (240 mmol, 24.0 eq.) acetic acid were added and the solution was allowed to stir at room temperature for 15 min. Zn powder (7.84 g, 120 mmol, 12 eq.) was then added in small portions, which resulted in gas formation. A cold water bath was used to keep the temperature in the flask under 40 °C. After complete addition, the reaction mixture was vigorously stirred for 16 h at room temperature. Thereafter, 20 mL of aqueous NH_4OH was added and the product was extracted from the aqueous phase with ethyl acetate in a separatory funnel (3 x 25 mL).

The combined organic layers were dried over $MgSO_4$; the solution was filtered through filter paper and the solvents were then removed under reduced pressure. The

crude product was purified by a bulb-to-bulb distillation using a short-path vacuum condenser. The product was transferred over at a maximum temperature of 154 °C (5 mbar) to yield 1.3 g (45 % yield) of a yellow oil. A ^{1}H NMR spectrum is included in Appendix III.

^{1}H NMR ($CDCl_3$, 400 MHz): δ [ppm] = 2.37-2.30 (m, 8H), 2.29-2.23 (m, 4H), 2.22 (s, 12H), 2.20 (s, 6H), 1.68-1.57 (m, 4H), 1.47-1.38 (m, 4H). ^{13}C NMR ($CDCl_3$, 100.7 MHz): δ [ppm] = 58.0, 57.8, 55.8, 45.6, 42.3, 25.7, 25.3. IR (film, NaCl): [cm^{-1}] = 2943 (s), 2812 (s), 2762 (s), 1459 (m), 1375 (w), 1303 (w), 1256 (w), 1212 (w), 1154 (w), 1122 (w), 1097 (w), 1042 (m), 967 (w), 834(w). MS (EI): m/z (%) = 287.32 (7), 286.31 (41) [M]+, 98.08 (28), 86.08 (44), 85.07 (100), 84.07 (41). HRMS (EI): calc. for $[M]^{+}$: 286.3097, found: 286.3091.

3.4.7 Synthesis of Compound 3.11, [1,1',1''-(Benzene-1,3,5-triyl)tris(*N*,*N*-dimethylmethanamine)]

The procedure was adapted from a previous literature method.[30] Dimethylamine in THF (30 mL of 2.0 M solution) was mixed with 75 mL dichloromethane cooled to 0 °C. 1,3,5-Benzenetricarbonyl trichloride (2.334 g, 8.79 mmol) was added dropwise to the stirring solution. The solution evolved a small amount of gas and turned yellow in colour. The solution was slowly warmed to 25 °C and stirred for 18 h.

The solvent was then removed *in vacuo* to leave a green-yellow solid, which was then dissolved in 10 mL of a 1.5 M $KOH_{(aq)}$ solution. The organic compounds were extracted from the alkaline solution by 4 x 30 mL chloroform extractions. The aqueous layer was discarded and the solvents from the combined organic layers were removed under reduced pressure to yield ~2 g of an off-white solid.

The intermediate solid (2.074 g) was dissolved in 200 mL of THF. The solution was cooled to 0 °C and 47 mL of 2.0 M $LiAlH_4$ in THF was added via dropping funnel. After the initial evolution of some gas, the solution was heated to reflux with stirring for 7 h. After the reaction was complete, the contents were cooled to 0 °C. Excess $LiAlH_4$ was neutralized by slowly adding 3.6 mL of H_2O dropwise, followed by 3.6 mL of 15% $NaOH_{(aq)}$ dropwise, and finally 10.8 mL of H_2O dropwise with vigorous stirring. The solution was then slowly warmed to 25 °C and stirred for 18 h. Precipitated solids were then washed with THF and removed from the solution via vacuum filtration. The organic liquid was dried with $MgSO_4$ and the solvents removed *in vacuo* to yield 1.845 g of a clear brown liquid. An impurity (~25:1, product/impurity) was observed in the ^1H NMR spectrum. The chemical shifts of this impurity matched those of BHT inhibitor found in THF.[48] Purification of the product was attempted using a bulb-to-bulb distillation using a short-path vacuum condenser. The liquid was transferred over at a maximum temperature of 111 °C (5 mbar), but the BHT impurity was also carried over into the distillate (b.p. 265 °C at 1.01 bar,[49] b.p. at 5 bar: ~118 °C).

^{1}H NMR ($CDCl_3$, 400 MHz): δ [ppm] = 7.13 (s, 3H), 3.40 (s, 6H), 2.23 (s, 18H). Reference: 7.15 (s, 3H), 3.39 (s, 6H), 2.22 (s, 18H).[50] ^{13}C NMR ($CDCl_3$, 100.7 MHz): δ [ppm] = 138.9, 128.8, 64.6, 45.5. HRMS (EI): calc. for $[M]^+$: 249.2206, Expected = 249.2205.

3.4.8 Synthesis of Compound 3.12, [1,1',1''-(Cyclohexane-1,3,5-triyl)tris(*N*,*N*,-dimethylmethanamine)]

Parts of this procedure were adapted from previous literature methods.[31,51] 1,3,5-Cyclohexanetricarboxylic acid (mixture of cis/trans, confirmed by ^{1}H NMR spectroscopy) (1.995 g, 9.2 mmol) was taken up in 40 mL dichloromethane to create a suspension. Oxalyl chloride (2.6 mL, 30.7 mmol) and one drop of anhydrous DMF were added to the solution. The solution was refluxed for 3 h, giving a yellow solution with white precipitate. The mixture was cooled to room temperature and the solvent was removed *in vacuo* leaving a solid which contained both the desired 1,3,5-cyclohexane tricarbonyl trichloride and unwanted salts. ^{1}H NMR (400 MHz, $CDCl_3$): δ [ppm] = 2.88 (t, J = 9 Hz, 3H), 2.69 (d, J = 13 Hz, 3H), 1.43 (q, J = 13 Hz, 3H).

The solid mixture was taken up in 50 mL THF and cooled to 0 °C. A 2.0 M dimethylamine solution in THF (35 mL) was added. The solution was warmed to room temperature and stirred for 18 h. The solvent was then removed *in vacuo* leaving a yellow solid. The solid was taken up in a solution of 2.2 g KOH in 20 mL H_2O. Organic contents

were then extracted with 3 x 40 mL chloroform washings. The organic washings were collected and the solvent removed *in vacuo* to yield ~2 g of a yellow liquid, *N,N,N',N',N'',N''*-hexamethylcyclohexane-1,3,5-tricarboxamide. ^{1}H NMR (400 MHz $CDCl_3$): δ [ppm] = 3.06 (s, 9H), 2.92 (s, 9H), 2.65 (q, J = 8 Hz, 3H), 1.86 (t, J = 8 Hz, 6H).

The liquid was dissolved in 80 mL THF and cooled to 0°C. An amount of 2.0 M $LiAlH_4$ in THF solution (58 mL, 116 mmol) was added dropwise to the solution. The solution was refluxed for 6 h and then cooled to 0 °C. The excess $LiAlH_4$ was quenched by addition of 4.4 mL H_2O, 4.4 mL 15 % $NaOH_{(aq)}$, and 13.2 mL H_2O. The solution was warmed to room temperature and stirred for 12 h. The precipitate was filtered off and washed with THF. The washings were combined with the original solution and dried with $MgSO_4$. The solvent was removed *in vacuo* to yield a yellow liquid. Purification of the liquid was attempted by performing a bulb-to-bulb distillation using a short-path vacuum condenser. The liquid was transferred over at a maximum temperature of 122 °C (5 mbar) affording 2.35 g of a faintly yellow liquid. The ^{1}H NMR spectrum showed that a small impurity was retained during the distillation in a ratio of roughly 20:1 product/impurity. The compound was assigned as residual BHT inhibitor from THF by ^{1}H NMR chemical shifts[48] and UV-Vis spectroscopy (λ_{max} = 277 nm in MeCN, Reference: λ_{max} = 279 nm in MeCN).[52] Crystalline solids of the product later formed upon cooling (m.p. 43 °C, uncorrected) and a structure was obtained by X-ray crystallography (see Appendix IV).

The varying ^{1}H NMR chemical shifts of cis/trans mixture of the starting material suggested that the product should also contain such a mixture. Several peaks of similar shape, but differing intensity, neighboured each other in the ^{1}H NMR spectrum of the product mixture.

cis,*cis*-1,3,5-Cyclohexanetricarboxylic acid: ^{1}H NMR (DMSO-d_6) δ [ppm] = 9.86 (bs, 3H), 2.36 (br t, 3H), 2.09 (br d, J = 12.8 Hz, 3H), 1.23 (q, J = 12.2 Hz, 3H).[53]

cis,*trans*-1,3,5-Cyclohexanetricarboxylic acid: ^{1}H NMR (DMSO-d_6) δ [ppm] = 12.28 (s, 3H), 2.81 (t, J = 2.2 Hz, 1H), 2.35 (tt, J = 12.4 Hz, 2H), 2.16 (d, J = 13 Hz, 2H), 2.04 (d, J = 13 Hz, 1H), 1.41 (dt, J = 13.2 Hz, J = 5 Hz, 2H), 1.33 (q, J = 12.7 Hz, 1H).[54]

^{1}H NMR ($CDCl_3$, 400 MHz): δ [ppm] = 2.18 (s, 18H), 2.07 (d, J = 7.0 Hz, 6H), 1.89 (d, J = 12.3 Hz, 3H), 1.52, (m, J= 7.1 Hz, 3H), 0.48 (q, J = 12.2 Hz, 3H). ^{13}C NMR ($CDCl_3$, 100.7 MHz): δ[ppm] = 67.1, 46.1, 37.1, 35.4. HRMS (EI): calc. for $[M]^{+}$: 255.2678, Expected = 255.2674. ^{1}H NMR spectra of the starting material and product mixture is available in Appendix III.

3.5 References

1) K. Sharavanan, H. Komber, D. Fischer, F. Böhme, *Polymer* **2004**, *45*, 2127-2132.

2) S.A. Rice, *J. Am. Chem. Soc*. **1956**, *78*, 5247-5252.

3) C. Wang, X. Luo, H. Luo, D-E. Jiang, H. Li, S. Dai, *Angew. Chem. Int. Ed*. **2011**, *50*, 4918-4922.

4) E.E. Chandler, *J. Am. Chem. Soc*. **1908**, *30*, 694-713.

5) E.Q. Adams, *J. Am. Chem. Soc.* **1916**, *38*, 1503-1510.

6) J. Greenspan, *Chem. Rev.* **1933**, *12*, 339-361.

7) N. Bjerrum, *Z. Physik. Chem*. **1923**, *106*, 219.

8) J.G. Kirkwood, F.H. Westheimer, *J. Chem. Phys*., **1938**, *6*, 506-512.

9) S. Yamazaki, T. Yoshida, Y. Muroga, I. Noda, *Polym. J.* **1999**, *31*, 1237-1242.

10) R.L. Gustafson, A.E. Martell, *J. Am. Chem. Soc*. **1959**, *81*, 525-529.

11) R. von Rometsch, A. Marxer, K. Miescher, *Helv. Chim. Acta* **1951**, *34*, 1611-1618.

12) D.E. Leyden, J.M. McCall Jr., *J. Phys. Chem.* **1971**, *75*, 2400-2402.

13) F. Basolo, R.K. Murmann, *J. Am. Chem. Soc*. **1952**, *74*, 5243-5246.

14) A. Gero, *J. Am. Chem. Soc*. **1954**, *76*, 5158-5159.

15) H. Ohtaki, M. Maeda, *Bull. Chem. Soc. Jpn*. **1973**, *46*, 2052-2056.

16) N.S. Hush, *J. Chem. Soc*. **1953**, 684-691.

17) *Gaussian 03, Revision C.02*, M.J. Frisch, G.W. Trucks, H.B. Schlegel, G.E. Scuseria, M.A. Robb, J.R. Cheeseman, J.A. Montgomery, Jr., T. Vreven, K.N. Kudin, J.C. Burant, J.M. Millam, S.S. Iyengar, J. Tomasi, V. Barone, B. Mennucci, M. Cossi, G. Scalmani, N. Rega, G.A. Petersson, H. Nakatsuji, M. Hada, M. Ehara, K. Toyota, R. Fukuda, J. Hasegawa, M. Ishida, T. Nakajima, Y. Honda, O. Kitao, H. Nakai, M. Klene, X. Li, J.E. Knox, H.P. Hratchian, J.B. Cross, V. Bakken, C. Adamo, J. Jaramillo, R. Gomperts, R.E. Stratmann, O. Yazyev, A.J. Austin, R. Cammi, C. Pomelli, J.W. Ochterski, P.Y. Ayala, K. Morokuma, G.A. Voth, P. Salvador, J.J. Dannenberg, V.G. Zakrzewski, S. Dapprich, A.D. Daniels, M.C. Strain, O. Farkas, D.K. Malick, A.D. Rabuck, K. Raghavachari, J.B. Foresman, J.V. Ortiz, Q. Cui, A.G. Baboul, S. Clifford, J.

Cioslowski, B.B. Stefanov, G. Liu, A. Liashenko, P. Piskorz, I. Komaromi, R.L. Martin, D.J. Fox, T. Keith, M.A. Al-Laham, C.Y. Peng, A. Nanayakkara, M. Challacombe, P.M.W. Gill, B. Johnson, W. Chen, M.W. Wong, C. Gonzalez, J.A. Pople, Gaussian, Inc.: Wallingford CT, **2004**.

18) C.M. Breneman, K.B. Wiberg, *J. Comput. Chem*. **1990**, *11*, 361-373.

19) R. Hoffmann, A. Imammura. W.J. Hehre, *J. Am. Chem. Soc*. **1968**, *90*, 1499-1509.

20) R.W. Alder, R.J. Arrowsmith, A. Casson, R.B. Sessions, E. Heilbronner, B. Kovač, H. Huber, M. Taagepera, *J. Am. Chem. Soc*. **1981**, *103*, 6137-6142.

21) J. Gębicki, A. Marcinek, C. Stradowski, *J. Phys. Org. Chem*. **1990**, *3*, 606-610.

22) Y. Geng, L. S. Romsted, *J. Phys. Chem. B* **2005**, *109*, 23629-23637.

23) X. Yang, Y-J. Fu, X-B. Wang, P. Slaviček, M. Mucha, P. Jungwirth, L-S. Wang, *J. Am. Chem. Soc.* **2004**, *126*, 876-883.

24) M. Demireva, J.T. O'Brien, E.R. Williams, *J. Am. Chem. Soc*. **2012**, *134*, 11216-11224.

25) E. Ciuffarin, M. Isola, P. Leoni, *J. Org. Chem*. **1981**, *46*, 3064-3070.

26) A. Domínguez, A. Fernández, N. González, E. Iglesias, L. Mentenegro, *J. Chem Educ*. **1997**, *74*, 1227-1231.

27) R. Bergeron, W.R. Weimar, Q. Wu, Y. Feng, J.S. McManis, *J. Med. Chem*. **1996**, *39*, 5257-5266.

28) R.A. da Silva, I.H.S. Estevam, L.W. Bieber, *Tetrahedron Lett*. **2007**, *48*, 7680-7682.

29) J.W. Bunting, D. Stefanidis, *J. Am. Chem. Soc*. **1990**, *112*, 779-786.

30) E.G. Knapick, P. Ander, J.A. Hirsch, *Synthesis* **1985**, 58-60.

31) K. Janabusa, A. Kawakami, M. Kimura, H. Shirai, *Chem. Lett*. **1997**, 191-192.

32) F. Barzagli, F. Mani, M. Peruzzini, *Energy Environ. Sci*. **2009**, *2*, 322-330.

33) D.J. Heldebrant, P.K. Koech, T. Ang, C. Liang, J.E. Rainbolt, C.R. Yonker, P.G. Jessop, *Green Chem*. **2010**, *12*, 713-721.

34) G. Sartori, D.W. Savage, *Ind. Eng. Chem. Fundam*. **1983**, *22*, 239-249.

35) A.K. Chakraborty, G. Astarita, K.B. Bischoff, *Chem. Eng. Sci.* **1986**, *41*, 997-1003.

36) R.J. Hook, *Ind. Eng. Chem. Res*., **1997**, *36*, 1779-1790.

37) J-Y. Park, S.J. Yoon, H. Lee, *Environ. Sci. Technol*. **2003**, *37*, 1670-1675.

38) G. Puxty, R. Rowland, A. Allport, Q. Yang, M. Brown, R. Burns, M. Maeder, M. Attalla, *Environ. Sci. Technol*. **2009**, *43*, 6427-6433.

39) P.D. Vaidya, E.Y. Kenig, *Chem. Eng. Technol*. **2007**, *30*, 1467-1474.

40) H.P. Mangalapally, H. Hasse, *Chem. Eng. Sci.* **2011**, *66*, 5512-5522.

41) T. Robert, S.M. Mercer, T.J. Clark, B.E. Mariampillai, P. Champagne, M.F. Cunningham, P.G. Jessop, *Green Chem.* **2012**, *14*, 3053-3062.

42) D.E. Kiely, A. Vishwanathan, B.P. Jarman, M. Manley-Harris, *J. Carbohydr. Chem.* **2009**,*28*, 348-368.

43) D. Ma, P.Y. Zavalij, L. Isaacs, L. *J. Org. Chem.* **2010**, *75*, 4786-4795.

44) M.W. Scoggins, *J. Chromatogr. Sci.* **1975**, *13*, 146-148.

45) J.R. Harjani, C. Liang, P.G. Jessop, *J. Org. Chem.* **2011**, *76*, 1683-1691.

46) J.J.E. Moreau, B.P. Pichon, C. Bied, M.W.C. Man, *J. Mater. Chem.* **2005**, *15*, 3929-3936.

47) E. Keinan, *Frictionless Molecular Rotary Motors*. WO Patent 2008/096360 A2, 08/14, **2008**.

48) H.E. Gottlieb, V. Kotlyar, A. Nudelman, *J. Org. Chem.* **1997**, *62*, 7512-7515.

49) D.M. Levermore, M. Josowicz, W.S. Rees Jr., J. Janata, *Anal. Chem.* **2001**, *73*, 1361-1365.

50) S.A. Young, G.E. Kiefer, L.R. Depalatis, *Targeting Chelants and Chelates*, WO Patent 2006/20779 A2, 02/23, **2006**.

51) I. Tomatsu, C.F.C. Fitié, D. Byelov, W.H. de Jeu, P.C.M.M. Magusin, M. Wübbenhorst, R.P.Sijbesma, *J. Phys. Chem. B* **2009**, *113*, 14158-14164.

52) L. Valgimigli, G. Brigati, G.F. Pedulli, G.A. DiLabio, M. Mastragostino, C. Arbizzani, D.F. Pratt, *Chem. Eur. J.* **2003**, *9*, 4997-5010.

53) T-L. Chan, Y-X. Cui, T.C.W. Mak, R-J. Wang, H.N.C. Wong, *J. Cryst. Spectrosco.* **1991**, *21*, 297-308.

54) K.E. Pryor, G.W. Shipps Jr., D.A. Skyler, J. Reebek Jr., *Tetrahedron* **1998**, *54*, 4107-4124.

Chapter 4

Recycling of Homogeneous Catalysts Using Switchable Water

4.1 Introduction

Homogeneous catalysts are often more active and selective than heterogeneous catalysts but are far more difficult to separate from the product. The development of new means to separate, recover, and recycle homogeneous catalysts is an important area of research for both industry and academia alike.[1,2] One approach, already industrialized in a few cases, is performing catalysis in an aqueous/organic biphasic mixture.[3-5] Such reactions involve the dissolution of a catalyst into the aqueous phase and the dissolution of the reagents into the organic solvent. The small partitioning of the reagent into the catalyst-bearing aqueous phase allows the reaction to proceed. Aqueous/organic biphasic systems are currently used for the industrial hydroformylation of short alkenes such as propene.[3] The hydroformylation system utilizes transition metals ligated by sulfonated phosphines to increase the water solubility of the catalyst, causing it to reside in the aqueous phase. After the reaction is completed, the product (organic) phase is decanted and the aqueous catalyst-bearing phase is used again.

Even though these aqueous/organic biphasic catalytic systems have the advantage of facile separation of catalyst from product, they can suffer from slow reaction rates. These result from the catalyst and the reactants being in two different phases, especially when the reactant (such as 1-octene or styrene) is so hydrophobic that its concentration in the aqueous phase is extremely low. One solution is to manipulate the hydrophilicity of

the catalyst by protonation/deprotonation of the ligands. This allows a reaction to be run in a monophasic organic solvent and the catalyst is later drawn into an aqueous phase, away from the products, using a pH change. This pH change is often enacted by introducing CO_2 into the aqueous phase (Fig 4.1a).[6-10] Similarly, catalysts which can be drawn into an aqueous phase based on temperature changes have also been explored (Fig. 4.1b).[11-13] Many of the ligands utilized in these examples however were tailor made and are thus not available on a commercial scale to make the system industrially viable. Another solution to this problem is to design a trigger to make the aqueous and organic phases merge into one phase during the catalysis and then to separate into two phases again after the reaction is complete. Demonstrations of this concept using thermomorphic liquids[14-16] (Fig. 4.1c) and analogously with fluorous compounds[17] have been performed. Unfortunately, many of these examples require the use of expensive and/or environmentally harmful components in the solvent system. CO_2-based organic/aqueous tunable solvents (OATS)[18-20] have also been previously published (Fig 4.1d). However, the OATS method required moderately high CO_2 pressures. Described herein is a method for achieving monophasic catalysis and biphasic separation in a similar vein to those methods. However through a new method using switchable water, these outcomes have been realized using mild reaction conditions, common reagents, with the reversible separations being performed at only 1 bar of CO_2.

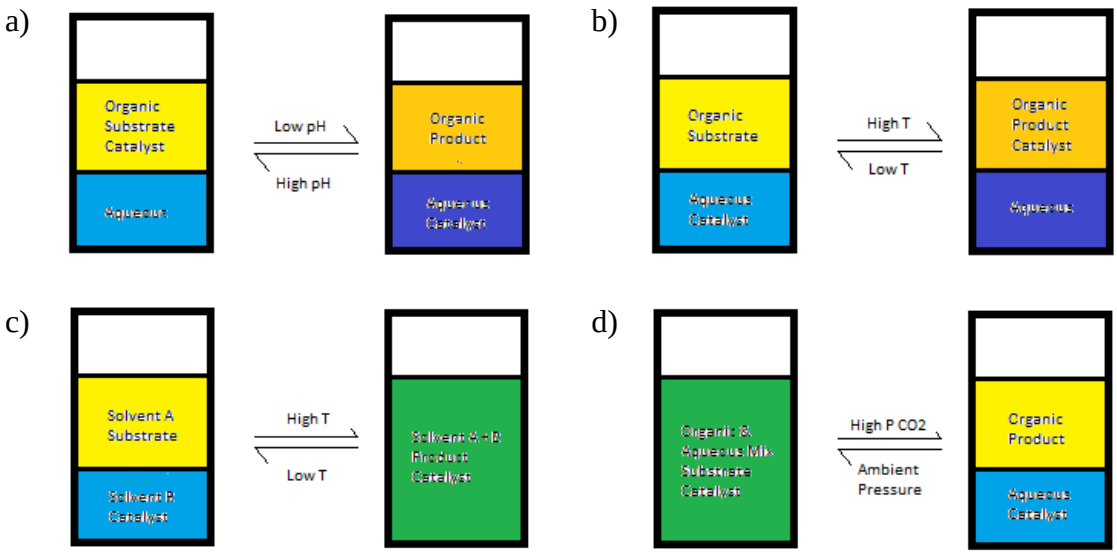

Fig. 4.1. Conceptual schemes of several examples of methods to achieve monophasic catalysis followed by biphasic separation of catalyst from product. a) Catalyst complexes with pH dependent aqueous solubility b) Catalyst complexes with temperature dependent aqueous solubility c) Catalysis performed in a thermomorphic liquid system d) Catalysis performed in an organic/aqueous tunable solvent system (OATS).

These results (except portions of sections 4.1, 4.2.4 & 4.2.5) have previously appeared in *Catalysis Science & Technology* **2012**, *2*, 1315-1318. The structure of the original manuscript has been modified to better reflect the progression of the study.

4.2 Results and Discussion

4.2.1 General Concept

We proposed that such switching between monophasic and biphasic aqueous/organic systems could be achieved at ambient pressure if the aqueous phase was

'switchable water'. Several combinations of switchable water and a water-miscible organic solvent were found to be a monophasic liquid mixture in the absence of CO_2, but a biphasic mixture in its presence. The proposed catalytic process involves homogeneous catalysis (such as hydroformylation of an alkene) in the aqueous/organic monophasic mixture, after which CO_2 is added (Fig. 4.2). The CO_2 would react with the amine, cause a rise in the ionic strength of the solution, and thereby trigger the salting out of both the organic solvent and the product from the aqueous phase. If a suitably hydrophilic catalyst is selected, the catalyst would then remain in the aqueous phase, isolated from the products of reaction. After decantation of the organic, product-bearing phase, the removal of CO_2 from the catalyst-bearing aqueous phase would then regenerate a low ionic strength aqueous phase that could now accept fresh reagents and organic solvent and the reaction could be repeated. The presence of the organic co-solvent (which is later salted out) would allow for higher loading of hydrophobic substrates than with water alone.

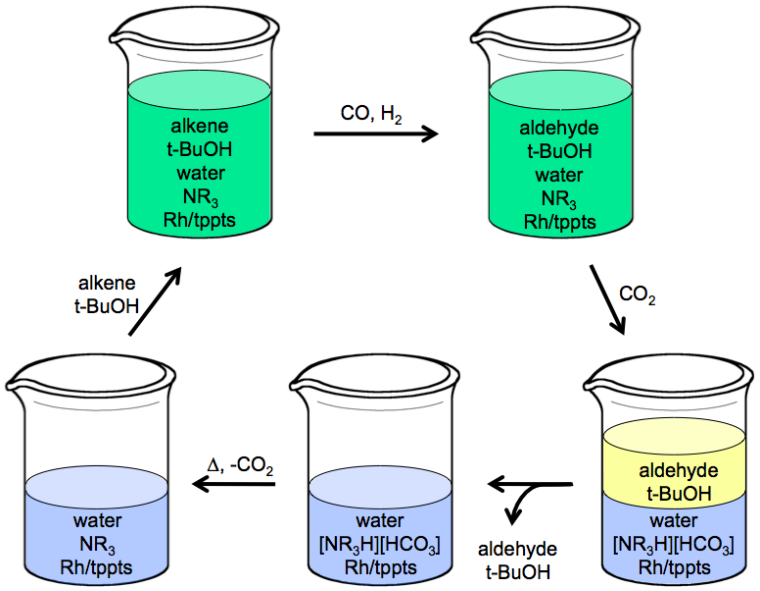

Fig. 4.2. Conceptual scheme of a monophasic hydroformylation and biphasic separation in a liquid mixture of switchable water and *tert*-butanol, the water-miscible organic co-solvent.

4.2.2 Initial Hydroformylation Studies

The hydroformylation of styrene was an attractive model system because its aldehyde products have potential use in pharmaceutical and fine chemical production and its water solubility is low[21] which would make a traditional aqueous/organic biphasic reaction inefficient. In Chapters 2 and 3 it was demonstrated that THF in a switchable water co-solvent mix could easily be forced out of the aqueous solution upon the addition of CO_2. However, initial studies into the hydroformylation of styrene found that this weakly coordinating organic solvent likely hindered the reaction as the initial conversion

of styrene never exceeded 10 % and quickly decreased to < 1 % upon recycling of the catalyst. Therefore other water-miscible organic solvents that could solubilize styrene and still later be salted out by our trialkylammonium bicarbonate salts were pursued. Preliminary tests showed that *tert*-butanol was an appropriate organic solvent choice. Ultimately the initial solvent system run was comprised of *tert*-butanol, water and 0.8 molar *N,N,N',N'*-tetramethyl-1,4-diaminobutane (TMDAB, Compound **2.3**).

With an established solvent system, hydroformylations and recycling studies were performed. Styrene, was reacted in the solvent system with synthesis gas (syngas) in the presence of a rhodium pre-catalyst ($[Rh(COD)Cl]_2$) and the sodium salt of sulfonated triphenylphosphine (TPPTS, $P(C_6H_4$-*m*-$SO_3Na)_3$) at 100 °C for 3 h (Fig. 4.3). After the reaction, CO_2 was bubbled through the solution, increasing the ionic strength and generating a biphasic system where the catalyst resided in the aqueous phase and the product resided in the *tert*-butanol phase. The organic phase could then be removed and analyzed. The low ionic strength form of the aqueous phase was then regenerated by expelling CO_2. This was achieved by heating to 65 °C and bubbling an inert gas through the solution. Under an inert atmosphere, a fresh supply of organic solvent and substrate was then added and the reaction was repeated (Table 4.1). Upon a single preliminary screening, aldehyde products were obtained with good conversions and selectivities over multiple cycles with varied regioselectivity (branched or linear, B:L). Unfortunately, deactivation of the catalyst occurred as the initial system suffered from decreasing conversions over the three cycles of the reaction.

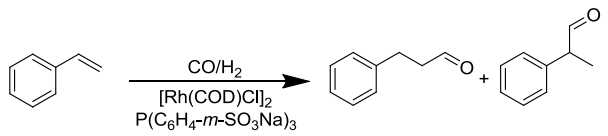

Fig. 4.3. Reaction scheme of the hydroformylation of styrene using a Rh pre-catalyst and water soluble phosphine, TPPTS.

Table 4.1. Conversions, selectivities, and regioselectivities (B:L) for the initial hydroformylation of styrene in a monophasic switchable water/*tert*-butanol mixture followed by separation in a biphasic switchable water/*tert*-butanol mixture. The switch between monophasic and biphasic is achieved through CO_2-induced phase separation.[a]

Cycle	% Conversion	% Aldehyde	B:L
1	98	98	10.2
2	96	98	5.7
3	63	99	4.7

[a] Compound **2.3** was used as the additive.

4.2.3 Optimization of the Hydroformylation Reaction

Deactivation of the catalyst may be due to the oxidation of the TPPTS, as was observed in ^{31}P NMR spectra, (Fig. 4.4, phosphine oxide peak found at δ ~30 ppm (Reference: 33.4 ppm[22] 34.5 ppm,[23] 31.6 ppm (2:1 H_2O/MeCN)[24]). Despite best efforts to remove molecular oxygen from the system, oxidation was still likely due to molecular oxygen as it is often found as an impurity in synthesis gas.[25] It is also possible that the

bidentate diamine, TMDAB, was contributing to catalyst deactivation. Leaching of TPPTS into the organic phase was likely negligible as no phosphines were detected in the salted out organic phases using ^{31}P NMR spectroscopy (Fig. 4.4). To test the effects of the amine additive upon the reaction, a single screening was performed using 1.4 molar of a monoamine, *N*,*N*-dimethylethanolamine (DMEA, Compound **2.1**) as the switchable water additive. Even with DMEA however, conversions decreased on the third cycle (Table 4.2). Additonally, a significant loss of aqueous phase volume during the later cycles was observed when DMEA was used. This was likely due to the greater potential of DMEA additive to partition into the organic phase than the TMDAB additive would upon CO_2 treatment as shown by model systems analyzed using ^{1}H NMR spectroscopy (Table 4.3).

It is essential for a switchable water additive to be retained in the aqueous phase for three reasons. 1) The retention of these ionogens serves to maintain a highly polar aqueous environment (when treated with CO_2) which would minimize the water content of the organic phase upon salting out. 2) Without high additive retention the resulting decrease in the aqueous phase volume would contribute to leaching of the catalyst into the organic solvent. 3) Additives must be retained so that sufficient ionic strength can be generated during the later cycles to afford salting out of the product-containing organic phases. A discoloration of the product-containing organic phase was observed and suggests that there was significant leaching of the catalyst over the cycles when DMEA was used (Fig. 4.5 & Table 4.4).

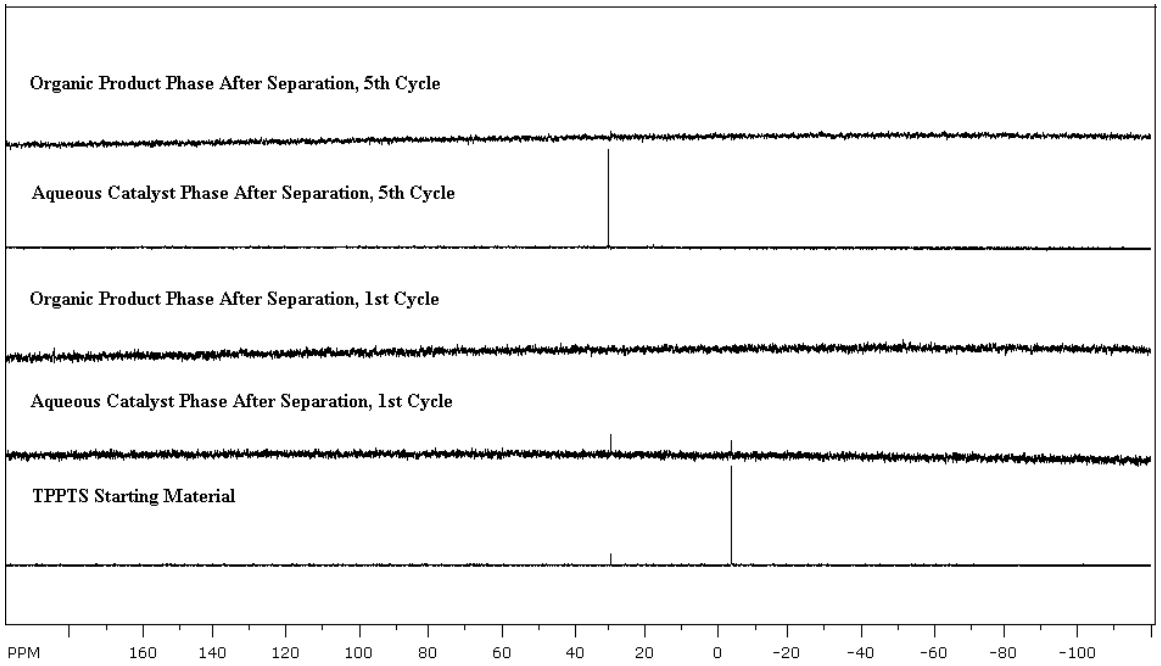

Fig. 4.4. ^{31}P NMR spectra of TPPTS starting material versus organic and aqueous layer after CO_2-induced separation from the first and fifth cycles of Table 4.5.

Table 4.2. Conversions, selectivities, and regioselectivities (B:L) for the hydroformylation of styrene in a monophasic switchable water/*tert*-butanol mixture followed by separation in a biphasic switchable water/*tert*-butanol mixture. The switch between monophasic and biphasic is achieved through CO_2-induced phase separation.[a]

Cycle	% Conversion	% Aldehyde	B:L
1	95	99	8.8
2	96	99	6.5
3	74	98	5.7

[a] Compound **2.1** was used as the additive.

Table 4.3. A comparison of the amount of *tert*-butanol salted out from 1:1 w/w solutions of *tert*-butanol and water with varied loadings of amines after 30 min of CO_2 treatment and the % retention of the amine in the aqueous phase.

Additive	Loading	% *tert*-butanol Removed[a]	% Additive Retained[a]
DMEA, **2.1**	1.4 molar	85 ± 1%	79 ± 6%
TMDAB, **2.3**	0.8 molar	81 ± 2%	91 ± 2%

[a] Determined by ^{1}H NMR spectroscopy. Experiments were performed in triplicate and standard deviations are reported as error.

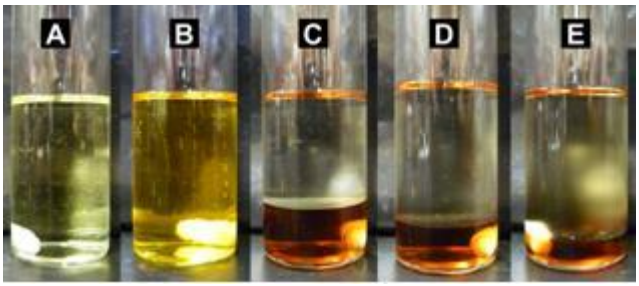

Fig. 4.5. Photographs of the cycling procedure for the hydroformylation of styrene using 1.40 molar DMEA (Compound **2.1**) as the switchable water additive. a) Solution before reaction. b) Solution after the reaction. c) Biphasic mixture after 30 min CO_2 treatment. d) Biphasic mixture after 30 min CO_2 treatment (2nd cycle). e) Biphasic mixture after 30 min CO_2 treatment (3rd cycle).

Table 4.4. The concentration (mg/L) of leached rhodium in the organic phase after separation by switchable water, as determined by ICP-MS. Samples were acquired from a typical reaction using DMEA as the switchable water additive.

Cycle 1	Cycle 2	Cycle 3
1.07 ± 0.04	3.63 ± 0.04	10.12 ± 0.25

It was thus prudent to explore the TMDAB system once more, but the initial phosphine loading was increased to hopefully overcome any potential catalyst deactivation by ligand oxidation. This modified system was able to be recycled for four runs with minimal loss of conversion and selectivity to the aldehyde products with only a slight loss of activity on the fifth cycle (Table 4.5, Entry 1). With a greater initial phosphine loading and therefore a greater initial ionic strength, the amount of styrene loaded into the system had to be decreased slightly so that it would remain soluble in the aqueous solvent. Because of the lower substrate loading, the reaction time was also decreased accordingly from 3 h to 1.5 h. Although high conversions were often observed for this system, some unreacted substrate was always observed in the gas chromatograms. The presence of unreacted material in all runs confirmed that catalyst activity was consistent until the final run and the substrate/catalyst ratio was appropriate. If quantitative conversions were obtained, no information about catalyst stability could be solicited. For example, with too high a catalyst loading, affording a low substrate/catalyst ratio, a large amount of catalyst deactivation might have occurred in the recycling stages,

but a large initial catalyst concentration would still have allowed for the reaction to be run to quantitative conversion. For Entry 1 of Table 4.5, consistent, but slightly below quantitative, conversions demonstrated that up until the final run, the catalytic activity was similar to the previous runs. Despite the presence of high concentrations of amine in the reaction mixture, no aldol by-products for these reactions were observed. A control experiment with no TPPTS in solution afforded poor conversion (< 6%) with a B:L ratio of roughly 0.8.

Table 4.5. Conversions, selectivites, and regioselectivites (B:L) for the hydroformylation of styrene in a modified (greater initial phosphine loading/lower substrate loading) monophasic water/tert-butanol mixture followed by separation in a biphasic water/tert-butanol mixture. The switch between monophasic and biphasic is achieved using the CO_2-induced phase separation of switchable water.[a]

Entry	Cycle	% Conversion	% Aldehyde	B:L
1[b]	1	99	97	7.5
	2	99	98	5.5
	3	99	99	5.2
	4	97	98	5.1
	5	73	99	5.2
2[c]	1	84	99	3.0
	2	77	99	3.4
	3	90	98	3.8
	4	83	99	3.8
	5	52	95	2.9

[a] Compound **2.3** was used as the additive. [b] Performed at 10 bar synthesis gas. [c] Performed at 5 bar synthesis gas.

To further confirm the stability of the catalytic species and the solvent system, the gas uptake for the hydroformylation of styrene over five cycles was monitored (Fig. 4.6). These reactions (Table 4.5, Entry 2) were performed at 5 bar syngas as opposed to 10 bar. There were two observed trends of note. First, the rate of gas uptake was greater than or equal to that of the first cycle for the first four cycles. As the second to fourth cycles of the reaction had faster gas uptake than the first cycle, this may have suggested the formation of a more active catalyst species. Second, a trend of decreasing gas uptake was observed after the second cycle to the fifth cycle with the fifth cycle showing the slowest gas uptake (the third and fourth cycles were quite similar but ultimately slower than the second cycle). This suggested that slight deactivation of the catalyst deactivation was occurring during the cycles but this was not greatly reflected in the % conversion until the fifth cycle.

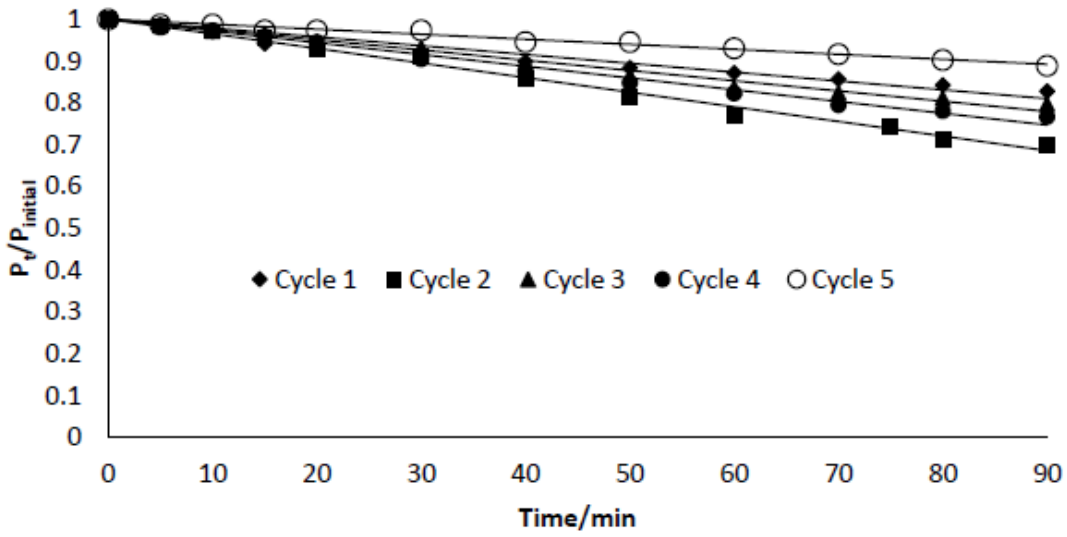

Fig. 4.6. A plot showing the ratio of pressure at time, *t*, over the total initial pressure (5 bar pressure of syngas (1:1 $CO:H_2$)) for the hydroformylation of styrene (Table 4.5, Entry 2).

The leaching of rhodium metal into the organic product phase was again monitored using ICP-MS through three cycles (Table 4.5, Entry 1). With an initial rhodium concentration of approximately 170 mg L^{-1} in solution, the TMDAB system showed low leaching of rhodium into the product-containing organic phase (Table 4.6), further demonstrating the potential utility of this system for catalysis. Of course, any leaching of precious metal catalysts is undesirable for industrial purposes. To this end, future research would have to delve into minimizing catalyst leaching into the organic product phase in conjunction with the development of non-precious metal catalysts.

Table 4.6. The concentration (mg/L) of leached rhodium in the organic phase after separation by switchable water, as determined by ICP-MS. Samples were acquired from Entry 1 of Table 4.5 where compound **2.3** was the additive used.

Cycle 1	Cycle 2	Cycle 3
1.04 ± 0.01	1.13 ± 0.02	1.52 ± 0.04

4.2.4 Regioselectivity Issues

A notable decrease in the branched/linear product ratio (B:L) was observed during the second cycles for all the hydroformylations of styrene with one exception (the lower pressure run, Entry 2 of Table 4.5, but pressure-dependent regioselectivity effects have been well-documented for the hydroformylation reaction[26]). For the latter cycles the regioselectivity remained consistent (Table 4.5, Entry 1). Additionally, as previously noted, gas uptake was found to be greater for cycles 2 through 4 compared to cycle 1. This finding, along with the regioselectivity effects described above, suggested that a change in the active catalyst species was occurring between cycles 1 and 2. Several hypotheses as to what may have happened to the active catalyst species are presented subsequently.

A profound colour change of the solutions occurred during the CO_2-induced phase separations (Fig. 4.7). We suspected that newly formed bicarbonate anions (which first form in solution during the initial introduction of CO_2 after the first hydroformylation) were complexing the rhodium, displacing some phosphine.

Coordination of bicarbonate to rhodium is well known.[27] When CO_2 is later removed from the system (to regenerate the monophasic system), it is possible that some of the bicarbonate remained complexed to the rhodium (as the original bright yellow solution was not completely regenerated). As the ligand system has already then incorporated bicarbonate after the first introduction of CO_2, a plateau of regioselectivity for later cycles is plausible. Introduction of CO_2 into the system before the first hydroformylation (to induce the phase separation) did not cause this colour change. It appeared the post-reaction metal species was susceptible to bicarbonate coordination but not the $[Rh(COD)Cl]_2$ pre-catalyst. Adding a bicarbonate salt to the system at the beginning is not possible due to the changes it causes in the phase behaviour of the system.

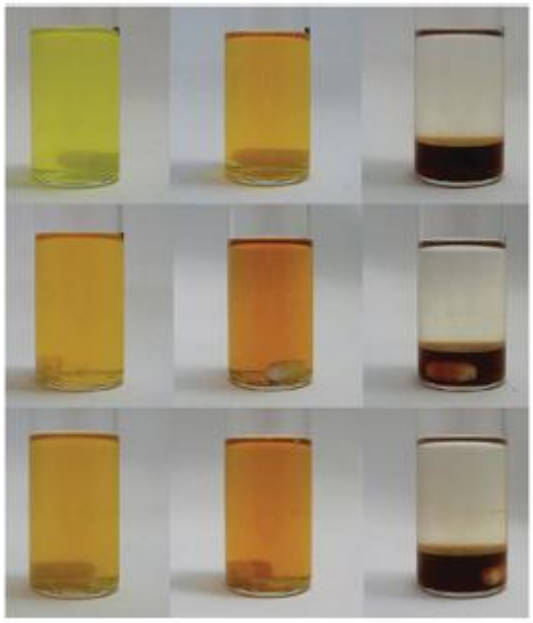

Fig. 4.7. Photographs of the hydroformylation of styrene in a mixture of *tert*-butanol and switchable water where compound **2.3** was the additive used. (Left) All reagents mixed before reaction or CO_2 treatment. (Centre) After completion of the hydroformylation reaction. (Right) After CO_2 treatment for 45 min. From Top to Bottom: Cycles 1 to 3 using the same catalyst and aqueous phase.

It is also possible that pH effects may have caused the diminished regioselectivity between the first and second cycles and the plateau after the second cycle. pH effects on the regioselectivity of biphasic hydroformylations have been noted previously.[28] When removing CO_2 to regenerate the biphasic system, it is likely that not all of the CO_2 is removed, as has been previously noted in Chapters 2 and 3. This would then prevent the

solvent from completely returning to the initial pH. In fact, the first cycle was performed at pH = 12.1, while subsequent cycles were performed with the pH being around 9.6. As the pH swing is relatively consistent for cycles two to five, this could have lead to the more consistent regioselectivity observed during the latter cycles.

Additionally, we hypothesized that the regioselectivity was diminishing due to the decreasing amount of TPPTS in the system through the cycles as TPPTS was oxidized (as was observed by ^{31}P NMR). In such a case, the regioselectivity would be expected to continually drop throughout the cycles as more and more TPPTS degrades. However such an effect was not observed. In a control experiment it was found that adding fresh TPPTS during the recycle stages (i.e. between cycles 1 and 2, 2 and 3, etc.) still did not maintain the high regioselectivity observed in the first cycle despite replenishment of the phosphine ligand. There was also the potential for a contribution of rhodium nanoparticles to the catalysis, assuming their formation in the system. Such nanoparticle formation was not studied; however work by several groups has previously shown that Rh(0) nanoparticles when used in hydroformylation reactions will in fact form molecular rhodium species and that those species are likely performing the catalysis.[29,30] Any potential nanoparticle formation was very unlikely to be dictating the regioselectivity of the aldehyde products. It is more likely that the presence of complexed bicarbonate and/or pH effects are the greater contributors to the initial drop of regioselectivity between cycles one and two and then the more consistent regioselectivity from cycles two to five.

4.2.5 Additional Catalytic Reactions

The hydroformylation of 1-octene was also briefly studied and showed good conversion and selectivity over three cycles (Table 4.7, Entry 1). The selectivity to the linear isomer over the branched isomer (see L:B, the linear to branched product ratio) is consistent with past literature.[8-10] The pressures used for these experiments were lower than typically used in the literature and slightly higher catalyst loadings were used; as a result the turnover numbers for the system were generally lower than previous examples (i.e. ~300 compared to ~1000).[8-10] The switchable water system afforded an average turnover frequency of 100 h^{-1} while recent work on traditional aqueous/organic biphasic hydroformylations of 1-octene using Rh/TPPTS afforded ~20 h^{-1}.[31]

Table 4.7. Conversions, selectivities, and regioselectivities (L:B) for the hydroformylation of 1-octene and using the switchable water system. $[Rh(COD)Cl]_2$ was used as the pre-catalyst and TPPTS as the ligand.

Cycle	% Conversion	% Aldehyde	L:B
1	99	98	2.0
2	99	99	3.3
3	99	99	3.3

The hydrogenation of styrene was also performed to demonstrate the potential versatility of this catalyst recycling system. Over three cycles, high conversions to

ethylbenzene were observed (94 %, 94 %, and 87 % respectively). No side-products were detected by gas chromatography and thus no selectivity is reported.

4.3 Conclusions

In summary, the first demonstration of using switchable water to conduct homogeneous catalysis in a monophasic solvent mixture and provide subsequent catalyst/product separation in a biphasic solvent mixture was presented. This method did not suffer from the traditional mass transfer issues that accompany biphasic reactions because the system was monophasic during the catalysis. Furthermore it could also tolerate alkenes of lower water solubility than traditional biphasic aqueous/organic catalytic systems. The hydroformylation and hydrogenation reactions performed in switchable water were run at low synthesis or hydrogen gas pressures, on short timescales, and with facile separation of catalyst from product because of CO_2-induced phase separation. Recycling of the catalyst solution was performed with ease by removing CO_2 from the solution by sparging with an inert gas and moderate heating. The Rh/TPPTS catalyst maintained high conversion, product selectivity, and good regioselectivity through recycling. This method for solving the inherent rate limitations of conventional biphasic catalysis did not require high pressure or expensive fluorous or ionic liquid solvents. Overall, the mild reaction conditions, high selectivity, low ligand

loading, and recyclability have made this system an attractive alternative to the previously described aqueous/organic biphasic systems.

4.4 Experimental

4.4.1 General Procedures

Chemicals were used as received, except for styrene, which was passed through an inhibitor remover column (Sigma Aldrich) before use to remove the 4-*tert*-butylcatechol inhibitor. Conversions and selectivities were determined by gas chromatography (Shimadzu GC-17A with an Agilient DB-5 column) using calibration curves. High pressure reactions were performed in 31 mL Parr reaction vessels. NMR spectroscopy was performed using a 400 MHz Bruker instrument. Rhodium analysis was performed using a Varian 820 ICP-MS. pH measurements were taken with a Thermo Scientific Orion 4 Star pH meter.

4.4.2 Reaction & Recycling Procedures

Standard Reaction Conditions: In a glass vial under N_2, 6 mL degassed *tert*-butanol and degassed 4 mL deionized H_2O were mixed. To this solution, 0.50 g of *N,N*-dimethylethanolamine or 0.47 g *N,N,N',N'*-tetramethyl-1,4-diaminobutane was added. Under N_2, triphenylphosphine-3,3',3"-trisulfonic acid trisodium salt hydrate (TPPTS, 21

mg or 54 mg for greater loading runs) and then chloro(1,5-cyclooctadiene)rhodium (I) dimer ($[Rh(COD)Cl]_2$, 1.4 mg) were then dissolved into the mixture to give a clear, yellow solution. The uninhibited styrene (0.15 mL or 0.10 mL for greater phosphine runs) was then pipetted into the aqueous mixture, which remained a single phase. The solution was transferred to a pressure vessel. The vessel was sealed and purged three times with synthesis gas (1:1 $CO:H_2$). The vessel was heated to 100 °C and pressurized to 10 bar of synthesis gas. The reaction was run, with stirring, for 3 h (1.5 h for runs with greater phosphine loading). When 1-octene was reacted, 0.30 mL was used and the reaction was run for 3 h. When the hydrogenation of styrene was performed, 0.10 mL of substrate was reacted under 5 bar of H_2 instead of syngas for 1 h.

After the reaction time, the vessel was cooled to 25 °C and the pressure was released. Under N_2, the golden yellow clear solution was transferred to a glass vial and capped with a rubber septum. A long narrow-gauge steel needle was inserted through the septum into the solution. A second needle was inserted through the septum to act as a gas outlet. CO_2 was introduced into the solution via the first needle, while the solution was stirred, at a flow rate of ~10 mL min^{-1} as measured by a J&W Scientific ADM 2000 Intelligent Flowmeter. CO_2 was bubbled through the solution for 30 min until a phase separation had occurred. The biphasic system consisted of a reddish brown, clear aqueous phase and a clear, colorless organic phase. Under a dynamic CO_2 atmosphere, the organic phase was extracted via syringe and analyzed by gas chromatography. The aqueous phase was then stored under CO_2 atmosphere for later recycling. By-products of styrene

hydroformylation were identified as ethylbenzene and acetophenone while 1-octene hydroformylation by-products were identified as octane and isomerized starting material. No 2-octanone was observed by GC after the hydroformylation of 1-octene.

To recycle the solvent and catalyst, the separated aqueous phase was placed in a 65 °C water bath and N_2 was introduced into the solution, with stirring, in a similar fashion to the CO_2 bubbling. After 45-60 min (45 min the DMEA was used, 60 min when the TMDAB additive was used), the aqueous phase reverted back to a clear, yellow solution. The solution was cooled to 25 °C and under N_2, 6 mL degassed *tert*-butanol and ~2 mL degassed H_2O were added to return the system to its original volume. Fresh uninhibited styrene (0.15 mL) was pipetted into the mixture and the reaction procedure described above was repeated. The uptake of gas shown in Fig. 4.6 was monitored using an Omega Engineering Inc PG-2000 digital pressure gauge.

4.5 References

1) *Catalyst Separation, Recovery and Recycling: Chemistry and Process Design*, D.J. Cole-Hamilton, R.P. Tooze, Eds., Springer: Dordrecht, **2006**.

2) M.J. Muldoon, *Dalton Trans*. **2010**, *39*, 337-338.

3) B. Cornils and E.G. Kuntz, In *Aqueous-Phase Organometallic Catalysis* 2nd ed., B. Cornils, W. G. Hermann, Eds., Wiley-VCH: Weinheim, **2004**.

4) U. Hintermair, W. Leitner, P.G. Jessop, In *Supercritical Solvents*, W. Leitner, P.G. Jessop, Eds., Wiley-VCH: Weinheim, **2010**.

5) L. Obrecht, P. Kamer, W. Laan, *Catal. Sci. Technol.* **2012**, *In Press* DOI: 10.1039/C2CY20538F.

6) A. Andreetta, G. Barberis, G. Gregorio, *Chim. Ind*. **1978**, *60*, 891.

7) A. Buhling, P.C.J. Kamer, P.W.N.M. van Leeuwen, J.W. Elgersma, K. Goubitz, J. Fraanje, *Organometallics* **1997**, *16*, 3027-3037.

8) A. Buhling, P.C.J. Kamer, P.W.N.M. van Leeuwen, J.W. Elgersma, *J. Mol. Catal. A: Chem*. **1997**, *116*, 297-308.

9) S. L. Desset, D.J. Cole-Hamilton, *Angew. Chem. Int. Ed*. **2009**, *48*, 1472-1474.

10) M. Mokhadinyana, S.L. Desset, D.B.G. Williams, D.J. Cole-Hamilton, *Angew. Chem. Int. Ed*. **2012**, *51*, 1648-1652.

11) Z. Jin, X. Zheng, B. Fell, *J. Mol. Catal. A: Chem*. **1997**, *116*, 55-58.

12) Z. Jin, Y. Wang, X. Zheng, In *Aqueous-Phase Organometallic Catalysis* 2nd ed., B. Cornils, W. G. Hermann, Eds., Wiley-VCH: Weinheim, **2004**.

13) A. Behr, G. Henze, R. Schomäcker, *Adv. Synth. Catal*. **2006**, *348*, 1485-1495.

14) D.E. Bergbreiter, P.L.Osburn, A.Wilson, E.M. Sink, *J. Am. Chem. Soc*. **2000**, *122*, 9058-9064.

15) D.E. Bergbreiter, P.L. Osburn, J.D. Frels, *J. Am. Chem. Soc*. **2001**, *123*, 11105-11106.

16) D.E. Bergbreiter, J. Tian, C. Hongfa, *Chem. Rev*. **2009**, *109*, 530-582.

17) J.A. Gladysz, R. Corrêa da Costa, In *Handbook of Fluorous Chemistry*, J.A. Gladysz, D.P. Curran, I.T. Horváth, Eds., Wiley-VCH: Weinheim, **2004**.

18) J. Lu, M.L. Lazzaroni, J.P. Hallet, A.S. Bommarius, C.L. Liotta, C.A. Eckert, *Ind. Eng. Chem. Res*. **2004**, *43*, 1586-1590.

19) J.P. Hallet, J.W. Ford, R. S. Jones, P. Pollett, C.A. Thomas, C.L. Liotta, C.A. Eckert, *Ind. Eng. Chem. Res*. **2008**, *47*, 2585-2589.

20) P. Pollett, R.J. Hart, C.A. Eckert, C.L. Liotta, *Acc. Chem. Res*. **2010**, *43*, 1237-1245.

21) *CRC Handbook of Chemistry and Physics*, 79th ed. D. R. Lide, Ed., CRC Press: Boca Raton, **1998**.

22) C. Larpent, H. Patin, *Tetrahedron* **1988**, *44*, 6107-6118.

23) G. Papadogianakis, J.A. Peters, L. Maat, R.A. Sheldon, *J. Chem. Soc., Chem. Commun*. **1995**, 1105-1106.

24) E.C. Warren, K.H. Shaughnessy, *J. Org. Chem*. **2005**, *70*, 6378-6388.

25) D. Wang, H.A. Wright, B.C. Ortego, S. Trinh, R. Espinoza, *Selective Removal of Oxygen from Syngas*, US Patent 6,992,112, 01/31, **2006**.

26) A.L. Watkins, C.R. Landis, *J. Am. Chem. Soc*. **2010**, *132*, 10306-10317.

27) T. Yoshida, D.L. Thorn, T. Okano, J.A. Ibers, S. Otsuka, *J. Am. Chem. Soc*. **1979**, *101*, 4212-4221.

28) R.M. Deshpande, Purwanto, H. Delmas, R.V. Chaudhari, *J. Mol. Cat. A: Chem*. **1997**, *126*, 133-140.

29) A.J. Bruss, M.A. Gelesky, G. Machado, J. Dupont, *J. Mol. Cat A: Chem* **2006**, *252*, 212-218.

30) M.R. Axet, S. Castillón, C. Claver, K. Philippot, P. Lecante, B. Chaudret, *Eur. J. Inorg. Chem.* **2008**, 3460-3466.

31) Z. Ma, X. Liu, G. Yang, C. Liu, *Fuel Process. Technol*. **2009**, *90*, 1241-1246.

Chapter 5

The Effect of Switchable Water on Clay Suspensions

5.1 Introduction

Current strip mining operations demand high water usage. For example, a net of 2–4.5 barrels of water are required for every barrel of bitumen produced by oil sand extraction.[1] After extraction of the desired materials, the leftover aqueous slurry of sand and clay is often deposited into tailing ponds, where the solids must be consolidated before the water can be reused. While the sand fraction rapidly settles to the bottom of such ponds, fine clay tailings can take from decades up to 150 years to settle out.[2] Conventional inorganic flocculants, including calcium salts, have been used to accelerate the rate of settling,[3-5] but salt additives result in water with high ionic strength, which must be treated by methods such as adsorption and membrane filtration[6] before the water can be recycled. High ionic strength solutions are not desired when recycled water is fed back into the extraction process. The challenge of facilitating the settling of clay particles to dewater the tailings in a technically, environmentally, and economically viable manner still remains. Research towards enhanced clay settling is also not limited solely to the mining industry: many other fields, including water treatment, can benefit from efficient, recyclable means of settling clays.[7]

We proposed that switchable water could be employed as a means to accelerate the settling of clay tailings from various industrial processes. In Chapter 2 compound **2.3** (TMDAB), was demonstrated as an effective and commercially available switchable

ionic strength additive. Upon introduction of CO_2 into a clay suspension containing the amine additive, the generated salt would greatly increase the ionic strength of the solution, in a manner similar to the result of adding typical inorganic salts. Removal of CO_2 by heating and sparging the solution with N_2 or air would then easily reverse the reaction and return the aqueous solution to a low ionic strength so the process water could be easily returned to the original extraction process. The increase in ionic strength could promote the accelerated settling of solids in a similar fashion to common flocculants such as $CaSO_4$ or other inorganic salts. Additionally, the facile removal of CO_2, to regenerate a low ionic strength solution, should allow for recycling of the process water without need for distillation or desalination, in contrast to common inorganic, non-switchable flocculants. Herein, the influence of TMDAB-based switchable water on the settling of several model clay suspensions and the recyclability of the process water is described.

The results in this chapter have previously appeared in *ChemSusChem* **2012**, DOI: 10.1002/cssc.201200465. The order of the manuscript has been modified in several places to better reflect the progression of the study.

5.2 Results and Discussion

5.2.1 The Effect of TMDAB on Kaolinite Suspensions

As the clay content in oil sands tailings is predominantly kaolinite (although composition does vary from sample to sample),[8-12] its suspension behaviour was the primary focus of this study; several experiments using montmorillonite were also performed. Kaolinite is a hydrous aluminum silicate of composition $Si_2Al_2O_5(OH)_4$.[13,14] The faces of the particles possess a permanent negative charge, while the charge on the edge surfaces is pH-dependent. Kaolinite clay fines naturally form stable colloidal suspensions in water unless the particles are too large.

Experiments were performed on three different samples of kaolinite taken from the same site (Edgar, Florida). The three samples possessed slightly different particle size distributions (with large polydispersity indices, PDIs) and zeta potentials in water (Table 5.1). Sample 3 should, in theory, have been the easiest of the three to settle because its zeta potential was the closest to zero. The large PDI values show that the samples contained wide distributions of particle sizes as would be expected in clay samples from strip mining operations.

Table 5.1. A comparison of the particle size, distribution, and zeta potentials in water of the three kaolinite samples studied.

Sample	Particle Size/nm	PDI	Zeta Potential/mV
1	1010	0.31	-48 ± 12
2	720	0.26	-36 ± 9
3	816	0.41	-25 ± 1

The bubbling of an inert gas (N_2) through the kaolinite suspensions had no effect on suspension stability. In a TMDAB aqueous solution, in the absence of CO_2, no observable effect on particle flocculation or settling was observed either. However, upon introduction of CO_2 to protonate the TMDAB in solution, settling was observed in a concentration dependent manner, as presented in Fig. 5.1. The settling profiles were plotted as time versus the percent height of the mudline (the interfacial plane between the clay slurry and the supernatant) relative to the total height of the suspension. Interestingly, an increase in TMDAB concentrations led to slower settling rates overall. The greatest settling rate was found in a CO_2-treated suspension with no TMDAB present. At 0.1 mM and 0.01 mM TMDAB (not shown) the settling profiles were found to be very similar to that of the CO_2-treated suspension without TMDAB. CO_2 alone can facilitate bulk settling in a clay colloid because the CO_2 forms carbonic acid in water and thereby lowers the pH. In fact, industry has already begun to inject CO_2 into tailing ponds to accelerate the settling of tailing fines[15-17] and the design for introduction and removal of CO_2 into these systems is already well developed.[18] All three samples of kaolinite showed similar trends in settling.

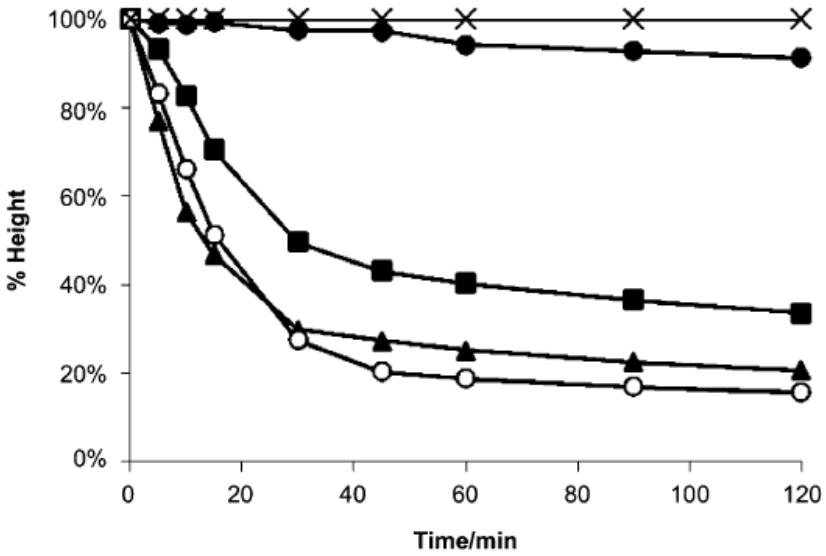

Fig. 5.1. A plot showing the settling profiles of CO_2-treated kaolinite (5 wt%) suspensions (sample 1) in 0 mM (○), 1 mM (▲), 10 mM (■), and 100 mM (●) TMDAB solutions at 25 °C. A control experiment using 10 mM TMDAB with no CO_2 treatment is also included (X).

While the addition of TMDAB did not improve the settling rate, it did lead to decreased turbidity of the supernatant (Fig. 5.2). In the presence of CO_2 alone, the turbidity was found to be 120 ± 15 NTU for sample 1, 40 ± 1 NTU for sample 2, and 60 ± 1 NTU for sample 3 after 2 h. As the concentration of TMDAB increased, the turbidity of the supernatant decreased and the turbidity became much more consistent between the three different clay samples (Figure 5.2). As was previously mentioned, when using TMDAB, a CO_2 treatment was essential; without CO_2, no supernatant was liberated

during the time period of the experiment and the resulting turbidities of these slow-settling suspensions were out of the upper range for the instrument (>1100 NTU). A TMDAB concentration of at least 1 mM was required to reduce the supernatant turbidity by an appreciable amount compared to the samples treated with only CO_2 and no TMDAB. A photographic time profile of the settling of a kaolinite suspension treated with 10 mM TMDAB and CO_2 is presented in Fig. 5.3. The resulting supernatant turbidity from suspensions under different treatment conditions is shown in Fig. 5.4. At higher concentrations of TMDAB (100 mM), traces of oxidized amine imparted a yellow color to the supernatant (Fig. 5.4). Thus, an important industrial design consideration would be a compromise between a desirable settling rate and water turbidity versus discoloration.

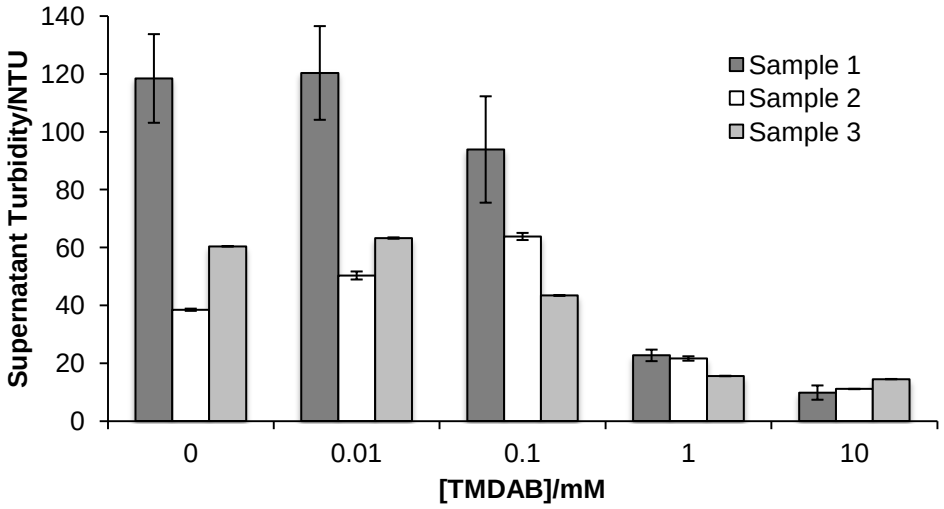

Fig. 5.2. A graph comparing the supernatant turbidities of 5 wt% kaolinite suspensions after 2 h of settling at varying TMDAB concentrations at 25 °C.

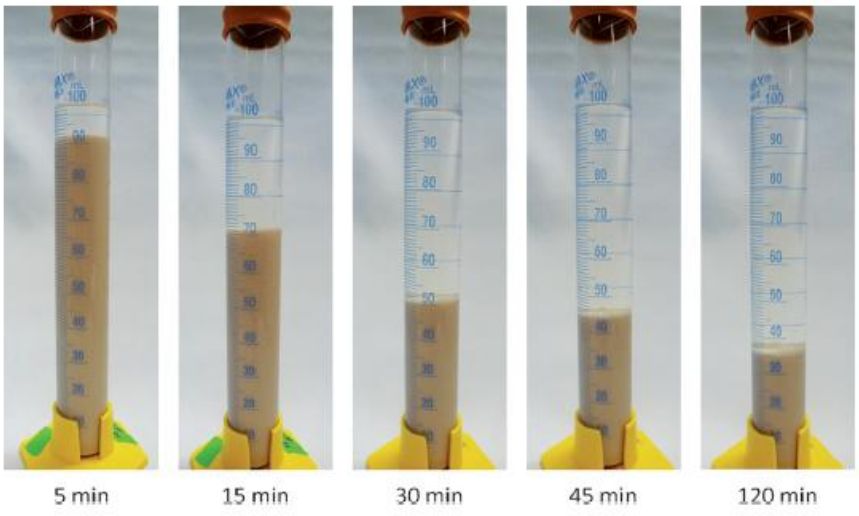

Fig. 5.3. A photographic settling profile of a typical CO_2-treated 5 wt% kaolinite suspension (sample #1) in a 10 mM TMDAB solution.

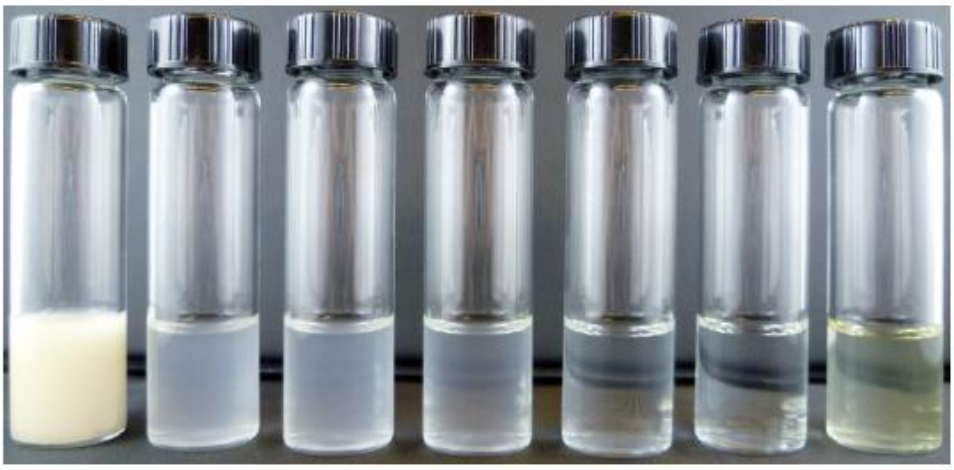

Fig. 5.4. Photographs of supernatants after 2 h of settling of 5 wt% kaolinite suspensions (sample 1). From left to right: no treatment, 0 mM, 0.01 mM, 0.1 mM, 1 mM, 10 mM, and 100 mM TMDAB. All suspensions containing TMDAB were subjected to CO_2 treatment.

The majority of bulk settling for both the 0 mM and 1 mM TMDAB-containing suspensions occurred within the first hour and reached a relatively constant slurry height after 2 h. However, the supernatant turbidity, because of unsettled particles still in suspension, continued to decrease over time as shown in Fig. 5.5. The turbidity of the supernatant of suspensions without any TMDAB present dropped from roughly 100 NTU after 2 h of settling to approximately 60 NTU after 7 h of settling. After 2 h, the turbidity of the 1 mM TMDAB-containing suspension was already lower than the turbidity of the CO2-only treated suspension after 7 h (21 NTU compared to 60 NTU). After 7 h of settling, the turbidity of the 1 mM TMDAB suspension decreased even further (15 NTU). For these experiments of extended length, a constant flow of CO_2 was maintained over top of the cylinders. This demonstrated that a short TMDAB/CO_2 treatment could yield better turbidity results than an extended CO_2-only treatment.

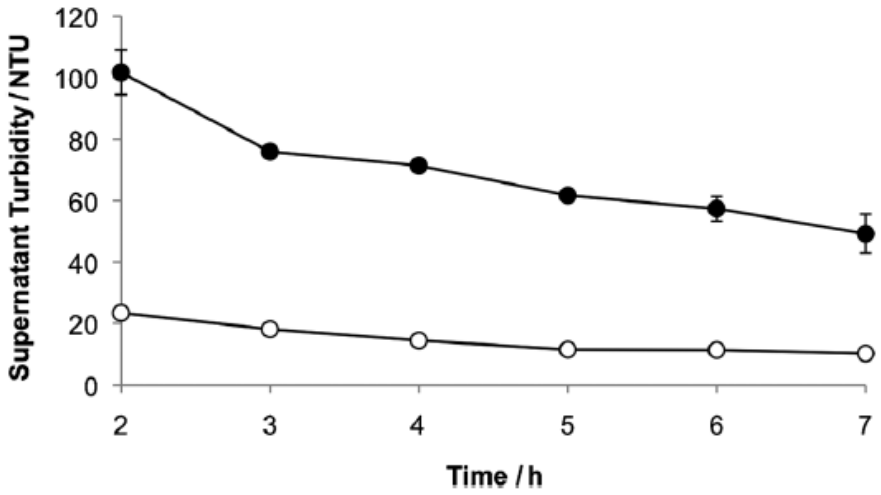

Fig. 5.5. A plot showing the supernatant turbidities of CO_2-treated (●) and 1 mM TMDAB-CO_2 treated (○) 5 wt% kaolinite suspensions (sample #1) over time. Samples were kept under a dynamic CO_2 headspace.

The zeta potential was used as a method of predicting colloidal system stability. At large zeta potential absolute values, the particles are highly charged and repel one another. This prevents the particles from flocculating and results in a stable suspension.[19] Flocculation generally takes place when the value of the zeta potential is less than a critical absolute value of about 30 mV.[20] The closer the zeta potential is to zero, the more it indicates weakened repulsive forces, which allows the particles to flocculate due to attractive van der Waals forces. The zeta potential and the flocculation value (the amount of electrolyte required to flocculate a clay colloid) are related parabolically; a slight change in zeta potential towards zero indicates a many-fold decrease in suspension

stability.[21] Fig. 5.6 shows the zeta potentials of kaolinite particles under different treatment conditions. A kaolinite colloid without any treatment or with TMDAB in the absence of CO_2 generally exhibited zeta potential values in the stable range (more negative than -30 mV). This was consistent with the suspension settling experiments as no settling was observed under these two conditions. The zeta potential of a CO_2-treated suspension with no additive indicated some destabilization of the system, however not to the extent that a TMDAB suspension treated with CO_2 did. This was also consistent with the settling test where settling occurred without CO_2, but the resulting supernatants were quite turbid. However, TMDAB (1 mM) in the presence of CO_2 was able to increase the zeta potential of the suspension components, to values closer to zero than -30 mV. This was once again reflected in the settling of clay and a clearer supernatant. Despite the kaolinite samples differing slightly in the magnitude of their zeta potentials under most treatment conditions, the general trends of destabilization by CO_2 and TMDAB were the same.

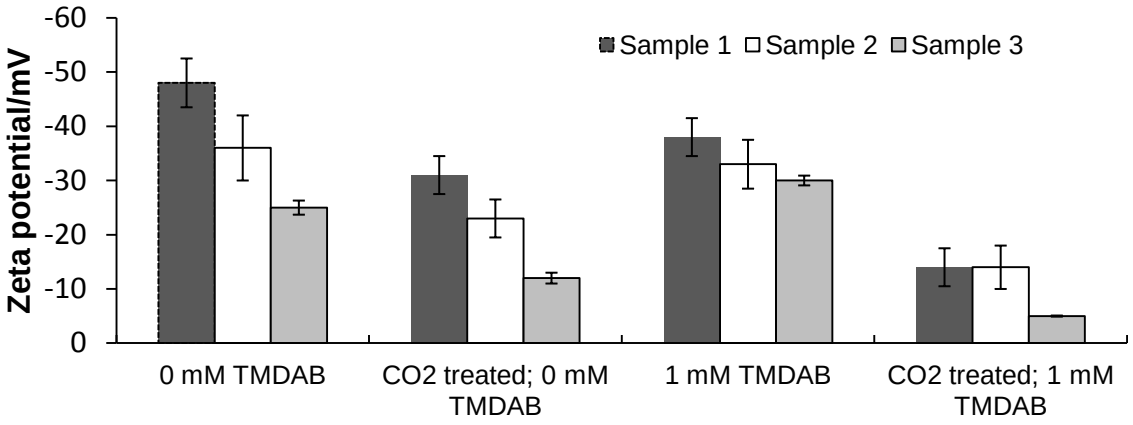

Fig. 5.6. A plot showing the zeta potential measurements for kaolinite suspensions created under four different treatment conditions.

5.2.2 The Effect of Clay Loading on Kaolinite Suspensions

To mimic more realistic clay loadings found in industrial samples, studies were undertaken with varied loadings of kaolinite. The kaolinite clay loading proved to have a large influence on the suspension settling characteristics. The settling time increased as clay loading increased (Fig. 5.7). This finding was consistent with the previous literature using more conventional additives.[22] Final turbidity was generally consistent between 2.5 wt% to 10 wt% suspensions (Fig. 5.8). The 10 wt% suspension was found to undergo densification from 10 wt% solids initially to up to 24 wt% after treatment. In terms of turbidity, the TMDAB in its protonated form exerted a similar effect on the clay suspension despite varied clay loadings; however greater loadings of kaolinite (>20 wt%)

did not settle with CO_2-treatment alone or with CO_2-treated 1 mM or 10 mM TMDAB solutions in the 2 h experiment range.

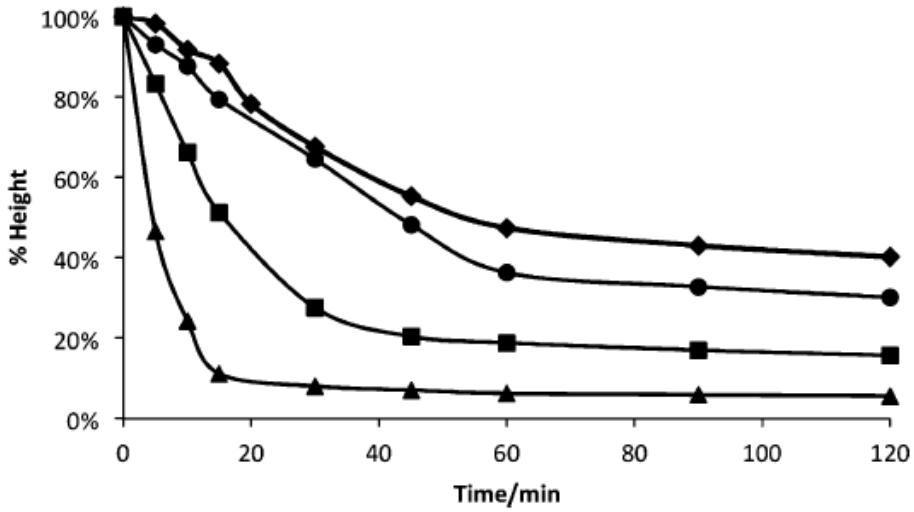

Fig. 5.7. A plot of the settling profiles of CO_2-treated kaolinite suspension (both samples #1 and #3 were tested and the result averaged) with 1 mM TMDAB at 2.5% (▲), 5% (■), 7.5% (●) 10.0% (♦) wt% loading.

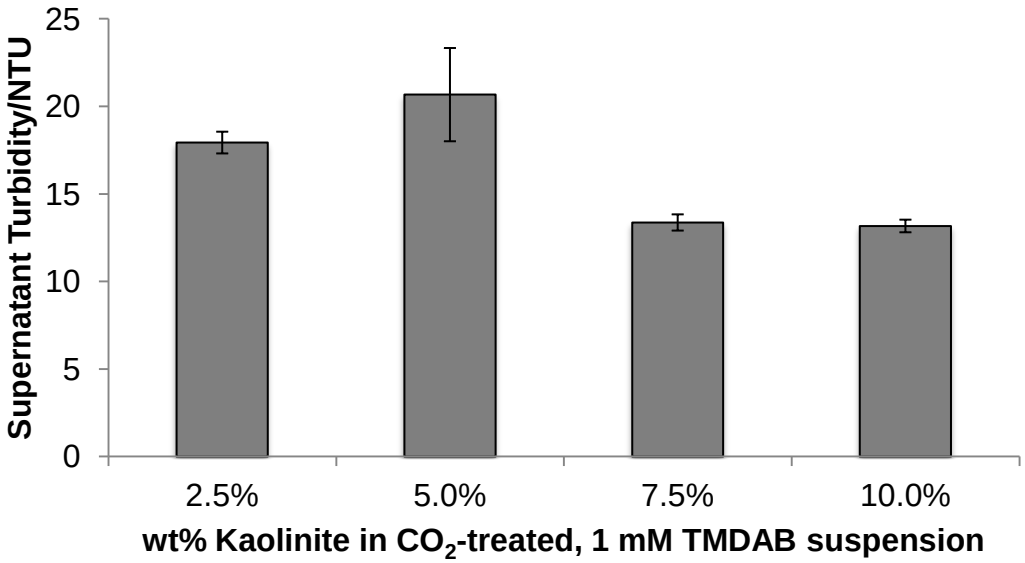

Fig. 5.8. A plot comparing the supernatant turbidities after 2 h of settling at varied clay loading levels for CO_2-treated suspensions in the presence of 1 mM TMDAB (both samples #1 and #3 were tested and an average is presented).

Experiments with mixtures of sand and clay were also performed, with higher solids content, to evaluate mixtures closer to those that would be found in oil sands tailings. For practical reasons, a larger vessel was required. Using a 250 mL graduated cylinder and a glass frit to introduce CO_2 more efficiently, a reasonable settling of a 10 wt% clay/10 wt% sand mixture in water with 1 mM TMDAB was achieved. The supernatant turbidity was found to be 31 ± 1 NTU after 2 h of settling; the slurry densified during that time to 29 wt%.

5.2.3 The Effect of pH and Ionic Strength on Kaolinite Suspensions

The ability of TMDAB and CO_2 together to promote clay settling could have been caused by their effect on the solution pH, their effect on the ionic strength, or specific chemical effects. Experiments were therefore designed to evaluate the effect of pH and ionic strength on clay settling to determine whether the promotion of settling could be explained by these two factors alone. TMDAB in its unprotonated form behaved as a base in an aqueous solution and raised the pH of the solution in a concentration-dependent manner. The ionic strength of such a solution was low but not zero due to some small amount of deprotonation of water, giving partial conversion to the hydroxide salt of the diamine. However, upon CO_2 treatment, the pH is lowered by the formation of carbonic acid, which protonates the TMDAB. Protonation of the diamine resulted in an increase in ionic strength of the solution via the formation of the corresponding alkylammonium bicarbonate salts.

The pH of kaolinite suspensions under different treatment conditions were measured (Table 5.2). To investigate whether the ability of TMDAB-CO_2 to promote settling of kaolinite suspensions was driven by solution pH, three suspensions were prepared with pH values that would correspond to those of 0 mM TMDAB (A), 1 mM TMDAB (B), and 10 mM TMDAB (C) suspensions after CO_2 treatment. The pH was adjusted using 1 M $HCl_{(aq)}$ and 1 M $NaOH_{(aq)}$. A defined interface between supernatant and slurry was observed in suspensions A and B, but not C. It was possible that the addition of NaOH to suspension C may have helped to disperse the clay, preventing

settling; however, the amount of NaOH added to raise the pH from 4.3 to 6.0 was quite small (ca. 0.2 mg per 100 g suspension). The bulk settling for A and B exhibited comparable trends. The supernatant turbidity of B, however, was higher than that of A (520 NTU compared to 64 NTU, Table 5.3). Lower pH values were favourable for kaolinite flocculation and increases in solution pH became increasingly unfavourable towards flocculation until solid settling was no longer observed at pH = 6. The supernatant turbidity also increased as the solution pH increased.

Table 5.2. The pH values of 5 wt% kaolinite suspensions (sample 2) under different treatment conditions and the resulting supernatant turbidity of the suspension after settling.

TMDAB/mM	Gas	Suspension pH	Supernatant Turbidity/NTU
0	air	4.9	n/a
0	CO_2	4.3	38 ± 1
1	air	7.1	n/a
1	CO_2	4.8	22 ± 2
10	air	10.4	n/a
10	CO_2	6.0	11 ± 1

Table 5.3. The supernatant turbidities after 2 h of settling for three 5 wt% kaolinite suspensions (sample 2) at different pH values adjusted with HCl and NaOH to mimic CO_2-treated (A) or TMDAB CO_2-treated (B & C) samples.

Suspension	pH	Supernatant Turbidity/NTU
A	4.3	64 ± 1
B	4.8	520 ± 5
C	6.0	No Settling (> 1100)

These results are in contrast to the turbidity experiments performed with TMDAB where a 1 mM solution generated a far less turbid supernatant than a 0 mM solution (Fig. 5.2). Additionally a 10 mM solution of TMDAB afforded clay settling where a solution without TMDAB but adjusted to the same pH did not. It was previously reported that at pH = 6 and below kaolinite particles can attract electrostatically and form "card-house" flocs,[22] but this electrostatic attraction diminishes with increasing pH. A definitive effect was exerted on suspension behaviour by changing pH, particularly on supernatant turbidity where a change in pH from 4.3 to 4.8 resulted in an 8-fold increase in turbidity; however TMDAB solutions of 1 mM and 10 mM generated solutions of lower turbidity than 0 mM solutions, despite being at a higher pH (Table 5.2). Hence, the effect of the additive on kaolinite settling cannot be explained by a pH effect alone.

To investigate whether TMDAB affected the behaviour of kaolinite suspensions though an ionic strength effect, suspensions without TMDAB present were prepared at the proper ionic strength using common inorganic salts. Equation 2.3 shows that ideally,

upon CO_2 treatment, 1 mM and 10 mM solutions of TMDAB imparted ionic strengths of 3 mM and 30 mM respectively. At the appropriate pH values, inorganic salts were dissolved in solution to impart the same ionic strengths in several model suspensions (Fig. 5.9). The pH was adjusted with 1 M $HCl_{(aq)}$ and 1 M $NaOH_{(aq)}$. The Hofmeister series indicates that different ions can exert different effects on particle interfacial chemistry,[23,24] so this notion must be kept in consideration during this model study. Additionally, a closely related lyotropic series has shown that different cations have varied effectiveness in coagulating a negatively charged colloidal suspension.[23,24] In the attempt to obtain a more general conclusion for the effect of ionic strength, three different additives were investigated for this model study: NaCl, $(NH_4)_2SO_4$, and the divalent $CaCl_2$.

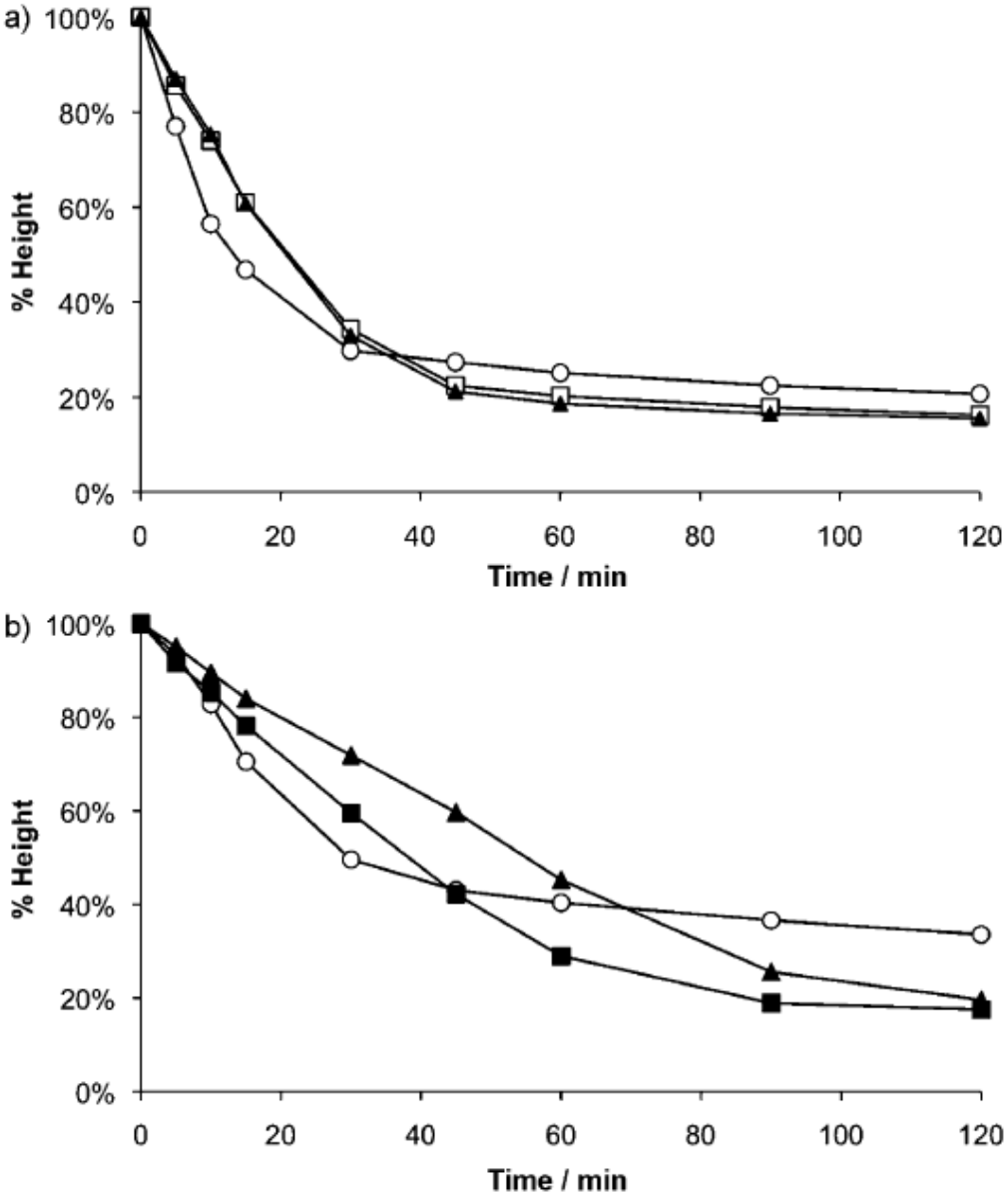

Fig. 5.9. (a) A plot showing the settling profiles of 5 wt% kaolinite suspensions (sample #2) in a 1 mM solution of TMDAB with CO_2 treatment (○), a solution of NaOH and NaCl having the same pH and ionic strength as the CO_2-treated 1 mM TMDAB suspension (□), and a solution of NaOH and ammonium sulfate having the same pH (4.8) and ionic strength as the CO_2-treated 1 mM TMDAB suspension (▲). **(b).** A plot showing the settling profiles of 5 wt% suspensions (sample #2) in a 10 mM solution of TMDAB with CO_2 treatment (○), a solution of NaOH and NaCl having the same pH and ionic strength as the CO_2-treated 10 mM TMDAB suspension (■), and a solution of NaOH and ammonium sulfate having the same pH (6.0) and ionic strength as the CO_2-treated 10 mM TMDAB suspension (▲).

A suspension with an ionic strength of 3 mM set by either NaCl or $(NH_4)_2SO_4$ yielded comparable settling profiles to each other and similar to that of a 1 mM TMDAB-CO_2 treated suspension (Fig. 5.9a). While the solely pH-corrected suspension C (Table 5.3) did not promote settling, increasing the ionic strength to 30 mM with either NaCl or $(NH_4)_2SO_4$ induced similar settling profiles as a suspension treated with 10 mM TMDAB and CO_2 (Figure 5.9b). It appeared that settling rates could be influenced by both pH and ionic strength. Higher concentrations of TMDAB imparted both increased pH and ionic strength; high pH impeded settling, while high ionic strength did the opposite. The observed decrease in settling rate that accompanied the increase in TMDAB concentration is consistent with these observations (Fig. 5.1). As shown in Table 5.4, protonated TMDAB provided a lower final turbidity than equal ionic strength solutions provided by the three inorganic salts studied. Following Schultz-Hardy relationships, divalent species should afford a lower critical coagulation concentration.[7] The lower turbidity observed from protonated TMDAB and $CaCl_2$ suspensions compared to NaCl or $(NH_4)_2SO_4$ suspensions seems reasonable. Interestingly, suspensions with TMDAB and $CaCl_2$ at higher ionic strength generated a less turbid supernatant while greater loadings of NaCl and $(NH_4)_2SO_4$ invoked the opposite effect in the supernatant (compare I = 3 mM to I = 30 mM, Table 5.4). As Na^+ ions are known to disperse wet clays,[25] this result seemed understandable.

Table 5.4. A comparison of the supernatant turbidities of 5 wt% kaolinite suspensions with ionic strengths of 3 mM or 30 mM using varied salts. pH was set at 4.75 for I = 3 mM and 5.95 for I = 30 mM and was adjusted by 1 M $NaOH_{(aq)}$ if necessary.

Clay Sample	Salt	Supernatant Turbidity (I = 3 mM)/NTU	Supernatant Turbidity (I = 30 mM)/NTU
1	TMDAB + CO_2	23 ± 4	10 ± 5
2	TMDAB + CO_2	22 ± 2	11 ± 1
2	NaCl	56 ± 10	119 ± 11
2	$(NH_4)_2SO_4$	99 ± 1	182 ± 11
2	$CaCl_2$	21 ± 2	26 ± 2

Zeta potential measurements also indicated that neither pH nor ionic strength gave an adequate explanation of the lower turbidity behaviour brought about by CO_2-treated aqueous TMDAB. Although the addition of electrolyte increased zeta potentials in comparison to the absence of electrolyte, increasing the concentrations of electrolyte (at the corresponding pH values) did not produce the same trend as increasing TMDAB concentration which had afforded zeta potential values well above (closer to zero than) -30 mV (Fig. 5.10).

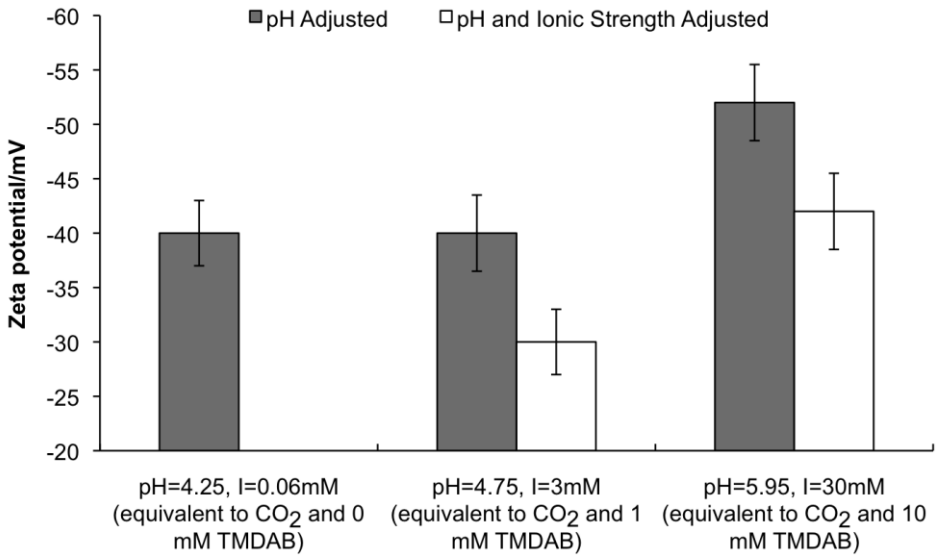

Fig. 5.10. A plot showing the zeta potentials for kaolinite suspensions (sample #2) with only pH adjusted using NaOH, or with both pH and ionic strength adjusted using NaOH and NaCl, to simulate conditions with CO_2 and TMDAB. (No experiment was performed with both pH and ionic strength adjusted to simulate CO_2 and 0 mM of TMDAB).

Although pH and ionic strength were both important factors that affected clay suspension behaviour, these two factors did not fully explain the mechanism through which TMDAB affected settling rates and supernatant turbidity as the results could not be duplicated using common inorganic salts at the same ionic strength and pH values. Other potential contributors including adsorption and inter-particle bridging by TMDAB had to be examined.

5.2.4 Recycling Studies

The previous studies indicated that a stable suspension of kaolinite clay could be formed in the presence of TMDAB in its unprotonated form. Upon treatment with 1 atm of CO_2, settling of the clay fines was observed. However, further treatment with 1 atm of N_2 at 65 °C for 1 h to sparge the aqueous slurry of CO_2 resulted in the reformation of a stable suspension, indicating that a reversible system was created with the use of TMDAB as switchable water additive. To further confirm this finding, zeta potential measurements after treatment with N_2 were obtained. The results show a complete restoration, within error, of the zeta potential to its original value (Fig. 5.11). This result suggested that the process water, if recovered after clay settling, could be used again and would not promote further clay settling until CO_2 is added once more. In processes such as oil sands separations, where clay settling is only wanted in the final step and not earlier, this reversible control of clay settling might be particularly useful.

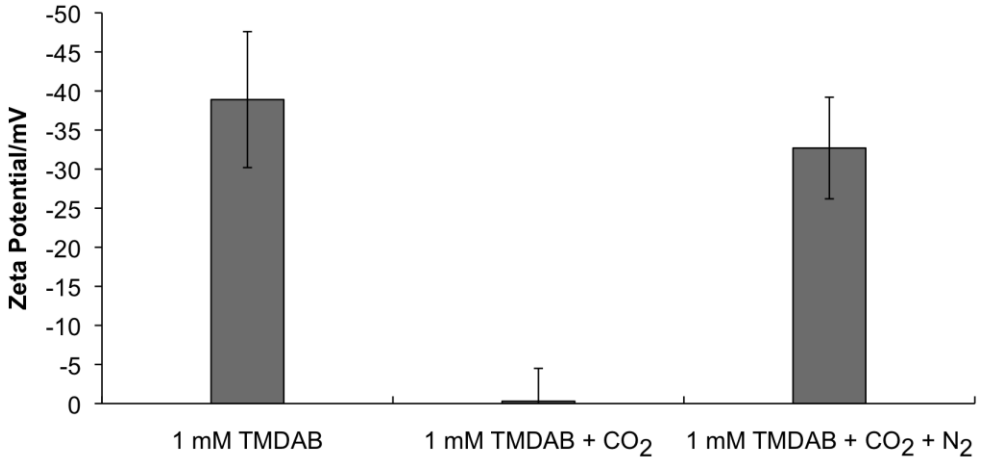

Fig. 5.11. A plot of the zeta potential of 5 wt% suspensions of kaolinite (sample 2) with 1 mM TMDAB, as a function of gas treatment.

It has been reported that ammonium cations can adsorb onto clay by ion exchange.[26] Sufficient adsorption of cationic species onto the negative faces of kaolinite particles could partially reverse surface charges in a localized manner, increasing the likelihood of electrostatic attractions in suspension.[26] In addition, since TMDAB in its protonated form has two charged sites at opposing ends, bridging flocculation could occur.[18] Bridging flocculation is possible when the mean end-to-end molecule distance is approximately equal to or larger than the interlayer spacing of the clay particle.[27] Kaolinite is non-expandable in water and its layer stacking geometry renders the interlayer spacing negligible;[28] as a result, TMDAB may adsorb on separate particles and draw them together. For these many reasons, binding of the additive to the clay surface may be partly responsible for the ability of the additive to promote settling; however, this

may also provide a mechanism for the additive to be lost to the clay slurry, preventing recycling of the process water.

To analyze the amount of amine additive that adsorbed onto the kaolinite clays, a chloroform extraction of the amine from the process water (supernatant) was performed. The chloroform extracts were analyzed by gas chromatography and the amount of amine present was calculated using calibration curves. Analyses were performed on two sets of supernatants from each of 0.1 mM, 1 mM, and 10 mM TMDAB suspension settling tests. As shown in Table 5.5, the amine additive loss was roughly 18% for the 10 mM solution but % adsorption of amine on the clay increased dramatically for both the 1 mM and 0.1 mM solutions.

Table 5.5. The percentage loss of original amine additives from aqueous solutions after CO_2-treatment and settling of kaolinite clays (sample #2, 5 wt% clay suspensions) as determined by Gas Chromatography.

[TMDAB]/mM	% Amine Lost
0.1	51 ± 20%
1	95 ± 3%
10	18 ± 7%

It would appear that for the two lower concentrations, amine would need to be added to recycled process water to make up for losses to the clay. If such make up amount of amine were not added, the amount of TMDAB remaining in solution would likely not be

sufficient to promote clay settling upon recycle. Indeed, as shown in Fig. 5.12, recycling of the supernatant from the 1 mM TMDAB suspension did not afford lower turbidity values than the CO_2-blank (0 mM TMDAB) sample (~40 NTU, Figure 5.2) after a recycle step and thus was not pursued further. For the 10 mM TMDAB suspensions, however, the losses to the clay were not large enough to inhibit the ability of remaining additive in solution to provide enhanced turbidity reduction, compared to a solely CO_2-treated sample, through three cycles (Figure 5.12). Under these loading conditions, the switchable water additive afforded a recyclable system for clay settling over three cycles.

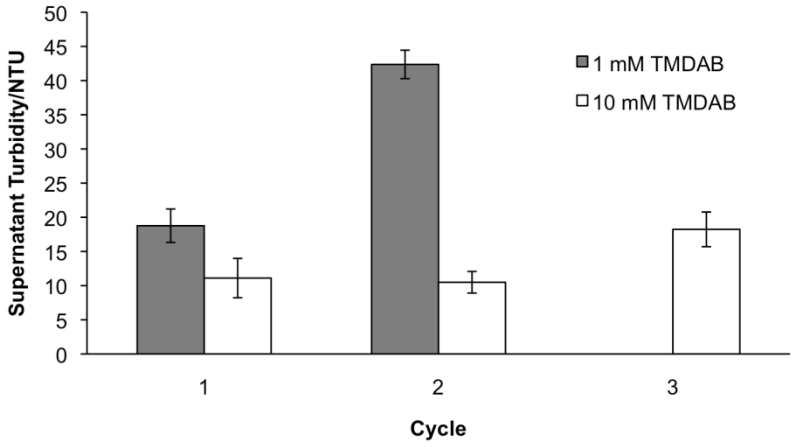

Fig. 5.12. A plot showing the supernatant turbidities from kaolinite suspensions 5 wt% (sample #2) during recycling of process water. A CO_2-only treated sample generated a turbidity of ~40 NTU.

5.2.5 The Effect of TMDAB on Montmorillonite Suspensions

Montmorillonite is a clay with an empirical formula $(Na,Ca)_{0.33}(Al,Mg)_2Si_4O_{10}(OH)_2 \cdot nH_2O$,[13,14] Montmorillonite is known as a swelling clay and adopts a gel-like consistency under aqueous conditions. This gel locks up large quantities of water, and poor dewaterability of the tailings ponds is associated with this property.[29] The montmorillonite sample studied was found to have a zeta potential of -41 ± 5 mV in water. The particle size of the sample was estimated by light microscopy and the average diameter was approximately 20 mm, however the particles appeared quite disperse by qualitative observation. The particle size was estimated for a dry montmorillonite sample due to the potential swelling of the clay in water.

No liquid separations from slurries were observed in 5 wt% montmorillonite suspensions under all treatment conditions investigated (0 mM TMDAB to 10 mM TMDAB). Neither CO_2 treatment nor TMDAB with and without CO_2 imparted any observable effect on particle flocculation or suspension settling.

When the montmorillonite loading was reduced to 2.5 wt%, settling was observed in a suspension treated with 10 mM TMDAB and CO_2 (Fig. 5.13), but settling was not observed with solely CO_2 treatment or 1 mM TMDAB with CO_2. Thus, the presence of TMDAB was essential in promoting settling of montmorillonite clay fines. Furthermore, the effect of TMDAB on the settling behavior of montmorillonite appeared to be an all-or-none response with a definable critical TMDAB concentration, somewhere between 1 and 10 mM TMDAB for the 2.5 wt% clay suspension. The observed critical TMDAB

concentration in montmorillonite suspensions could be in part related to a critical coagulation concentration (CCC), which is defined as the minimum concentration of an electrolyte required to cause flocculation of a given colloid in a given time.[28] It is known that the CCC for montmorillonite is in general considerably higher than for kaolinite.[30] Additionally, under weakly acidic conditions, kaolinite readily flocculates at negligible CCC values, which explains the ability of the CO_2-only treatment of a suspension to provide coagulation of kaolinite but not montmorillonite.

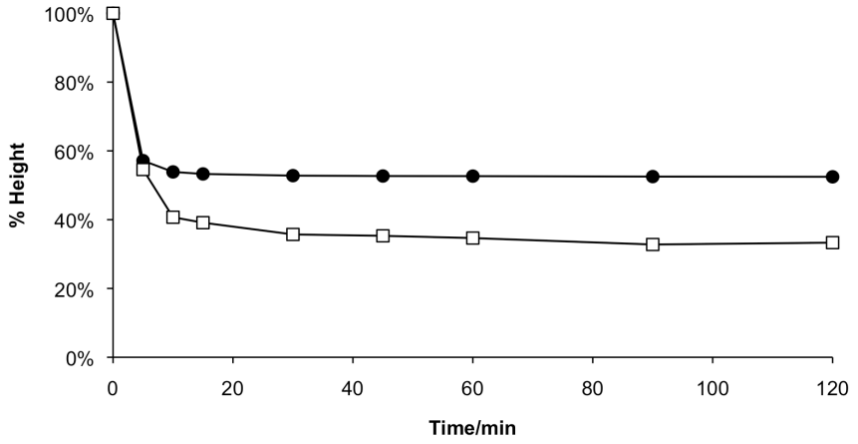

Fig. 5.13. A plot showing the settling profiles of CO_2-treated montmorillonite suspensions with 10 mM TMDAB at 2.5 wt% (●) and 1 wt% (□) loading of clay in water.

Unlike kaolinite suspension settling, which was a function of clay loading level, the time required to achieve settling of montmorillonite suspensions appeared to be

independent of clay loading (Fig. 5.13). The majority of settling at both 2.5 wt% and 1 wt% loading levels in CO_2-treated 10 mM TMDAB occurred within the first 15 min. The supernatant turbidity of 1 wt% montmorillonite CO_2-treated 10 mM TMDAB after 2 h of settling was 6 ± 1 NTU. It was qualitatively noted that the turbidity change in a montmorillonite suspension also exhibited an all-or-none response. However, when such a response occurred the supernatant became very clear qualitatively in a short period of time. This was unlike the kaolinite suspensions, where the decrease in turbidity was gradual over time.

5.3 Conclusions

The effects of TMDAB, a switchable water additive, on the settling trends of kaolinite and montmorillonite suspensions have been described. For kaolinite suspensions, TMDAB, when protonated by carbonic acid, improved the rate of settling compared to the rate in unmodified water but not compared to carbonated water. The TMDAB/CO_2 combination promoted a greater reduction of turbidity, and therefore a better settling of small fines, compared to CO_2 without an amine additive. Montmorillonite solids settled in the presence of the TMDAB/CO_2 combination but not with CO_2 alone. The ability of protonated TMDAB to promote the settling of clay could not be solely attributed to pH and ionic strength effects. Some specific effects such as a possible bridging by the tethered ammonium cations of TMDAB assisted the coagulation

of the clays. This was supported by the observation of some losses of the TMDAB in solution to the clay solids. Because TMDAB is a switchable water additive that can easily be protonated and deprotonated by the introduction and removal of CO_2, the process water containing TMDAB at an appropriate concentration was able to be recycled through three cycles.

This proof of principle study was able to demonstrate that CO_2-switchable additives could potentially afford a means to settle clays more efficiently and in a recyclable fashion. However, the use of small molecule additives on an industrial scale would not likely be economically or environmentally viable for several reasons. 1) The volatility of the amine additive, which would be dissolved in tailings ponds open to the atmosphere, would ultimately lead to undesirable emissions into the atmosphere. 2) Any additive lost to the clays would need to be extracted before the solids could be returned into the environment so that nitrogen-containing compounds would not be released into the neighbouring soils and/or bodies of water. 3) Despite a potential economic benefit, a life-cycle assessment into the use of small molecule additives would likely prove to be more environmentally damaging than the current methods of settling clays using CO_2 alone (even in a closed-loop system). In an attempt to remedy these issues, the Jessop group has recently developed a set of polymeric amine additives which have been shown to settle clays, as well as tailings samples, in a more efficient and recyclable fashion than in the study previously described.[31] The use of larger polymeric structures affords lower volatility and greater additive recovery and will help to mitigate many of the concerns

noted. With the continued study of these CO_2-triggered additives, faster and easier recycling of process water used in strip mining procedures may be achieved in the future.

5.4 Experimental

5.4.1 Clays

Three separate samples of kaolinite (taken from Edgar, Florida) were purchased from Ward's Natural Science (Rochester, New York) several months apart from one another and were used as received. They are referred to as samples #1 through #3. The particle sizes were determined using a Nano-ZS90 Zetasizer.

Several montmorillonite (taken from Panther Creek, Colorado) studies were also performed using a single sample from Ward's Natural Science, which was used as received. The dry particle size was estimated using a calibrated Nikon Eclipse E600-POL microscope.

5.4.2 Supernatant Turbidity and Settling Studies

Kaolinite suspensions were prepared in duplicate by adding clay fines to 100 mL of aqueous solution containing varied concentrations of TMDAB. The effects of changing clay loadings (2.5 wt%, 5 wt%, 7.5 wt%, and 10 wt%) and TMDAB concentrations (0, 0.01, 0.1, 1, 10 mM) on settling behavior were investigated. The

mixtures were stirred with a magnetic stirrer for 15 minutes at 500 RPM in a 250 mL glass beaker prior to transfer to the graduated cylinder. Both CO_2-treated as well as no-CO_2 treatment or CO_2 removed forms of TMDAB were investigated for their effect on clay settling. For the CO_2-treated experiments, CO_2 was bubbled through the mixture in the graduated cylinder using a 20-gauge needle for 1 h at a flow rate of 100-150 mL min^{-1} as measured by a Varian Intelligent Digital Flowmeter. Such conditions afforded CO_2 saturation of the system at equilibrium. The cylinder was then sealed with a rubber septum to maintain the CO_2 headspace and solid settling was monitored over 2 h with an Eberbach brand cathetometer. Supernatant from each settling experiment was sampled and its turbidity was measured in triplicate using a turbidimeter (TB200, Orbeco-Hellige). Montmorillonite suspensions were prepared similarly to the kaolinite suspensions but at 1 wt% and 2.5 wt% loadings. Supernatant from each settling experiment was sampled and its turbidity was measured using the aforementioned instrumentation.

Deionized water with a resistivity of 18.2 MΩ·cm (Synergy® UV, Millipore) was used throughout this study. CO_2 (Supercritical Chromatographic Grade, 99.998%, Praxair) was used as received. White quartz sand (50+70 mesh) was purchased from Sigma Aldrich (St. Louis, Missouri) and used as received. TMDAB was purchased from TCI (Portland, Oregon) and used without further purification. 100 mL graduated cylinders (Kimble Kimax, single metric scale, 26 mm i.d., 20025H 50) were used for all settling tests unless otherwise noted. Consistency in cylinder dimensions was particularly

important, as it has been reported that container height can influence settling rate.[32] To account for potential bridging effects from the glassware, several duplicate experiments were performed in graduated cylinders that were base treated by immersing the glass in 0.1 M NaOH for 24 h beforehand. Ultimately, no difference in settling behavior was observed between untreated or base-treated glassware experiments.

5.4.3 pH and Ionic Strength Effect Studies

The pH of three 5 wt% kaolinite suspensions were measured using a Thermo Scientific Orion 4 pH meter. The suspensions studied were: 0 mM TMDAB, 1 mM TMDAB, and 10 mM TMDAB, all with CO_2-treatment. To investigate the effect of pH on suspension settling behaviour, similar 5 wt% kaolinite suspensions were prepared in duplicate, and the pH of each suspension was adjusted with 1 M $HCl_{(aq)}$ and/or 1 M $NaOH_{(aq)}$ to match the pH conditions of a completed CO_2-treatment. To investigate the effect of ionic strength on suspension settling behavior, the pH was again corrected to match the pH of a corresponding treatment condition, and the ionic strength was then adjusted with NaCl, ammonium sulfate, or $CaCl_2$ to mimic the CO_2-treated systems. Ionic strength was initially calculated using the assumption that all basic sites on the TMDAB are protonated by carbonic acid. The small contribution to the ionic strength by either $NaOH_{(aq)}$ or $HCl_{(aq)}$ for pH adjustment was considered negligible.

5.4.4 Zeta Potential Experiments

Zeta potentials were measured using a Nano-ZS90 Zetasizer instrument (Malvern) using a folded capillary cell. Clay fines (25 mg) were added to 10 mL of aqueous solutions containing varying concentrations of TMDAB. A suspension was created using a vortex mixer. All CO_2 treatments were conducted in Fisher four dram vials for 1 hour. When necessary, the pH was adjusted with 1 M $HCl_{(aq)}$ and 1 M $NaOH_{(aq)}$. Twelve scans were collected for each measurement and each measurement run in triplicate.

5.4.5 Liquid-Liquid Extraction to Quantify TMDAB in Supernatant

Initially, calibration curves for the chloroform extraction of TMDAB from aqueous solutions were established. A series of amine aqueous solutions with known concentrations were prepared. To 2 mL aliquots of each solution, 700 mg NaCl was added and after dissolution the solution was mixed with 3 mL chloroform. The organic fraction was extracted and analyzed by gas chromatography using a Shimadzu GC-17A Gas Chromatograph (2 μL injections on an Agilent DB-5 column). The resulting signal was plotted against initial amine concentration to provide a calibration curve for the extractions. To 2 mL aliquots of supernatant process water taken from 5 wt% clay suspensions, 15% $NaOH_{(aq)}$ was added to make the solution alkaline (usually requiring less than one drop) to deprotonate all the additive in solution. To this basic solution, 700 mg of NaCl was added. After dissolution of the salt, 3 mL of chloroform was added and

the solution was stirred for 5 min. The organic layer was extracted and analyzed for amine content by means of gas chromatography (2 μL injections). Two samples at each concentration were run in duplicate and average remaining concentrations and standard deviations were calculated. The percentage loss of amine to clay adsorption was calculated from the difference between the starting and measured concentrations in solution.

5.4.6 Recycling Procedure

A 5 wt% kaolinite suspension at 1 mM or 10 mM TMDAB was prepared and studied in a similar fashion to the above settling and turbidity studies. After completion of the initial CO_2 treatment, solids were removed from the system via vacuum filtration. The filtrate was then heated at 65 °C while N_2 (Praxair, 99.998%) was bubbled through the filtrate using a 20-gauge needle for 30 min at 100-150 mL min^{-1} to remove CO_2 from the solution. A 5 wt% kaolinite suspension using new clay was then prepared with the N_2-treated filtrate and any deficit in solution volume was made up with new deionized water. Settling and turbidity studies were then performed again to observe effects from recycling of the supernatant.

5.5 References

1) M. Griffiths, A. Taylor, D. Woynillowicz, *Troubled Waters, Troubling Trends: Technology and Policy Options to Reduce Water use in Oil and Oil Sands Development in Alberta*, The Pembina Institute: Drayton Valley, Alberta, **2006**.

2) P.M. Fedorak, D.L. Coy, M.J. Salloum, M.J. Dudas, *Can. J. Microbiol*. **2002**, *48*, 21-33.

3) R.K. Schofield, H.R. Samson, *Discuss. Faraday Soc*. **1954**, *18*, 135-145.

4) L.S. Kotylar, B.D. Sparks, R. Schutte, *Clay Miner*. **1996**, *44*, 121-131.

5) R.J. Chalaturnyk, J. Don Scott, B. Ozüm, *Pet. Sci. Technol*. **2002**, *20*, 1025-1046.

6) E.W. Allen, *J. Environ. Eng. Sci*. **2008**, *7*, 499-524.

7) J.M. Montogmery, *Water Treatment Principles and Design*, John Wiley & Sons: New York, **1985**.

8) F. Camp, *Can. J. Chem. Eng*. **1977**, *55*, 581-591.

9) S. Ramachandra Rao, *Int. J. Miner. Process*. **1980**, *7*, 245-253.

10) O. Omotoso, R.J. Mikula, *Appl. Clay Sci*. **2004**, *25*, 37-47.

11) R. Mikula, O. Omotoso, *Clay. Sci*. **2006**, *12 Supp. 2*, 177-182.

12) S. Motta Cabrera, J. Bryan, A. Kantzas, *J. Can. Pet. Technol*. **2010**, *49*, 8-19.

13) *Origin and Mineralogy of Clays*, B. Velde, Ed. Springer: New York, **2005**.

14) R.F. Giese, C.J. van Oss, *Colloid and Surface Properties of Clays and Related Minerals, Surface Science Series*, Vol. 105, Marcel Dekker Inc.: New York, 2002.

15) J.G. Matthews, W.H. Shaw, M.D. Mackinnon, R.G. Cuddy, *Int. J. Surf. Min. Reclam. Environ*. **2002**, *16*, 24-39.

16) R.J. Mikula, R. Zrobok, O.Omotoso, *J. Can. Pet. Technol*. **2004**, *43*, 48-52.

17) R. Zhu, Q. Liu, Z. Xu, J.H. Masliyah, A. Khan, *Energy Fuels* **2011**, *25*, 2049-2057.

18) Canadian Association of Petroleum Producers, *Shrinking the Tailings Pond*. http://www.capp.ca/energySupply/innovationStories/Land/ShrinkingTheTailingsPond (*accessed 08/2012*).

19) A.V. Delgado, F. González-Caballero, R.J. Hunter, L.K. Koopal, J. Lyklema, *J. Pure Appl. Chem*. **2005**, *77*, 1753-1805.

20) D.H. Everett, *Basic Principles of Colloid Science*, Royal Society of Chemistry: London, **1988**.

21) H. Jenny, R.F. Reitemeier, *J. Phys. Chem*. **1935**, *39*, 593-604.

22) A.S. Michaels, J.C. Bolger, *Ind. Eng. Chem. Fundam*. **1962**, *1*, 24-33.

23) M.G. Cacace, E.M. Landau, J.J. Ramsden, *Q. Rev. Biophys*. **1997**, *30*, 241-277.

24) G. Para, E. Jarek, P. Warszynski, *Adv. Colloid Interface Sci*. **2006**, *122*, 39-55.

25) J.D. Oster, I. Shainberg, J.D. Wood, *Soil Sci. Soc. Am. J*. **1980**, *44*, 955-959.

26) S.L. Swartzen-Allen, E. Matijevic, *Chem. Rev*. **1974**, *74*, 385-400.

27) J. Swenson, M.V. Smalley, H.L.M. Hatharasinghe, *Phys. Rev. Lett*. **1998**, *81*, 5840-5843.

28) H. van Olphen, *An Introduction to Clay Colloid Chemistry: For Clay Technologists, Geologists, and Soil Scientists*, 2nd ed. John Wiley & Sons: New York, **1977**.

29) M.A. Kessick, *J. Can. Pet. Technol*. **1979**, *18*, 49-52.

30) S. Goldberg, H.S. Forster, *Clay Miner*. **1991**, *39*, 375-380.

31) T. Robert, S.M. Mercer, T.J. Clark, B.E. Mariampillai, P. Champagne, M.F. Cunningham, P.G. Jessop, *Green Chem.* **2012**, *14*, 3053-3062.

32) A.M. Gaudin, M.C. Fuerstenau, S.R. Mitchell, *Mining Eng.* **1959**, *11*, 613-616.

Chapter 6

Towards the Development of CO_2-Switchable Chiral Resolving Agents

6.1 Introduction

The methods of obtaining enantio-enriched chiral compounds are numerous and ever-growing. Novel and elegant methodologies for synthesis and/or separation are often a major ambition of today's synthetic and analytical chemist; demonstrating their high competency in their respective fields. In industrial fine chemical production however, the time needed to develop such elegant methodologies is often not present. To remain economically viable, industry (particularly the pharmaceutical industry) must be able to synthesize large quantities of fine chemicals efficiently and therefore is restricted by the practicality of a methodology, time-to-market, short patent lifetimes, and production costs.[1] Often then to obtain enantio-enriched materials, industry must employ chiral resolution by crystallization methods. Although generally considered a less elegant and lower yielding method than stereoselective synthesis, resolutions are often more practical in the long term due their robustness, generality, and reliability.

Chiral resolution by crystallization affords separation of racemates through the direct crystallization of separate enantiomers (racemic conglomerates) or by the exploitation of varied physical properties of their diastereomeric derivatives or salts, formed via a reaction with a enantiopure chiral resolving agent. In efforts to improve production cost and minimize environmental impact, industry has already begun to employ strategies to recycle chiral resolving agents.[2] Unfortunately, such strategies often

require the addition of auxiliary chemicals, such as inorganic acids and bases, to achieve reclamation of the value-added chiral resolving agent. Although the costs are minimized, hazardous wastes could still be generated. A chiral resolving agent that could provide resolved enantiomers efficiently but could also be recycled without the addition of excess environmentally damaging materials might be a useful green innovation for the chemical enterprise.

The generation of enantio-enriched alcohols is an active area of research in chiral resolution as well as stereoselective synthesis. Kinetic resolution is a popular method of generating enantio-enriched alcohols. This method typically employs a preferential acylation reaction on one enantiomer, thereby enriching the slower reacting enantiomer. These kinetic resolutions usually consist of a transesterification reaction and have been performed both enzymatically[3] and catalytically.[4] The procedure generally involves interception of an achiral acylating agent, prior to reaction with the racemic alcohol, by an enzyme or chiral catalyst, thereby imparting chirality onto the modified acylating agent. In fact, strong nitrogenous bases such as amidines,[5] a common motif used in the Jessop group, have previously been demonstrated as chiral catalysts for the kinetic resolutions of alcohols. Preferential oxidation of one alcohol enantiomer has also emerged as a viable means of kinetic resolution. It has become an attractive method of resolution as it can offer a means of boosting yields over 50 % as the unwanted prochiral ketone generated in the resolution can be re-racemized upon later reduction.[4] In terms of resolution by diastereomeric crystallization, typical methods involve either covalent or

ionic functionalization of the alcohol. Acid catalyzed-esterification of an alcohol using an enantiopure chiral carboxylic acid affords diastereomeric esters which can be separated. Half esters formed from achiral dicarboxylic acids and racemic alcohols can later form diastereomeric salt pairs with an enantiopure chiral base, such as an amine.[6] Of course both of these methods then require material intensive chemical modifications after the resolution to remove the chiral resolving agent to yield the desired alcohol enantiomer. A resolution method that employs a simple means of liberating the desired alcohol enantiomer while allowing for easy reclamation of the chiral resolving agent would prove quite beneficial.

We proposed that CO_2-switchable chemistry can be used to generate chiral resolving agents which would be easier to recover and recycle, facilitating the reduction of waste produced by chiral resolutions which use diastereomeric crystallizations. As shown in Fig. 6.1, an enantiopure amidine base, B, could be reacted in the presence of a racemic alcohol ((**S**)-R-OH & (**R**)-R-OH), which has been converted to the respective alkyl-carbonic acids via reaction with CO_2. The subsequent acid/base reaction and formation of the amidinium alkyl-carbonate salts would result in a diastereomeric salt pair. Resolution could be achieved by the removal of one diastereomer away from the other by selective precipitation. The later removal of CO_2 by heating and/or sparging with an inert gas would then liberate the alcohol from the salt and provide the enriched enantiomer. The amidine resolving agent could then be recovered and recycled for another resolution. Alternatively, if direct removal of CO_2 failed, the alkyl-carbonate

anion could be displaced by water, where the bicarbonate anion would substitute in for the alkyl-carbonate, thereby liberating the alcohol. Recovery and recycling of the amidine would then be performed in the same fashion as previously described. In this chapter, the initial screening of the reactivity of a series of chiral nitrogenous bases with racemic CO_2-generated alkyl-carbonic acids is presented.

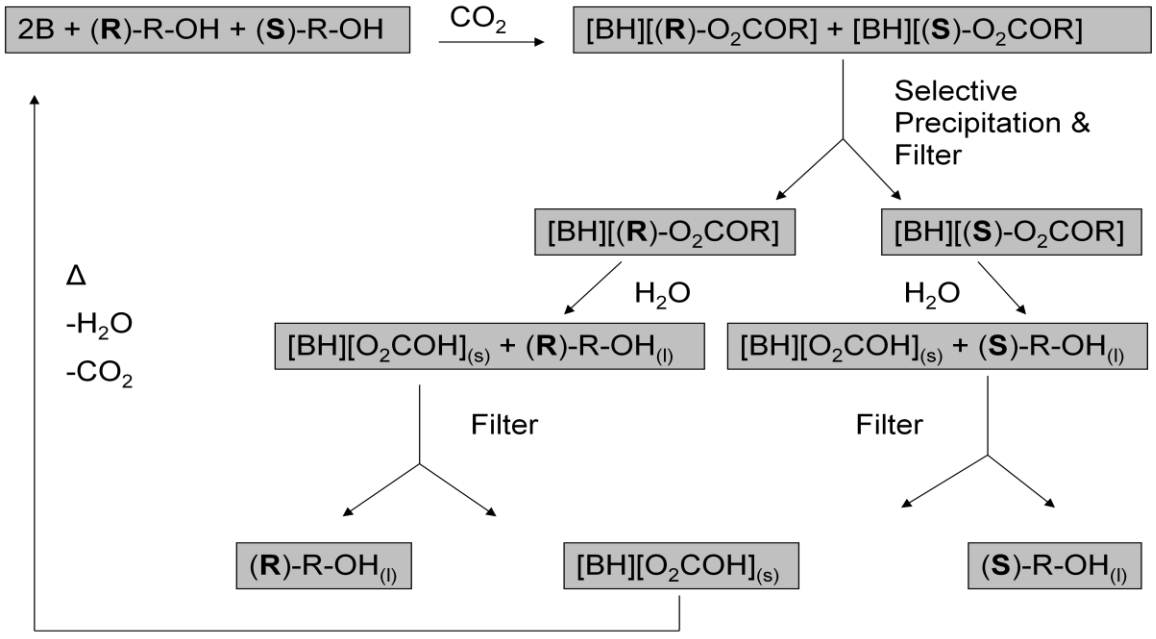

Fig. 6.1. Conceptual reaction scheme of CO_2-switchable chiral resolving agents. B is an enantiopure chiral base.

6.2 Results and Discussion

6.2.1 Chiral Imidazoline Frameworks

The initial design strategy for the generation of the library of chiral amidines to test for applicability as resolving agents was based on incorporating a high degree of rigidity in the molecules' scaffolds to hopefully assist the latter crystallization step in the chiral resolution. Imidazolines, the cyclic analogues of amidines, with appended aryl functionalities were thus first selected as a subset of frameworks to synthesize and test for reactivity (Fig. 6.2)

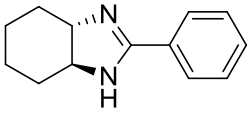

6.1

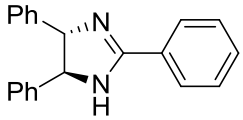

6.2

Fig. 6.2. Molecular structures of the initial imidazolines synthesized as candidates for CO_2-switchable chiral resolving agents.

Initial synthetic endeavors were modeled on the reaction of diamines with carboxylic acids as described by Shi (Fig. 6.3).[7] This preparation had already been successfully used to synthesize imidazoline head groups for CO_2-switchable surfactants.[8] However this procedure appeared to only be successful for aliphatic carboxylic acids, such as those that were used in the surfactant syntheses, as all attempts to invoke

cyclization with the aryl carboxylic acids were unsuccessful. It seemed that these reactions always terminated at an amide-type intermediate.

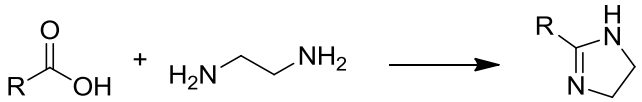

Fig. 6.3. Reaction scheme for the synthesis of imidazolines from a diamine and carboxylic acid, described by Shi.[7]

The synthesis of these imidazolines was later achieved using a method developed by Togo where a diamine was reacted with an aldehyde, rather than a carboxylic acid, in the presence of molecular iodine (Fig. 6.4),[9] *tert*-butyl hypochlorite,[10], or 1,3-diiodo-5,5-dimethylhydantoin (DIH).[11]

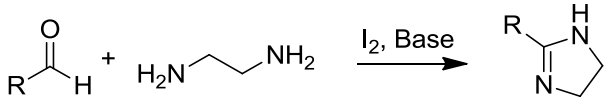

Fig. 6.4. Reaction scheme for the synthesis of imidazolines from a diamine and aldehyde, described by Togo.[9]

When the DIH method was employed, compounds **6.1** and **6.2** were synthesized successfully, but in low to moderate yields. Due to cost considerations and low yields of

these reactions, the racemic version of **6.1** and the *meso* isomer of **6.2** were synthesized for the initial testing.

Both compounds **6.1** and **6.2** were reacted with methanol and CO_2 (1 atm) and were subsequently analyzed by ^{1}H and ^{13}C NMR spectroscopy. It was hypothesized that the appearance of some diagnostic peaks, such as the alkyl-carbonate peak (~165 ppm) in the ^{13}C NMR spectrum, would signify reaction between the imidazoline and methyl-carbonic acid. Unfortunately, no definitive evidence of reaction was acquired for either compound using any of the spectroscopic methods. This result was later found to be quite plausible as the pK_{aH} values of compounds **6.1** and **6.2** were determined by acid/base titration to be 9.1 and 8.3 (aqueous scale) respectively. The low basicity of either species could have certainly prohibited a large formation of any alkyl-carbonate salt.

The synthesis of compound **6.3** (Fig. 6.5), from (**R**)-BINAM, was also attempted but was ultimately not successful. The failure of the reaction was likely due to the high rigidity or strain that would have had to have been incorporated into the 7-membered heterocyclic ring while the (**R**)-BINAM framework itself is already constrained. Upon later analysis using prediction software,[12] the pK_{aH} of the biphenyl analogue of compound **6.3** was predicted to be 3.5, so it was unlikely that compound **6.3** would have functioned in the manner desired.

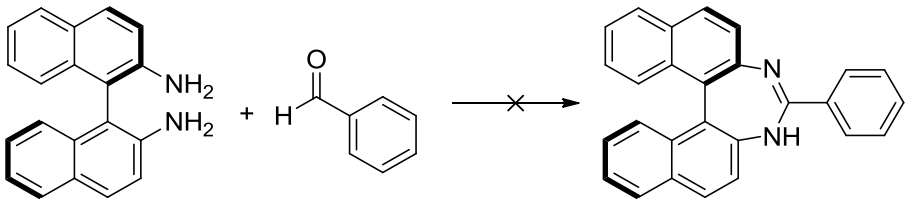

Fig. 6.5. The reaction scheme of the envisioned, but unsuccessful, synthesis of a (**R**)-BINAM-based chiral heterocycle, compound **6.3**, using the method developed by Togo.[11]

6.2.2 Cinchona Alkaloid-Based Amidines

The disappointing results for the insufficiently-basic imidazolines led to the need to develop stronger chiral bases stemming from different organic frameworks. The linear analogue to the imidazoline, the amidine, was envisioned as an appropriate basic functional group for this project. A subset of amidines, the acetamidines, had previously been demonstrated as being easily formed from primary amines[13] and has been a popular motif in the Jessop group.[14] If a suitable enantiopure chiral amine framework could be generated, the grafting of the amidine onto that molecule would potentially generate a sufficiently basic enantiopure chiral molecule to act as a resolving agent as desired.

The cinchona alkaloid family was selected as a base framework on which to construct a chiral amidine due to their inherent and well-known ability to transmit and/or discriminate chirality from other molecules. In addition to their roles as food additives, chiral ligands, promoters, and organocatalysts (for which they are quite popularly used today),[15] cinchona alkaloids had been previously used as chiral resolving agents for

diastereomeric crystallizations.[6] Combining a series of well-established transformations, the synthetic strategy towards an amidine-alkaloid involved a number of steps. Many however could be performed in one-pot (Fig. 6.6).

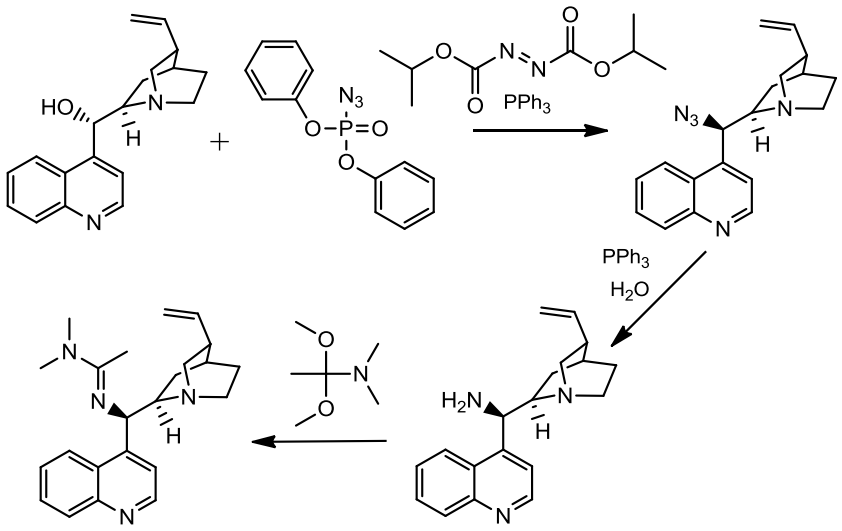

Fig. 6.6. Proposed synthetic route to generate amidine-functionalized cinchona alkaloids.

The initial transformation would involve the substitution of the alcohol functionality at the 9-position into an azide via a Mitsunobu reaction (which would invert the stereochemistry at that position). Subsequent conversion to a primary amine would occur in the same pot via a Staudinger reduction and the triple salt of the alkaloid would later be isolated.[16] After release of the free amine, the installation of the amidine would occur via a procedure that was initially developed by Scoggins[13] and later refined by Jessop.[17]

Initial synthesis was directed towards the functionalization of hydroquinine, compound **6.4** (Fig. 6.7), to afford an amidine-hydroquinine, compound **6.6**. Synthesis to give the amino-triple salt intermediate (compound **6.5**) appeared successful by ^{1}H NMR spectroscopy. However, the isolation of the HCl triple salt proved extremely difficult and isolated yields never exceeded 1 % and thus subsequent reactions were not pursued. Hypothesizing that packing effects may have been leading to the significantly less than expected yields at the crystallization step, the pseudo-enantiomer of the hydroquinine, hydroquinidine (compound **6.7**, Fig. 6.8) was proposed as a new framework.

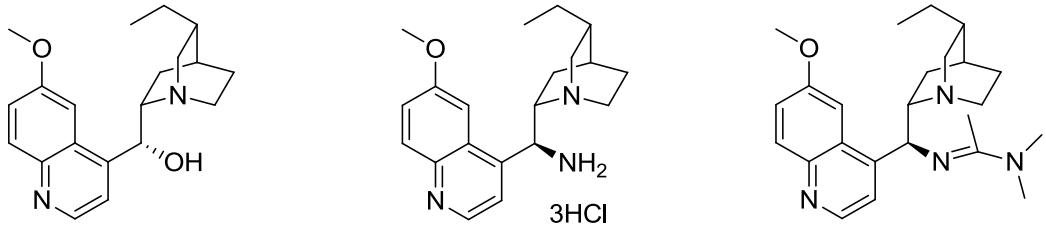

6.4 **6.5** **6.6**

Fig. 6.7. Molecular structure of hydroquinine and its functionalized analogues generated by the reactions highlighted in Fig. 6.6.

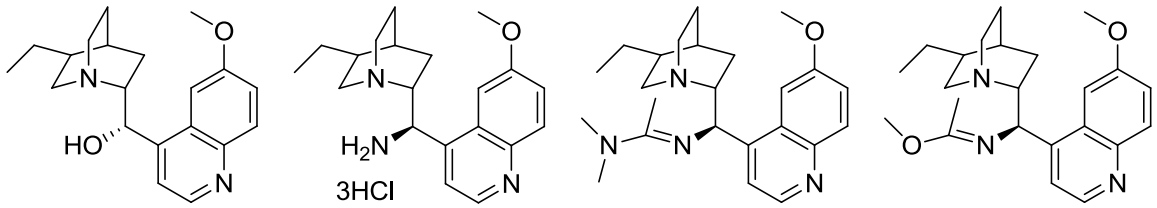

6.7 **6.8** **6.9** **6.10**

Fig. 6.8. Molecular structures of hydroquinidine and the subsequent products and side-product generated by the reactions highlighted in Fig. 6.6.

The reaction of hydroquinidine to the 9-amino-hydroquinidine proceeded smoothly and the triple HCl salt (compound **6.8**) was isolated in a 13 % yield using a modified work-up developed by MacMillan and co-workers.[18] Although the yield was still quite low, enough product was generated to move to subsequent transformations. The installation of the amidine functionality was pursued utilizing a number of synthetic procedures.[17] The product, compound **6.9**, appeared to have formed but was always accompanied by an unknown alkaloid side product as seen in the ^{1}H and ^{13}C NMR spectra. HRMS studies suggested that the side product was the imidate ester (compound **6.10**) of the alkaloid. Such imidate esters have been known to be common side products in these amidine syntheses,[17] however all attempts to minimize their formation were unsuccessful. Purification of the free base, as well as the triple HCl salt, by column chromatography was also unsuccessful, as was the purification of the triple HCl salt of

the compound **6.9** by recrystallization. Unfortunately in all cases the salts of the imidate ester co-crystallized with the desired amidine product.

The mixture of compounds **6.9** and **6.10** was then screened for reactivity with CO_2 and several alcohols. An equimolar mixture (using the assumption that all of the alkaloid mixture was in fact the amidine) with 1-phenylethanol or methanol was dissolved in a dry deuterated solvent. When put under an atmosphere of CO_2, no spectroscopic evidence of reactivity was obtained. When in the presence of a large molar excess of dry methanol however, a small peak in the ^{13}C NMR spectrum around 165 ppm was observed, suggesting some formation of an alkyl-carbonate species, but this peak was only observed in polar organic solvents, such as acetonitrile.

6.2.3 Other Amidine and Guanidine Frameworks

An isolable linear amidine was needed to either confirm or deny the capacity of the functional group as a candidate for a CO_2-based chiral resolving agent for racemic alcohols. Using a simpler organic framework, (**R**)-1-(1-napthyl)ethylamine (compound **6.11**, Fig. 6.9), the amidine analogue (compound **6.12**) was generated by using the typical amidine synthetic procedure,[17] but unfortunately an imidate ester impurity was likely generated once more.

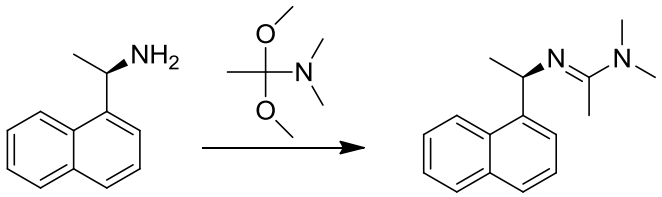

6.11 **6.12**

Fig. 6.9. Molecular structure of (**R**)-1-(1-naphthyl)ethylamine and the amidine analogue generated as a chiral resolving agent candidate.

When compound **6.12** was dissolved in a dry deuterated solvent and put under a CO_2 atmosphere in the presence of a large molar excess of dry methanol, the diagnostic peak for an alkyl-carbonate was again observed in the ^{13}C NMR spectrum, but again only when a polar organic solvent was used. Unfortunately, when equimolar amounts of compound **6.12** and 1-phenylethanol, 2-butanol, or methanol were dissolved in a dry deuterated solvent and put under CO_2, no spectroscopic evidence of reaction was obtained. Utilizing CS_2 as opposed to CO_2 as the acid gas also produced no reactivity at equimolar loadings of the amidine and the alcohol. It would appear that the amidine can elicit the formation of alkyl-carbonate species in the presence of CO_2, but only in much greater concentrations of the alcohol. As small alkyl-carbonic acids have acidities similar, if not greater, to that of carbonic acid,[19] it is unlikely that these bases were disallowing the formation of the alkyl-carbonate salts. It would seem that the initial generation of alkyl-carbonic acids, although well documented in switchable-polarity solvents (SPS)[20]

and CO_2-expanded liquids,[21] seems to be the large issue for these systems. It is possible that the deuterated solvents used (acetonitrile, dichloromethane, benzene) may have adversely affected the salt formation as the species were only ever observed in acetonitrile, but preparing a neat reaction of the amidine and racemic alcohol (as would be done in an SPS) was not feasible at this stage of the project. Additionally, the concentrations of the alcohols and amidines that were studied were quite low compared to those that appear in a SPS system. Additionaly, the CO_2 pressure used was significantly lower in these experiments than the pressures used in gas-expanded liquids. It may be possible that these varied parameters, in addition to potential solvent effects, were the contributing factors to the lack of alkyl-carbonic acid formation. Currently, these factors would appear to be disallowing these bases to act as candidates for chiral resolving agents of alcohols. In the future, the alkyl-carbonic acids must be readily generated and must react sufficiently with the strong chiral base at equimolar loadings to afford an efficient resolution system.

Even stronger bases, the guanidines, were also envisioned as candidates for chiral resolving agents. Two targets, compounds **6.13** and **6.14** (Fig. 6.10), were selected, stemming from the (**R**)-BINAM and amino-hydroquinidine frameworks respectively. The synthesis of **6.13** was pursued using a literature preparation,[22] but unfortunately no formation of the cyclic guanidine was observed and only starting material was recovered.

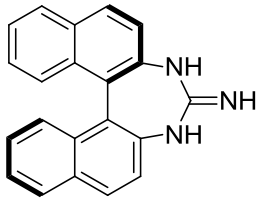

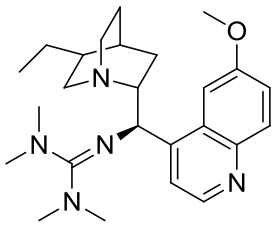

6.13 **6.14**

Fig. 6.10. Molecular structures of two envisioned chiral guanidine bases to test for applicability as chiral resolving agents.

Compound **6.14** was to be generated via a Vilsmeier salt intermediate of *N,N,N'N'*-tetramethyurea[23] and although the formation of the intermediate salt appeared complete by ^{1}H NMR spectroscopy, no trace of the desired guanidine-hydroquinidine product was observed. In the future, guanidines will need to be successfully synthesized and isolated before any conclusions about their use as CO_2-based chiral resolving agents can be made.

6.3 Conclusions

Synthetic efforts towards building a library of chiral nitrogenous bases (or achiral models) to screen for their reactivity as CO_2-switchable chiral resolving agents for the diastereomeric crystallization of racemic alcohols was presented. Although in several cases the compounds synthesized proved insufficiently basic, non-isolable, or

unattainable, a few examples did show reactivity with methanol and CO_2, forming the corresponding acid-base salt pair with methyl-carbonic acid. Unfortunately, in these cases, the concentration of methanol was required to be much greater than that of the amidine base for any alkyl-carbonate salt formation to occur. At this stage of research, these bases cannot function as chiral resolving agents for racemic alcohols as equimolar reactivity is required.

6.4 Experimental

6.4.1 General Procedures

Chemicals were used as received. NMR spectroscopy was performed using a 400 MHz Bruker instrument. pH measurements for titrations to determine pK_{aH} values were taken with a Thermo Scientific Orion 4 Star pH meter. Opitcal rotation was measured using an Atago AP-300 automatic polarimeter. All unsuccessful syntheses followed literature procedure as previously referenced.

6.4.2 Imidazoline Synthetic Procedures

Representative Synthesis:[11] *trans*-1,2-Diaminocyclohexane (0.777 g) was dissolved in 40 mL of *tert*-butanol in a 250 mL round-bottom flask. Benzaldehyde (0.683 g) was pipetted into the solution and N_2 was bubbled through the solution at 25 °C for 30

min. 1,3-Diiodo-5,5-dimethylhydantoin (DIH, 1.414 g) was added to the solution which caused the clear, colourless solution to turn a dark orange/brown colour. The solution was heated to 50 °C for 150 min. While slowly cooling to 25 °C, the solution was quenched by the addition of a saturated $Na_2SO_{3(aq)}$ solution which generated a biphasic system where the organic layer turned yellow in colour.

The organic compounds were extracted into chloroform and washed with saturated solutions of $K_2CO_{3(aq)}$ and brine. The organic extracts were then dried over $MgSO_4$. The solvent was removed *in vacuo* to yield a dark brown solid. The solid was recrystallized in hot acetone to yield the product in low-moderate yields.

Compound **6.1**, 2-phenyl-3a-4,5,6,7,7a-hexahydro-1*H*-benzo[d]imidazole: (28 % isolated yield) m.p. 180-181 °C (180-181 °C)[24] ^{1}H NMR ($CDCl_3$, 400 MHz): δ [ppm] = 7.77 (d, J = 7.7 Hz, 2H), 7.44-7.35 (m, 3H), 3.12 (m, 2H), 2.29, (m, 2H), 1.85 (m, 2H), 1.54 (m, 2H), 1.36 (m, 2H). These chemical shifts match the literature (only the chemical shifts for the (+)-enantiomer are available): 7.74-7.72 & 7.37-7.28 (m, 5H), 3.10 (m, 2H), 2.29 (m, 2H), 1.84 (m, 2H), 1.54 (m, 2H), 1.36 (m, 2H).[25] HRMS (EI): calc. for $[M]^+$: 200.1311, Expected = 200.1313. The structure was confirmed by X-ray crystallography, see Appendix IV.

Compound **6.2**, *meso*-2,4,5-triphenyl-4,5-dihydro-1*H*-imidazole (70 % isolated yield) m.p. 126-128 °C (124 – 127 °C).[26] ^{1}H NMR ($CDCl_3$, 400 MHz): δ [ppm] = 7.99 (d, J =

6.4 Hz, 2H), 7.54-7.47 (m, 3H), 7.07-6.95 (m, 10H), 5.30, (s, 2H). These chemical shifts match the literature: 7.97 (d, J = 6.9 Hz, 2H), 7.49-7.47 (m, 3H), 7.00-6.95 (m, 10H), 5.45 (s, 2H).[25] HRMS (EI): calc. for $[M]^+$: 298.1476, Expected = 298.1470.

6.4.3 Amidine-Alkaloid Synthetic Procedures

Representative Synthesis:[13,16-18] Hydroquinidine (2.005 g) and triphenylphosphine (TPP, 1.944 g) were added to 40 mL of THF to create a slurry. The slurry was cooled to 0 °C and put under a N_2 atmosphere. Diisopropylazodicarboxylate (DIAD, 1.80 mL) was added to the slurry drop-wise where all solids dissolved and solution took on an orange colour. Diphenylphosphoryl azide (DPPA, 1.98 mL) was then added drop-wise. The solution was warmed to 25 °C and stirred under N_2 for 4 h. If any solid precipitated out during this time, 10 mL of extra THF was added to re-dissolve the solid.

The solution was then heated to 45 °C for 2 h. The solution was then opened to air and 1.948 g TPP was added. The solution became a light yellow colour and gas was evolved. The solution was then stirred under air for another 2 h at 45 °C. Afterwards, 3 mL of H_2O was added the solution and it was stirred again at 45 °C for 18 h. The solvents were then removed *in vacuo* to yield a golden yellow solid.

The solid was partitioned between 50 mL dichloromethane and 50 mL of 2 M $HCl_{(aq)}$. The aqueous acidic layer was washed with 3 x 15 mL of dichloromethane. The water and acid were removed *in vacuo* to yield a bubbly yellow solid. The solid was

dissolved in hot methanol and ethyl acetate was added drop-wise to induce a small amount of precipitation. The solution was then cooled to -18 °C where more solids precipitated. The solids were collected by vacuum filtration to yield 13 % of the HCl triple salt of the alkaloid.

Compound **6.8**, m.p. 216 – 218 °C, dec., uncorrected (224 – 226 °C, dec.).[16] ^{1}H NMR (d_4-MeOH, 400 MHz): δ [ppm] = 9.21 (d, J = 5.7 Hz, 1H), 8.51 (d, J = 5.7 Hz, 1H), 8.32 (d, J = 9.3 Hz, 1H), 8.05, (d, J = 2.0 Hz, 1H), 7.95 (dd, J = 9.4 Hz, 2.4 Hz, 1H), 6.09 (d, J = 10.4 Hz, 1H), 4.70 (q, J = 19.4 Hz, 9.6 Hz, 1H), 4.19 (s, 3H), 3.81-3.53 (m, 4H), 2.15-1.91 (m, 4H), 1.62-1.22 (m, 4H), 0.98 (t, J = 7.2 Hz, 3H). *Reference 16 reports ^{1}H NMR shifts in $CDCl_3$, but the salt is sparingly soluble and a ^{1}H NMR spectrum could not be acquired. The ^{1}H NMR of the free-base does match the literature however (see next paragraph).* Literature reference chemical shifts: ($CDCl_3$) 8.93 (d, J = 4.0 Hz, 1H), 8.16 (d, J = 9.5 Hz, 1H), 8.08 (d, J = 5.5 Hz, 1H), 7.79 (dd, J = 2.0 Hz, 9.0 Hz, 1H), 7.69 (d, J = 2.0 Hz, 1H), 5.56 (d, J = 10.0 Hz, 1H), 4.04-4.10 (m, 1H), 3.64 (s, 3H), 3.55 (dd, J = 10.2, 11.7 Hz, 1H), 3.45-3.50 (m, 1H), 3.38 (ddd, J = 3.7 Hz, 12.4 Hz, 22.0 Hz, 1H), 3.22 (ddd, J = 1.4 Hz, 8.0 Hz, 11.7 Hz, 1H), 1.94 (t, J = 8.5 Hz, 1H), 1.79-1.84 (bs, 3H), 1.21-1.41 (m, 4H), 0.77 (t, J = 7.3 Hz, 3H).[16]

Free-base: ^{1}H NMR ($CDCl_3$) δ [ppm] = 8.78 (d, J = 4.5 Hz, 1H), 8.06 (d, J = 9.2 Hz, 1H), 7.55 (bs, 1H), 7.43 (bs, 1H), 7.40 (dd, J = 9.2 Hz, 2.6 Hz, 1H), 4.68 (bs, 1H), 3.99

(s, 3H), 3.07-2.92 (m, 4H), 2.62 (m, 1H), 1.93 (m, 1H), 1.57-1.36 (m, 6H) 1.09 (m, 1H), 0.90 (t, J = 7.3 Hz, 3H). These chemical shifts match the literature: ($CDCl_3$) 8.74 (d, J = 4.6 Hz, 1H), 8.02 (d, J = 9.2 Hz, 1H), 7.62 (bs, 1H), 7.50 (d, J = 4.4 Hz, 1H), 7.38 (dd, J = 9.2 Hz, 2.6 Hz, 1H), 4.66 (d, J = 10.1 Hz, 1H), 3.94 (s, 3H), 3.03 (m, 4H), 2.64 (m, 1H), 1.91(s, 1H), 1.53-1.27 (m, 6H), 1.09 (s, 1H), 0.90 (t, J = 7.3 Hz, 3H).[27]

Compound **6.8**, was then partitioned between 25 mL dichloromethane and 25 mL 2 M $NaOH_{(aq)}$. The aqueous layer was washed with 2 x 15 mL of dichloromethane. The organic extracts were collected and solvents removed *in vacuo* to yield a viscous yellow oil. The oil was dissolved in minimal THF and a minimum of 1.2 equivalents of dimethylacetamide dimethyl acetal was added. The solution was stirred at 25 °C for 18 h. The mixture was then dried under vacuum at 55 °C for 4 h to yield a brown oil (~3 % crude yield) likely containing the amidine-alkaloid product (compound **6.9**) and the side product imidate ester (compound **6.10**) as suggested by HRMS. If such was the case, the amidine/ester ratio appeared to be roughly 2:1 by ^{1}H NMR spectroscopy. HRMS (EI): calc. for $[M]^+$: 394.2719, Expected = 394.2733. Imidate Ester $[M]^+$: 381.2432, Expected = 381.2416.

6.4.4 Synthesis of Compound 6.12, (R)-*N*,*N*,-dimethyl-*N*'-(1-(napthalen-1-yl)ethyl)acetimidamide

This procedure was modified from a literature procedure.[17] Dimethylacetamide dimethyl acetal (0.1960 g) was placed in a 25 mL round bottom flask. Over 5 min, 0.1952 g of (**R**)-1-(1-napthylethylamine) was added dropwise while stirring the solution at 25 °C. The solution was stirred for another 10 min. then left to sit for 18 h at 25 °C. The solution was then dried under vacuum at 75 °C for 3 h to afford a yellow oil. Purification of the product was attempted using a bulb-to-bulb distillation using a short-path vacuum condenser. The liquid was transferred over at a maximum temperature of 156 °C (5 mbar) and 0.376 g of a yellow oil was obtained. The ^{1}H NMR spectra showed that an impurity was retained during the distillation (hypothesized to be the corresponding imidate ester)[17] in a ratio of roughly 10:1 product/impurity.

$[\alpha]_D^{22}$ = -214.5 (c 0.015, Ethanol). ^{1}H NMR ($CDCl_3$, 400 MHz): δ [ppm] = 8.25 (d, J = 8.4 Hz, 1H), 7.81 (dd, J = 6.9, 1.4 Hz 1H), 7.75 (d, J = 7.0 Hz, 1H), 7.65 (d, J= 8.1 Hz, 1H), 7.44-7.33 (m, 3H), 5.13 (q, J = 6.6 Hz, 1H), 2.89 (s, 6H), 1.76 (s, 3H), 1.48 (d, J = 7.0 Hz, 3H). ^{13}C NMR ($CDCl_3$, 100.7 MHz): δ [ppm] = 157.9, 144.7, 134.0, 130.7, 128.9, 126.4, 125.9, 125.3, 125.0, 123.9, 123.8, 54.8, 38.1, 26.4, 13.1 HRMS (EI): calc. for $[M]^+$: 240.1621, Expected = 240.1626.

6.4.5 Base Reactivity Screening Procedure

In an NMR tube, ~20 mg of a nitrogenous base was dissolved in a dry deuterated solvent (acetonitrile, dichloromethane, or benzene). An equimolar amount of a dry alcohol (methanol, 1-phenylethanol, or 2-butanol) was added and the NMR tube was sealed with a rubber septa. In several cases a large molar excess (generally 10-fold molar excess) of the alcohol was added. A narrow gauge steel was then inserted through the septa and into the solution. A second needle was put through the septa, but not into the liquid, to act as a gas outlet. CO_2 was bubbled through the solution at a flow rate of 3-5 mL min^{-1}, as measured by a flowmeter, for 1-2 h. The needles were then removed and the contents of the solution were analyzed by ^{1}H and ^{13}C NMR spectroscopy to identify the formation of alkyl-carbonate species.

6.5 References

1) B.A. Astleford, L.O. Weigel, *Resolution Versus Stereoselective Synthesis in Drug Development: Some Case Histories*, In Chirality in Industry II: Developments in the Manufacture and Applications of Optically Active Compounds, A.N. Collins, G.N. Sheldrake, J. Crosby, Eds., John Wiley & Sons: New York, **1997**.

2) Y. Fujima, M. Ikunaka, T. Inoue, J. Matsumoto, *Org. Process Res. Dev*. **2006**, *10*, 905-913.

3) B. Wang, L. Jiang, J. Wang, J. Ma, M. Liu, H. Yu, *Tetrahedron: Asymmetry* **2011**, *22*, 980-985.

4) H. Pellissier, *Adv. Synth. Catal*. **2011**, *353*, 1613-1666.

5) X. Li, H. Jiang, E.W. Uffman, L. Guo, Y. Zhang, X. Yang, V.B. Birman, *J. Org. Chem*. **2012**, *77*, 1722-1737.

6) J. Jacques, A. Collett, S.H. Wilen, *Enantiomers, Racemates, and Resolutions*, John Wiley & Sons: New York, **1981**.

7) Z. Shi, H. Gu, *Synth. Commun*. **1997**, *27*, 2701-2707.

8) L.M. Scott, T. Robert, J.R. Jarjani, P.G. Jessop, *RSC Adv*. **2012**, *2*, 4925-4931.

9) M. Ishihara, H. Togo, *Tetrahedron* **2007**, *63*, 1474-1480.

10) M. Ishihara, H. Togo, *Synthesis* **2007**, 1939-1942.

11) S. Takahashi, H. Togo, *Heterocycles* **2008**, *76*, 507-514.

12) S.W. Karickhoff, L.A. Carreira, S.H. Hilal, *SPARC Online pKa Calculator* http://archemcalc.com/sparc/ (accessed Aug. 2012).

13) M.W. Scoggins, *J. Chromatogr. Sci*. **1975**, *13*, 146-148.

14) P.G. Jessop, S.M. Mercer, D.J. Heldebrant, *Energy Environ. Sci*. **2012**, *5*, 7240-7253.

15) *Cinchona Alkaloids in Synthesis and Catalysis: Ligands, Immobilization, and Organocatalysis*, C.E. Song, Ed. Wiley-VCH: Weinheim **2009**.

16) S.H. McCooey, S.J. Connon, *Org. Lett*. **2007**, *9*, 599-602.

17) J.R. Harjani, C. Liang, P.G. Jessop, *J. Org. Chem*. **2011**, *76*, 1683-1691.

18) P. Kwiatkowski, T.D. Beeson, J.C. Conrad, D.W.C. MacMillan, *J. Am. Chem. Soc.* **2011**, *133*, 1738-1741.

19) J.L. Gohres, A.T. Marin, J. Liu, C.L. Liotta, C.A.Eckert, *Ind. Eng. Chem. Res*. **2009**, *48*, 1302-1306.

20) P. G. Jessop, D. J. Heldebrant, L. Xiaowang, C. A. Eckert, C. L. Liotta, *Nature* **2005**, *436*, 1102.

21) K.N. West, C. Wheeler, J.P. McCarney, K.N. Griffith, D. Bush, C.L. Liotta, C.A. Eckert, *J. Phys. Chem. A* **2001**, *105*, 3947-3948.

22) H.M. Lovick, F.E. Michael, *Tetrahedron Lett*. **2009**, *50*, 1016-1019.

23) P.G. Jessop, L. Phan, A. Carrier, S. Robinson, C.J. Dürr, J. R. Harjani, *Green Chem*. **2010**, *12*, 809-814.

24) F. Winternitz, M. Mousseron, R. Dennilauler, *Bull. Soc. Chim. Fr.* **1956**, 382-391.

25) C. Dauwe, J. Buddrus, *Synthesis* **1995**, 171-172.

26) D.C. Braddock, J.M. Redmond, S.A. Hermitage, A.J.P. White, *Adv. Synth. Catal.* **2006**, *348*, 911-916.

27) L. Zhang, M-M. Lee, S-M. Lee, J. Lee, M. Cheng, B-S. Jeong, H-G. Park, S-S. Jew, *Adv. Synth. Catal.* **2009**, *351*, 3063-3066.

Chapter 7

Conclusions and Recommendations

7.1 Switchable Water

The initial development and optimization of switchable water, described in chapters 2 and 3, demonstrated the potential utility of this aqueous solvent system. The wide variety of industrial processes which incorporate changes in salinity and ionic strength offer a multitude of research projects to pursue and screen for compatibility with switchable water. Although a small amount of additive optimization, to generate ionogens with as great a change in ionic strength possible, was performed, future work should involve the continued improvement of these amine-based additives. It is quite likely that larger polymeric additives will prove the most fruitful as they have the potential to generate cations of even higher valency upon reaction with CO_2. The design principles identified in chapter 3 should assist in the efficient generation of larger polymeric additives.

The use of switchable water as a recyclable homogenous catalyst recovery system, described in chapter 4, offered an efficient, viable alternative to traditional organic/aqueous biphasic systems. The hydroformylation was demonstrated for several alkenes of low water-solubility. These substrates are in contrast to those transformed using traditional systems as these systems cannot efficiently accommodate these alkenes. Future work on this catalyst recycling system should include the continued optimization of conditions, catalyst, and the screening of more ligands for the hydroformylation

reaction. Elucidating the cause of the diminished regioselectivity during later cycles of styrene hydroformylations should also be examined further. The use of Rh/bicarbonate pre-catalysts may offer a means of probing the effect of adding bicarbonate in the system prior to CO_2 treatment. Studies into the pH effects on styrene hydroformylations should also be pursued. By performing catalysis at varied pH, the effect on regioselectivity could be more easily monitored. Additionally, new reactions should be screened to further expand the utility of this mono- to biphasic catalysis system.

Switchable water was also demonstrated as a recyclable working solvent for the improved settling of clay suspensions in chapter 5. This proof of principle study was quite exciting as the efficient settling of tailings and subsequent water reclamation from strip mining is of particular relevance to the Canadian energy sector. Studies towards improving the loading of additive and efficiency of recycling are already being pursued in the Jessop group using larger polymeric switchable water additives. These additives have already proven to be more useful than the small molecule additives described in chapter 5 due to their enhanced capacity for the generation of ionic strength and their greater retention in water upon recycling. Optimization studies involving real-world tailings samples on industrial scales will be necessary in the future to further demonstrate the utility of this solvent system for settling of clay-based suspensions.

In closing, the switchable water project has proven to be a quite fruitful research project. The versatility of the concept has opened a vast amount of future research with potential industrial utility. As stated previously, the purpose of researching green

chemistry-based concepts, such as switchable water, is to move future green technologies towards industry where they can have the greatest impact both economically and environmentally. I hope that in the future, the research presented here will assist with the incorporation of switchable water, in addition to other CO_2-switchable technologies, into current and new industrial processes.

7.2 Switchable Chiral Resolving Agents

The concept of an easily recyclable and minimally material-intensive chiral resolving agent is an interesting one. Unfortunately, as described in chapter 6, none of the chiral bases generated seemed to possess sufficient reactivity to achieve the necessary diastereomeric salt formation required of a CO_2-based resolving agent. In the future, additional linear amidines and guanidines should be synthesized as they generally possess greater basicity than the imidazolines, which were found to be insufficiently basic in this study. The synthesis of strong chiral bases stemming from the cinchona alkaloids should be continued in the future as some reactivity between the crude amidine mixture and a CO_2-treated alcohol was demonstrated. Designing an improved plan for synthesis which minimizes the formation of imidate ester impurity and/or developing an improved plan for isolation which involves fewer crystallization steps or allows for chromatographic separation may provide a more fruitful result in the future.

Beyond the bases synthesized, the disappointing results may have stemmed in part from other contributing factors. The carboxylation of the racemic alcohols, to form the alkyl-carbonic acids, appeared to be difficult to achieve under the mild conditions employed. The subsequent deprotonation of the acid by the generated bases to form the alkyl-carbonate, which would have confirmed the initial formation of the alkyl-carbonic acid, only seemed to occur at high concentrations of the alcohol and only in polar organic solvents. Due to cost and yield considerations, the reaction of the base and alcohol was never scaled-up to afford a potential 1:1 reaction of base and alcohol at a high enough concentration of the alcohol. In the future, reactions on half gram scales or larger should be attempted to either of confirm or deny whether the carboxylation of the racemic alcohol is a key determining factor of subsequent diastereomeric salt pair formation in the presence of a strong chiral base.

Of course, the selective isolation of one diastereomeric salt over the other, as well as recycling of the resolving agent, must still be achieved to provide proof of principle of the idea. With continued research, I am confident that this concept will be demonstrated to provide yet another interesting switchable-CO_2 based technology with potential industrial utility.

Appendix I

Calculation of the Extent of Amine Protonation by Carbonic Acid as Monitored by ^{1}H NMR Spectroscopy.

Compound **2.1**, DMEA

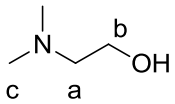

^{1}H NMR Chemical Shifts (D_2O) δ = 2.35(a), 3.54 (b) 2.08 (c).

Table A1.1. ^{1}H NMR chemical shifts of Compound **2.1** in D_2O given a series of treatments.

Condition	δ_a	δ_b	δ_c	$\delta_b - \delta_a$	$\delta_b - \delta_c$
None	2.35	3.53	2.08	1.19	1.45
HCl Run 1	3.12	3.74	2.75	0.61	0.98
HCl Run 2	3.10	3.71	2.72	0.61	0.99
HCl Run 3	3.11	3.73	2.74	0.62	0.99
HNO_3 Run 1	3.11	3.73	2.76	0.62	0.97
HNO_3 Run 2	3.10	3.73	2.75	0.63	0.98
HNO_3 Run 3	3.08	3.73	2.72	0.65	1.01

Average $\delta_b - \delta_a$: 0.63 ± 0.01 when fully protonated

Average $\delta_b - \delta_c$: 0.99 ± 0.01 when fully protonated

$$\%\ Protonation = 1 - \frac{(\delta_{b,100\%} - \delta_{a,100\%}) - (\delta_{b,x\%} - \delta_{a,x\%})}{(\delta_{b,100\%} - \delta_{a,100\%}) - (\delta_{b,0\%} - \delta_{a,0\%})}\, x\ 100$$

$$\%\ Protonation_{Error} = \left(\sqrt{\left(\frac{0.01}{0.63}\right)^2}\right) x\ 100\ =\ 1.6\ \%\ (a), 1.0\ \%\ (c)$$

Reported % protonation is thereby ± 1.6 % at a minimum.

For (a):

$$\%\ Protonation = \left(1 - \frac{(0.63) - \left(\delta_{b,x\%} - \delta_{a,x\%}\right)}{(0.63) - (1.19)}\right) x\ 100$$

For (c):

$$\%\ Protonation = \left(1 - \frac{(0.99) - \left(\delta_{b,x\%} - \delta_{c,x\%}\right)}{(0.99) - (1.45)}\right) x\ 100$$

Table A1.2. The approximate % protonation of compound **2.1**, in D_2O, as a function of CO_2 treatment or CO_2 removal (by sparging with N_2 and heating to 75 °C) as monitored by ^1H NMR spectroscopy.

Condition	**δ_a**	**δ_b**	**δ_c**	**$\delta_b - \delta_a$**	**$\delta_b - \delta_c$**	**% Protonated referenced to ($\delta_b - \delta_a$)**	**% Protonated referenced to ($\delta_b - \delta_c$)**
5 min CO_2	2.63	3.57	2.30	0.94	1.27	45 %	39 %
10 min CO_2	3.06	3.70	2.70	0.64	1.00	98 %	98 %
20 min CO_2	3.11	3.72	2.74	0.61	0.98	~ 100 %	~ 100 %
90 min CO_2	3.10	3.72	2.74	0.62	0.98	~ 100 %	~ 100 %
60 min N_2	2.91	3.67	2.56	0.76	1.11	77 %	74 %
120 min N_2	2.86	3.64	2.52	0.78	1.12	73 %	72 %
240 min N_2	2.62	3.60	2.41	0.98	1.19	38 %	44 %
300 min N_2	2.55	3.59	2.24	1.04	1.35	27 %	22 %

Compound **2.2**, MDEA

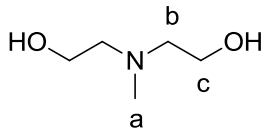

Table A1.3. ^{1}H NMR chemical shifts of Compound **2.2** in D_2O given a series of treatments.

Condition	**δ_a**	**δ_b**	**δ_c**	**$\delta_c - \delta_a$**	**$\delta_c - \delta_b$**
None	2.13	2.47	3.55	1.42	1.08
Av. HCl	2.74	3.15	3.77	1.03	0.62
Av. HNO_3	2.80	3.21	3.80	1.00	0.59

Table A1.4. The approximate % protonation of compound **2.2**, in D_2O, as a function of CO_2 treatment or CO_2 removal (by sparging with N_2 and heating to 75 °C) as monitored by ^{1}H NMR spectroscopy.

Condition	**δ_a**	**δ_b**	**δ_c**	**$\delta_c - \delta_a$**	**$\delta_c - \delta_b$**	**% Protonated referenced to ($\delta_c - \delta_a$)**	**% Protonated referenced to ($\delta_c - \delta_b$)**
5 min CO_2	2.27	2.62	3.60	1.33	0.98	23 %	21 %
10 min CO_2	2.67	3.07	3.72	1.05	0.65	89 %	88 %
20 min CO_2	2.80	3.21	3.78	0.98	0.57	~ 100 %	~ 100 %
90 min CO_2	2.78	3.19	3.77	0.99	0.58	~ 100 %	~ 100 %
60 min N_2	2.43	2.80	3.66	1.23	0.86	45 %	45 %
240 min N_2	2.20	2.54	3.59	1.39	1.05	7 %	7 %
300 min N_2	2.18	2.53	3.59	1.41	1.06	4 %	5 %

Compound **2.3**, TMDAB

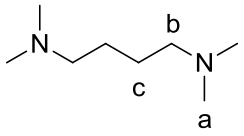

Table A1.5. ^{1}H NMR chemical shifts of Compound **2.3** in D_2O given a series of treatments.

Condition	**δ_a**	**δ_b**	**δ_c**	**δ_a - δ_c**	**$\delta_b - \delta_c$**
None	2.07	2.22	1.34	0.72	0.88
Av. HCl	2.78	3.08	1.71	1.07	1.37
Av. HNO_3	2.83	3.12	1.72	1.11	1.40

Table A1.6. The approximate % protonation of compound **2.3**, in D_2O, as a function of CO_2 treatment or CO_2 removal (by sparging with N_2 and heating to 75 °C) as monitored by ^{1}H NMR spectroscopy.

Condition	**δ_a**	**δ_b**	**δ_c**	**$\delta_a - \delta_c$**	**$\delta_b - \delta_c$**	**% Protonated referenced to ($\delta_a - \delta_c$)**	**% Protonated referenced to ($\delta_b - \delta_c$)**
10 min CO_2	2.78	3.08	1.68	1.10	1.40	~100 %	~ 100 %
120 min N_2	2.78	2.53	1.57	0.96	1.21	65 %	66 %
240 min N_2	2.51	2.31	1.46	0.85	1.05	36 %	35 %

Compound **2.4**

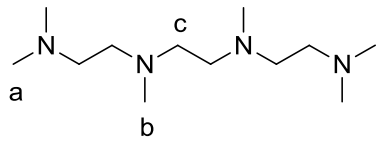

Table A1.7. ^{1}H NMR chemical shifts of Compound **2.4** in D_2O given a series of treatments.

Condition	δ_a	δ_b	δ_c	$\delta_c - \delta_a$	$\delta_c - \delta_b$
None	2.05	2.08	2.39	0.34	0.31
1/4 HCl	2.41	2.18	2.54	0.13	0.36
1/2 HCl	2.78	2.25	2.65	-0.13	0.40
Full HCl	2.91	2.85	3.55	0.64	0.70
1/4 HNO_3	2.40	2.16	2.52	0.12	0.36
1/2 HNO_3	2.74	2.25	2.63	-0.11	0.38
Full HNO_3	2.90	2.88	3.58	0.66	0.70

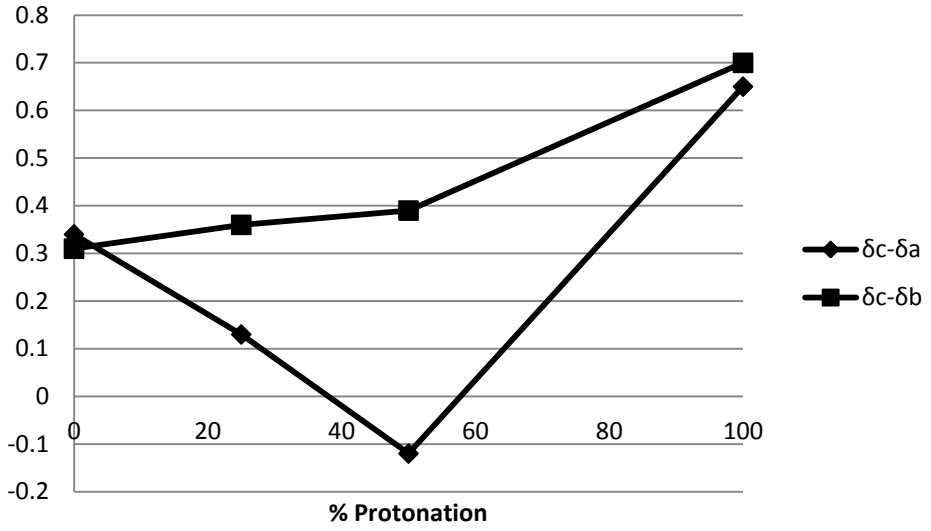

Fig. A1.1. A plot of the differences between a series of ^{1}H NMR chemical shifts of compound **2.4**, in D_2O, as a function of % protonation, achieved by the addition of strong acids.

Table A1.8. The approximate % protonation of compound **2.4**, in D_2O, as a function of CO_2 treatment or CO_2 removal (by sparging with N_2 and heating to 75 °C) as monitored by ^{1}H NMR spectroscopy.

Condition	**δ_a**	**δ_b**	**δ_c**	**$\delta_c - \delta_a$**	**$\delta_c - \delta_b$**	**% Protonated referenced to graph**
20 min CO_2	2.65	2.17	2.57	-0.08	0.40	~ 50 %
60 min CO_2	2.67	2.19	2.59	-0.08	0.40	~ 50 %
90 min CO_2	2.67	2.19	2.59	-0.08	0.40	~ 50 %
60 min N_2	2.18	2.10	2.44	0.26	0.34	~ 25 %
180 min N_2	2.14	2.08	2.43	0.29	0.35	~ 20 %
240 min N_2	2.13	2.09	2.43	0.30	0.34	~ 20 %

Compound **2.5**

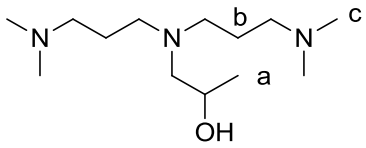

Table A1.9. ^{1}H NMR chemical shifts of Compound **2.5** in D_2O given a series of treatments.

Condition	**δ_a**	**δ_b**	**δ_c**	**$\delta_b - \delta_a$**	**$\delta_c - \delta_a$**
None	1.17	1.65	2.20	0.48	1.03
1/3 HCl	1.04	1.64	2.35	0.60	1.31
2/3 HCl	1.08	1.78	2.70	0.70	1.62
Full HCl	1.15	2.04	2.85	0.89	1.70
1/3 HNO_3	1.05	1.67	2.86	0.62	1.19
2/3 HNO_3	1.07	1.80	2.89	0.73	1.82
Av. HNO_3	1.19	2.15	2.87	0.96	1.68

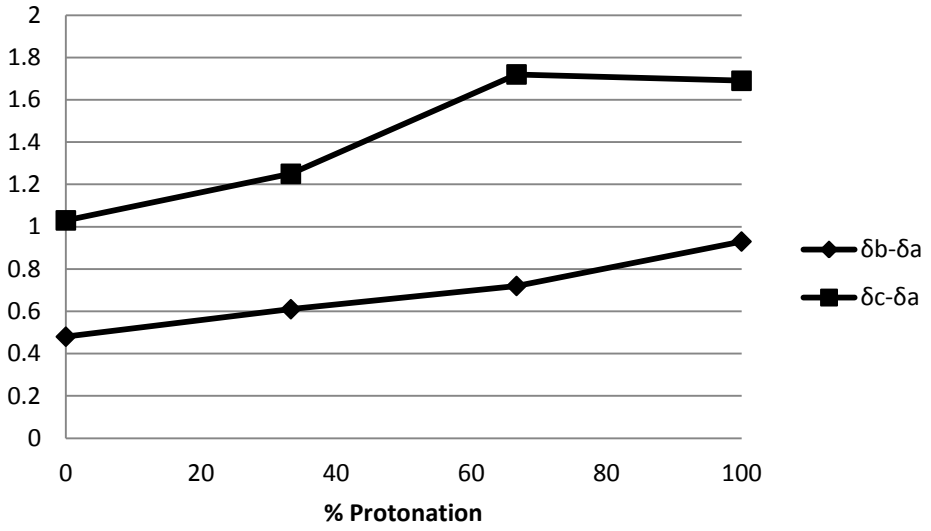

Fig. A1.2. A plot showing the difference between a series of ^{1}H NMR chemical shifts of compound **2.5**, in D_2O, as a function of % protonation achieved by the addition of strong acids.

Table A1.10. The approximate % protonation of compound **2.5**, in D_2O, as a function of CO_2 treatment or CO_2 removal (by sparging with N_2 and heating to 75 °C) as monitored by ^{1}H NMR spectroscopy.

Condition	**δ_a**	**δ_b**	**δ_c**	**$\delta_b - \delta_a$**	**$\delta_c - \delta_a$**	**% Protonated referenced to graph**
10 min CO_2	1.01	1.77	2.71	0.76	1.70	~ 75 %
20 min CO_2	1.01	1.78	2.71	0.77	1.70	~ 75 %
90 min CO_2	1.01	1.78	2.71	0.77	1.70	~ 75 %
60 min N_2	1.02	1.65	2.40	0.63	1.38	~ 35 %
120 min N_2	1.07	1.67	2.38	0.60	1.31	~ 30 %

Compound **3.11**

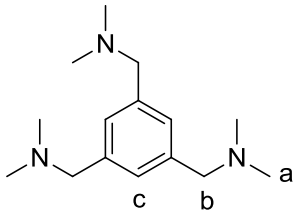

Table A1.11. ^{1}H NMR chemical shifts of Compound **3.11** in D_2O given a series of treatments.

Condition	δ_a	δ_b	δ_c	$\delta_c - \delta_a$	$\delta_c - \delta_b$
None	2.12	3.42	7.13	5.01	3.71
Av. HCl	2.90	4.45	7.79	4.89	3.34
Av. HNO_3	2.87	4.41	7.72	4.85	3.31

Table A1.12. The approximate % protonation of compound **3.11**, in D_2O, as a function of CO_2 treatment or CO_2 removal (by sparging with N_2 and heating to 75 °C) as monitored by ^{1}H NMR spectroscopy.

Condition	δ_a	δ_b	δ_c	$\delta_c - \delta_a$	$\delta_c - \delta_b$	**% Protonated referenced to ($\delta_c - \delta_a$)**	**% Protonated referenced to ($\delta_c - \delta_b$)**
30 min CO_2	2.82	4.34	7.70	4.88	3.36	93 %	92 %
60 min CO_2	2.79	4.31	7.66	4.87	3.35	~ 100 %	95 %
90 min CO_2	2.82	4.34	7.70	4.88	3.36	93 %	92 %
60 min N_2	2.20	3.59	7.20	5.00	3.61	7 %	26 %
120 min N_2	2.20	3.52	7.21	5.01	3.69	~ 0%	5 %
180 min N_2	2.17	3.48	7.18	5.01	3.70	~ 0%	3 %

Compound **3.12**

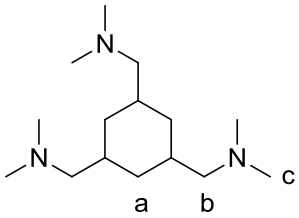

Table A1.13. ^{1}H NMR chemical shifts of Compound **3.12** in D_2O given a series of treatments.

Condition	**δ_a**	**δ_b**	**δ_c**	**$\delta_b - \delta_a$**	**$\delta_c - \delta_a$**
None	0.51	2.18	2.14	1.67	1.63
Av. HCl	0.93	3.11	2.91	2.18	1.98
Av. HNO_3	0.84	3.02	2.83	2.18	1.99

Table A1.14. The approximate % protonation of compound **3.12**, in D_2O, as a function of CO_2 treatment or CO_2 removal (by sparging with N_2 and heating to 75 °C) as monitored by ^{1}H NMR spectroscopy.

Condition	**δ_a**	**δ_b**	**δ_c**	**$\delta_b - \delta_a$**	**$\delta_c - \delta_a$**	**% Protonated referenced to ($\delta_b - \delta_a$)**	**% Protonated referenced to ($\delta_c - \delta_a$)**
30 min CO_2	0.88	3.06	2.87	2.18	1.99	~ 100 %	~ 100 %
60 min CO_2	0.89	3.07	2.88	2.18	1.99	~ 100 %	~ 100 %
90 min CO_2	0.91	3.09	2.90	2.18	1.99	~ 100 %	~ 100 %
60 min N_2	0.63	2.49	2.40	1.86	1.77	37 %	39 %
180 min N_2	0.62	2.44	2.36	1.82	1.74	29 %	31 %
420 min N_2	0.56	2.30	2.25	1.74	1.69	14 %	17 %

Appendix II

Computational Modeling of the Atomic Charges of Diammonium Dications

Level of Theory: B3LYP/6-311G(d,p) (pop=chelpg, mul = 1, charge = 2 e.u.)

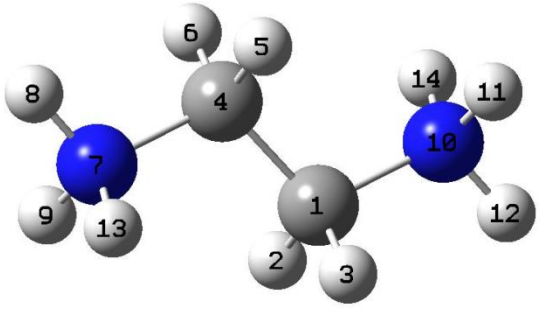

Fig. A2.1. Optimized gas-phase geometry of 1,2-diammoniumethane cation.

Table A2.1. CHELPG charges of gas-phase 1,2-diammoniumethane cation.

Atom	Charge	Atom	Charge	Atom	Charge	Atom	Charge
C1	0.0653	C4	0.0673	N7	-0.5047	N10	-0.5047
H2	0.1282	H5	0.1279	H8	0.4116	H11	0.3847
H3	0.1281	H6	0.1278	H9	0.3851	H12	0.4112
				H13	0.3852	H14	0.3847

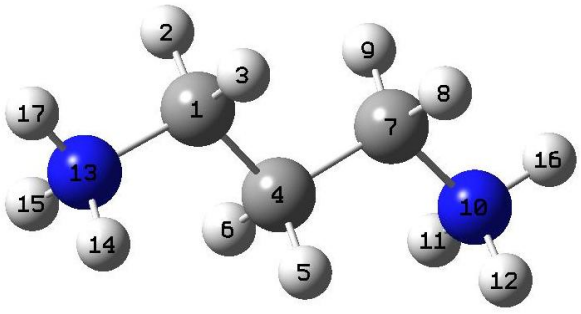

Fig. A2.2. Optimized gas-phase geometry of 1,3-diammoniumpropane cation.

Table A2.2. CHELPG charges of gas-phase 1,3-diammoniumpropane cation.

Atom	Charge	Atom	Charge	Atom	Charge	Atom	Charge	Atom	Charge
C1	0.0947	C4	-0.1673	C7	0.0941	N10	-0.4214	N13	-0.4221
H2	0.1069	H5	0.1077	H8	0.1070	H11	0.3571	H14	0.3573
H3	0.1069	H6	0.1077	H9	0.1070	H12	0.3572	H15	0.3575
						H16	0.3748	H17	0.3749

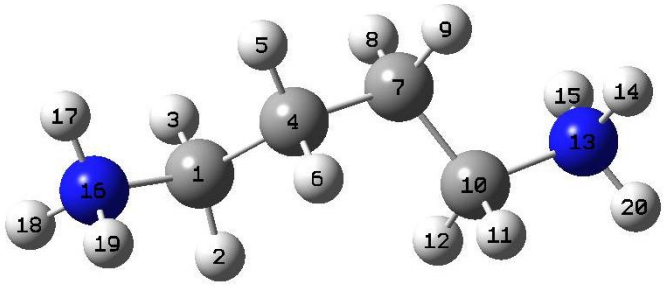

Fig. A2.3. Optimized gas-phase geometry of 1,4-diammoniumbutane cation.

Table A2.3. CHELPG charges of gas-phase 1,4-diammoniumbutane cation.

Atom	Charge	Atom	Charge	Atom	Charge
C1	0.1258	C4	-0.0986	C7	-0.0987
H2	0.0766	H5	0.1000	H8	0.0717
H3	0.0957	H6	0.0716	H9	0.1000
Atom	**Charge**	**Atom**	**Charge**	**Atom**	**Charge**
C10	0.1260	N13	-0.4923	N16	-0.4922
H11	0.0957	H14	0.3671	H17	0.3671
H12	0.0766	H15	0.3689	H18	0.3849
		H20	0.3849	H19	0.3688

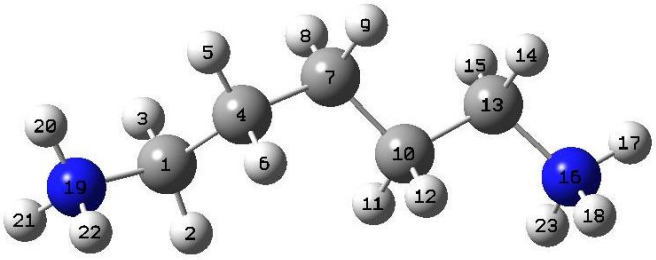

Fig. A2.4. Optimized gas-phase geometry of 1,5-diammoniumpentane cation.

Table A2.4. CHELPG charges of gas-phase 1,5-diammoniumpentane cation.

Atom	Charge	Atom	Charge	Atom	Charge	Atom	Charge
C1	0.1181	C4	-0.0344	C7	-0.0637	C10	-0.0912
H2	0.0796	H5	0.0687	H8	0.0480	H11	0.0459
H3	0.0953	H6	0.0548	H9	0.0791	H12	0.0700
Atom	**Charge**	**Atom**	**Charge**	**Atom**	**Charge**		
C13	0.1287	N16	-0.4845	N19	-0.5319		
H14	0.0906	H17	0.3765	H20	0.3745		
H15	0.0913	H18	0.3609	H21	0.3900		
		H23	0.3623	H22	0.3711		

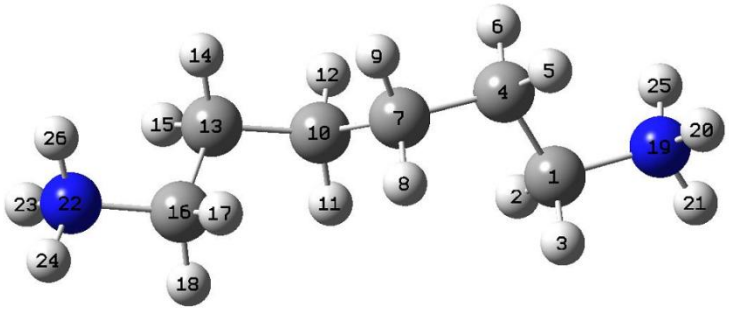

Fig. A2.5. Optimized gas-phase geometry of 1,6-diammoniumhexane cation.

Table A2.5. CHELPG charges of gas-phase 1,6-diammoniumhexane cation.

Atom	Charge	Atom	Charge	Atom	Charge	Atom	Charge
C1	0.1702	C4	-0.1216	C7	-0.0355	C10	-0.0384
H2	0.0656	H5	0.0788	H8	0.0230	H11	0.0237
H3	0.0789	H6	0.0689	H9	0.0750	H12	0.0755
Atom	**Charge**	**Atom**	**Charge**	**Atom**	**Charge**	**Atom**	**Charge**
C13	-0.1207	C16	0.1696	N19	-0.5121	N22	-0.5141
H14	0.0689	H17	0.0659	H20	0.3656	H23	0.3660
H15	0.0790	H18	0.0793	H21	0.3783	H24	0.3790
				H25	0.3653	H26	0.3659

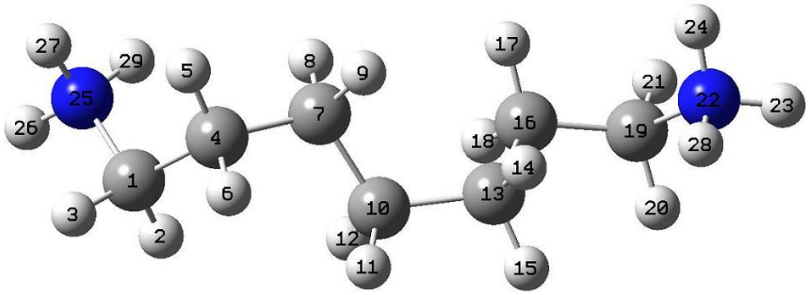

Fig. A2.6. Optimized gas-phase geometry of 1,7-diammoniumheptane cation.

Table A2.6. CHELPG charges of gas-phase 1,7-diammoniumheptane cation.

Atom	Charge	Atom	Charge	Atom	Charge	Atom	Charge	Atom	Charge
C1	0.1537	C4	-0.2084	C7	0.0979	C10	-0.0431	C13	-0.0046
H2	0.0598	H5	0.0877	H8	-0.0274	H11	0.0400	H14	0.0184
H3	0.0887	H6	0.1130	H9	0.0282	H12	0.0340	H15	0.0410
Atom	**Charge**	**Atom**	**Charge**	**Atom**	**Charge**	**Atom**	**Charge**		
C16	-0.0677	C19	0.0592	N22	-0.4054	N25	-0.4520		
H17	0.0409	H20	0.1020	H23	0.3565	H26	0.3606		
H18	0.0714	H21	0.1020	H24	0.3447	H27	0.3522		
				H28	0.3210	H29	0.3416		

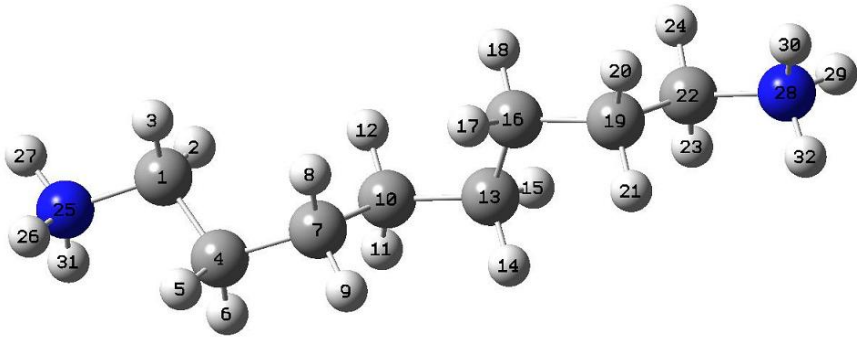

Fig. A2.7. Optimized gas-phase geometry of 1,8-diammoniumoctane cation.

Table A2.7. CHELPG charges of gas-phase 1,8-diammoniumoctane cation.

Atom	Charge	Atom	Charge	Atom	Charge	Atom	Charge	Atom	Charge
C1	0.1695	C4	-0.1094	C7	-0.0319	C10	0.0030	C13	-0.0493
H2	0.0614	H5	0.0656	H8	0.0247	H11	0.0344	H14	0.0394
H3	0.0737	H6	0.0612	H9	0.0646	H12	0.0059	H15	0.0256
Atom	**Charge**	**Atom**	**Charge**	**Atom**	**Charge**	**Atom**	**Charge**	**Atom**	**Charge**
C16	-0.0302	C19	-0.1460	C22	0.1578	N25	-0.5009	N28	-0.5155
H17	0.0590	H20	0.0768	H23	0.0742	H26	0.3589	H29	0.3751
H18	0.0378	H21	0.0743	H24	0.0831	H27	0.3720	H30	0.3641
						H31	0.3579	H32	0.3632

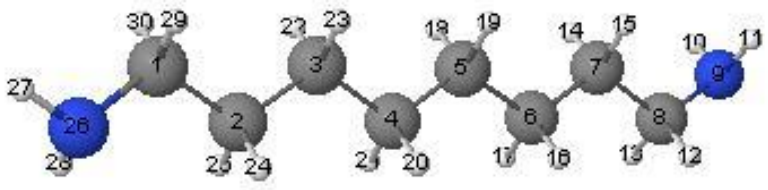

Fig. A2.8. Optimized gas-phase geometry of 1,8-diamnooctane.

Table A2.8. CHELPG charges of gas-phase 1,8-diamnooctane.

Atom	Charge	Atom	Charge	Atom	Charge	Atom	Charge	Atom	Charge
C1	0.4446	C2	0.1133	C3	-0.1635	C4	0.0980	C5	0.2381
H29	-0.0127	H24	-0.0207	H22	0.0116	H20	-0.0250	H18	-0.0547
H30	-0.1102	H25	-0.0090	H23	-0.0029	H21	-0.0394	H19	-0.0536
Atom	**Charge**	**Atom**	**Charge**	**Atom**	**Charge**	**Atom**	**Charge**	**Atom**	**Charge**
C6	-0.0472	C7	-0.0807	C8	0.5622	N9	-1.0337	N26	-1.0306
H16	-0.0300	H14	-0.0161	H12	-0.0521	H10	0.3493	H27	0.3650
H17	-0.0246	H15	-0.0145	H13	-0.0525	H11	0.3486	H28	0.3458

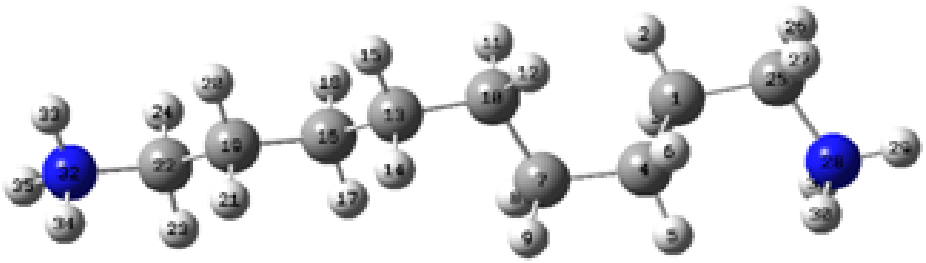

Fig. A2.9. Optimized gas-phase geometry of 1,9-diammoniumnonane cation.

Table A2.9. CHELPG charges of gas-phase 1,9-diammoniumnonane cation.

Atom	Charge	Atom	Charge	Atom	Charge	Atom	Charge	Atom	Charge
C1	-0.0631	C4	-0.0884	C7	0.0456	C10	-0.0123	C13	-0.0156
H2	0.0615	H5	0.0256	H8	0.0003	H11	0.0204	H14	0.0224
H3	0.0568	H6	0.0500	H9	0.0279	H12	0.0275	H15	0.0279
Atom	**Charge**	**Atom**	**Charge**	**Atom**	**Charge**	**Atom**	**Charge**	**Atom**	**Charge**
C16	0.0387	C19	-0.1377	C22	0.1503	C25	0.0754	N28	-0.4493
H17	0.0048	H20	0.0689	H23	0.0753	H26	0.0938	H29	0.3609
H18	0.0131	H21	0.0646	H24	0.0744	H27	0.0967	H30	0.3339
								H31	0.3540
Atom	**Charge**								
N32	-0.4694								
H33	0.3514								
H34	0.3514								
H35	0.3621								

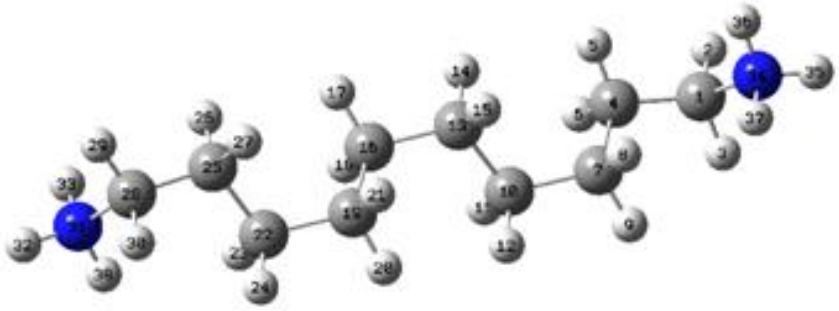

Fig. A2.10. Optimized gas-phase geometry of 1,10-diammoniumdecane cation.

Table A2.10. CHELPG charges of gas-phase 1,10-diammoniumdecane cation.

Atom	Charge	Atom	Charge	Atom	Charge	Atom	Charge	Atom	Charge
C1	0.0505	C4	-0.1065	C7	-0.0173	C10	-0.0217	C13	0.0047
H2	0.0985	H5	0.0631	H8	0.0127	H11	0.0334	H14	0.0086
H3	0.1034	H6	0.0899	H9	0.0364	H12	0.0292	H15	0.0093
Atom	**Charge**	**Atom**	**Charge**	**Atom**	**Charge**	**Atom**	**Charge**	**Atom**	**Charge**
C16	00048	C19	-0.0217	C22	-0.0173	C25	-0.1065	C28	0.0505
H17	0.0086	H20	0.0292	H23	0.0127	H26	0.0631	H29	0.0985
H18	0.0093	H21	0.0334	H24	0.0364	H27	0.0899	H30	0.1033
Atom	**Charge**	**Atom**	**Charge**						
N31	-0.4148	N34	-0.4148						
H32	0.3451	H35	0.3451						
H33	0.3456	H36	0.3456						
H38	0.3201	H37	0.3210						

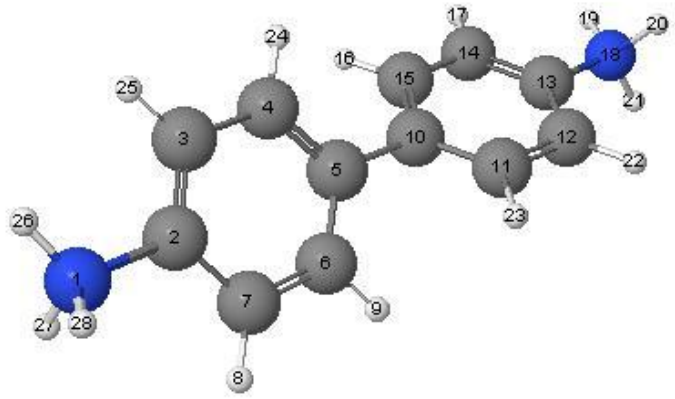

Fig. A2.11. Optimized gas-phase geometry of [1,1'-biphenyl]-4,4'-diammonium cation.

Table A2.11. CHELPG charges of gas-phase [1,1'-biphenyl]-4,4'-diammonium cation.

Atom	**Charge**	**Atom**	**Charge**	**Atom**	**Charge**	**Atom**	**Charge**	**Atom**	**Charge**
C2	0.2405	C3	-0.1939	C4	-0.0451	C6	-0.0391	C7	-0.2056
C5	0.0464	H25	0.1697	H24	0.1213	H9	0.1186	H8	0.1798
Atom	**Charge**	**Atom**	**Charge**	**Atom**	**Charge**	**Atom**	**Charge**	**Atom**	**Charge**
C10	0.0464	C11	-0.0391	C12	-0.2056	C14	-0.1939	C15	-0.0457
C13	0.2404	H23	0.1186	H22	0.1798	H17	0.1697	H16	0.1213
Atom	**Charge**	**Atom**	**Charge**						
N1	-0.5655	N18	-0.5655						
H26	0.3927	H19	0.3927						
H27	0.3907	H20	0.3907						
H28	0.3900	H21	0.3900						

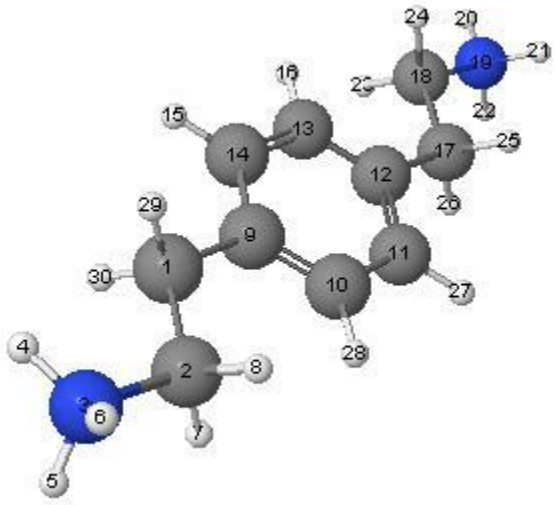

Fig. A2.12. Optimized gas-phase geometry of 2,2'-(1,4-phenylene)-diethanammonium cation.

Table A2.12. CHELPG charges of gas-phase 2,2'-(1,4-phenylene)-diethanammonium cation.

Atom	Charge	Atom	Charge	Atom	Charge	Atom	Charge	Atom	Charge
C1	-0.2652	C2	0.4108	C9	0.1331	C10	-0.1698	C11	-0.1060
H29	0.0967	H7	0.0158			H28	0.1078	H27	0.1400
H30	0.0967	H8	0.0158						
Atom	**Charge**	**Atom**	**Charge**	**Atom**	**Charge**	**Atom**	**Charge**	**Atom**	**Charge**
C12	-0.0861	C13	-0.1146	C14	-0.1603	C17	-0.2467	C18	0.3075
		H16	0.0952	H15	0.1518	H25	0.0992	H23	0.0483
						H26	0.0992	H24	0.0483
Atom	**Charge**	**Atom**	**Charge**						
N3	-0.6289	N19	-0.5610						
H4	0.3780	H20	0.3785						
H5	0.3940	H21	0.3742						
H6	0.3940	H22	0.3742						

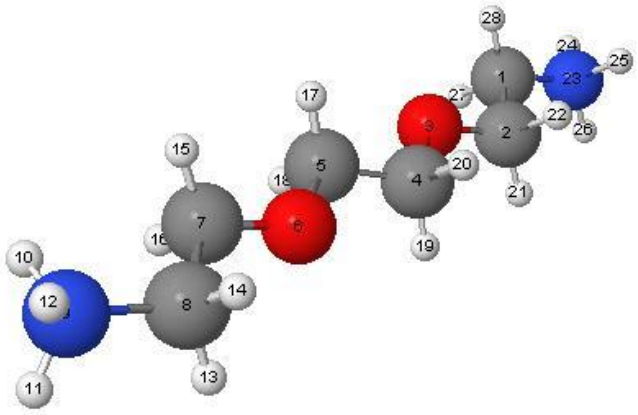

Fig. A2.13. Optimized gas-phase geometry of 2,2'-[ethane-1,2-diylbis(oxy)diethanammonium cation.

Table A2.13. CHELPG charges of gas-phase 2,2'-[ethane-1,2-diylbis(oxy)diethanammonium cation.

Atom	**Charge**	**Atom**	**Charge**	**Atom**	**Charge**	**Atom**	**Charge**	**Atom**	**Charge**
C1	0.1488	C2	0.2510	O3	-0.1635	C4	0.3174	C5	0.2650
H27	0.0942	H21	0.0212			H19	0.0224	H17	0.0268
H28	0.0942	H22	0.212			H20	0.0224	H18	0.0268
Atom	**Charge**	**Atom**	**Charge**	**Atom**	**Charge**	**Atom**	**Charge**	**Atom**	**Charge**
O6	-0.0472	C7	0.3674	C8	0.0606	N9	-0.4582	N23	-0.5609
		H15	0.0012	H13	0.1030	H10	0.3175	H24	0.3966
		H16	0.0012	H14	0.1030	H11	0.3715	H25	0.3708
						H12	0.3715	H26	0.3708

Appendix III

^{1}H NMR Spectra

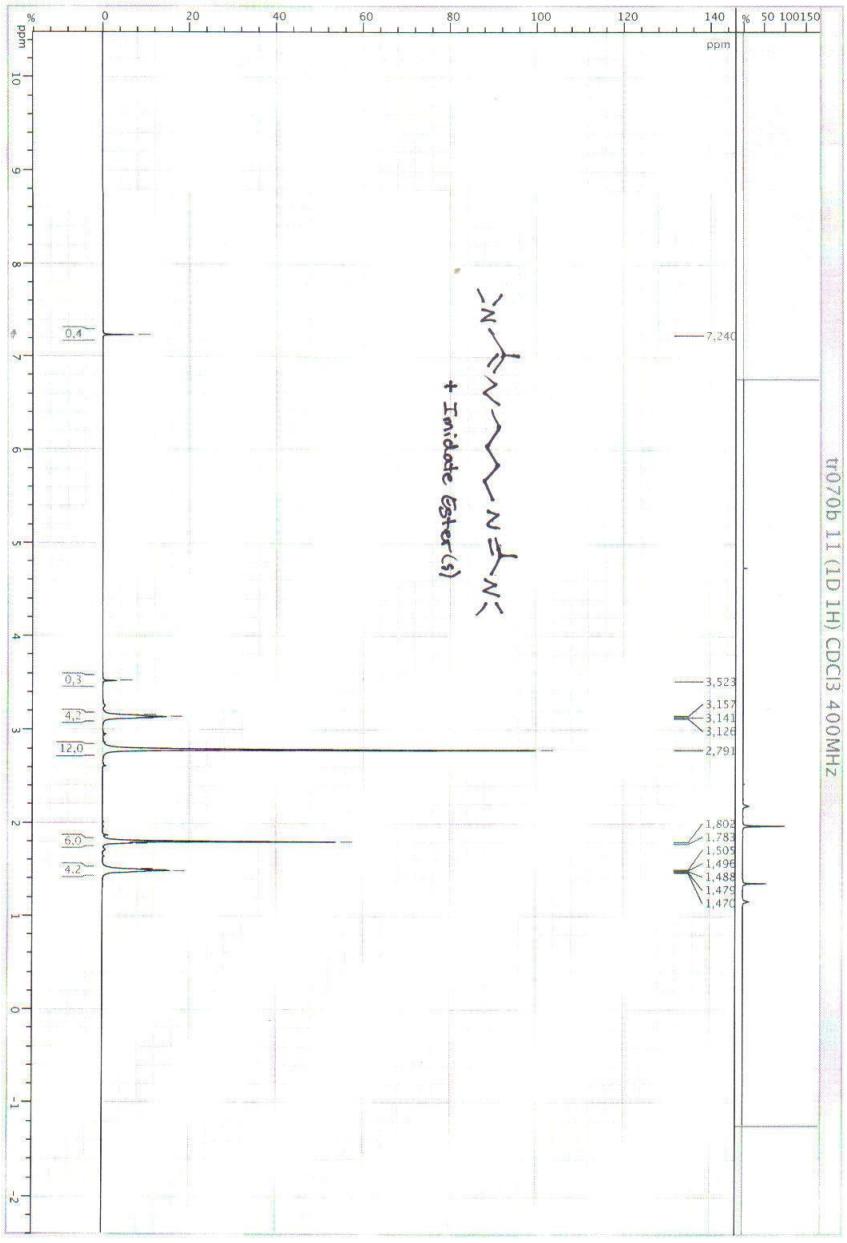

Fig. A3.1. ^{1}H NMR spectrum of compound **3.1** and imidate ester(s) impurity in $CDCl_3$.

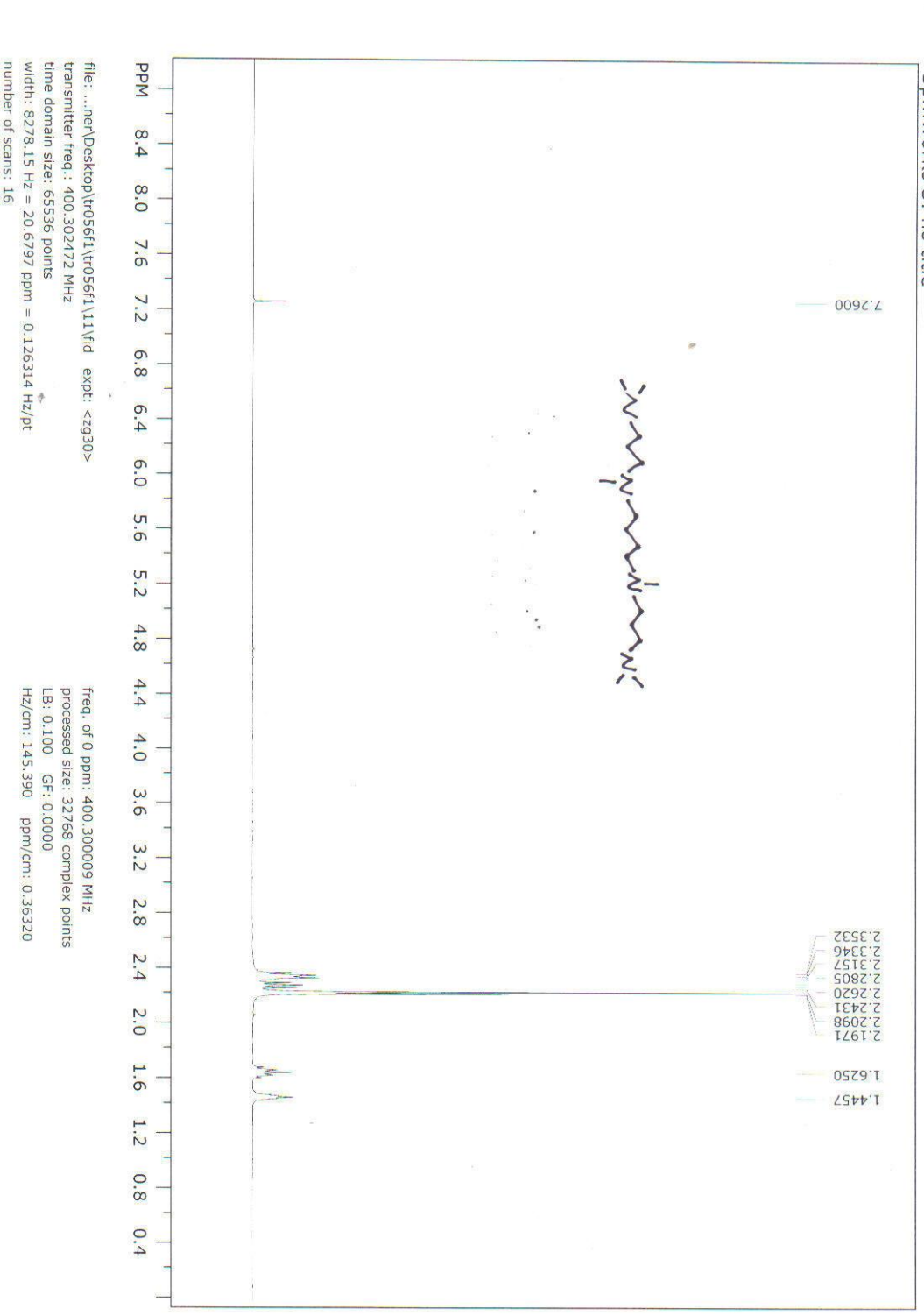

Fig. A3.2. ^{1}H NMR spectrum of compound **3.10** in $CDCl_3$.

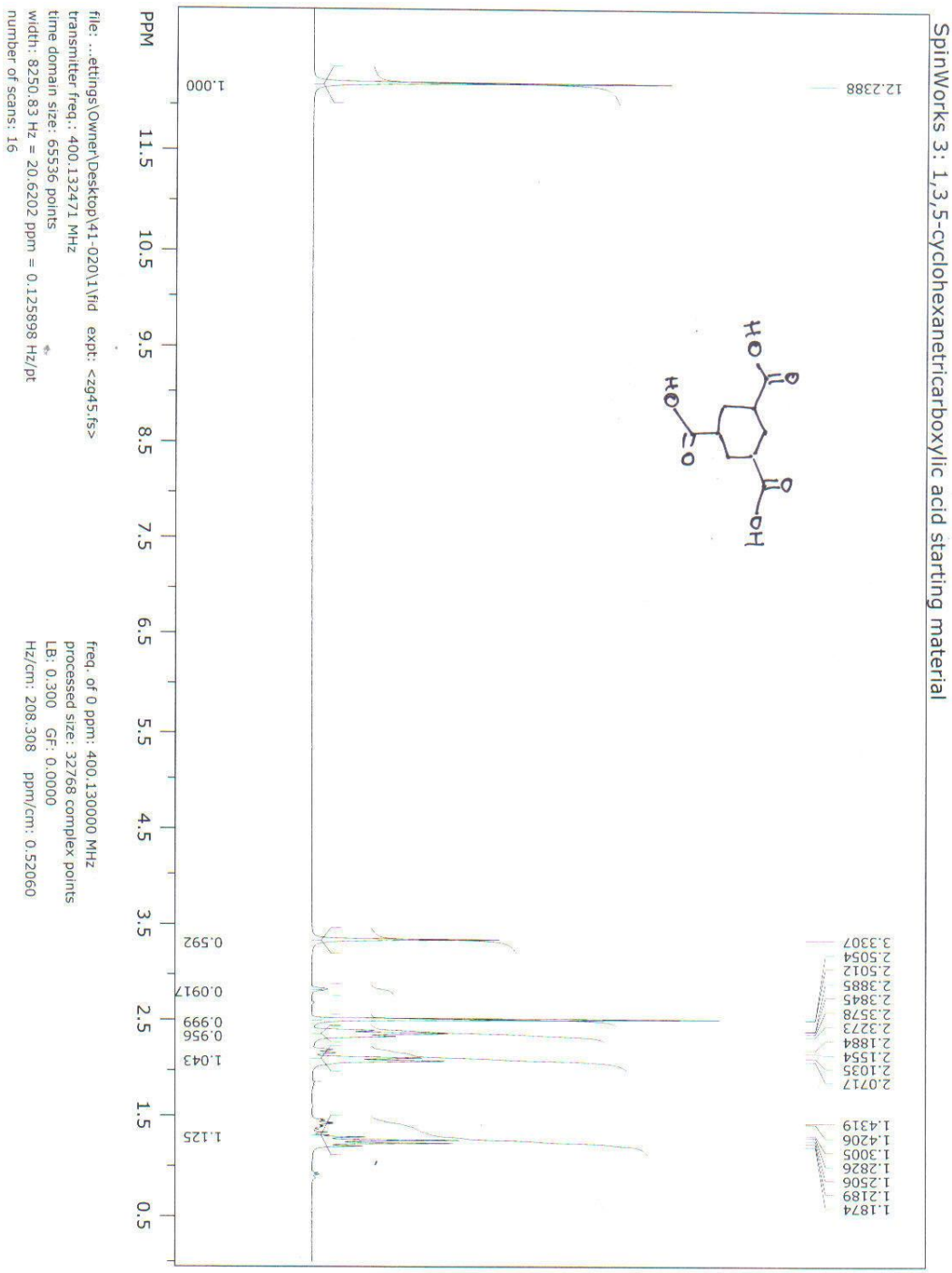

Fig. A3.3. ^{1}H NMR spectrum of 1,3,5-Cyclohexanetricarboxylic acid starting material (cis/trans mixture) used for the synthesis of compound **3.12**, in DMSO-d_6.

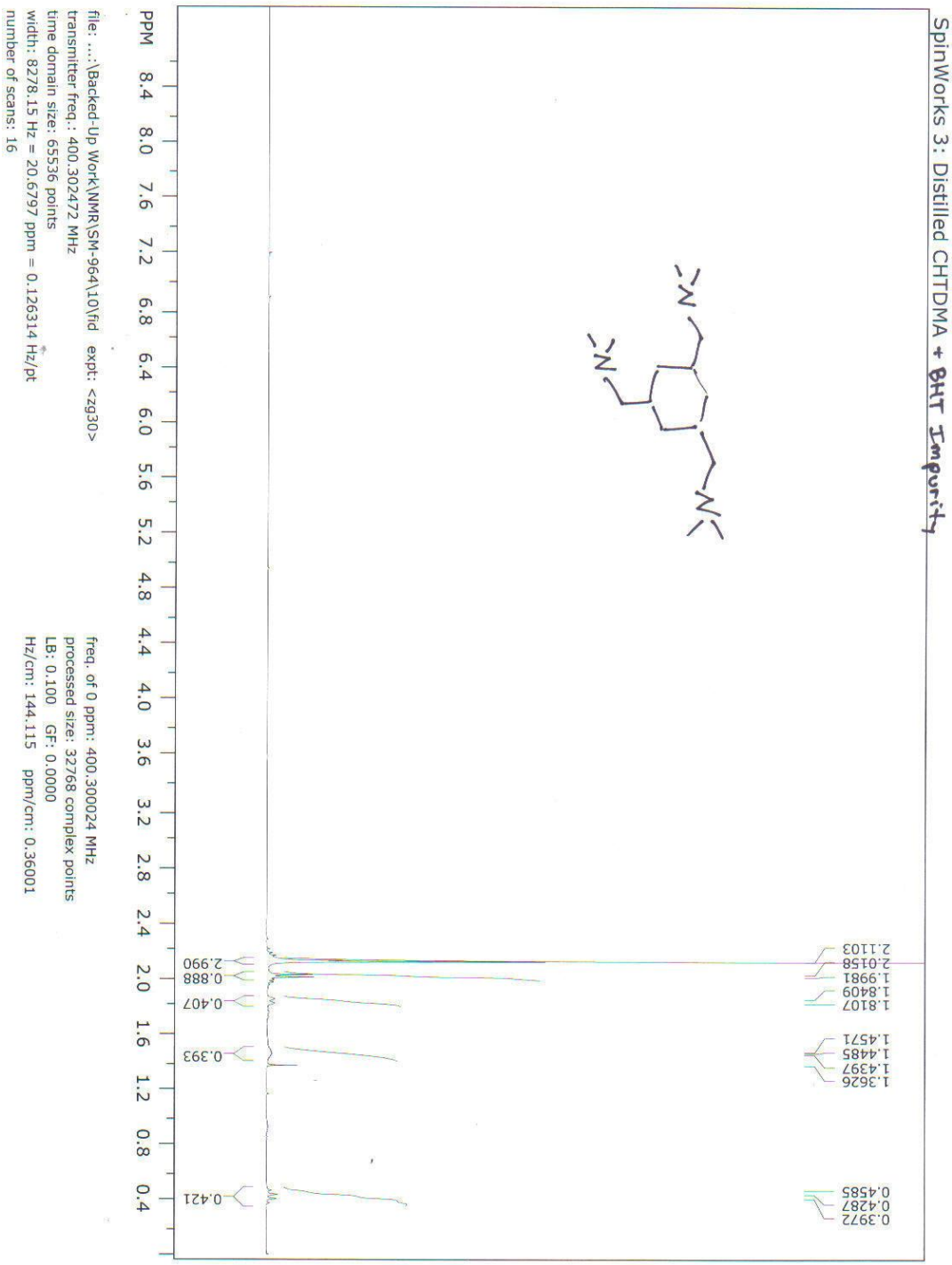

Fig. A3.4. ^{1}H NMR spectrum of compound **3.12** and BHT impurity in $CDCl_3$.

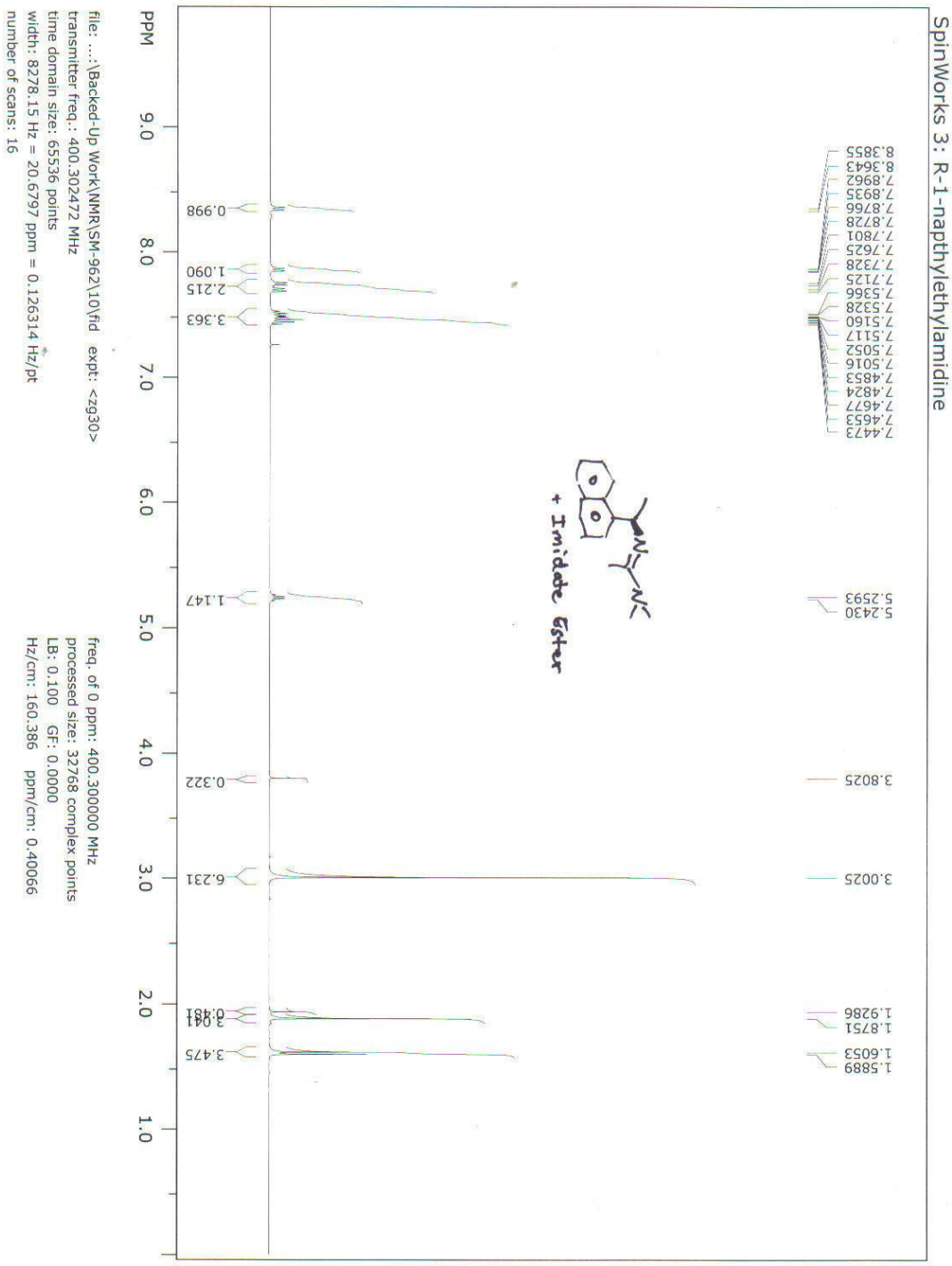

Fig. A3.5. ^{1}H NMR spectra of compound **6.12** and imidate ester impurity in $CDCl_3$.

Appendix IV

Crystal Data

Compound 3.12

A crystal of the compound (colorless, plate-shaped, size 0.20 x 0.20 x 0.06 mm) was mounted on a glass fiber with grease and cooled to -93 °C in a stream of nitrogen gas controlled with Cryostream Controller 700. Data collection was performed on a Bruker SMART APEX II X-ray diffractometer with graphite-monochromated Mo K_α radiation (λ = 0.71073 Å), operating at 50 kV and 30 mA over 2Θ ranges of 5.36 ~ 51.90º. No significant decay was observed during the data collection.

Data were processed on a PC using the Bruker AXS Crystal Structure Analysis Package:[1] Data collection: APEX2 (Bruker, 2006); cell refinement: SAINT (Bruker, 2005); data reduction: SAINT (Bruker, 2005); structure solution: XPREP (Bruker, 2005) and SHELXTL (Bruker, 2000); structure refinement: SHELXTL; molecular graphics: SHELXTL; publication materials: SHELXTL. Neutral atom scattering factors were taken from Cromer and Waber.[2] The crystal is hexagonal space group *R*-3, based on the systematic absences, *E* statistics and successful refinement of the structure. The structure was solved by direct methods. Full-matrix least-square refinements minimizing the function $\sum w (F_o^2 - F_c^2)^2$ were applied to the compound. All non-hydrogen atoms were refined anisotropically. The H atoms on C(1) and C(2) were located from difference Fourier maps, and the rest H atoms were placed in geometrically calculated positions,

with C-H = 0.99(CH_2), and 0.98(CH_3) Å, and refined as riding atoms, with Uiso(H) = 1.5UeqC(CH_3) or 1.2 UeqC(other C). In addition, the methyl groups were refined with AFIX 137, which allowed the rotation of the methyl groups whilst keeping the C-H distances and X-C-H angles fixed.

Convergence to final R_1 = 0.0482 and wR_2 = 0.1314 for 974 (I>2σ(I)) independent reflections, and R_1 = 0.0636 and wR_2 = 0.1464 for all 1296 (R(int) = 0.0223) independent reflections, with 67 parameters and 0 restraints, were achieved.[3] The largest residual peak and hole to be 0.193 and – 0.200 e/Å^3, respectively. Crystallographic data, atomic coordinates and equivalent isotropic displacement parameters, bond lengths and angles, anisotropic displacement parameters, hydrogen coordinates and isotropic displacement parameters, and torsion angles are given in Table 1 to 6. The molecular structure and the cell packing are shown in Figures A2.1 and A2.2.

_____

[1] Bruker AXS Crystal Structure Analysis Package:

Bruker (2000). SHELXTL. Version 6.14. Bruker AXS Inc., Madison, Wisconsin, USA.

Bruker (2005). XPREP. Version 2005/2. Bruker AXS Inc., Madison, Wisconsin, USA.

Bruker (2005). SAINT. Version 7.23A. Bruker AXS Inc., Madison,Wisconsin, USA.

Bruker (2006). APEX2. Version 2.0-2. Bruker AXS Inc., Madison, Wisconsin, USA.

[2] Cromer, D. T.; Waber, J. T. *International Tables for X-ray Crystallography*; Kynoch Press: Birmingham, UK, 1974; Vol. 4, Table 2.2 A.

[3] $R_1 = \sum | |Fo| - |Fc| | / \sum |Fo|$

$wR_2 = \{\sum [w (Fo^2 - Fc^2)^2] / \sum [w(Fo^2)^2]\}^{1/2}$

($w = 1 / [\sigma^2(Fo^2) + (0.0744P)^2 + 1.186P]$, where $P = [\text{Max}(Fo^2, 0) + 2Fc^2] / 3$)

a)

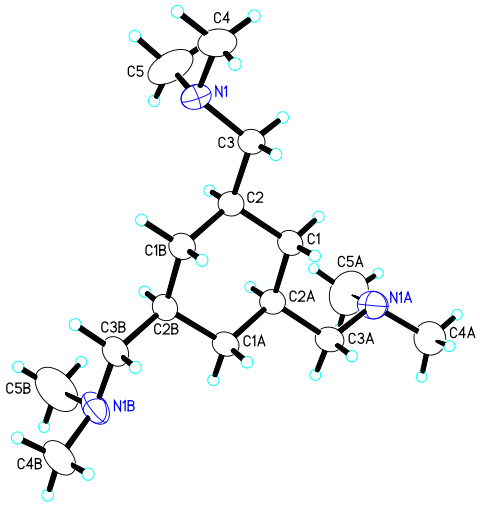

b)

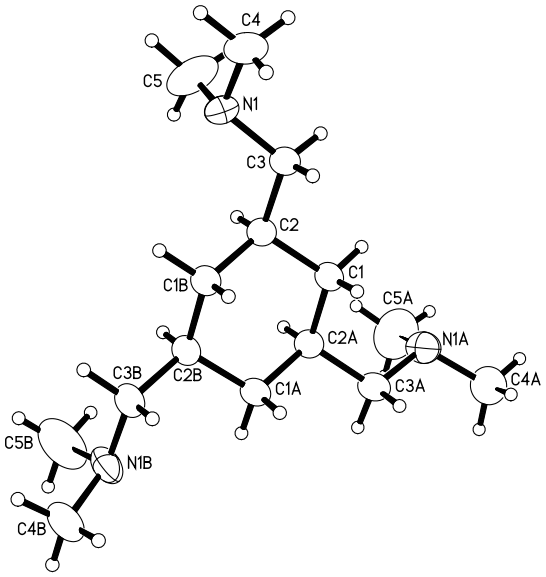

Fig. A4.1. Molecular Structure (Displacement ellipsoids for non-H atoms are shown at the 50% probability level and H atoms are represented by circles of arbitrary size).

a)

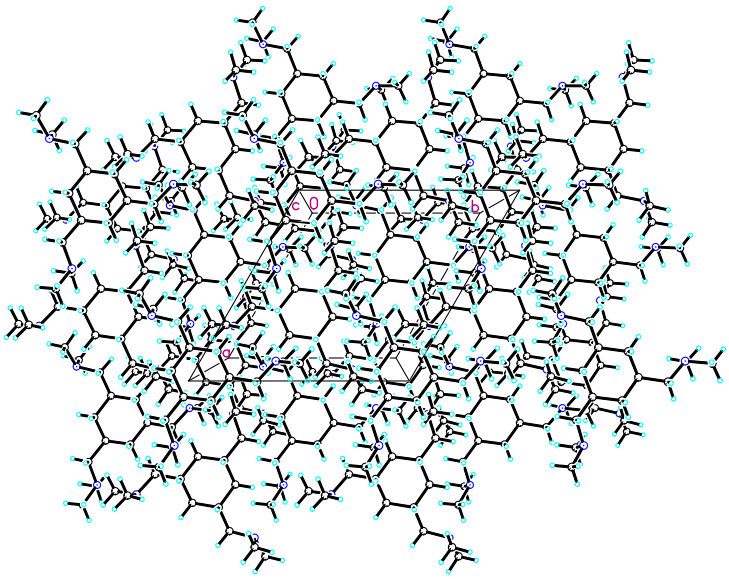

b)

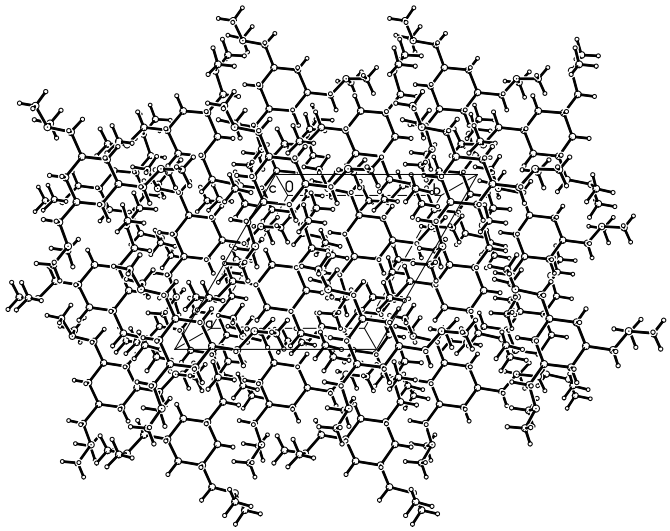

Fig. A4.2. Unit cell packing.

Table A4.1. Crystal data and structure refinement for Compound **3.12**.

Identification code	pj35	
Empirical formula	C15 H33 N3	
Formula weight	255.44	
Temperature	180(2) K	
Wavelength	0.71073 Å	
Crystal system	Hexagonal	
Space group	R-3	
Unit cell dimensions	a = 10.3969(4) Å	α= 90°.
	b = 10.3969(4) Å	β= 90°.
	c = 28.4886(15) Å	γ = 120°.
Volume	2666.9(2) $Å^3$	
Z	6	
Density (calculated)	0.954 Mg/m^3	
Absorption coefficient	0.057 mm^{-1}	
F(000)	864	
Crystal size	0.20 x 0.20 x 0.06 mm^3	
Theta range for data collection	2.68 to 26.95°.	
Index ranges	-12<=h<=13, -13<=k<=9, -32<=l<=36	
Reflections collected	3702	
Independent reflections	1296 [R(int) = 0.0223]	
Completeness to theta = 26.95°	99.5 %	
Absorption correction	Multi-scan	
Max. and min. transmission	0.9966 and 0.9888	
Refinement method	Full-matrix least-squares on F^2	
Data / restraints / parameters	1296 / 0 / 67	
Goodness-of-fit on F^2	1.053	
Final R indices [I>2sigma(I)]	R1 = 0.0482, wR2 = 0.1314	
R indices (all data)	R1 = 0.0636, wR2 = 0.1464	
Largest diff. peak and hole	0.193 and -0.200 $e.Å^{-3}$	

Table A4.2. Atomic coordinates (x 10^4) and equivalent isotropic displacement parameters (Å^{2}x 10^3) for Compound **3.12**. U(eq) is defined as one third of the trace of the orthogonalized U^{ij} tensor.

	x	y	z	U(eq)
N(1)	3358(1)	-706(1)	864(1)	44(1)
C(1)	5381(1)	3526(1)	992(1)	34(1)
C(2)	5172(1)	2030(1)	832(1)	32(1)
C(3)	3691(1)	770(1)	1012(1)	37(1)
C(4)	2129(2)	-1839(2)	1138(1)	56(1)
C(5)	3011(2)	-955(2)	371(1)	82(1)

Table A4.3. Bond lengths [Å] and angles [°] for Compound **3.12**.

N(1)-C(5)	1.440(2)
N(1)-C(3)	1.4570(15)
N(1)-C(4)	1.4585(18)
C(1)-C(2)#1	1.5228(16)
C(1)-C(2)	1.5274(16)
C(1)-H(1A)	0.981(15)
C(1)-H(1B)	0.988(15)
C(2)-C(1)#2	1.5228(16)
C(2)-C(3)	1.5270(16)
C(2)-H(2A)	1.031(14)
C(3)-H(3A)	0.9900
C(3)-H(3B)	0.9900
C(4)-H(4A)	0.9800
C(4)-H(4B)	0.9800
C(4)-H(4C)	0.9800

C(5)-H(5A)	0.9800
C(5)-H(5B)	0.9800
C(5)-H(5C)	0.9800

C(5)-N(1)-C(3)	112.19(13)
C(5)-N(1)-C(4)	109.76(12)
C(3)-N(1)-C(4)	110.24(11)
C(2)#1-C(1)-C(2)	112.50(11)
C(2)#1-C(1)-H(1A)	108.5(8)
C(2)-C(1)-H(1A)	108.3(8)
C(2)#1-C(1)-H(1B)	109.3(8)
C(2)-C(1)-H(1B)	110.6(8)
H(1A)-C(1)-H(1B)	107.5(11)
C(1)#2-C(2)-C(3)	111.88(10)
C(1)#2-C(2)-C(1)	110.48(11)
C(3)-C(2)-C(1)	110.05(9)
C(1)#2-C(2)-H(2A)	107.7(7)
C(3)-C(2)-H(2A)	109.5(7)
C(1)-C(2)-H(2A)	107.1(7)
N(1)-C(3)-C(2)	114.43(10)
N(1)-C(3)-H(3A)	108.7
C(2)-C(3)-H(3A)	108.7
N(1)-C(3)-H(3B)	108.7
C(2)-C(3)-H(3B)	108.7
H(3A)-C(3)-H(3B)	107.6
N(1)-C(4)-H(4A)	109.5
N(1)-C(4)-H(4B)	109.5
H(4A)-C(4)-H(4B)	109.5
N(1)-C(4)-H(4C)	109.5
H(4A)-C(4)-H(4C)	109.5
H(4B)-C(4)-H(4C)	109.5
N(1)-C(5)-H(5A)	109.5

N(1)-C(5)-H(5B)	109.5
N(1)-C(5)-H(5C)	109.5

Symmetry transformations used to generate equivalent atoms:

#1 -x+y+1,-x+1,z #2 -y+1,x-y,z

Table A4.4. Anisotropic displacement parameters ($Å^2 x\ 10^3$) for pj35. The anisotropic displacement factor exponent takes the form: $-2\pi^2[\ h^2\ a^{*2}U^{11} + ...\ + 2\ h\ k\ a^*\ b^*\ U^{12}\ ]$

	U^{11}	U^{22}	U^{33}	U^{23}	U^{13}	U^{12}
N(1)	32(1)	28(1)	64(1)	-12(1)	-2(1)	10(1)
C(1)	27(1)	28(1)	48(1)	-2(1)	0(1)	15(1)
C(2)	27(1)	28(1)	40(1)	-2(1)	-1(1)	13(1)
C(3)	26(1)	29(1)	54(1)	-6(1)	-1(1)	12(1)
C(4)	39(1)	31(1)	84(1)	-4(1)	-1(1)	7(1)
C(5)	88(2)	54(1)	72(1)	-28(1)	-3(1)	12(1)

Table A4.5. Hydrogen coordinates ($x\ 10^4$) and isotropic displacement parameters ($Å^2 x\ 10^3$) for Compound **3.12**.

	x	y	z	U(eq)
H(1A)	5348(15)	3528(15)	1336(5)	40
H(1B)	4562(16)	3662(14)	876(5)	40
H(2A)	5168(15)	2034(14)	470(5)	38
H(3A)	3696	802	1359	45
H(3B)	2886	941	901	45

H(4A)	1934	-2825	1041	84
H(4B)	1239	-1761	1085	84
H(4C)	2388	-1692	1472	84
H(5A)	2755	-1971	289	123
H(5B)	3875	-249	187	123
H(5C)	2167	-813	301	123

Table A4.6. Torsion angles [°] for Compound **3.12**.

C(2)#1-C(1)-C(2)-C(1)#2	54.72(17)
C(2)#1-C(1)-C(2)-C(3)	178.77(9)
C(5)-N(1)-C(3)-C(2)	-71.06(16)
C(4)-N(1)-C(3)-C(2)	166.29(11)
C(1)#2-C(2)-C(3)-N(1)	-58.92(15)
C(1)-C(2)-C(3)-N(1)	177.85(10)

Symmetry transformations used to generate equivalent atoms:

#1 -x+y+1,-x+1,z #2 -y+1,x-y,z

Compound 6.1

A crystal of the compound (brown, plate-shaped, size 0.30 x 0.25 x 0.06 mm) was mounted on a glass fiber with grease and cooled to -93 °C in a stream of nitrogen gas controlled with Cryostream Controller 700. Data collection was performed on a Bruker SMART APEX II X-ray diffractometer with graphite-monochromated Mo K_α radiation (λ = 0.71073 Å), operating at 50 kV and 30 mA over 2θ ranges of 4.04 ~ 52.00º. No significant decay was observed during the data collection.

Data were processed on a PC using the Bruker AXS Crystal Structure Analysis Package:[1] Data collection: APEX2 (Bruker, 2006); cell refinement: SAINT (Bruker, 2005); data reduction: SAINT (Bruker, 2005); structure solution: XPREP (Bruker, 2005) and SHELXTL (Bruker, 2000); structure refinement: SHELXTL; molecular graphics: SHELXTL; publication materials: SHELXTL. Neutral atom scattering factors were taken from Cromer and Waber.[2] The crystal is tetragonal space group $P4_2/nbc$, based on the systematic absences, *E* statistics and successful refinement of the structure. The structure was solved by direct methods. Full-matrix least-square refinements minimizing the function $\sum w (F_o^2 - F_c^2)^2$ were applied to the compound. All non-hydrogen atoms were refined anisotropically. The structure is disordered with molecules on the same sites of the lattice can orient in two different ways, with a equal chance and related to each other through a 2-fold axis (See Fig. A3.1(i)). The hydrogen atoms cannot be included into the refinement due to the disorder, which leads to the 5 Level B Alerts from the CheckCIF report.

Convergence to final R_1 = 0.1162 and wR_2 = 0.3917 for 782 (I>2σ(I)) independent reflections, and R_1 = 0.1367 and wR_2 = 0.4181 for all 1104 (R(int) = 0.0394) independent reflections, with 125 parameters and 0 restraints, were achieved.[3] The largest residual peak and hole to be 0.114 and – 0.126 e/Å^3, respectively. Crystallographic data, atomic coordinates and equivalent isotropic displacement parameters, bond lengths and angles, anisotropic displacement parameters, and torsion angles are given in Table 1 to 5. The molecular structure and the cell packing are shown in Figures A3.1 and A3.2.

_____

[1] Bruker AXS Crystal Structure Analysis Package:
Bruker (2000). SHELXTL. Version 6.14. Bruker AXS Inc., Madison, Wisconsin, USA.
Bruker (2005). XPREP. Version 2005/2. Bruker AXS Inc., Madison, Wisconsin, USA.
Bruker (2005). SAINT. Version 7.23A. Bruker AXS Inc., Madison,Wisconsin, USA.
Bruker (2006). APEX2. Version 2.0-2. Bruker AXS Inc., Madison, Wisconsin, USA.

[2] Cromer, D. T.; Waber, J. T. *International Tables for X-ray Crystallography*; Kynoch Press: Birmingham, UK, 1974; Vol. 4, Table 2.2 A.

[3] $R_1 = \sum | |Fo| - |Fc| | / \sum |Fo|$

$wR_2 = \{\sum [w (Fo^2 - Fc^2)^2] / \sum [w(Fo^2)^2]\}^{1/2}$

($w = 1 / [\sigma^2(Fo^2) + (0.200P)^2]$, where $P = [\text{Max} (Fo^2, 0) + 2Fc^2] / 3$)

a)

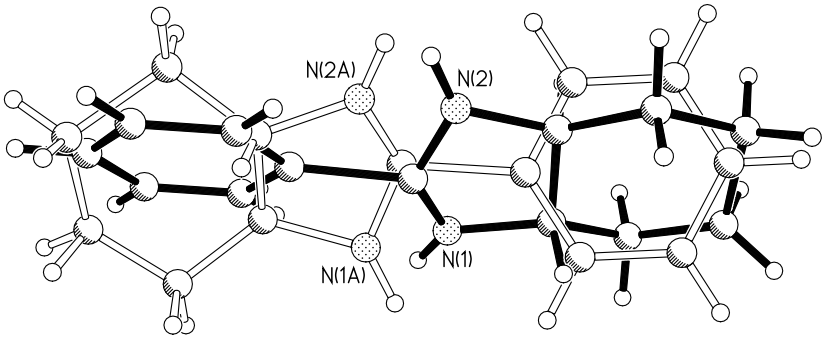

b)

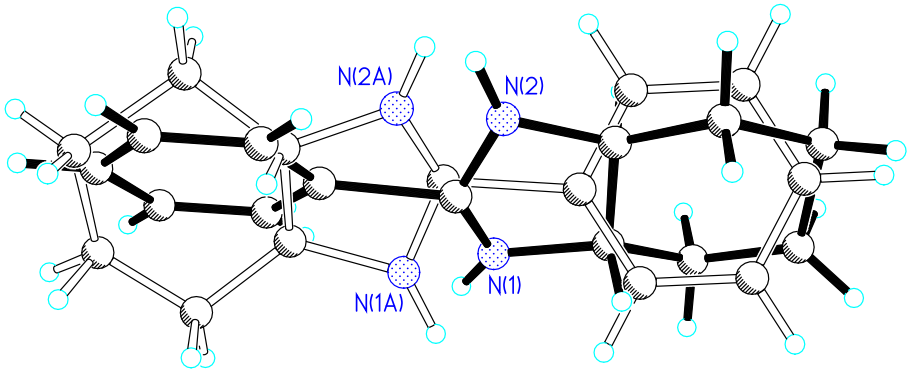

a)

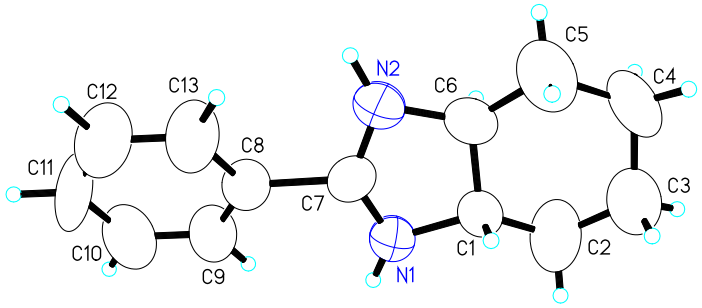

b)

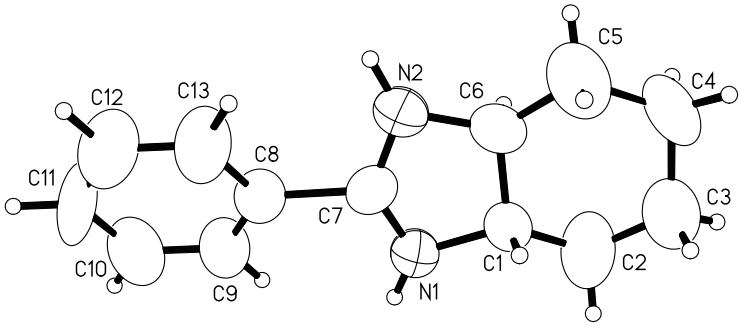

Fig. A4.3. Molecular structure i) A drawing showing the disorder of the structure (two different orientations of the molecules appear at the same lattice sites at an equal chance, 50% each). ii) Molecular Structure (Displacement ellipsoids for non-H atoms are shown at the 50% probability level and H atoms are represented by circles of arbitrary size.)

a)

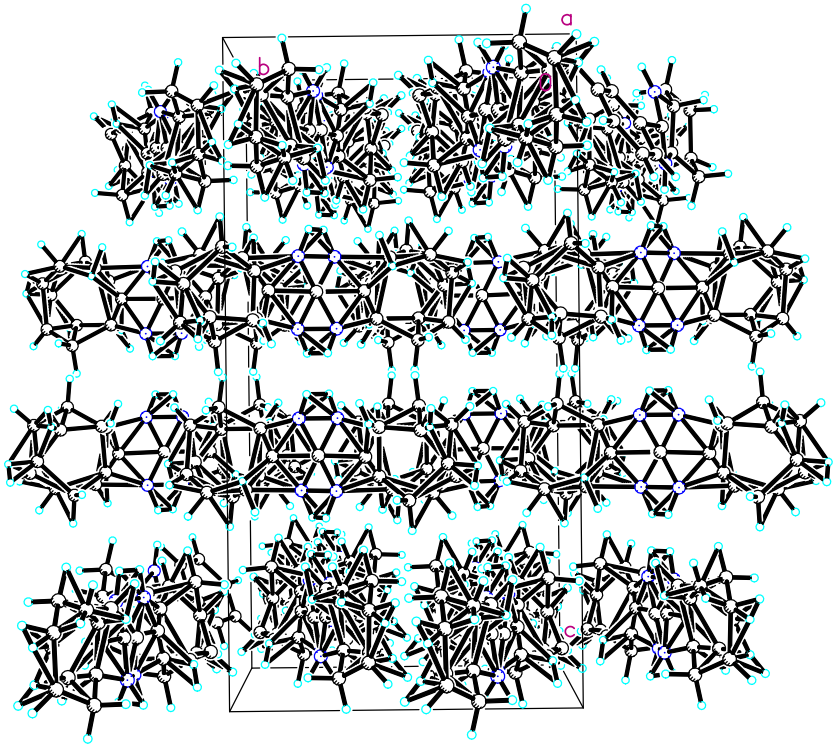

b)

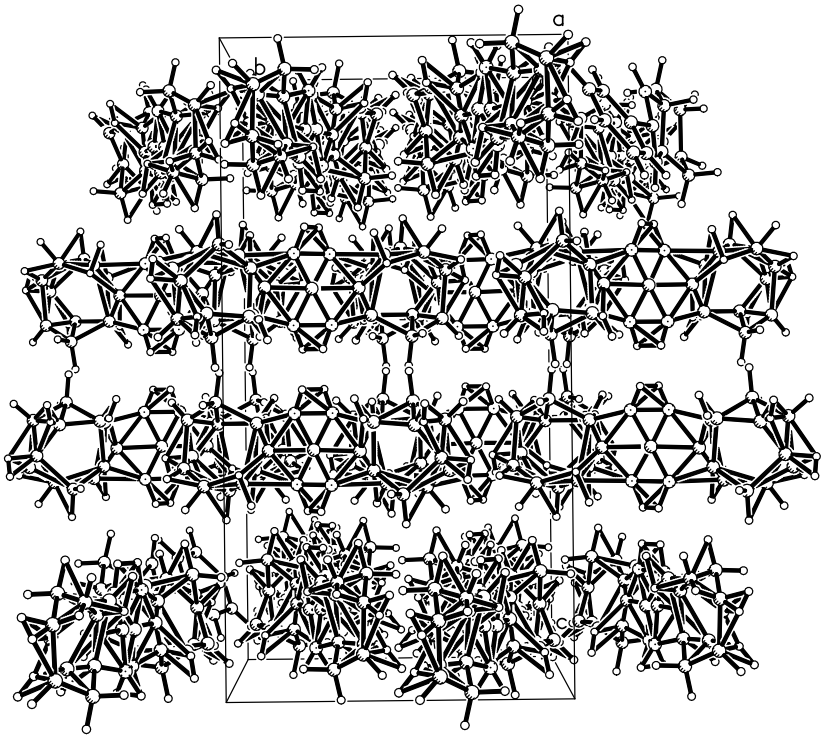

Fig. A4.4. Unit cell packing

Table A4.7. Crystal data and structure refinement for Compound **6.1**.

Identification code	pj42
Empirical formula	C13 H17 N2
Formula weight	201.29
Temperature	180(2) K
Wavelength	0.71073 Å
Crystal system	Tetragonal
Space group	P4(2)/nbc

Unit cell dimensions	a = 10.5477(3) Å	α= 90°.
	b = 10.5477(3) Å	β= 90°.
	c = 20.1254(7) Å	γ = 90°.
Volume	2239.03(12) $Å^3$	
Z	4	
Density (calculated)	0.597 Mg/m^3	
Absorption coefficient	0.036 mm^{-1}	
F(000)	436	
Crystal size	0.30 x 0.25 x 0.06 mm^3	
Theta range for data collection	2.02 to 26.00°.	
Index ranges	-13<=h<=13, -13<=k<=13, -24<=l<=24	
Reflections collected	27294	
Independent reflections	1104 [R(int) = 0.0394]	
Completeness to theta = 26.00°	100.0 %	
Absorption correction	Multi-scan	
Max. and min. transmission	0.9979 and 0.9894	
Refinement method	Full-matrix least-squares on F^2	
Data / restraints / parameters	1104 / 0 / 125	
Goodness-of-fit on F^2	1.775	
Final R indices [I>2sigma(I)]	R1 = 0.1162, wR2 = 0.3917	
R indices (all data)	R1 = 0.1367, wR2 = 0.4181	
Largest diff. peak and hole	0.144 and -0.126 e.$Å^{-3}$	

Table A4.8. Atomic coordinates (x 10^4) and equivalent isotropic displacement parameters ($Å^2$x 10^3) for Compound **6.1**. U(eq) is defined as one third of the trace of the orthogonalized U^{ij} tensor.

	x	y	z	U(eq)
N(1)	2473(5)	3065(4)	4312(2)	68(2)
N(2)	2181(5)	3021(4)	3198(2)	77(2)

C(1)	1782(7)	4238(6)	4156(4)	67(2)
C(2)	1886(11)	5459(9)	4494(5)	138(4)
C(3)	1033(10)	6381(9)	4210(6)	110(3)
C(4)	1002(15)	6508(12)	3439(9)	110(4)
C(5)	939(9)	5140(9)	3078(5)	113(3)
C(6)	1860(7)	4284(7)	3425(4)	67(2)
C(7)	2330(14)	2510(30)	3744(2)	45(3)
C(8)	3106(4)	1120(4)	3726(3)	59(2)
C(9)	3952(5)	702(4)	4187(3)	78(2)
C(10)	4444(6)	-489(5)	4139(3)	96(2)
C(11)	4091(7)	-1262(5)	3631(3)	92(5)
C(12)	3245(7)	-843(6)	3170(3)	104(3)
C(13)	2753(5)	347(5)	3217(3)	99(3)

Table A4.9. Bond lengths [Å] and angles [°] for Compound **6.1**.

N(1)-C(7)	1.295(16)
N(1)-C(1)	1.470(8)
N(2)-C(7)	1.235(17)
N(2)-C(6)	1.449(9)
C(1)-C(2)	1.461(12)
C(1)-C(6)	1.474(10)
C(2)-C(3)	1.443(13)
C(3)-C(4)	1.558(17)
C(4)-C(5)	1.617(19)
C(5)-C(6)	1.499(11)
C(7)-C(8)	1.68(3)
C(8)-C(9)	1.361(3)
C(8)-C(13)	1.361(3)
C(9)-C(10)	1.363(3)

C(10)-C(11)	1.360(3)
C(11)-C(12)	1.361(3)
C(12)-C(13)	1.363(3)

C(7)-N(1)-C(1)	97.7(13)
C(7)-N(2)-C(6)	98.7(15)
C(2)-C(1)-N(1)	127.2(6)
C(2)-C(1)-C(6)	115.5(6)
N(1)-C(1)-C(6)	102.4(5)
C(3)-C(2)-C(1)	111.3(9)
C(2)-C(3)-C(4)	117.7(8)
C(3)-C(4)-C(5)	111.8(9)
C(6)-C(5)-C(4)	107.5(9)
N(2)-C(6)-C(1)	107.3(6)
N(2)-C(6)-C(5)	124.0(7)
C(1)-C(6)-C(5)	116.7(6)
N(2)-C(7)-N(1)	127(3)
N(2)-C(7)-C(8)	115.1(12)
N(1)-C(7)-C(8)	111.0(12)
C(9)-C(8)-C(13)	119.9
C(9)-C(8)-C(7)	126.0(5)
C(13)-C(8)-C(7)	113.9(5)
C(8)-C(9)-C(10)	120.1
C(11)-C(10)-C(9)	120.0
C(10)-C(11)-C(12)	119.9
C(11)-C(12)-C(13)	120.1
C(8)-C(13)-C(12)	120.0

Symmetry transformations used to generate equivalent atoms:

Table A4.10. Anisotropic displacement parameters ($Å^2 x\ 10^3$)for compound **6.1**. The anisotropic displacement factor exponent takes the form: $-2\pi^2[\ h^2 a^{*2} U^{11} + ... + 2\ h\ k\ a^*\ b^*\ U^{12}\ ]$

	U^{11}	U^{22}	U^{33}	U^{23}	U^{13}	U^{12}
N(1)	95(3)	58(2)	53(3)	1(2)	0(2)	12(2)
N(2)	100(4)	77(3)	53(3)	7(2)	-6(2)	21(3)
C(1)	85(5)	57(3)	58(3)	7(3)	5(3)	12(3)
C(2)	205(11)	96(5)	112(6)	-25(5)	-21(7)	56(6)
C(3)	121(7)	89(6)	120(7)	9(5)	8(6)	25(5)
C(4)	125(8)	75(6)	131(7)	45(7)	10(6)	21(6)
C(5)	110(6)	104(6)	124(6)	16(5)	-15(5)	28(5)
C(6)	72(4)	63(4)	65(5)	14(3)	12(3)	-9(3)
C(7)	19(8)	62(2)	54(2)	-5(3)	1(2)	-7(8)
C(8)	58(3)	56(4)	64(4)	-7(3)	-9(3)	-11(2)
C(9)	76(4)	70(4)	87(5)	2(3)	-7(4)	20(4)
C(10)	87(5)	77(5)	125(6)	15(4)	-3(4)	5(4)
C(11)	75(5)	52(5)	148(13)	-42(6)	-13(6)	14(3)
C(12)	111(6)	88(5)	114(6)	-32(4)	-36(5)	0(5)
C(13)	113(7)	81(5)	102(6)	-24(4)	-50(5)	23(4)

Table A4.11. Torsion angles [°] for Compound **6.1**.

C(7)-N(1)-C(1)-C(2)	-159.4(12)
C(7)-N(1)-C(1)-C(6)	-23.4(10)
N(1)-C(1)-C(2)-C(3)	-178.5(8)
C(6)-C(1)-C(2)-C(3)	50.1(12)
C(1)-C(2)-C(3)-C(4)	-47.4(15)
C(2)-C(3)-C(4)-C(5)	46.0(16)

C(3)-C(4)-C(5)-C(6)	-43.6(13)
C(7)-N(2)-C(6)-C(1)	-4.6(10)
C(7)-N(2)-C(6)-C(5)	-145.5(10)
C(2)-C(1)-C(6)-N(2)	160.5(7)
N(1)-C(1)-C(6)-N(2)	18.2(7)
C(2)-C(1)-C(6)-C(5)	-55.3(10)
N(1)-C(1)-C(6)-C(5)	162.4(7)
C(4)-C(5)-C(6)-N(2)	-172.7(8)
C(4)-C(5)-C(6)-C(1)	49.7(10)
C(6)-N(2)-C(7)-N(1)	-15.6(15)
C(6)-N(2)-C(7)-C(8)	-163.7(12)
C(1)-N(1)-C(7)-N(2)	27.3(15)
C(1)-N(1)-C(7)-C(8)	176.5(10)
N(2)-C(7)-C(8)-C(9)	142.7(10)
N(1)-C(7)-C(8)-C(9)	-10.5(18)
N(2)-C(7)-C(8)-C(13)	-42.1(17)
N(1)-C(7)-C(8)-C(13)	164.7(10)
C(13)-C(8)-C(9)-C(10)	0.0
C(7)-C(8)-C(9)-C(10)	174.9(9)
C(8)-C(9)-C(10)-C(11)	0.0
C(9)-C(10)-C(11)-C(12)	0.0
C(10)-C(11)-C(12)-C(13)	0.0
C(9)-C(8)-C(13)-C(12)	0.0
C(7)-C(8)-C(13)-C(12)	-175.5(8)
C(11)-C(12)-C(13)-C(8)	0.0

Symmetry transformations used to generate equivalent atoms: